OF 2000-8

New Nouveau
Brunswick

Open File

Natural Resources and Energy
Minerals and Energy Division

TILL PROVENANCE AND GLACIAL HISTORY OF THE PETITCODIAC (NTS 21 H/14) MAP AREA, SOUTHEASTERN NEW BRUNSWICK

Geoffrey M. Allaby

ISSN 1205-7150
ISBN 1-55236-749-5
2000

Price $6.75

Open File 2000-8

Till Provenance and Glacial History of the Petitcodiac (NTS 21 H/14) Map Area, Southeastern New Brunswick

Recommended citation:

ALLABY, G.M. 2000. Till provenance and glacial history of the Petitcodiac (NTS 21 H/14) map area, southeastern New Brunswick. New Brunswick Department of Natural Resources and Energy, Minerals and Energy Division, Open File 2000-8, 217 p.

This report has been reprinted by:

Minerals and Energy Division
Department of Natural Resources and Energy
New Brunswick

Hon. Jeannot Volpé
Minister of Natural Resources and Energy

July, 2000

New Nouveau
Brunswick

Natural Resources and Energy
Minerals and Energy

Open File 2000-8

Till Provenance and Glacial History of the Petitcodiac (NTS 21 H/14) Map Area, Southeastern New Brunswick

Geoffrey M. Allaby

ISSN 1205-7150
ISBN 1-55236-749-5

2000

TILL PROVENANCE AND GLACIAL HISTORY OF THE PETITCODIAC (NTS 21 H/14) MAP AREA, SOUTHEASTERN NEW BRUNSWICK

By

Geoffrey M. Allaby
B.Sc., University of New Brunswick, 1997

A Thesis Submitted in Partial Fulfillment of
the Requirements for the Degree of

Master of Science

In the Department of

Geology

Supervisor: B.E. Broster, Ph.D., Geology

Examining Board: R.F, Miller, Ph.D., Geology, Chair
E. Hildebrand, Ph.D., Engineering

This thesis is accepted.

....

Dean of Graduate studies

THE UNIVERSITY OF NEW BRUNSWICK

January, 2000

ABSTRACT

Mapping of surficial deposits and examination of till clast lithologies have contributed to an understanding of the Late Wisconsinan glacial stratigraphy and ice movement in the Petitcodiac map area (NTS 21H/14) of southeastern New Brunswick. Clast and matrix samples were collected from basal till at 2 km intervals across the map area. Ice-flow directions were inferred from the till matrix geochemistry and clast provenance data, as well as from orientation of glacial landforms and striae.

Only a single basal till unit was recognised in the Petitcodiac map area, suggesting that glacial sediments were deposited by a regional ice sheet during the last (Late Wisconsinan) glaciation. The dispersal of till components and the ice-flow data indicate that the dominant ice-flow direction fluctuated between south-southwest and southeast over the entire map area.

In the eastern half of the study area drumlinoid features, rat-tails, striations, geochemical dispersal in the till matrix, and clast dispersal record late easterly and northeasterly ice-flow events. It is likely that ice flow gradually shifted from south-southeast, toward a more easterly direction, as the ice sheet thinned during deglaciation. Eventually the thinning ice sheet became confined by regional topography, and an ice divide developed as ice streamed around the eastern border of the Caledonian Highlands. The ice divide separated ice moving northeastward toward Chignecto Bay, from ice moving southwestward down the Kennebecasis Valley.

Evaluation of the glacial dispersal of till constituents has provided new prospecting targets in the study area. Dispersal of till clasts suggests a local occurrence of unmapped volcanic units, which are often associated with mineralisation in the region. Furthermore, geochemical dispersal indicates that there is potential for local mineralised zones along some faults.

ACKNOWLEDGEMENTS

First and foremost I would like to thank my supervisor, Dr. B. E. Broster, for providing me with this great opportunity to further my academic career and for the invaluable advice he provided throughout the project. I would also like to thank Dr., R. Pickerill, Dr. R. Miller, and Dr. E. Hildebrand for critically reviewing my thesis and greatly enhancing its quality.

I would like to express my thanks to the New Brunswick Department of Natural Resources and Energy, Fredericton for their logistical support. My summers spent working with the people at DNRE will be fondly remembered. Throughout my thesis I drew on the experience and knowledge of several of the staff at DNRE, most notably of whom is A. G. (Toon) Pronk, who always found time to help me develop my ideas. I would also like to thank A. A. Seaman for his encouragement and for helping to keep the science in my thesis "honest", R. Bolden for his assistance and good company both in the field and the lab, D. Nenuopal for his assistance with identification of clast lithologies, M. MacLeod for providing me background information on the geology in the study area, and the student field assistants Connie Manning and Lora Clowater for their "deep" conversations and hard work. M. Parkhill, S. McCutcheon, and M. Laybourne also deserve recognition for allowing me the opportunity to gain valuable work experience in the Bathurst area, northern New Brunswick.

I thank the staff at UNB for their good-natured jokes and support. Thanks to technicians Todd Jewett and Dave Pirie for helping me out with my stubborn computer;

Calvin Nash and Ancel Murphy for providing first rate thin sections; and Angel Gómez for helping me with my slides.

I would like to thank my fellow graduate students for making my stay in Fredericton an enjoyable one. Special thanks to Andrew Stumpf taking me under his wing, being a sounding board for my ideas, and his great company. Thanks to Marni, Jim, Bill, Jürgen, Chris, Heather, Martin, John, Ron, Mal, Brad, Tracey, Alain, Donovan, Graham, Yvette, Ellie, and Ali for their great soccer games, potlucks, and nights on the town in Fredericton. I would also like to extend my gratitude to Dr. T. Al, Dr. A. Park, Dr. T. Dunn, Dr. R. Turner, Dr. Nick Susak and Dr. J. Tong for their encouragement and advice throughout the past 2 years.

Thanks to my many friends I have made over the past years; especially my Valley View buds John, Austin, Andy, Matt, and Mike, and my roommates Pat and Rick 'n Beth. I would also like to thank Mélanie for her unwavering support and expanding my appreciation of the Arts (especially music) during the last year of my thesis. Finally, I would like to extend my gratitude to my family for providing so much encouragement and support throughout the last seven years of my university career.

TABLE OF CONTENTS

LIST OF TABLES

* denotes abbreviated table titles.

LIST OF FIGURES

* denotes abbreviated figure captions.

CHAPTER 1

INTRODUCTION

1.1. The New Brunswick Model

Mapping the southern margin of the Late Wisconsinan Laurentide ice sheet in New Brunswick has been crucial to the understanding of the Quaternary geology in Atlantic Canada. Debate regarding the limits of the Laurentide ice sheet in New Brunswick presently rests on the timing of its southerly expansion out of Québec.

Several geologists favour the development of a regional ice sheet from local ice domes in New Brunswick prior to the arrival of the Laurentide ice sheet (Rampton and Paradis, 1981; Rampton et al., 1984; Vincent and Prest, 1987; Pronk et al., 1989; Rappol, 1989). The regional ice sheet is thought to have blocked most of the subsequent southward expansion of the Laurentide ice sheet in the Maritimes (Rampton et al., 1984; Rappol, 1989). This model proposes a "minimal" intrusion of the Laurentide ice sheet into New Brunswick and is supported by the orientation of micro-scale glacial erosional features such as nailhead striae, bi-directional striae, rat-tails, and glacigenic fractures (Flint, 1951; Rampton et al., 1984; Pronk et al., 1989).

Some geologists propose that the Laurentide ice sheet overrode most of New Brunswick approximately 18,000 years ago, prior to the development of local ice domes (Grant, 1977; Hughes et al., 1985). Hughes et al. (1985) argued that the Laurentide Ice Sheet downwasted approximately 16,000 years ago, leaving remnant ice domes in the Maritimes. They suggest that micro-scale erosional features only record the more recent glacial ice-flow directions. However, their model does not account for the absence of

Precambrian Shield erratics from Québec in central and northeastern New Brunswick (David and Lebuis, 1985; Pronk et al., 1989).

Both models indicate that an ice mass developed during the Late Wisconsinan on the Appalachian Mountains in northwestern New Brunswick, blocking the southward movement of Laurentide ice into the province (Grant, 1977; Rampton et al., 1984; Hughes et al., 1985; Pronk et. al., 1989; Rappol, 1989). The "damming" of Laurentide ice by an "Appalachian Ice Divide" in northern New Brunswick may have allowed a regional ice system, consisting of relatively small ice centres, to develop in the Maritimes. Interactions among these ice centres could account for the complex ice-flow patterns indicated by erratic dispersal and micro-scale erosional features found throughout the province. Presently, the chronology of the flow events and the maximum thickness of the New Brunswick ice sheet remain uncertain.

Robert Chalmers (1890, 1895) was the first to report the complex ice-flow patterns within New Brunswick in his observations of striae and geomorphological features. He attributed the complex ice-flow patterns to the interactions between local ice domes. Subsequent studies suggest that the regional ice flow ranged from south-southeast to east in southeastern New Brunswick during the Late Wisconsinan (Rampton et al., 1984; Foisy and Prichonnet, 1991; Seaman, 1991; Munn, 1995; Munn et al., 1996). Presently, it is thought that the shifts in flow direction occurred in response to fluctuations in the relative strengths of three local ice centres as glaciation progressed (Rampton et al., 1984).

A late northward ice-flow event originating from an ice mass on the Caledonia Zone in southeastern New Brunswick has recently been proposed by Foisy and

Prichonnet (1991) based on two striae sites found on the Salisbury map area. The new evidence provided by Foisy and Prichonnet (1991) contradicts a notion advanced by Rampton et al. (1984) that the Caledonia Zone was a nunatak during the Late Wisconsinan (Figure 1.1). The present study area for this project, located immediately south of the Salisbury map sheet, is ideally located to evaluate whether the Caledonia Zone was a nunatak or covered by a remnant ice mass during the Late Wisconsinan deglaciation. Southeastern New Brunswick is believed to have been essentially ice-free at approximately 13 ka. (Rampton et al., 1984).

1.2. Purpose and Scope

Fieldwork was conducted in southeastern New Brunswick on the Petitcodiac map area (NTS 21H/14, Figure 1.2) during the summers of 1997 and 1998 as part of a regional surficial mapping project co-ordinated by A. G. Pronk of the New Brunswick Department of Natural Resources and Energy. The primary focus of the project was to characterise the areal distribution of lithological and chemical components in till units. To meet this objective, sampling of till was conducted at 2 km spacing covering the map area (Figure 1.3). Data from this study were used to delineate glacial dispersal of the clast and matrix components in till originating from distinct bedrock units or mineral occurrences. These dispersal patterns were then used to establish the approximate lengths of clast and geochemical dispersal trains originating from distinctive bedrock units in the Petitcodiac area. Once the direction and average distance of glacial dispersal and the transport distances for the various components of the till were determined, attempts were made to associate unknown till geochemical anomalies and till clasts with their bedrock sources. In addition, the regional background levels of selected elements were established to meet

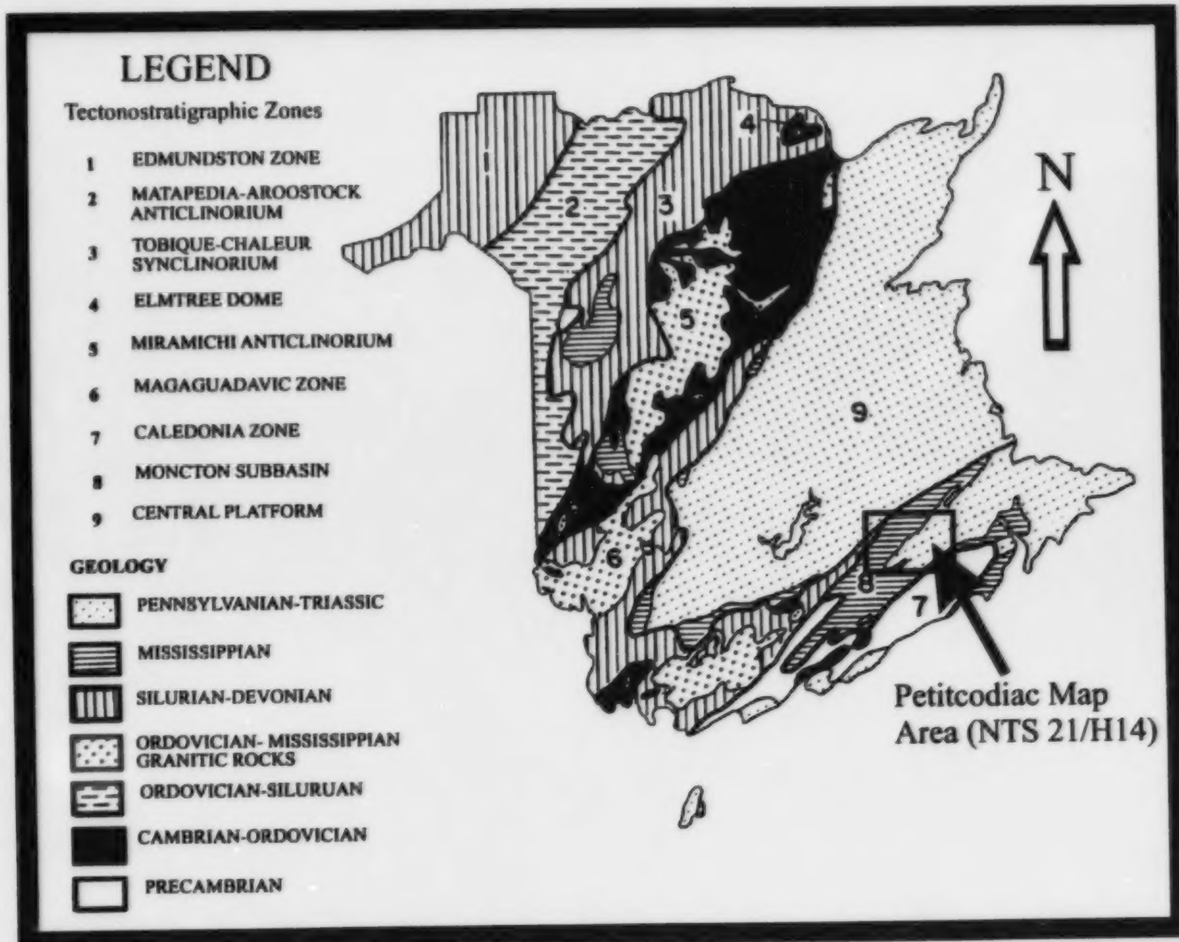

Figure 1.1: Tectonostratigraphic zones and general geology of New Brunswick (after Rampton et. al., 1984).

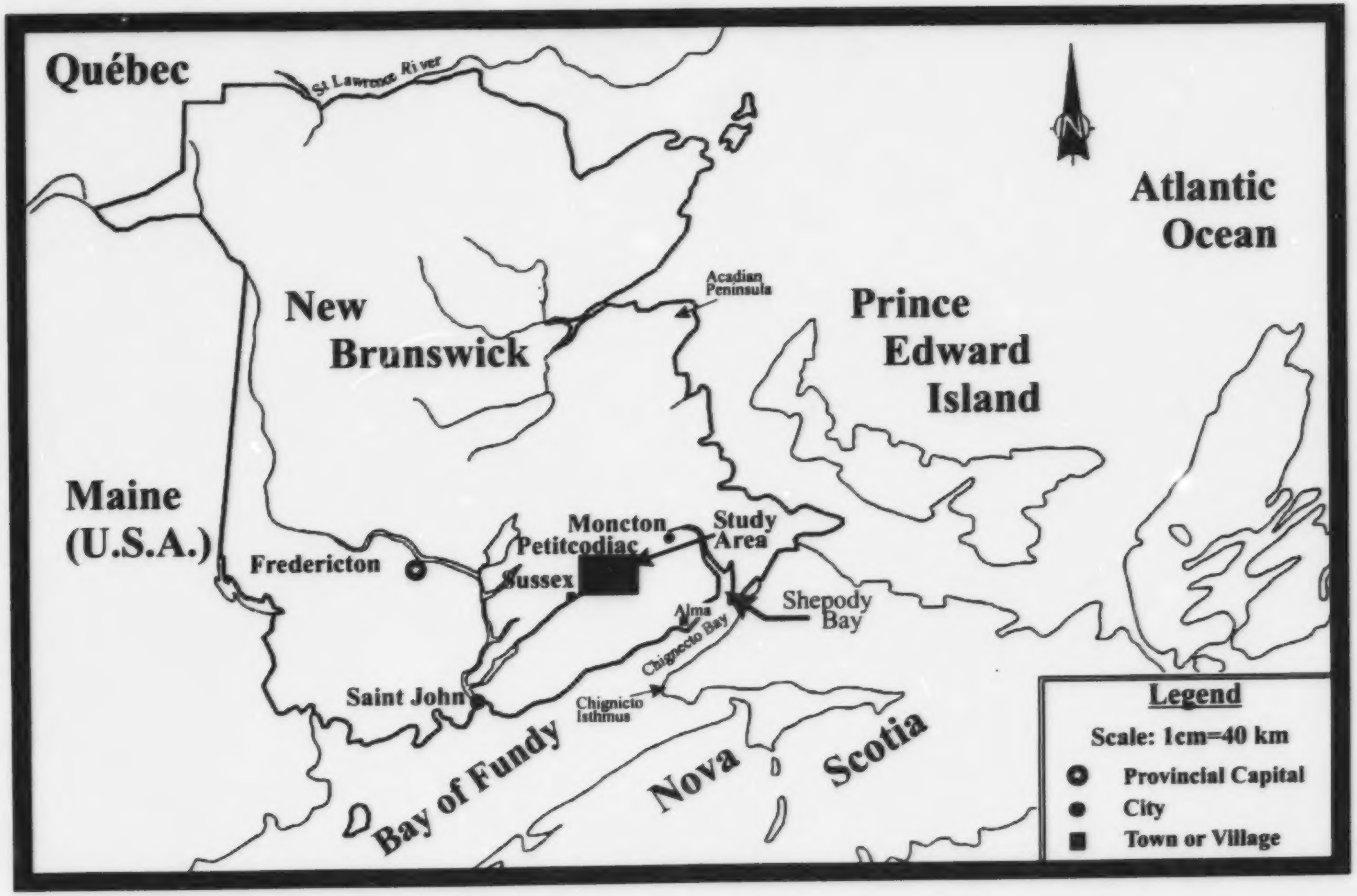

Figure 1.2 : Location of study area in southeastern New Brunswick.

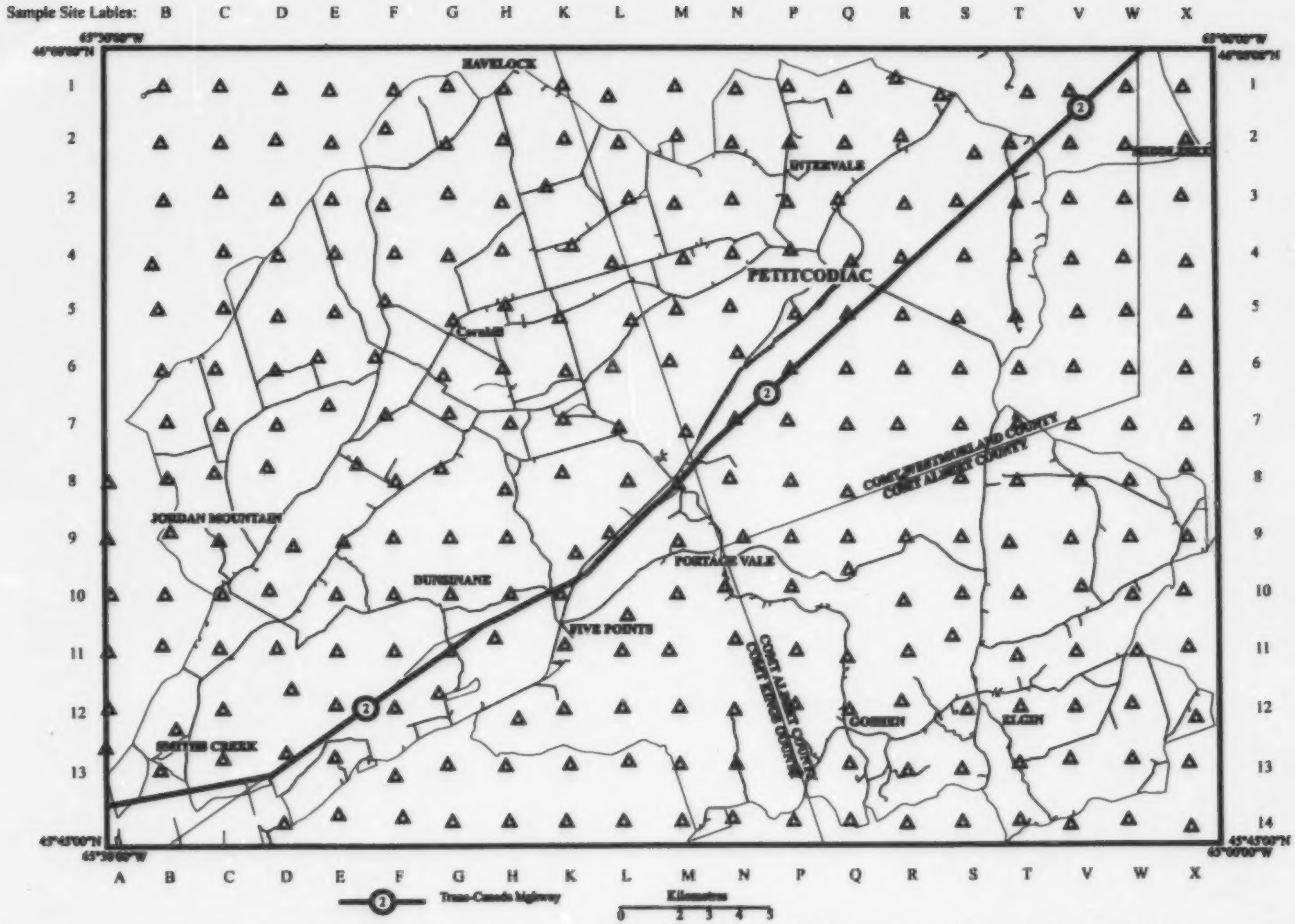

Figure 1.3: Sample site locations in the Petitcodiac (21 H/14) map area. The triangles marking the sample sites are accurate to within 50m.

the growing environmental concerns for industry. Levinson (1974) suggested that C-horizon soil sampling is particularly useful for establishing the natural elemental background levels because the geochemistry of the samples has not been significantly altered since glacial times.

A secondary objective was to map erosional and geomorphological ice-flow indicators such as striae, rat-tails, grooves, and drumlinoid features to assess whether they reflect the debris transport direction, or simply the ice-flow directions during deglaciation. These data were also used to check the plausibility of a suspected northward ice-flow event in New Brunswick (Seaman, 1989, 1991; Foisy and Prichonnet, 1991).

The final objective was to evaluate the relationship between the granular texture of the till and its source lithology because the potential for elemental partitioning into particular grain sizes is an important consideration in drift exploration studies (see Chapter 2.2). This issue was addressed statistically by performing a Spearman's rank correlation analysis on the till matrix geochemistry and grain size data.

Many of the interpretations of these data will be used by the Department of Natural Resources, in conjunction with several other provincial mapping projects at the 1:50 000 scale, to produce a better understanding of the surficial geology and the ice-flow history for New Brunswick. Eventually, the results of this study may also be integrated into an independent study of the Fundy Model Forest soils and land use plans.

1.3. Location and Access to the Study Area

The study area is located in southeastern New Brunswick, Canada, and encompasses approximately 1092 km^2 (Figures, 1.2, 1.3). The area is defined by the National Topographic Series Petitcodiac map area (NTS 21H/14, scale 1:50 000). Situated between Moncton and Sussex, the map sheet is bounded by longitudes 65º30′ and 65º00′, and by latitudes 45º45′ and 46º00′.

The Petitcodiac map area can be accessed via the Trans-Canada Highway (Route 2) and provincial highways (Figure 1.4). Most of the sample locations are accessible by vehicle using the extensive network of secondary and logging roads. Skidder, game and snowmobile trails provide additional access by foot. Most sites required short hikes through wooded areas to maintain a consistent sampling grid.

1.4. Physiography

New Brunswick is located in the Appalachian Region of Canada (Bostock, 1970). The general physiography (Figure 1.5) of the province has evolved mainly from tectonic and erosional processes during the Cretaceous and Tertiary periods, subsequently undergoing only minor modification during the Quaternary (Rampton et al., 1984). The Petitcodiac map area is located within the Caledonian Highlands physiographic unit, a subdivision of the New Brunswick Highlands (Bostock, 1970; Rampton et al., 1984). In the southeastern corner of the map sheet, the topography becomes increasingly hilly where glacially streamlined ridges rise 120 m to 250 m from the valley floors. In contrast, the northern regions exhibit much less topographic expression having a gently undulating plateau-like surface interrupted by occasional clusters of rolling hills (Rampton and Paradis, 1981; Seaman, 1987).

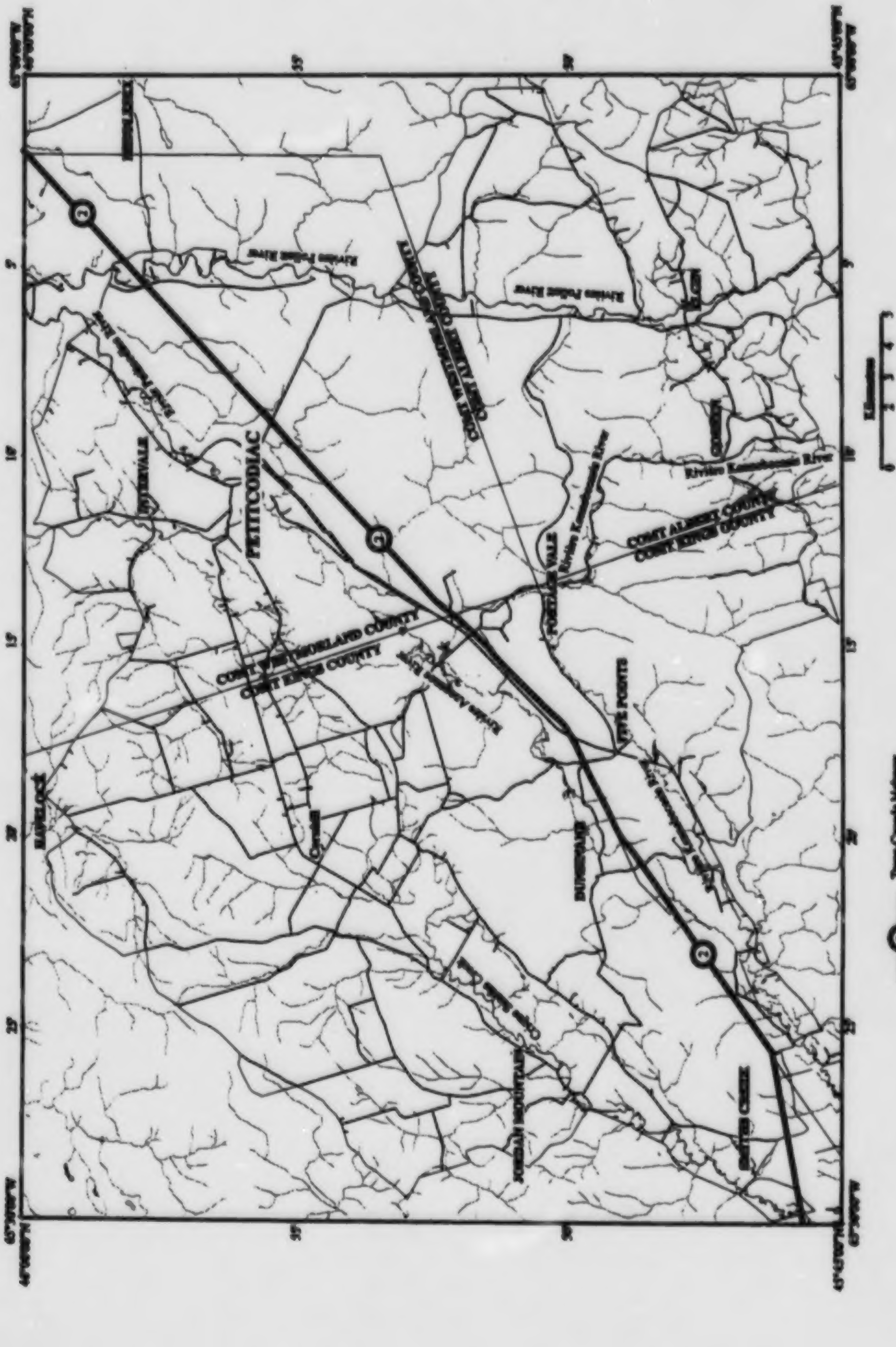

Figure 1.4: Map of infrastructure and drainage in the Petitcodiac area.

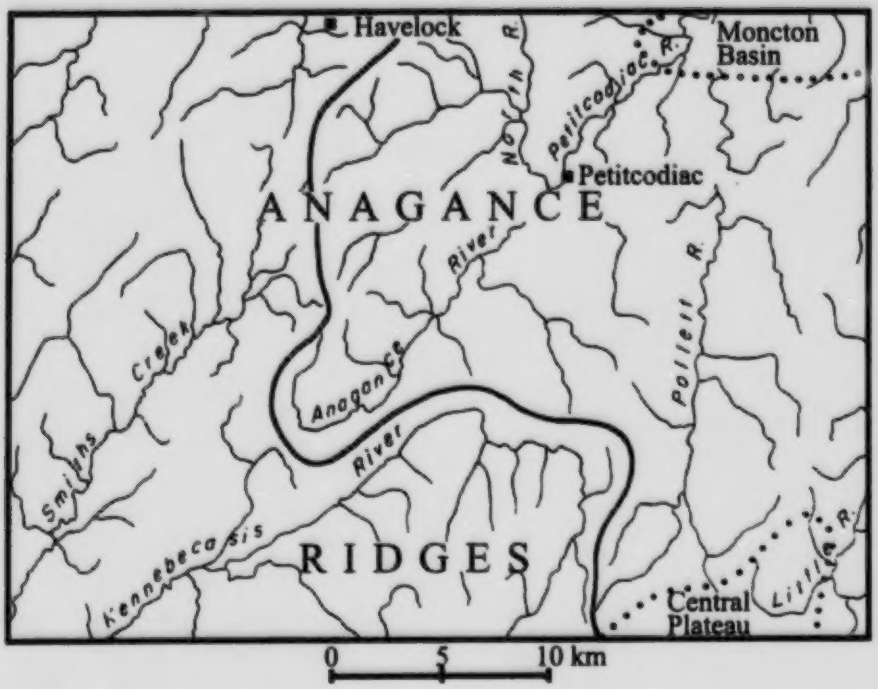

physiographic boundary

drainage basin boundary

Saint John River drainage basin to the west
Petitcodiac River drainage basin to the east

Figure 1.5: Physiography and drainage of the Petitcodiac area (after Seaman, 1987)

The study area can be further subdivided based on its geology and geo–morphology into three units; the Central Plateau, Moncton Basin, and Anagance Ridges (Figure. 1.5). The Anagance Ridges constitute the largest portion of the map area, and it is characterised by northeast-southwest ridge and valley topography (Rampton and Paradis, 1981). Major topographical features parallel local structural trends with relief ranging from 100 to 200 m at elevations of about 20 to 300 m. In the northeast, the map sheet encompasses a small part of the Moncton Basin. The basin's gently undulating surface lies below an elevation of 75 m. In the eastern region of the Petitcodiac map area, a small portion of the Central Plateau gently slopes toward the southwest. On the plateau, relief is typically 30 to 90 m and the elevation ranges from 160 to 325 m.

1.5. Drainage

The regional drainage system can be characterised as a trellis drainage pattern, reflecting the underlying bedrock structure and geology (Rampton and Paradis, 1981). The regional drainage network follows valleys that are deeply incised into bedrock. Along valleys, modern drainage channels have eroded into glaciofluvial and glaciolacustrine sediments. The eroded sediment is presently being redeposited as modern fluvial sediments by the larger rivers. Outside of the valleys and basins, surface drainage flows through a veneer of till and colluvial sediments overlying bedrock.

The field area straddles two major drainage basins (Figure 1.5). Within the western half of the map area, the Saint John River basin drains toward the southwest into the Bay of Fundy. Rivers in the eastern half of the map area flow northeastward into the Petitcodiac River system. Drainage is generally good in both of the basins.

In the Saint John River drainage basin (Figure 1.5), the Kennebecasis River and a tributary, Smiths Creek, follow the regional southwestward structural and topographic trend. Tributaries run perpendicular to the regional structural trend, cutting across the dividing ridges. In the Petitcodiac River drainage basin (Figure 1.5), the main tributaries emptying into the Petitcodiac River are the Little, Pollett, Anagance, and North rivers. Throughout the map area, the major rivers tend to occupy U-shaped valleys, indicating they have been glacially scoured at some point in the past. Moving westward across the study area, the valleys gradually change from being relatively deeply incised with most of the glaciofluvial material being plastered along the valley as kames and kame terraces, into valleys that are very broad and filled with large amounts of glaciofluvial outwash material. One notable exception to the general northeast-southwest orientation of the regional valley system is the Pollett River valley, oriented north-south perpendicular to the local bedrock stratigraphy.

CHAPTER 2

PRINCIPLES OF DRIFT PROSPECTING IN GLACIATED TERRAINS

2.1. Glacial Transport and Deposition of Debris

Until recently, glacial-overburden has largely been viewed as a hindrance to exploration programs in Canada. It is estimated that 97% of Canada has been glaciated at some point during the Quaternary Period (Nichol and Bjorklund, 1973). Until the early 1980s, traditional exploration programs primarily used geophysics and bedrock mapping to locate mineral deposits. This situation has recently changed in response to fluctuations in the global market, which have rendered many of the known deposits economically unfeasible. Consequently, till clast dispersal and geochemical exploration techniques, being relatively inexpensive (Broster and Huntley, 1995), have been steadily gaining recognition by the private sector.

To effectively conduct an overburden sampling program in glaciated terrain, the project geologist must acquire a good understanding of the glacial history of the region. Many drift prospecting programs have failed to identify the sources of geochemical anomalies and boulder trains in glaciated sediments because the glacial history and the mechanics of ice flow in the region were poorly understood. The dynamic ice-flow mechanics found at the base of the glacier can result in dramatic changes in the modes of entrainment and deposition of glacial debris, even on a local scale. These changes in glacial flow mechanics affect the composition of the deposited sediments. Thus, ground reconnaissance by a competent geologist is important.

Till composition, like many glacial and modern (derived) water-laid sediments, is closely related to its bedrock source (Dreimanis, 1976). According to Shilts (1976, p. 222), "... all Quaternary and modern sediments in glaciated areas can be regarded as derivatives of bedrock." He proposed that till is a "first derivative" sediment because it is derived from bedrock through the glacial comminution process and deposited directly by the ice. Thus, geochemical and clast dispersal patterns found in till reflect the directions of ice movement, often providing a clear indication of ice-flow direction.

Portions of the glacial load can undergo fluvial transport and sorting. Such sediments are termed "second derivative" sediments and include eskers, kames and proglacial outwash (Shilts, 1976, 1993). These sediments are often originally deposited as till, which has subsequently been eroded by subglacial and proglacial meltwaters that redistribute the silt and clay-sized particles throughout the glaciofluvial system.

Silt and clay that was flushed through the glaciofluvial system and deposited as glaciomarine and glaciolacustrine sediments are termed "third derivative" sediments (Shilts, 1976, 1993). These sediments have a complex transportation history, having been eroded from large areas of bedrock by glacial ice or subglacial meltwater. They subsequently undergo fluvial, and lacustrine or marine transportation, resulting in a high degree of fluvial mixing and sorting.

Both secondary and tertiary sediments are generally derived from much larger regions than primary sediments, which tend to reflect the local bedrock lithologies (Shilts, 1976, 1993). For this reason, overburden sampling programs conducted in glaciated terrains using secondary and tertiary sediments have lower success rates. Thus,

only primary sediments (in this case ablation and basal till) were collected during this study.

2.2. Till Texture

2.2.1. Till Stratigraphy

Textural differences among glacial deposits can prove useful for evaluating the regional till stratigraphy (Dreimanis and Fenton, 1976; Broster and Dreimanis, 1981; Szabo and Angle, 1983). Changes in the glacigenic modes of entrainment and transport, associated with oscillating periods of glaciation and deglaciation, produce distinctly different degrees of homogenisation and stratification of geochemical and textural attributes within each corresponding till unit (Gilberg, 1977; Broster, 1986). The differences in basal ice environments associated with each period of glaciation are reflected in the texture of its sediments. Thus, the textural differences may provide a "fingerprint" for identifying till units. Recognition of stratigraphically different till units is extremely important when sampling in areas that have experienced multiple ice-flow events with very different flow directions. Failure to consistently sample within the same stratigraphic till unit can distort glacial clast and geochemical dispersal trains.

2.2.2. Textural Evolution

The recognition of the bimodal distribution of lithic components in till has aided the understanding of the distribution of minerals in glacial deposits. According to Dreimanis and Vagners (1969, 1971), sediments that have been transported by glacial ice tend to break down into at least two grain size "modes". The clast-sized mode is the fraction of the till that is coarser than 2.5 cm (this changes depending on the source material) and is related to proximal bedrock sources. During glacial transport of bedrock

clasts, comminution gradually reduces their particle size to the finer matrix-sized mode of till (Dreimanis and Vagners, 1969, 1971). Therefore, the fine fraction (<1–2mm) of the till matrix usually reflects the composition of distal bedrock sources.

2.2.3. Mineral Terminal Grades

The texture of the matrix (portion of till <2 mm) is defined by the terminal grades of the mineral constituents in the source rocks. Dreimanis and Vagners (1969, 1971) suggested that a mineral's terminal grade represents the maximum degree of particle-size reduction without degrading its inherent crystal structure or chemical composition. The characteristics of a mineral's terminal grade are a function of factors such as its original size(s) and shape(s) in the source rock, as well as the mineral's resistance to comminution during glacial transport (Driemanis and Vagners, 1969, 1971). Generally, the coarsest terminal grades fall in the sand (63–500 μm) and coarse silt (16–63 μm) regimes and are commonly derived from igneous and metamorphic minerals (Dreimanis and Vagners, 1969, 1971). Conversely, the finer portions of the till matrix are dominated by the mineralogy of sedimentary rocks with low quartz content. The fine portion of the till matrix is commonly defined as the medium to fine silt (4–16 μm) and clay (<4 μm) particle sizes (Dreimanis, 1976).

2.2.4. Chemical Partitioning of the Till Matrix

The wide range in the hardness of mineral grains in till produces a "rudimentary" partitioning of metals and minerals among particular grain sizes (Bolviken and Gleeson, 1979; Shilts, 1984, 1993, 1995; Dilabio, 1988; Coker and DiLabio, 1989). Coarser fragments (sand to coarse silt-sized particles) tend to be enriched in lithophile trace elements because their "host" minerals generally exhibit a relatively high resistivity

to abrasion and weathering. On the other hand, chalcophile trace elements are usually associated with minerals that are more susceptible to weathering and abrasion; therefore they tend to be enriched in the clay fractions in the till.

The chemical properties of the minerals are also important in the elemental partitioning among grain size fractions (Bolviken and Gleeson, 1979; Shilts, 1984, 1993, 1995; DiLabio, 1988; Coker and DiLabio, 1989; Berrow and Mitchell, 1991). Minerals whose terminal grain size falls in the clay fraction are generally capable of adsorbing or absorbing cations. Thus, cations that are liberated from rock debris during glacial communition and weathering processes tend to become adsorbed or absorbed by clay-sized particles in till, causing "secondary" enrichment in the cation content of the clay fraction (Bolviken and Gleeson, 1979; Shilts, 1984, 1993, 1995, Dilabio, 1988; Coker and DiLabio, 1989; Berrow and Mitchell, 1991). Given the possibility of secondary enrichment of cations in the till, it is important to measure the clay content of the matrix when comparing the geochemical data for mobile cations obtained from different sample sites.

Post-depositional weathering reduces many chalcophile and ferromagnesian minerals to clay-sized particles, further enriching the fine fraction of the till in cations (Bolviken and Gleeson, 1979; Shilts, 1984, 1993, 1995; DiLabio, 1988; Coker and DiLabio, 1989). Following deposition, tills are often weathered to depths greater than 2 m, making it difficult to obtain an unweathered sample. Therefore, the contribution of chalcophile and ferromagnesian minerals to the geochemical signature of a weathered till sample may be an important consideration for some drift prospecting projects.

2.3. Soil Processes

Soil is defined by pedologists as the "naturally" occurring, unconsolidated, mineral or organic material at the earth's surface that is capable of supporting plant growth and is at least 10cm thick (Kauranne et al., 1992). In the narrower sense of glacial geology, soil is considered to be the chemically differentiated upper layer of the overburden (Kauranne et al., 1992). Soil formation is controlled by several variables including climate, biological activity, porosity/composition of the parent material, topography, water content and time, which determine the type and depth of the soil (Agriculture Canada Expert Committee on Soil Survey, 1987; Kauranne et al., 1992). In glaciated regions the depth of the soil profile is limited by the short time since glaciation (<10 000 years), and the cool climate. In Canada, podzols and tundra soils are the most common soil types (Kauranne et al., 1992).

For the purposes of soil sampling, there are three horizons of interest in New Brunswick (Agriculture Canada Expert Committee on Soil Survey, 1987)(Figure 2.1). The A-horizon is commonly grey and heavily leached. This horizon is typically thin (1–10 cm) and is depleted in water-soluble elements and compounds. Below the A-horizon, a "zone of accumulation" referred to as the B-horizon forms where most of the mobile components leached out of the A-horizon precipitate. The transition from the A-horizon to the B-horizon is marked by a change in colour and texture. The B-horizon is generally red, reflecting its enriched iron oxide content, and has a silty texture. The thickness of the B-horizon is variable, but in New Brunswick it is generally 15 to 30 cm. At the base of the profile unweathered parent material may be found in a C-horizon and is generally the preferred sampling medium for till provenance studies.

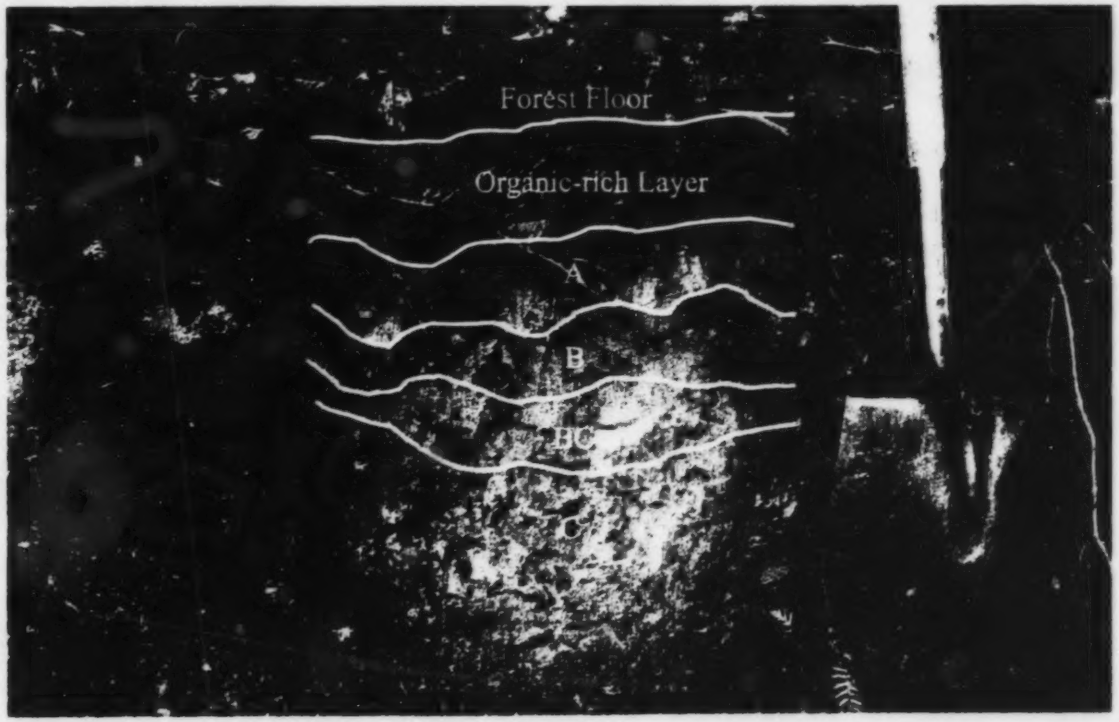

Horizons:

A: The leached zone.

B: Zone of Accumulation.

BC: Transition Zone

C: Unweathered parent material.

Figure 2.1: A typical soil profile in southeastern New Brunswick.
(photo taken in the Petitcodiac map area).

As weathering of the parent material progresses, horizontal layering develops through leaching and precipitation (Agriculture Canada Expert Committee on Soil Survey, 1987). Weathering produces post-depositional geochemical dispersion in the soil profiles of glacial deposits. There are three main mechanisms by which secondary dispersion can occur; 1) hydromorphic 2) electrochemical and 3) gaseous (Bolviken and Gleeson, 1979). Ultimately, the post-depositional change toward a more oxidising Eh/pH environment drives *in situ* geochemical dispersion in the overburden above the water table. In other words, mineral phases that are unstable in the oxidising conditions found in the upper part of the soil horizon are most susceptible to weathering.

Drainage is another important factor when determining the extent weathering has affected the partitioning of elements within the profile. Typically, poor drainage results in increased weathering rates that, in turn, can release several elements such as Co, Cr, Ni, V, and Zn from the coarse and fine sands. This can produce a corresponding enrichment of these elements in the silt and clay fractions. Most of the weathering and enrichment of the fine fractions occur *in situ*, producing no significant translocation of elements downward through the soil profile (Levinson, 1974).

CHAPTER 3

PREVIOUS WORK

3.1. Glacial Studies

3.1.1. Glacial History of Southeastern New Brunswick

During the late 1800s, numerous erosional markings were found on bedrock surfaces throughout the Atlantic Provinces, creating debate about their origin (Grant, 1977). Chalmers (1885) and Matthew (1872) pioneered surficial studies in New Brunswick. Matthew (1872, 1879) was the first to report on the geography of New Brunswick. Chalmers produced regional surficial maps for most of the province and was the first to postulate the development of a regional ice system consisting of local ice caps (Chalmers 1885, 1890, 1895, 1902). Chalmers' conclusion was based on erosional features that suggested divergent ice-flow patterns, which he interpreted as evidence supporting the presence of relatively small ice caps coexisting with a large external ice sheet. By mapping the erosional features, he was able to identify a strong southeast-trending ice-flow pattern for southern New Brunswick. However, the chronology of glacial flow events is still poorly understood, due in part to the absence of datable sediments and pre-late Wisconsinan glacial artefacts (Rampton et al., 1984).

In 1884 and 1885, Chalmers suggested the existence of small local ice caps on some of the plateaux in southeastern New Brunswick, including the Caledonian Highlands. He argued that the presence of highly weathered surficial deposits on the northern slopes of the Caledonian Highlands indicated the glaciers were not very erosive locally. From investigations of the erosional patterns on both sides of the Bay of Fundy,

Chalmers (1890) identified an ice source northeast of the Chignecto isthmus (Figure 1.2). He proposed that ice flowed from this ice source (the Escuminac) in a southwesterly direction across the Caledonian Highlands and into New Brunswick during the Late Wisconsinan. He also suggested a minor outflow of ice radiating from a remnant ice cap on the Caledonian Highlands (Chalmers, 1890), but the timing of this event is still debated (e.g. Rampton et al., 1984; Foisy and Prichonnet, 1991).

Rampton et al. (1984) divided the Late Wisconsinan glacial history of New Brunswick into five ice-flow "phases" based on the relative strengths of local ice domes. The five consecutive phases are 1) Chignecto; 2) Bantalor; 3) Millville/ Dungarvon; 4) Plaster Rock; and 5) Chaleur phases. The chronology of the phases was based primarily on cross-cutting striae relationships. Furthermore, the timing of each phase was loosely constrained using radiometric-dating techniques on organics found within glacial deposits (Rampton et al., 1984).

The Chignecto phase marked the growth and retreat of the Escuminac Ice Centre, located just north of Prince Edward Island (Rampton et al., 1984). As the ice centre expanded, ice advanced; 1) down into Chignecto Bay (Figure 1.2) past Alma, and across the Chignecto isthmus, and 2) up across the Acadian Peninsula (Rampton et al., 1984). During the growth of the Escuminac Ice Centre, its ice flow was diverted around the Caledonian Highlands (Rampton et al., 1984), indicating that the ice flow was topographically controlled.

A complex interaction between eastward-flowing and northward-flowing ice is suggested by the clast dispersion from a diabase dyke running the length of the Acadian Peninsula and the position of interlobate moraines, indicating that a second ice centre was

active during the Chignecto phase (Rampton et al., 1984). Additional evidence of interfingering between the two ice centres may be recorded by ice-flow erosional indicators and in a till unit at Stoney Creek, located just northwest of Hillsborough (Foisy and Prichonnet, 1991). A change in the orientation of ice-flow erosion indicators, and the intermediate composition of the till was interpreted as evidence of the confluence between southeastward-flowing and southwestward-flowing ice masses in the Stoney Creek area (Rampton et al., 1984; Foisy and Prichonnet, 1991).

According to Rampton et al. (1984), the southwest-flowing ice at Stoney Creek originated from the Escuminac Ice Centre. He proposed that the southeastward-flowing ice mass was flowing from an ice centre located in the interior of New Brunswick, which he named the Gaspereau Ice Centre. It is likely that ice from the Gaspereau Ice Centre flowed southeastward across the southwestern end of the Caledonian Highlands during the Chignecto phase.

Evidence of Escuminac ice in the Fundy region is provided by deltas formed during deglaciation where meltwater channels reached the sea near St. Martins and Chignecto Bay (Rampton et al., 1984; Foisy and Prichonnet, 1991). The Chignecto phase is assigned to the early Late Wisconsinan in the range of 15 to 18 ka. based on radiocarbon dating of whalebone found in marine clays post-dating the Chignecto phase (Rampton et al., 1984).

Following the conclusion of the Chignecto phase, the Gaspereau Ice Centre expanded over most of southeastern New Brunswick during the Bantalor phase (Rampton et al., 1984). As the influence of the Gaspereau ice centre increased in the Saint John area, the direction of ice flow gradually rotated counter-clockwise toward a more south-

southeastward direction. The glacial maximum during the Bantalor phase occurred between approximately 13.5 to 13.3 ka. (Rampton et al., 1984).

The end of the Bantalor phase marked the disintegration of several ice centres in New Brunswick, leaving active residual ice caps throughout the province (Rampton et al., 1984). Foisy and Prichonnet (1991) suggest that during deglaciation a residual ice cap occupied the Caledonian Highlands, contradicting an earlier interpretation by Rampton et al. (1984) that the Caledonian Highlands remained unglaciated throughout the Late Wisconsinan. It is believed that southeastern New Brunswick was essentially ice-free at the conclusion of the Bantalor phase (Rampton et al., 1984). The disintegration of active ice caps in New Brunswick is believed to have concluded by approximately 12 ka. (Rampton et al., 1984).

3.1.2. Glacial Studies in the Petitcodiac Map Area

The absence of datable sediments and the insufficient number of stratigraphic exposures have limited surficial studies in the Petitcodiac map sheet area (NTS 21/14). Brief descriptions of the local soils and surficial geology are found in soil survey report for southeastern New Brunswick (Aalund and Wicklund, 1950). Additional information is found in regional mapping projects of the surficial geology in New Brunswick (Chalmers, 1890; Rampton et al., 1984), and in compilation of all published striae data for New Brunswick (Seaman, 1989).

In southeastern New Brunswick, the regional ice-flow direction during the Late Wisconsinan ranged between south-southwest and southeast (Rampton et al., 1984; Munn, 1995; Munn et al., 1996). Within the Petitcodiac map area, similar ice-flow directions have been documented (Chalmers, 1890, Rampton et. al., 1984, Seaman 1987;

1991). However, in the eastern part of the map area, Chalmers (1890) described striae and grooves that indicate northeastward ice flow. His observations were refuted by Rampton et al. (1984), but have since gained support from discovery of similar striae orientations in the Hillsborough area, located immediately east of the Petitcodiac map area (Foisy and Prichonnet, 1991).

Hamilton and Carroll (1975) described aggregate resources in the Petitcodiac map area in their preliminary report. Further aggregate mapping by Seaman (1987) revealed that the ice movement was generally southward in the western half of the Petitcodiac map area. This interpretation is supported by north-south trending eskers, as well as ice-contact stratified drift and morainic material plastered against the north side of bedrock obstacles. However, he did not encounter any ice-flow erosional indicators, such as rat-tails and striae, to confirm his interpretation. Seaman (1987) further suggested that extensive morainic and ice-contact deposits along the sides of the Kennebecasis River valley record the positions of ice margins that were relatively stable for a long time.

The presence of a till-like unit found overlying clean, deltaic gravel at Five Points (Figure 1.4) was interpreted by Seaman (1987) as a local glacial re-advance into the Kennebecasis River valley. Unfortunately, the gravel has since been excavated, preventing further investigation of the site. The till-like unit was reportedly overlain by two units, 1) a massively structured sand and gravel, 0.9 to 1.8 m thick, and 2) an immature ablation-like unit containing abundant soft sandstone clasts (Seaman, 1987). Further evidence of glacial re-advance was found by Seaman (1987) near Cornhill (Figure 1.4), where a deltaic sequence and an esker segment are both overlain by till.

3.2. Geologic Setting

3.2.1. Bedrock Geology

Geologic contacts are not well constrained due to poor bedrock exposure throughout most of the Petitcodiac map area. Mapped bedrock units range from Precambrian to Upper Carboniferous in age, but Carboniferous marine and non-marine sedimentary rock underlie most of the study region (Figure 3.1).

Igneous units and lesser amounts of sedimentary strata outcrop in the southeastern part of the map area, forming the Caledonia Zone (Figures 1.2 and 3.1). These consist of a variety of folded and faulted Precambrian felsic and mafic volcanic units with interbedded sedimentary rocks, which are intruded by Cambrian granitic, granodioritic, dioritic, and gabbroic rocks. Similar rock units are also found in the western half of the map area at Jordan Mountain, where Cambrian basement rock is exposed (Figure 3.1).

Most of the Carboniferous sedimentary strata are relatively undeformed, with the more resistant units forming ridges (Figure 3.1). Regional contacts trend northeast-southwest. The strata consist primarily of shale, sandstone, and conglomerate that are Lower Carboniferous to Upper Carboniferous in age. Less significant amounts of Carboniferous clastic sedimentary rocks comprised of limestone and gypsum are found principally in the Havelock area (Figure.3.1), but also occur in narrow bands scattered throughout the map area.

3.2.2.Tectonostatigraphic History of the Petitcodiac Map Area

Carboniferous sedimentary rocks of the Petitcodiac area are situated in the Moncton Subbasin, which is part of the Late Paleozoic Maritimes Basin (Williams, 1974). The Moncton Subbasin is approximately 30 km wide, 150 km long, and up to 5 to

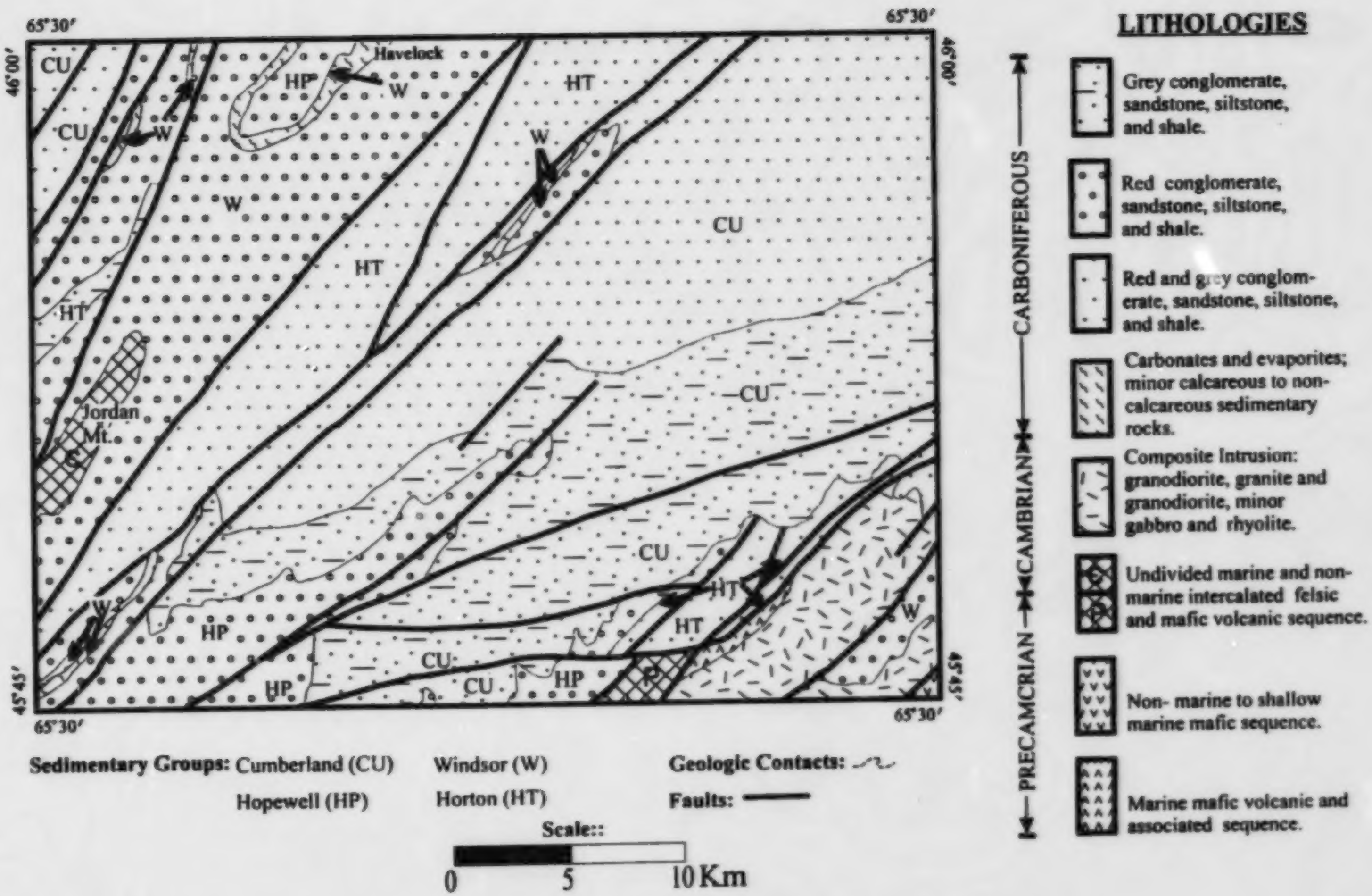

Figure 3.1: Geologic Map of the Petitcodiac Area (modified from McLeod et al., 1994).

6 km deep (St. Peter, 1992). In the Petitcodiac map area the Carboniferous sedimentary units were deposited over Precambrian and Lower Paleozoic deformed crystalline rocks of the Avalon Terrane during three main depositional events in an arid or semi-arid environment (St. Peter, 1992).

The oldest depositional sequence comprises the Horton Group (Figure 3.1) and consists of three conformable formations ranging in total from 3 to 5 km in thickness (St. Peter, 1992). Deposition of sediments occurred in response to the fault-controlled or thermal-related subsidence occurring in the subbasin. An angular unconformity exists at the base of the sequence where it directly overlies the Avalon Terrane (St. Peter, 1992).

Following a period of tectonic quiescence, renewed subsidence resulted in the deposition of the Windsor Group (Figure 3.1) during the Middle Viséan (St. Peter, 1992). Local crustal sagging led to the inundation by the Windsor Sea into the subbasin. Rapid subsidence followed, impounding the sea and producing evaporite deposits associated with the Windsor Group. A shift from local down-flexing or sagging of the subbasin to fault-controlled subsidence occurred during late Windsor time, which continued into Hopewell time, allowing for the deposition of the Hopewell Group (Figure 3.1). Gentle tilting with no significant folding of the Windsor and Hopewell beds occurred by the Namurian. Uplift produced a "pre-Cumberland" angular unconformity and erosion of the Windsor/Hopewell sediments (St. Peter, 1992).

By the late Namurian or early Westphalian, crustal downwarping led to thermal subsidence of the lithosphere (Bradley, 1982), which resulted in the deposition of the Cumberland Group (Figure 3.1). These sediments were transported from a distal southwesterly source by northeast-flowing highly sinuous rivers. The gentle-

macroscopic folding responsible for the Havelock syncline is associated with this final stage of tectonism (St. Peter, 1992).

3.2.3. Mineral Occurrences

The majority of the mineral exploration was conducted in the 1970s and 80s. Presently there are no base metal deposits of economic interest found locally, but there is an active limestone quarry located at Havelock containing sub-economic gypsum occurrences. More recent work by St. Peter (1992) has suggested that cupriferous deposits in the Carboniferous strata may be genetically related to faults in the southeastern section of the Moncton Subbasin.

Glacial dispersal of material from mineral occurrences may provide valuable information about the direction of glacial flow. There are eight areas of known base metal mineralisation in the study area (Figure 3.2) that may be useful as "point sources" for glacial dispersal.

In the Jordan Mountain area (Figure 3.2, Site 1) a base metal occurrence associated with a shear zone in a massive rhyolite host rock contains chalcocite, malachite, silver and gold (Rose and Johnson, 1990; Merlini, 1998). The shear zone ranges from 3 to 4 m wide and is approximately 210 m long. Mineralisation is disseminated in the rhyolite host rock and is concentrated along irregular seams. A second occurrence (Figure 3.2, Site 2) at Jordan Mountain contains manganite intergrown with pyrolusite and reduced amounts of hausmannite and psilomelane (Rose and Johnson, 1990; Merlini, 1998). This near-surface mineralisation is found in massive lenses, blebs and stringers in the cement of a Lower Carboniferous Hillsborough Formation conglomerate unit.

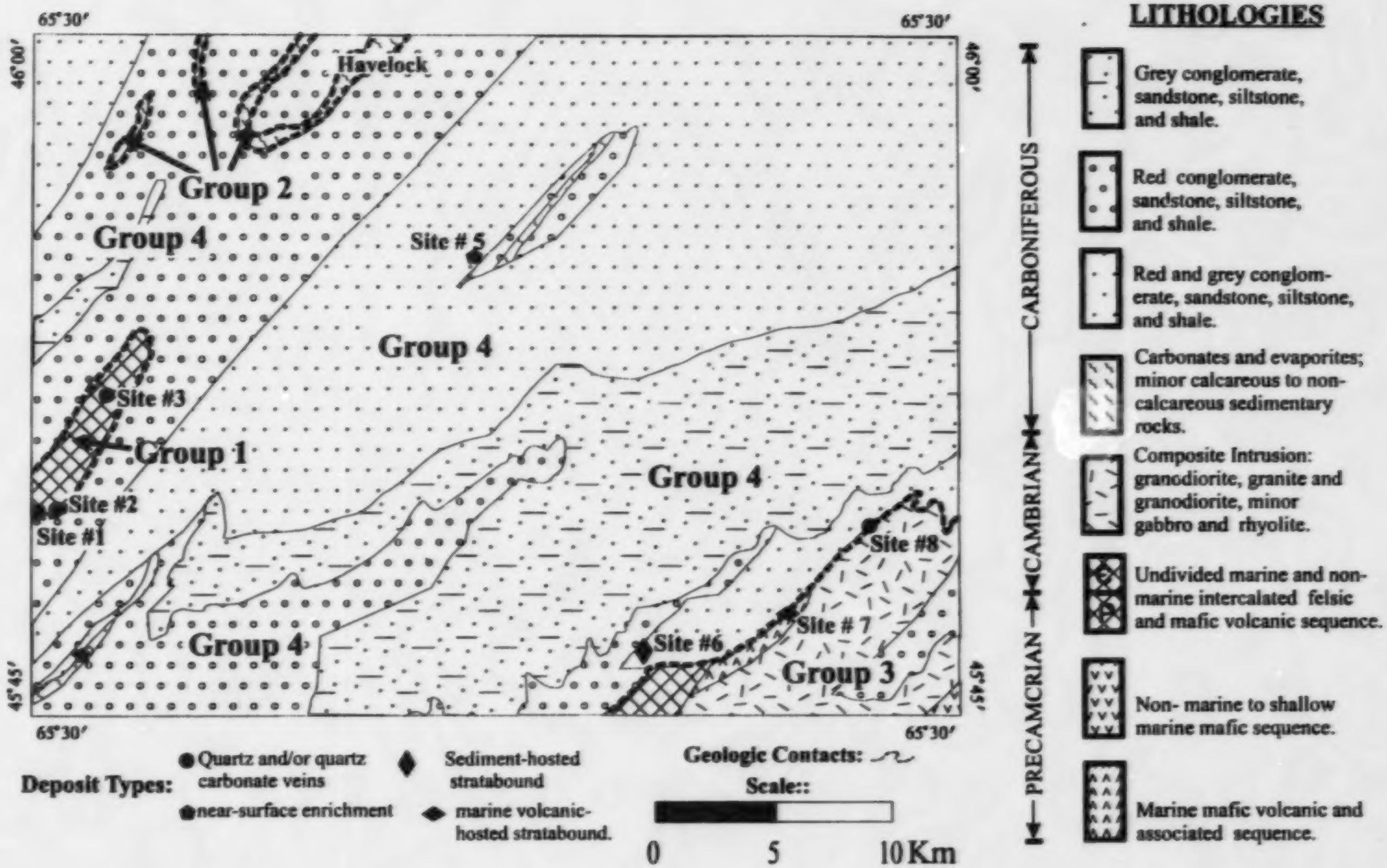

Figure 3.2: Mineral occurrences and main bedrock "groups" useful for till provenance studies (bedrock geology after McLeod et al., 1994): group 1 is synonymous with Jordon Mountain and group 3 is synonymous with the Caledonia Zone.

Approximately 4 km northeast of Jordan Mountain at Windgap Brook (Figure 3.2, Site 3) lenticular quartz veins containing sulphides and gold, cut a dark grey quartzose slate (Rose and Johnson, 1990; Merlini, 1998). The mineralised zone is 10 m wide and 23 m long.

South of Jordan Mountain at Smiths Creek (Figure 3.2, Site 4), disseminated chalcocite and malachite occur in the matrix of a grey conglomerate (Rose and Johnson, 1990; Merlini, 1998). The mineralised zone is less than 30 cm thick. Red sandstone, red conglomerate, and Windsor Group limestone overlie the grey conglomerate. A similar zone of mineralisation is found near Hillgrove (Figure 3.2, Site 5) (Rose and Johnson, 1990; Merlini, 1998).

Near Goshen (Figure 3.2, Site 6), primary and secondary minerals occur in a fanglomerate matrix, as coatings on the pebbles, and as infillings of fractures and cavities (Rose and Johnson, 1990; Merlini, 1998). Additional smaller occurrences are found locally. These shallow sub-economic occurrences contain manganese-oxides, covellite, chalcopyrite, malachite, azurite, copper, and silver (Rose and Johnson, 1990; Merlini, 1998).

In the Precambrian Coldbrook Group, the felsic tuffs near Elgin (Figure 3.2, Site 7) contain lenses of quartz and carbonate, hosting disseminated zinc and copper sulphides along with traces of gold (Rose and Johnson, 1990; Merlini, 1998). In some places the lenses occur in intensely drag-folded schistose zones (Rose and Johnson, 1990; Merlini, 1998).

At Gowland Mountain (Figure 3.2, Site 8) a large tabular body of fault breccia, striking at 068°, is composed of felsic rock cemented by manganese oxides (Rose and

Johnson, 1990; Merlini, 1998). The fault breccia contains massive botryoidal psilomelane, braunite, as well as crystals and needles of manganite in vugs with barite. The mineralised zone dips at 80° northeast averaging 1 m in width for approximately 60 m (Rose and Johnson, 1990; Merlini, 1998).

CHAPTER 4

METHODOLOGY

4.1. Field Methods

The New Brunswick Department of Natural Resources and Energy (DNRE.) undertook regional overburden sampling in the Petitcodiac area in the last two weeks of the summer field season of 1993. Sampling was conducted under the supervision of Toon Pronk, a Quaternary Geologist with the Minerals branch. In 1997, the author became involved with the project and field sampling was completed during the summer. In 1998, the author conducted surficial mapping in co-operation with the Department of Natural Resources and Energy Branch.

Overburden sampling of the Petitcodiac map area (NTS 21/H14) was completed on a 2-km grid based on the UTM gridlines (Figure 1.3). A total of 274 samples, including four field duplicates, were collected from hand-dug pits, road cuts, and natural exposures (Appendix I). The field duplicates were taken from four sample sites to evaluate the precision of the sampling procedure (Appendix II). Sample pits were generally 0.5 m in diameter and were dug to a depth sufficient to penetrate well into the C-horizon. Pit depths ranged from 0.4 to 1.0 m and the soil profile was logged. The soil profile, as well as the local topography and vegetation were recorded in accordance to the standard forestry site classification card (Zelazny et al., 1989). Additional information about the local drainage at each sample site and the till texture and consistency is found in Appendix III.

Between 50 to 100 clasts were collected from the C- horizon from each sample pit. These clasts typically ranged from 2 cm to 10 cm in diameter, but fragments broken off larger clasts with a rock hammer were taken to avoid sampling bias. Samples from the C-horizon of the till matrix were collected for geochemical analysis and archiving purposes. At each site, an additional sample of till matrix was taken from the B-horizon for future use in land use applications and research. Approximately 2 L and 1 L of matrix was taken from the B and C-horizons respectively. Basal till was the preferred sampling medium; however, ablation till was sampled where basal till could not be found within a 500 m radius of the sample site. Basal and ablation till were distinguished based on the criteria outlined in Dreimanis (1976).

Bedrock exposures encountered during the till sampling were inspected for directional ice-flow indicators. A suite of hand samples representing the "unique" bedrock units was collected to aid in clast provenance studies. Finally, the distribution and type of ice-contact glaciofluvial deposits were examined to evaluate the late stage basal ice conditions.

4.2. Laboratory Methods

Approximately 50 to 100 clasts were examined from each of the 270 sites. The clasts collected from the C-horizon of till were first identified in hand specimen. Clast identification was conducted on an unweathered surface using a hand lens. Questionable specimens, along with the "representative suite" of hand samples collected from the local bedrock units, were sent to the University of New Brunswick (Fredericton campus) thin section lab. Unpolished thin sections were prepared, permitting a more detailed

examination of the clast under an optical microscope. The thin sections obtained from the clasts were then compared to the thin sections obtained from the "representative suite" to aid in the identification of the clast's bedrock origin. The relative proportions of indicator lithologies were then recorded for each site (Appendix IV).

The matrix of each field sample was dry sieved by Rex Bolden and the author to obtain approximately 30 g for each of the minus 2 mm and minus 63 μm grain size fractions. For the C-horizon samples, geochemical analysis of the minus 63 μm fraction collected from the till matrix was performed by Activation Laboratories Limited (ACTLABS) for 48 base metal, trace, and rare earth elements (Appendix V: Part A). Stream sediment standards and sample splits were included with the sample suite to evaluate the precision and accuracy of the geochemical analysis.

Precisely 100 g of minus 2 mm till matrix from each sample were used for granulometric analysis. The relative proportions of sand, silt, and clay in the sample were determined according to the modified hydrometer method (Bouyoucos, 1962).

4.3. Statistical Methods

Lithological and elemental geochemical concentrations were contoured using Surfer® 6.01 computer software. Because the data was irregularly spaced, a kriging geostatistical treatment of the data was performed in Surfer® 6.01 to extrapolate unbiased contours between data points. Additional geochemical contour plots not presented in the body of the thesis can be found in Appendix V (Part B).

A non-parametric Spearman's rank correlation analysis was performed using the Statistical Package for Social Sciences (SPSS8.0 for Windows®) to examine covariance among granulometric, lithological, and geochemical data (Appendix VI).

CHAPTER 5

RESULTS AND INTERPRETATIONS

5.1. Till Characteristics

Till blankets most of the bedrock the Petitcodiac area. Basal till (sensu stricto, Dreimanis, 1976) was the most common glacial sediment encountered and was the preferred sample medium. However, at sample locations where basal till was not available, ablation till was collected for analysis. In southern New Brunswick, ablation till is commonly derived from local sources resulting in a geochemical signature similar to that of basal till (Seaman, 1992; Stumpf, 1995). Lithophile and rare earth element concentrations have been found to be slightly elevated in ablation till, but still exhibit dispersal patterns similar to those found in basal till.

Only one stratigraphic unit of till was observed during fieldwork. The average thickness of till ranged from 0.5 m to 2 m and was found to be highly variable in colour, texture, and its degree of compactness. The degree of till compactness was independent of the sample location or topographical position. However, till compaction, texture, and colour were closely related to the parent material.

Podzolic soils (senso stricto, Agriculture Canada, 1987) were encountered at most sample locations. The A-horizon is usually thin, ranging from 1 to 15 cm. Below the A-horizon, in the B-horizon, colour varied from yellowish red to olive brown and thickness varied from 10 to 30 cm. At the bottom of the soil profile the C-horizon closely reflected the colour of the parent material. The C-horizon was typically much more compact and contained a higher abundance of fine particle grades.

5.2. Lithological Analysis

Representative suites of the major bedrock units in the study area were collected and thin sectioned for comparison with till clasts. For the purposes of till clast provenance studies, the bedrock units can be grouped into four main lithological units based on their composition and origin (Figure 3.2). Group 1 is located in the Jordan Mountain anticline and represents part of the Cambrian basement rock. The core of the anticline is mapped as Cambrian greywacke, felsic and green mafic volcanic units (McLeod et al., 1994). The limbs of the anticline consist of Silurian gabbro, diorite, and granodiorite rocks. Group 2 is composed of bedrock units identified by McLeod et al. (1994) as Lower Carboniferous limestone, gypsum, and anhydrite. The most significant occurrence of group 2 is located at the Havelock syncline, with multiple smaller units outcropping along faults. The third group encompasses the Caledonia tectonostratigraphic zone (sensu stricto, Rampton et al., 1984). This group consists of large composite intrusions of granite, granodiorite, diorite, and minor gabbro and rhyolite (McLeod et al., 1994). There are also marine felsic and mafic volcanics with associated sedimentary units found in group 3. Finally, group 4 contains Upper Carboniferous and Lower Carboniferous sedimentary units of red and grey mudstone, sandstone, and conglomerate (McLeod et al., 1994). This group is geographically the most extensive of the four groups.

At each of the 270 sample locations, till clasts were collected. The clast lithological data is presented in Appendix IV. Clast dispersal was examined by measuring the relative abundance (i.e. percentage) of seven main indicator lithologies at each sample site. The seven indicator lithologies are; felsic volcanic, mafic igneous,

felsic intrusive, metamorphosed igneous, quartz and quartzite, limestone/evaporite, and sedimentary clasts.

5.2.1. Felsic Volcanic Clasts

Felsic volcanic units are found in lithologic groups 1 and 3 (Figure 3.2). In the western half of the study area, felsic volcanic clasts typically have a porphyritic texture and range from greyish pink to pink in colour. Immature porphyritic felsic volcanics clasts were observed in a Windsor Group conglomerate outcrop near the base of Jordan Mountain (Figure 3.1) during fieldwork, indicating that they have undergone fluvial transport during the Lower Carboniferous. The displacement of these clasts during pre-glacial times may have offset many of the dispersal trains in the region making interpretation of felsic volcanic clast dispersal questionable. In thin section, they are very similar to the Cambrian felsic volcanics found at Jordan Mountain (group 1). High abundance of felsic volcanics occur in discontinuous ribbon-shaped anomalies elongated away from Jordan Mountain in directions trending from northeast, east, southeast, to due south over distances of up to 25 km (Figure 5.1).

In the southeast corner of the study area (group 3, Figure 3.2), felsic volcanic clasts are restricted to the till overlying the Caledonia Zone. The absence of felsic volcanic clasts in the till overlying the Moncton Subbasin (Figure 1.5) suggests that ice did not flow northward over felsic volcanic bedrock units found toward the south in the Caledonia Zone.

In the northwestern corner of the map area, felsic tuff erratics produce a dispersal train 15 km long, elongated southward (Figure 5.2). There are no mapped felsic tuff units

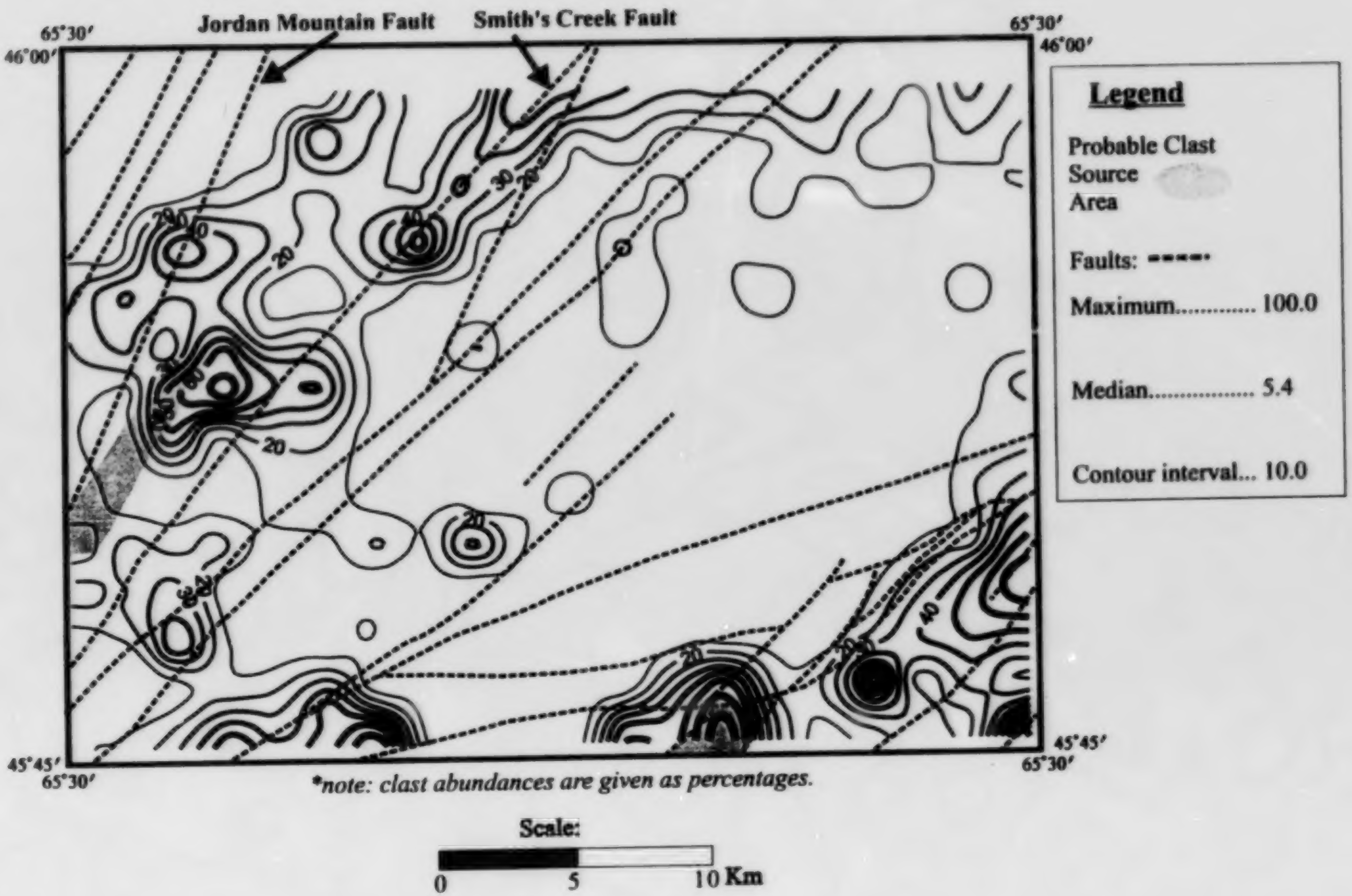

Figure 5.1: Contouring of felsic volcanic clast abundance in the till.

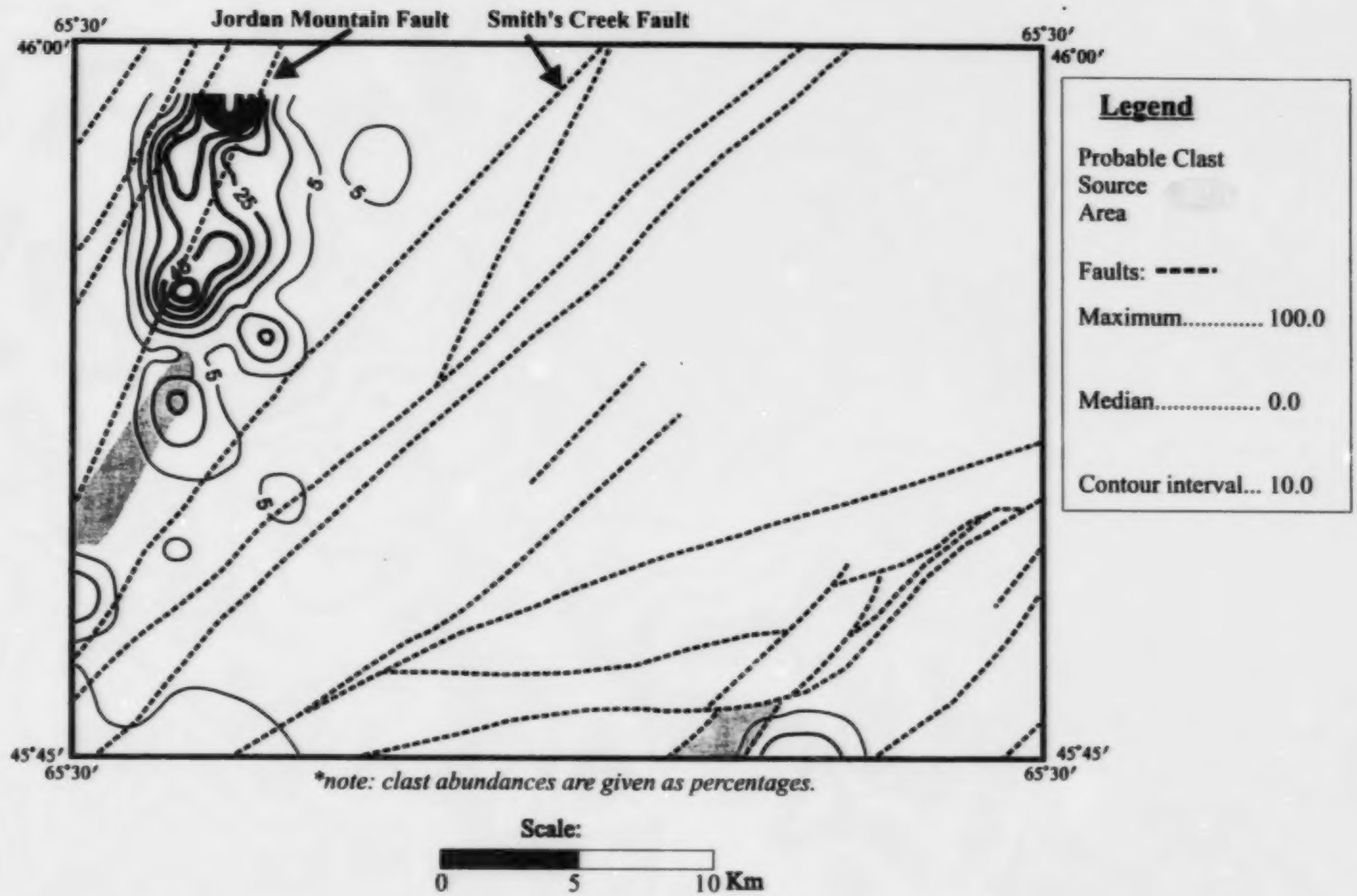

Figure 5.2: Contouring of felsic volcanic tuff clast abundance in the till.

in the immediate vicinity of the erratics, but the shape of their dispersal train suggests that a bedrock source is probably located north of the study area.

5.2.2. Mafic Igneous Clasts

Mafic volcanic bedrock units are found in three places: 1) in group 1 (Figure 3.2) at Jordan Mountain; 2) in group 3 in the Caledonia Zone; and 3) just outside of the northwestern vicinity of the study area. In the northwestern section of the map area, a high abundance of mafic extrusive clasts are present in the till. The tail of the dispersal train is fan-shaped and extends southward into the study area approximately 7 km. In the vicinity of the Caledonia Zone, few mafic volcanic clasts are observed in the till. Near Jordan Mountain, the clasts are found in the Anagance River valley (Figure 1.4), forming "bulls-eye" shaped patterns (Figure 5.3). Mafic intrusive clasts were also encountered in the till overlying Jordan Mountain, but do not appear to be significantly dispersed by glacial ice.

5.2.3. Felsic Intrusive Clasts

The felsic intrusive clasts ranged from granitic to dioritic in composition. The felsic intrusive bedrock units are geographically coincident with the three mafic volcanic sources (Figure 3.2), but granitic and granodiorite clasts are found more widely dispersed in the till (Figure 5.4). In the Jordan Mountain and Caledonia Zone (Figure 3.2), these clasts are restricted to the local till. In the north-central section of the map area, the till contains a high abundance of granite and granodiorite clasts, forming a large dispersal train extending approximately 15 km towards the southwest. In contrast, diorite clasts are not widely distributed in the till and exhibit no significant regional dispersal patterns.

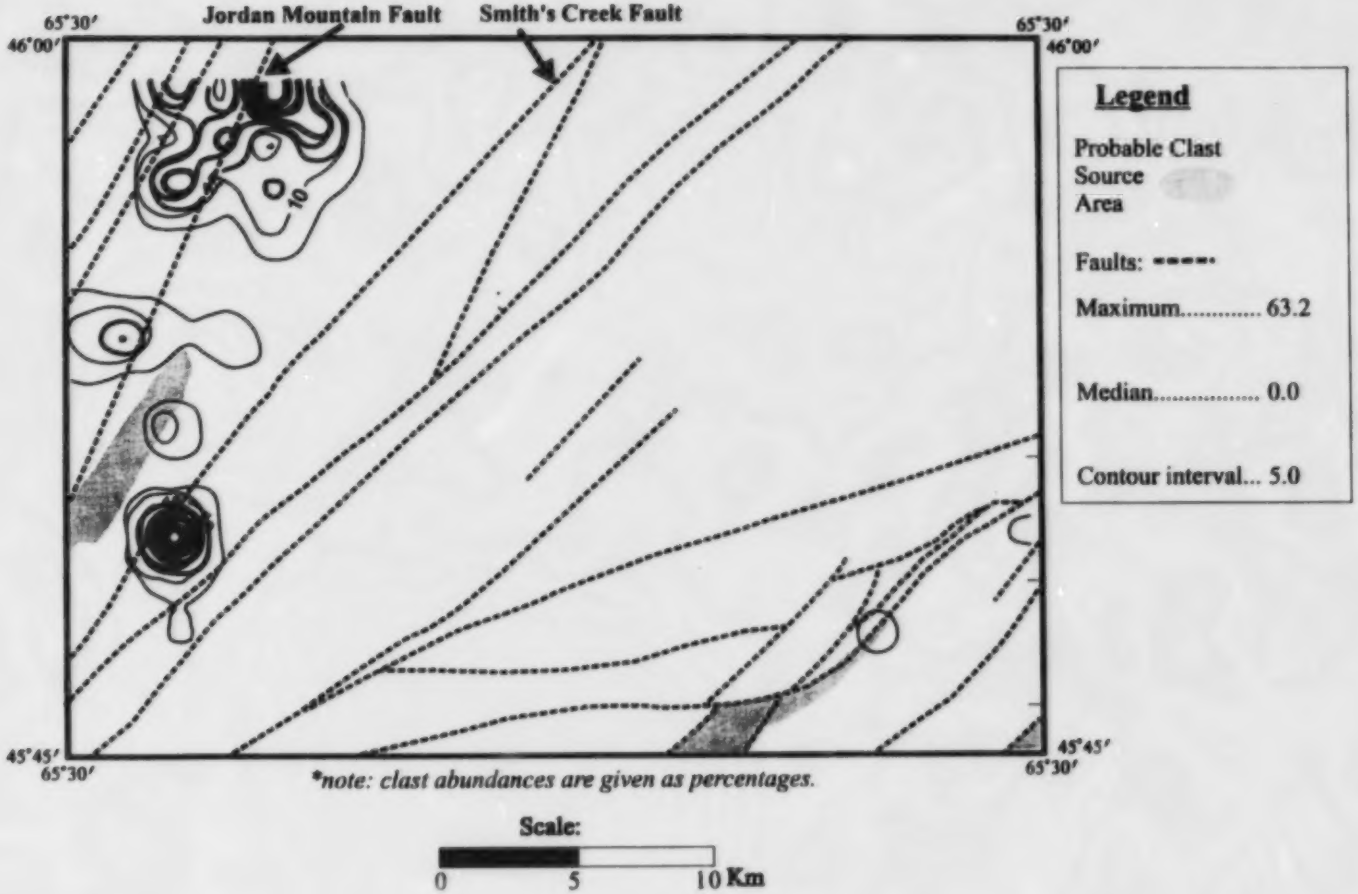

Figure 5.3: Contouring of mafic volcanic clast abundance in the till.

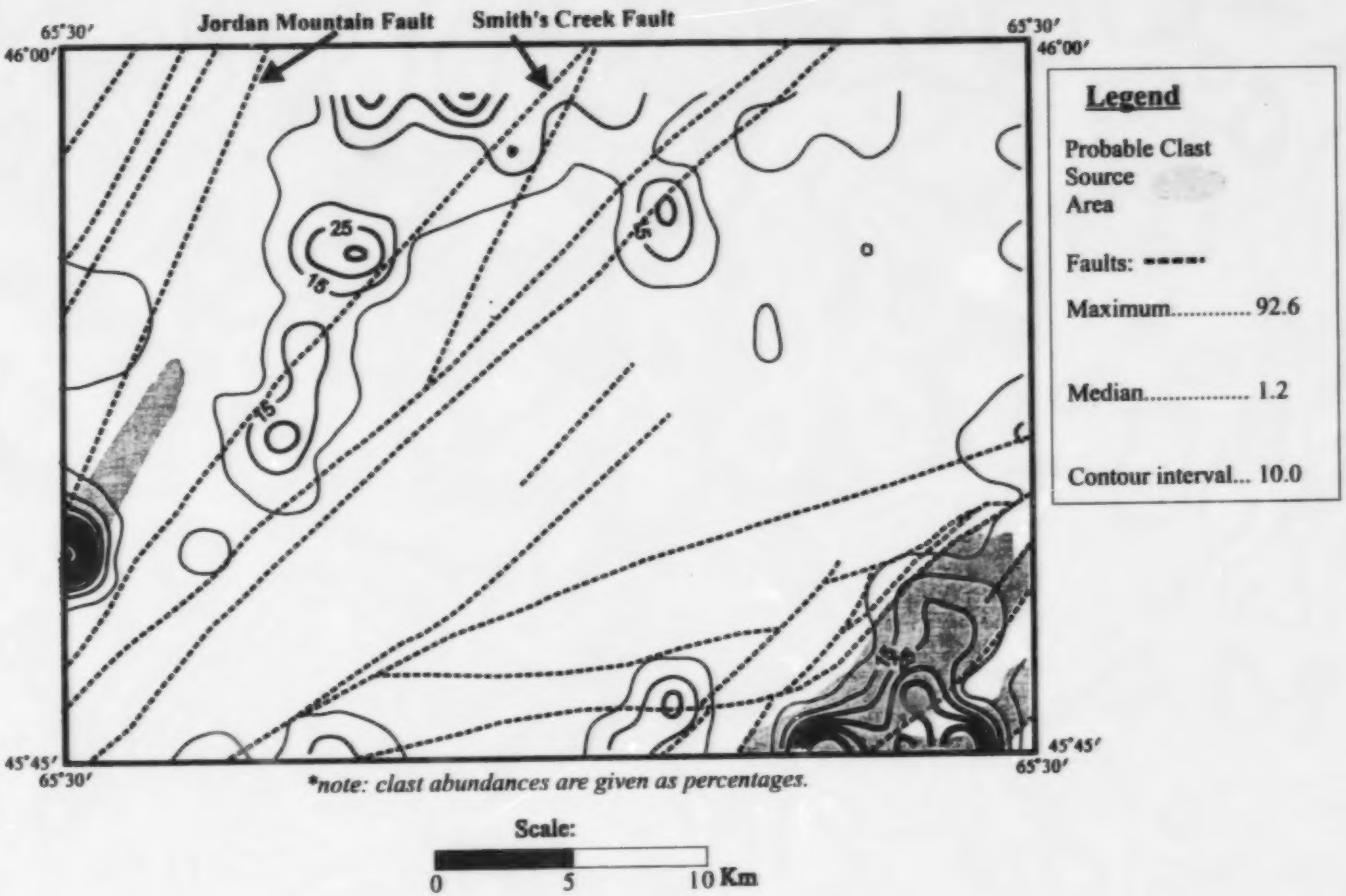

Figure 5.4: Contouring of granite/granodiorite clast abundance in the till.

5.2.4. Metamorphosed Sedimentary Clasts

Igneous rocks displaying moderate- to high-grade metamorphism were observed mainly in till overlying the Caledonia Zone (Figure 1.1). These till clasts were probably derived from a local bedrock source(s) and do not exhibit evidence of glacial dispersal.

5.2.5. Quartz and Quartzite Clasts

Angular quartz clasts are abundant in the north-central portion of the study area (Figure 5.5) and appear to be associated with the local fault system. No insight into the ice-flow directions is provided by the distribution of angular quartz or quartzite in the overlying till cover.

5.2.6. Evaporite Clasts

No limestone or evaporites till clasts were observed at any of the sample sites.

5.2.7. Sedimentary Clasts

The complex Carboniferous sedimentary stratigraphy of group 4 (Figure 3.2) is not mapped in detail, making it difficult to interpret glacial dispersal of till clasts from bedrock sources. Clasts were divided into groups of red or grey sedimentary bedrock (Figures 5.6, 5.7) and then subdivided into conglomerates, sandstones, and mudstones/siltstones. In the western half of the study area, the proportion of sedimentary clasts in the till is relatively low. However, in the part of the Moncton Subbasin located within the northeastern corner of the study area (Figure 1.1), grey sandstone clasts are abundant in the till (Figure 5.8), most likely suggesting that the glacial ice was more erosive locally than in the west.

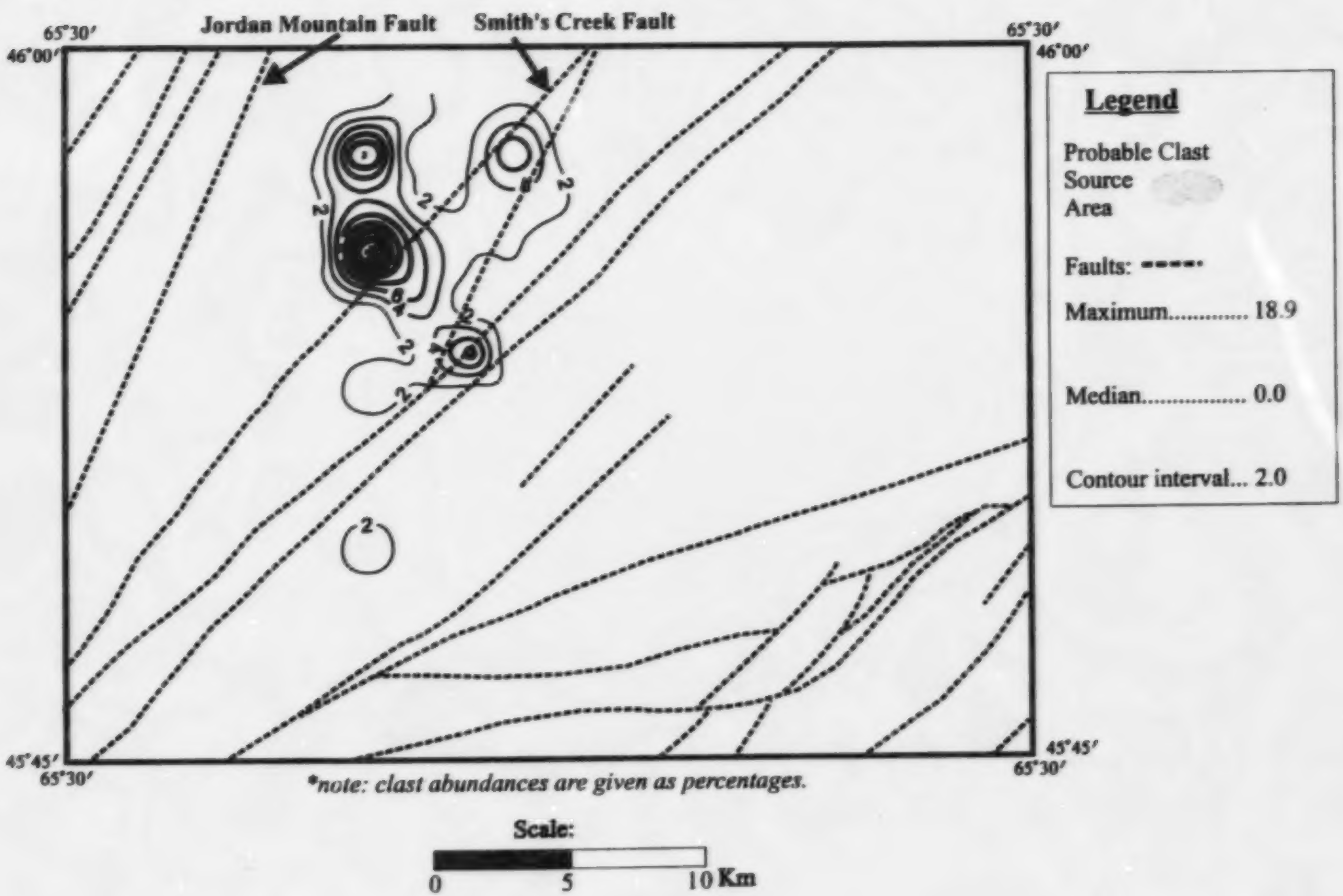

Figure 5.5: Contouring of angular quartz clast abundance in the till.

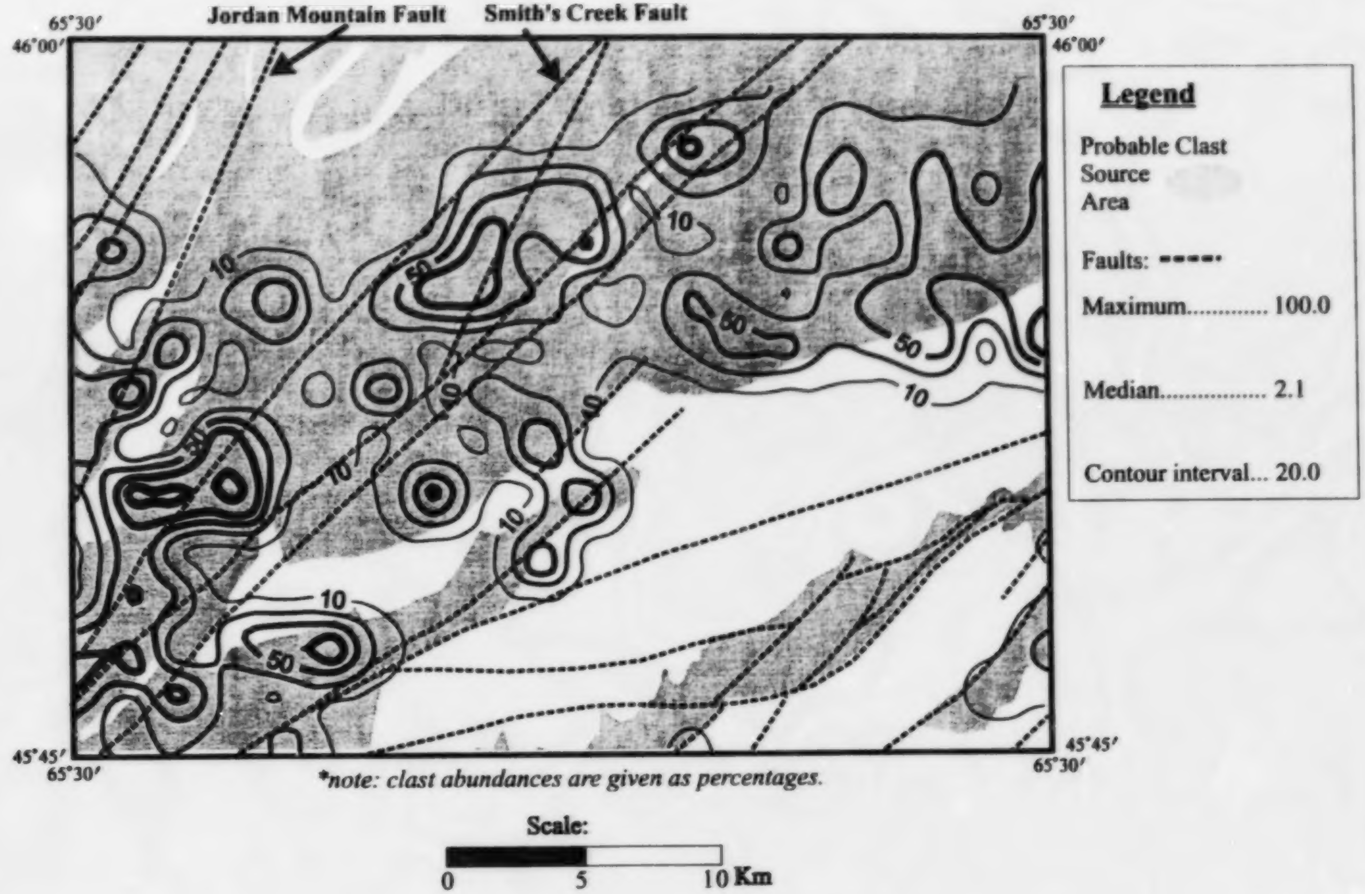

Figure 5.6: Contouring of red sedimentary clast abundance in the till.

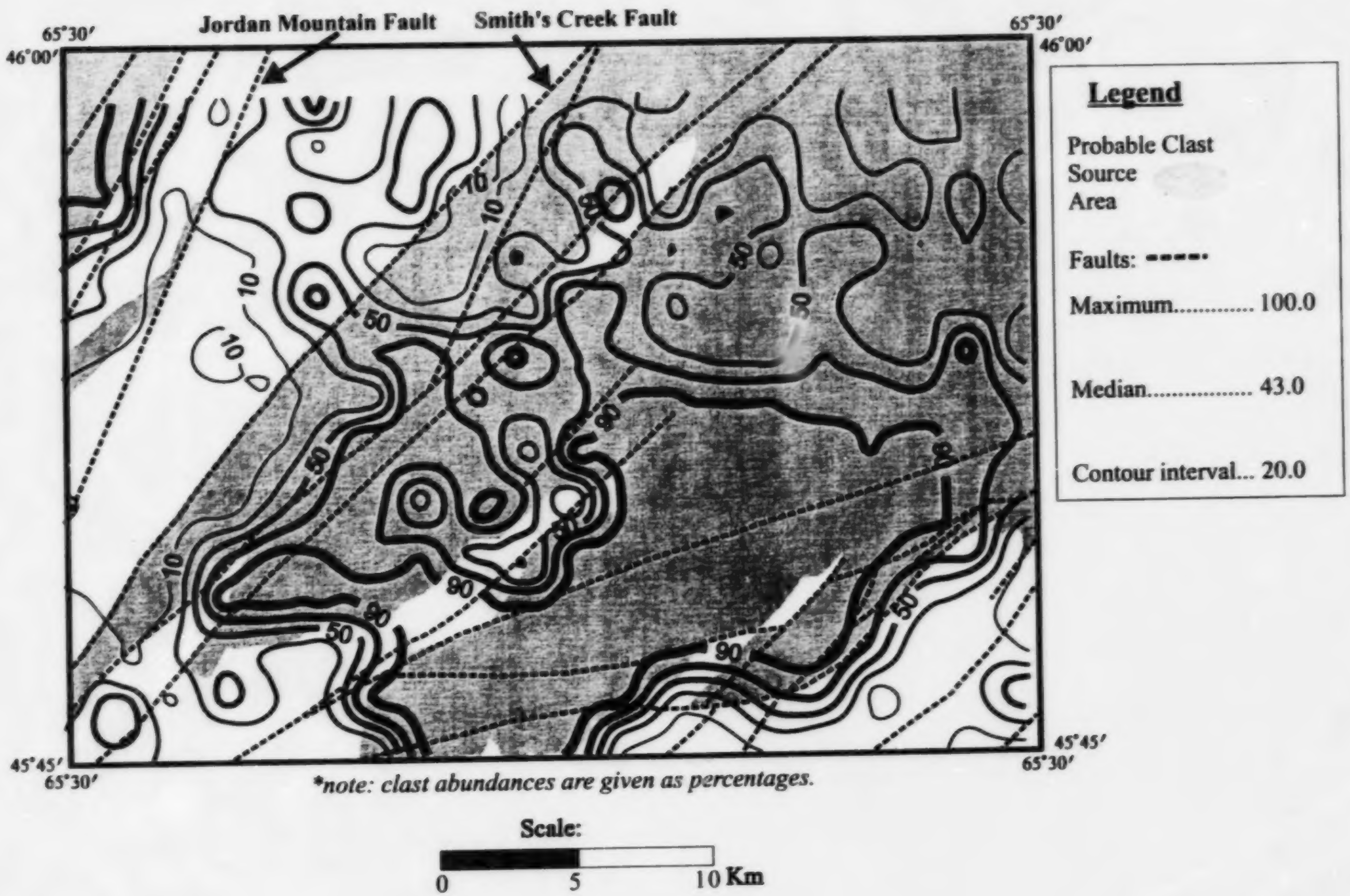

Figure 5.7: Contouring of grey sedimentary clast abundance in the till.

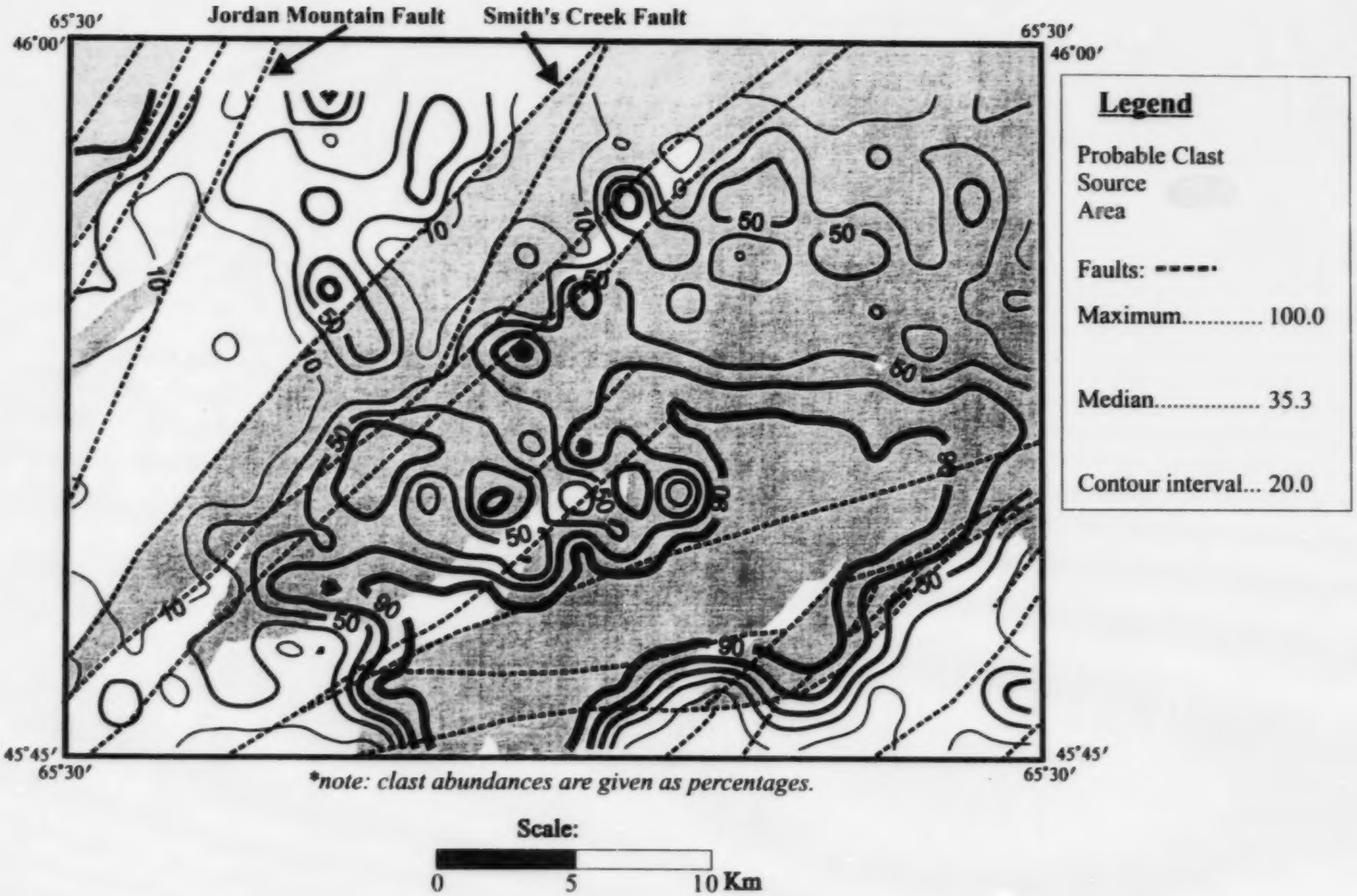

Figure 5.8: Contouring of grey sandstone clast abundance in the till.

5.3. Geochemical Analysis

Instrumental precision and accuracy were evaluated by running a series of lake sediment standards at random intervals with the till samples. For each element the accepted values were compared with the experimental values of the standards (Appendix II: Table II–a). Most elements display good agreement between their accepted and experimental values.

Sample splits were prepared to evaluate the geochemical variability within each till matrix sample. Each sample split was prepared from a randomly chosen till matrix sample by dividing it into two portions. The two portions of the sample were analysed and their geochemistry was compared for each element (Appendix II: Table II–b). Comparison of the splits was performed graphically (Appendix II: Figures 1–17).

Field duplicates were collected randomly at different sites to evaluate the local variability in till geochemistry (Appendix II: Table II–c). Comparison of the duplicates was done graphically (Appendix II: Figures 18–34). No systematic errors were found in the data, suggesting that the sampling protocols were adequate for obtaining representative samples of till.

The regional background concentrations for 48 elements examined in this study were assigned median concentration values. "Anomalous" concentrations for each element were based on threshold values outside two standard deviations from the median (Appendix VI: Table VI–a). Assuming normal distribution, this includes the lower 4.66th and the upper 95.44th percentiles. However, for most elements only the upper 95.44th percentile was considered because instrumental response is poor at concentration ranges below the 4.66th percentile.

Geochemical dispersal patterns in the till matrix were similar to those described by Balzer and Broster (1994), Munn (1995), and Stumpf (1995). Typical dispersal trains were relatively short (4–6 km) and irregular. The length of the dispersal train from point sources, such as mineralised zones, was observed to be dependent on topography. Sources located in topographic lows orientated transverse to ice flow generally display little glacial dispersion. Conversely, sources on topographic highs or ridges produce longer dispersal trains (c.f. Hornibrook et al., 1991).

In the following sections the geochemical data (Appendix V: Part A) will be subdivided into four main groups using Goldschmidt's (1937, 1954) classification system: lithophile, chalcophile, siderophile, and rare earth elements (after Stumpf, 1995). Only elements that exhibit well-defined glacial dispersal are presented in this chapter.

5.3.1. Lithophile Elements

Concentrations of 23 lithophile elements (Al, Ba, Be, Br, Ca, Cr, Cs, Hf, K, La, Mg, Mn, Na, Rb, Sc, Sr, Ta, Ti, Th, U, V, W, Y) were analysed in the till matrix samples. The concentrations for several of these elements (Al, Ba, Cr, Na, Sc, Th) appear to be significantly enriched in till overlying some faults within the western half of the study area (Figures 5.9, 5.10, 5.11, 5.12, 5.13, 5.14). These elements generally have short and irregular dispersal trains. The flow directions inferred from elongate dispersal trains suggest flow directions ranging from east, southeast, and southwest. However, geochemical anomalies elongated in a southwesterly direction may be an artefact of the northeast-southwest trend of the local fault system, and not a product of glacial dispersion. Till overlying the large composite intrusion in the Caledonia Zone is strongly enriched in strontium (Figure 5.15). No dispersal of calcium or magnesium was observed

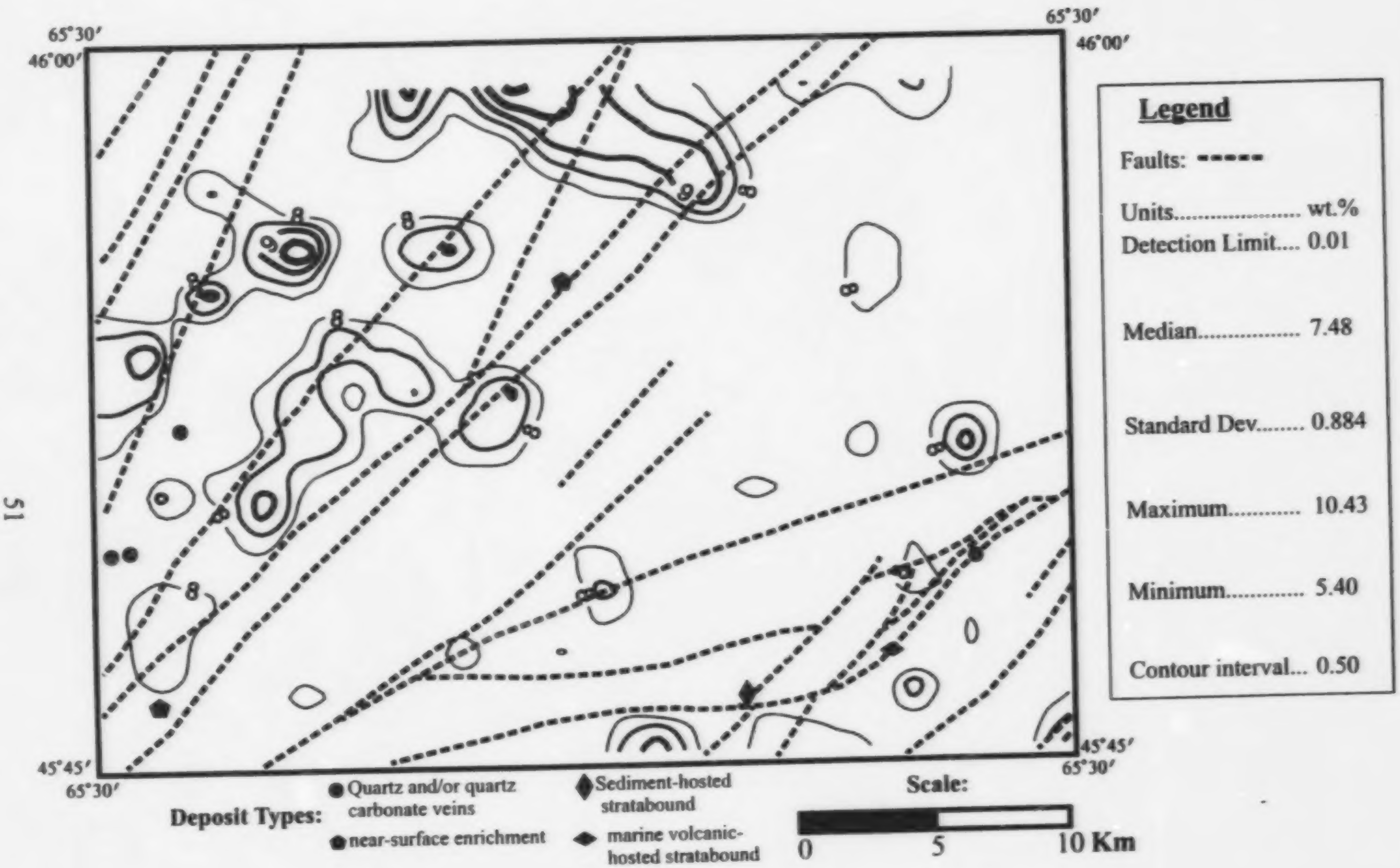

Figure 5.9: Contouring of aluminium concentrations in the till matrix.

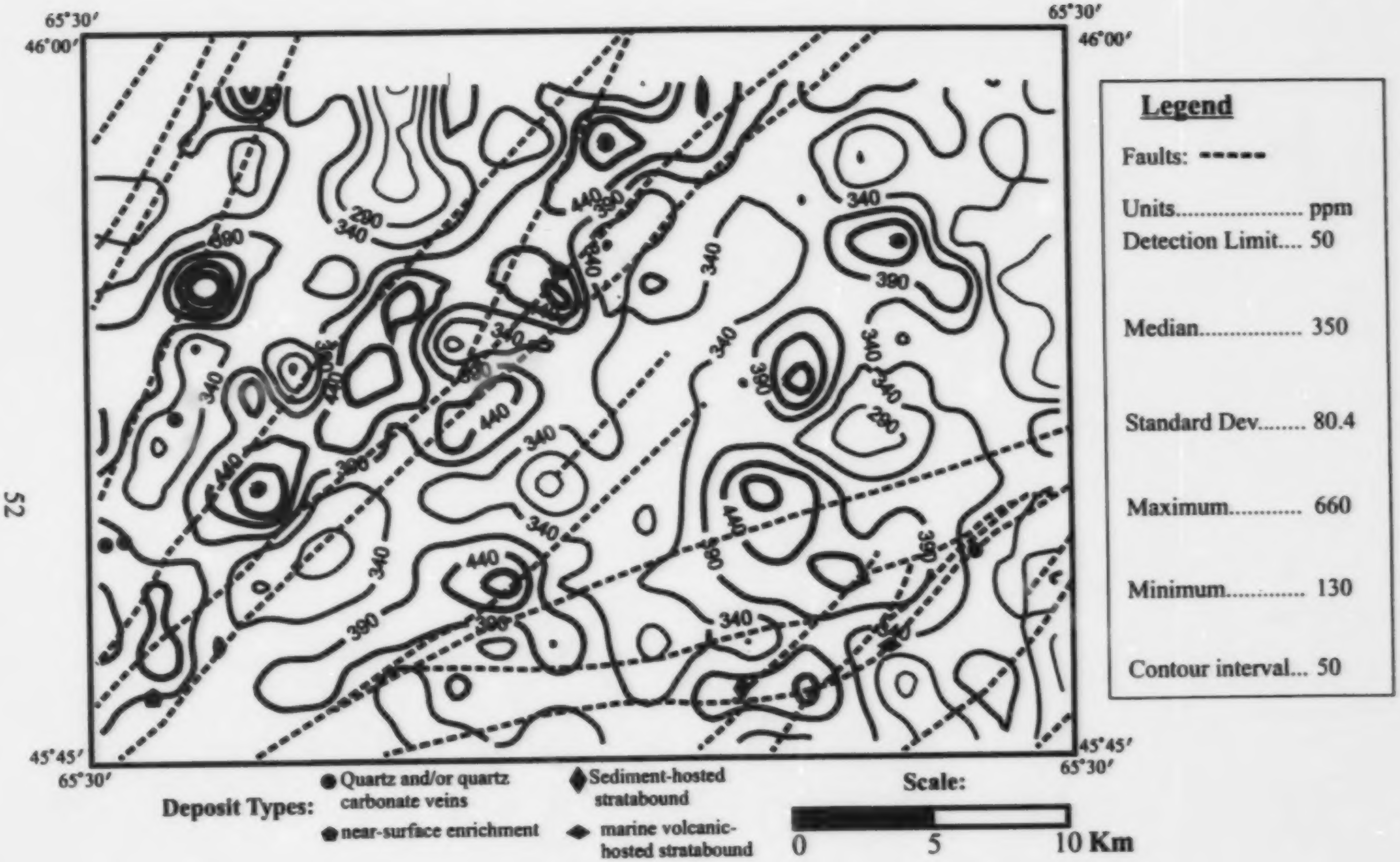

Figure 5.10: Contouring of barium concentrations in the till matrix.

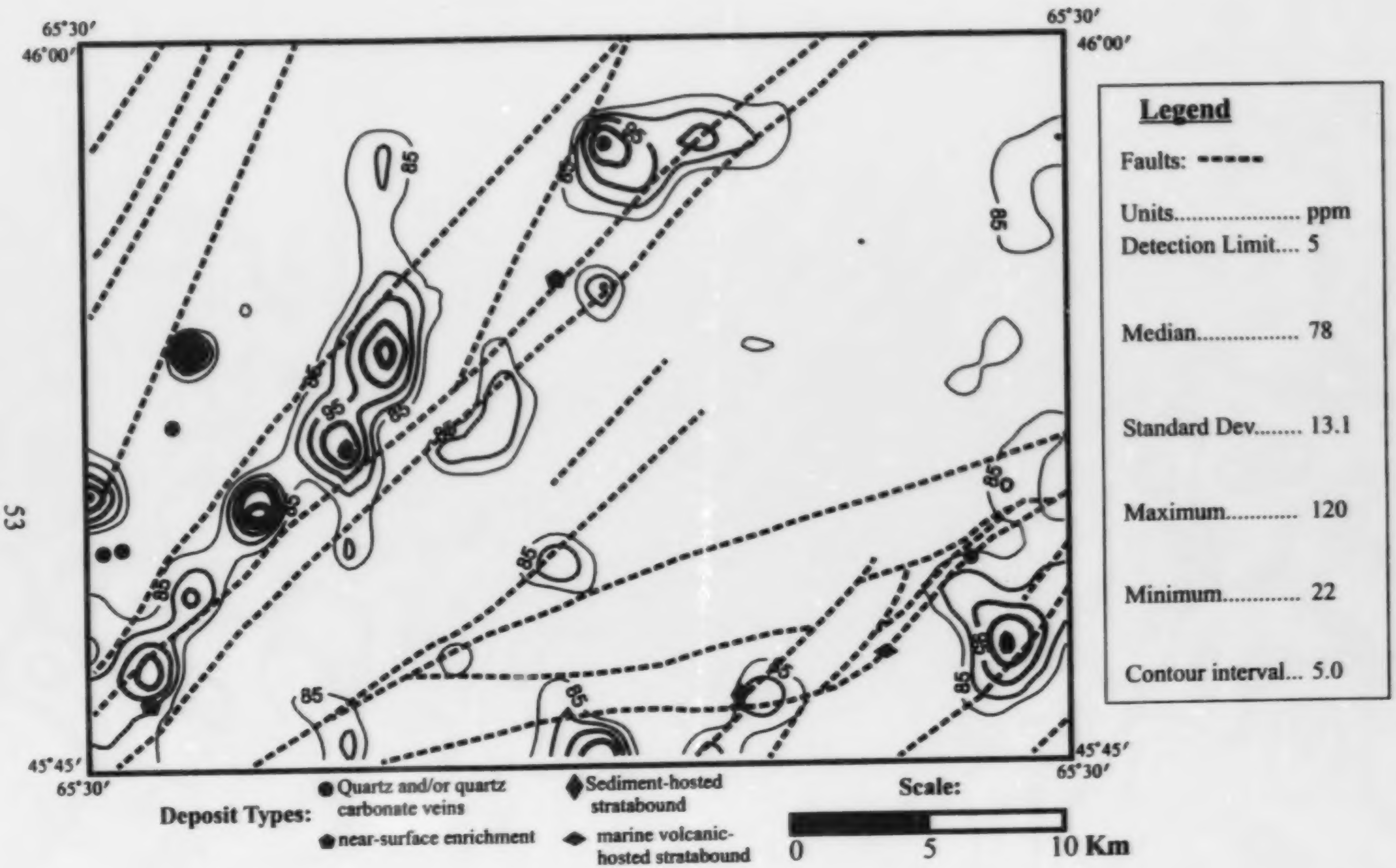

Figure 5.11: Contouring of chromium concentrations in the till matrix.

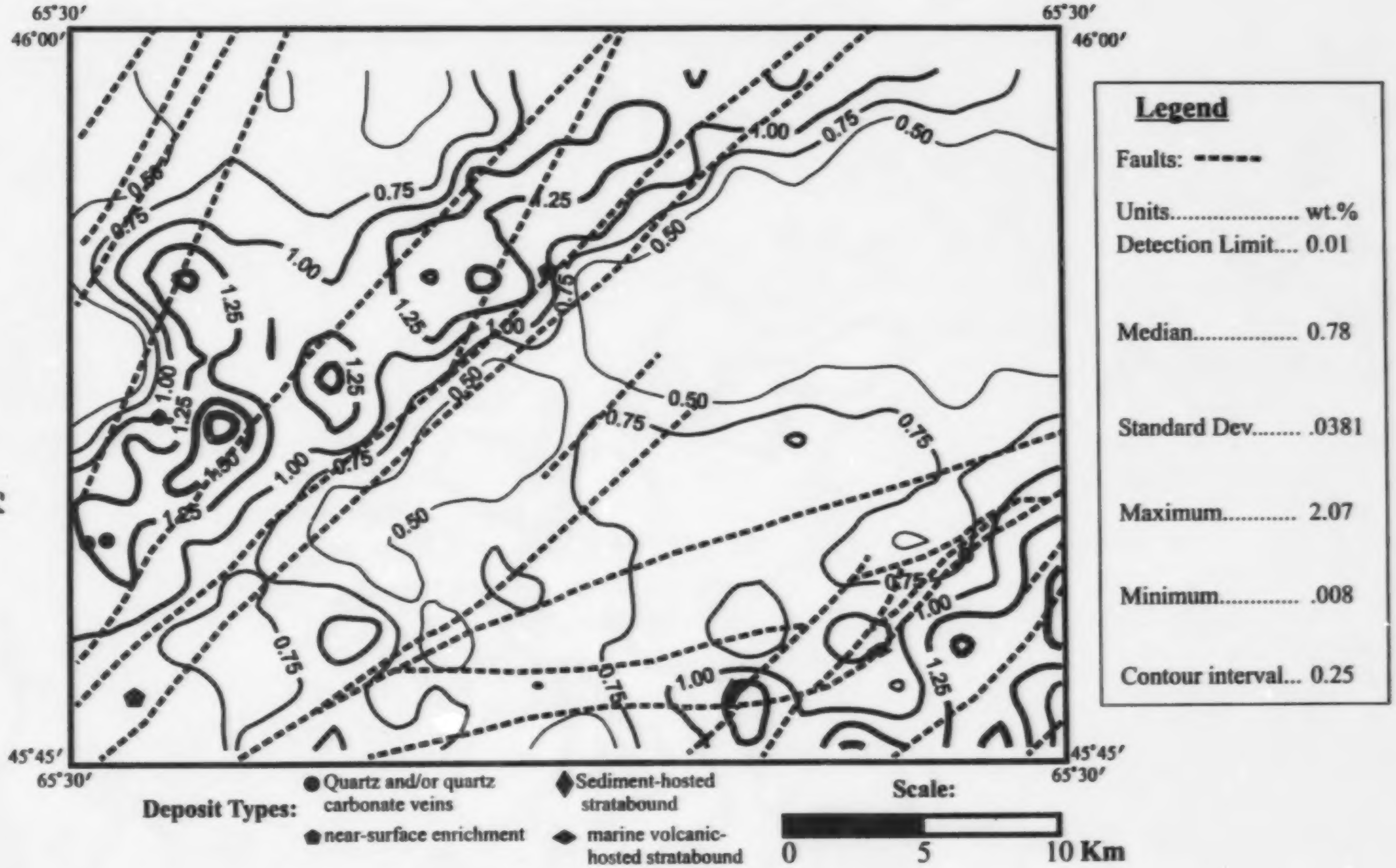

Figure 5.12: Contouring of sodium concentrations in the till matrix.

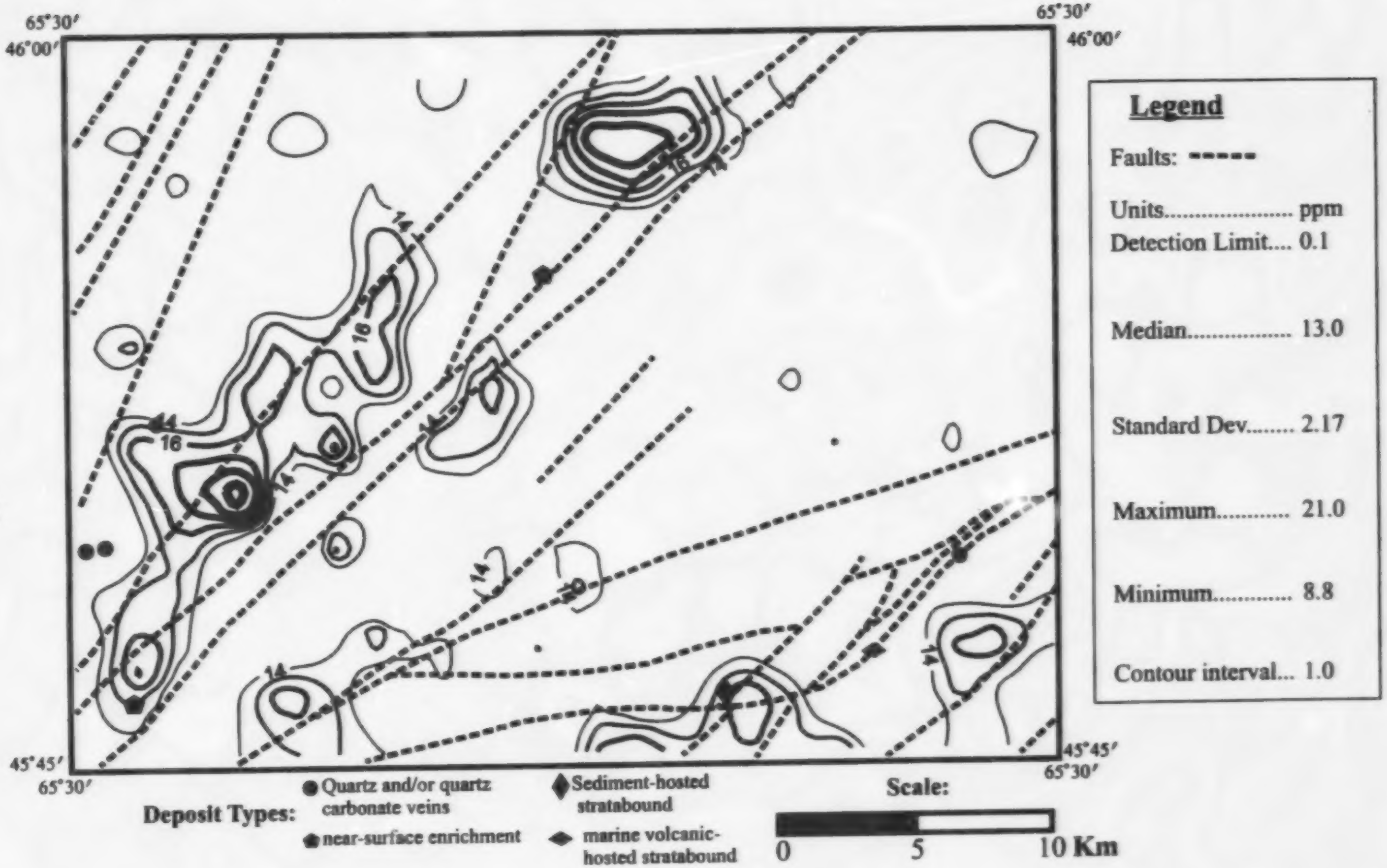

Figure 5.13: Contouring of scandium concentrations in the till matrix.

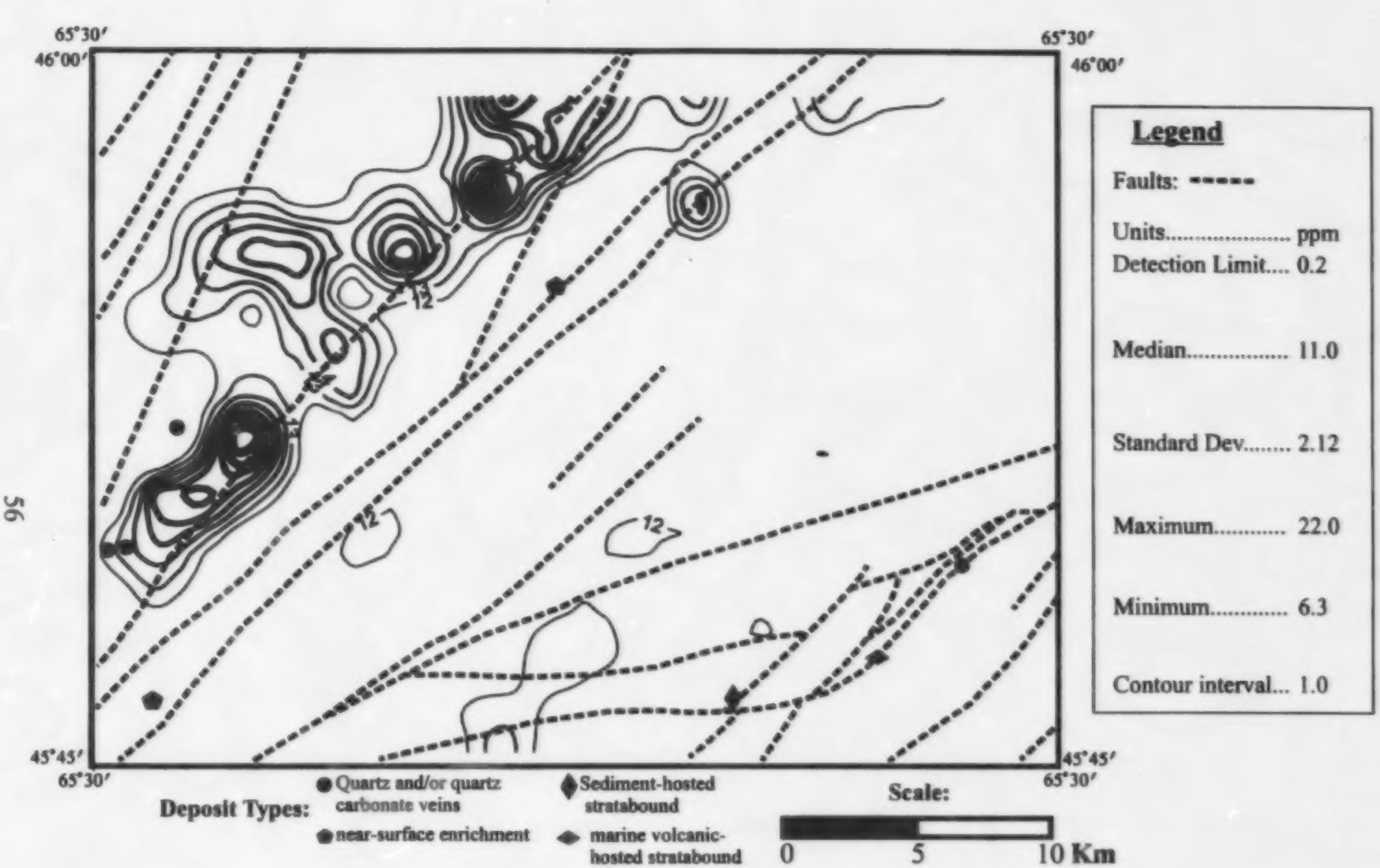

Figure 5.14: Contouring of thorium concentrations in the till matrix.

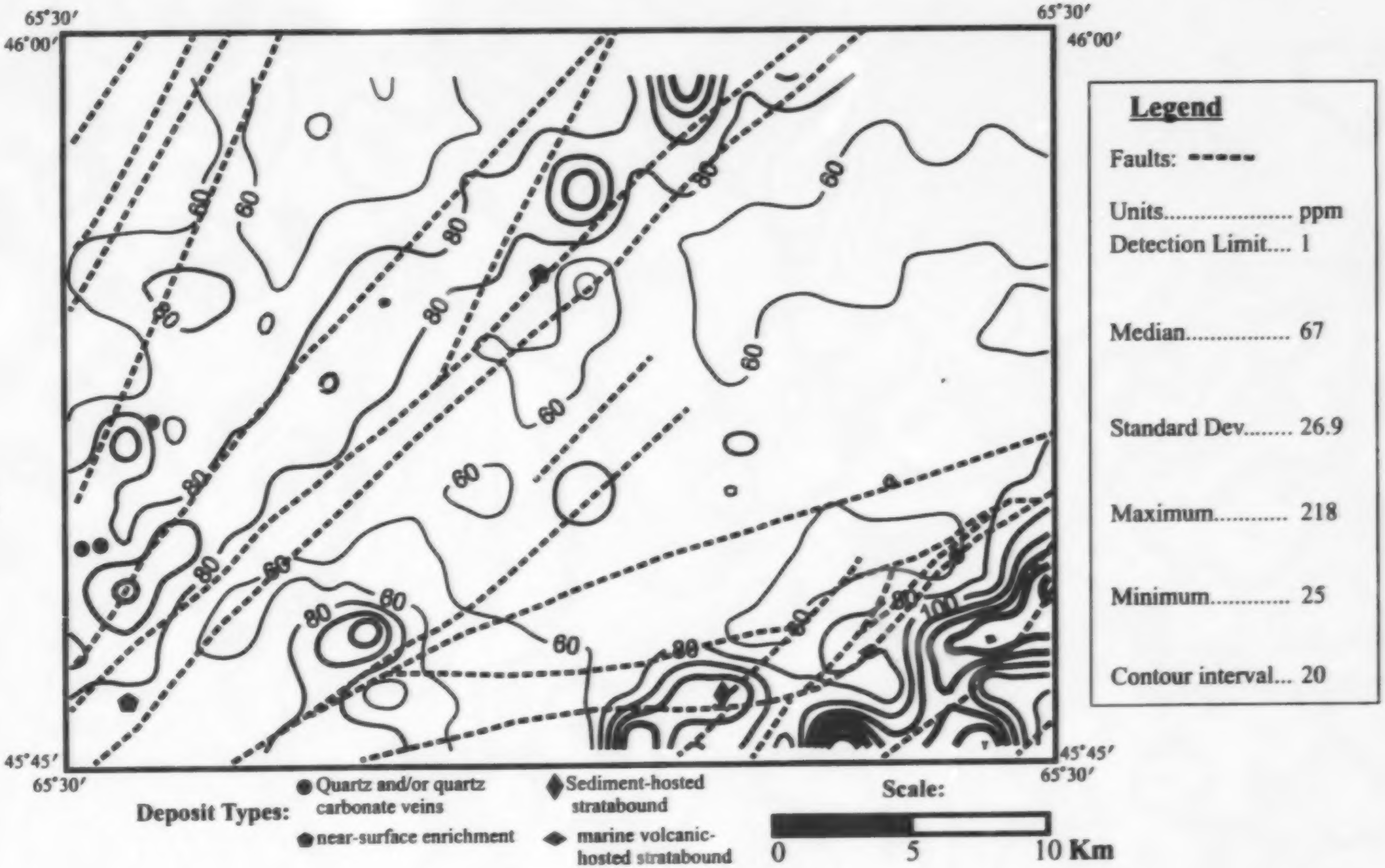

Figure 5.15: Contouring of strontium concentrations in the till matrix.

from the Windsor Group limestone and evaporite in the Havelock area (Appendix IV: Figures 1 and 2).

5.3.2. Chalcophile Elements.

A total of 10 chalcophile elements (Ag, As, Bi, Cd, Cu, Hg, Pb, Sb, Se, and Zn) were examined for evidence of glacial dispersal. Elevated concentrations of arsenic appear to be associated with two known base metal occurrences (Figure 5.16). High mercury and copper concentrations were observed over the large composite intrusion in the Caledonia Zone and may be associated with the mineral occurrence near Elgin (Figures 5.17, 5.18). High concentrations of lead and zinc occur in irregularly shaped anomalies that are probably associated with the local fault system (Figures 5.19, 5.20).

5.3.3. Siderophile Elements

Eight siderophile elements were analysed (Au, Co, Fe, Ir, Mo, Ni, P, Sn) during this study. Elevated nickel concentrations appear to be associated with the local fault system (Figure 5.21). In the north-central portion of the map area, the nickel concentration decreases in an easterly direction. Gold also appears to be associated with faults, occurring in "bulls-eye" shaped anomalies that do not exhibit significant dispersal (Figure 5.22).

5.3.4. Rare Earth Elements.

Seven elements (Ce, Eu, Lu, Nd, Sm, Tb, and Yb) were examined for evidence of dispersal in till. Several of the rare earth element anomalies appear to be associated with the local faults. The mineralised zone on Jordan Mountain has elevated concentrations of lutetium, samarium, and ytterbium, in the overlying till (Figures 5.23, 5.24, and 5.25).

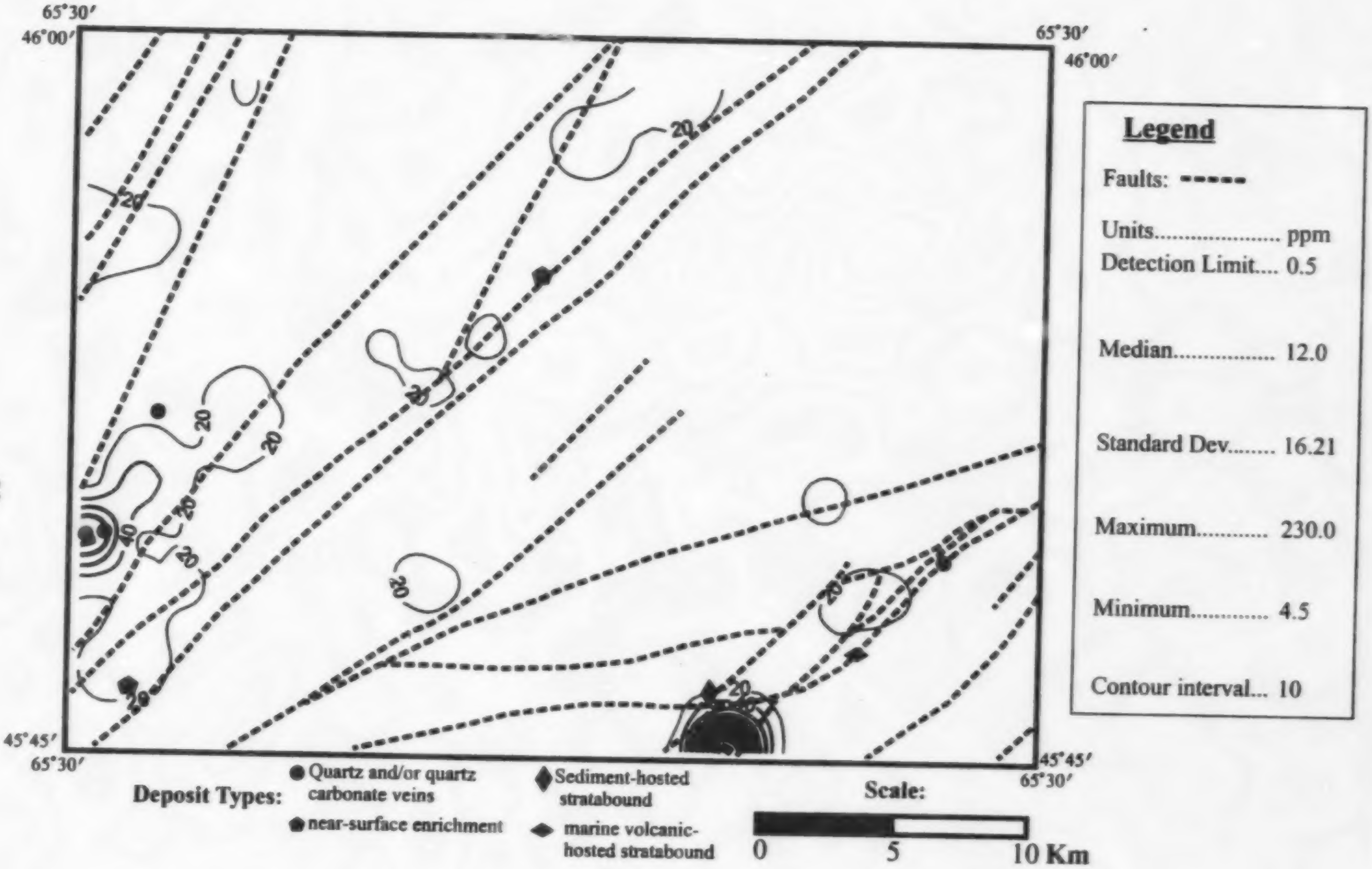

Figure 5.16: Contouring of arsenic concentrations in the till matrix.

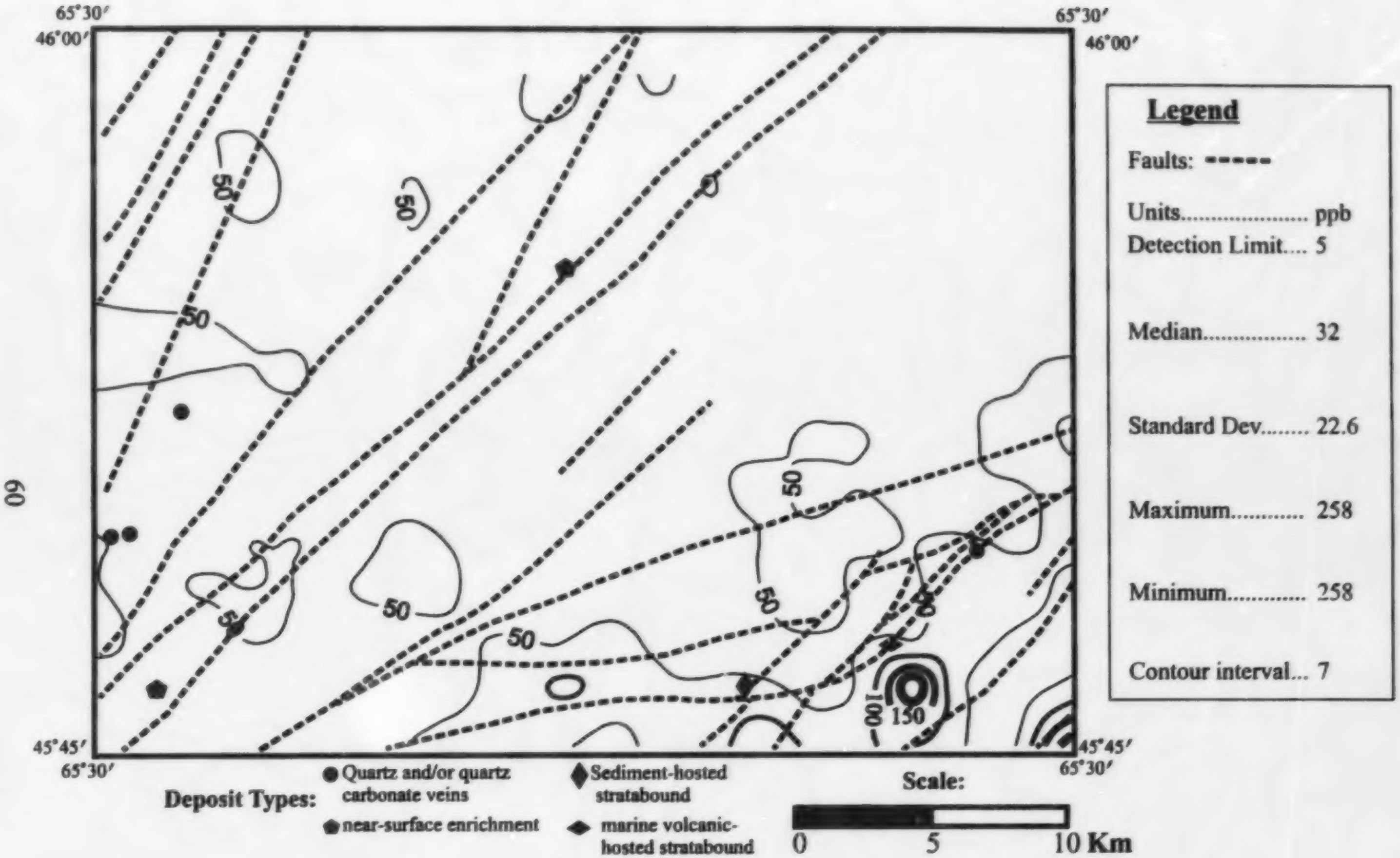

Figure 5.17: Contouring of mercury concentrations in the till matrix.

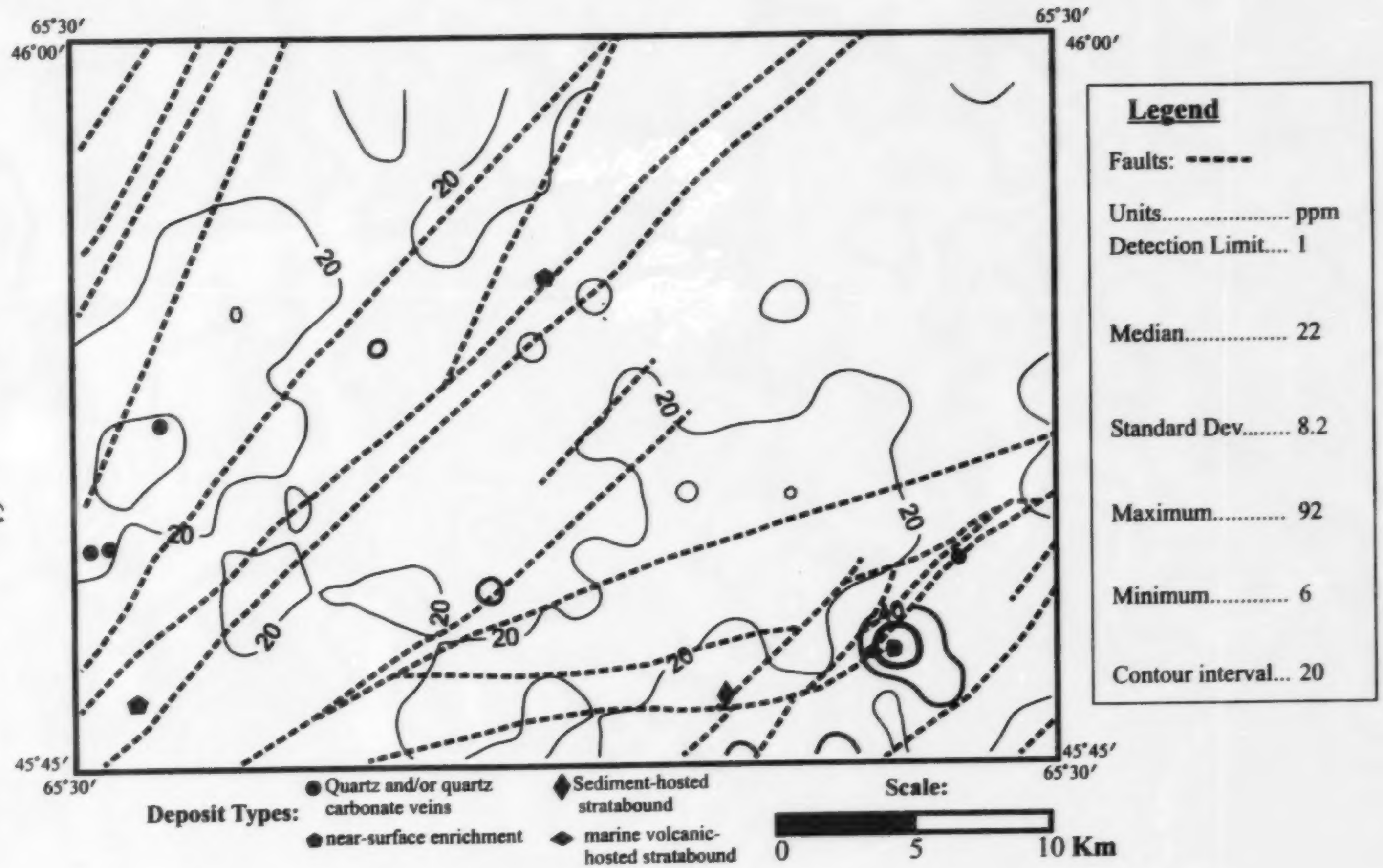

Figure 5.18: Contouring of copper concentrations in the till matrix.

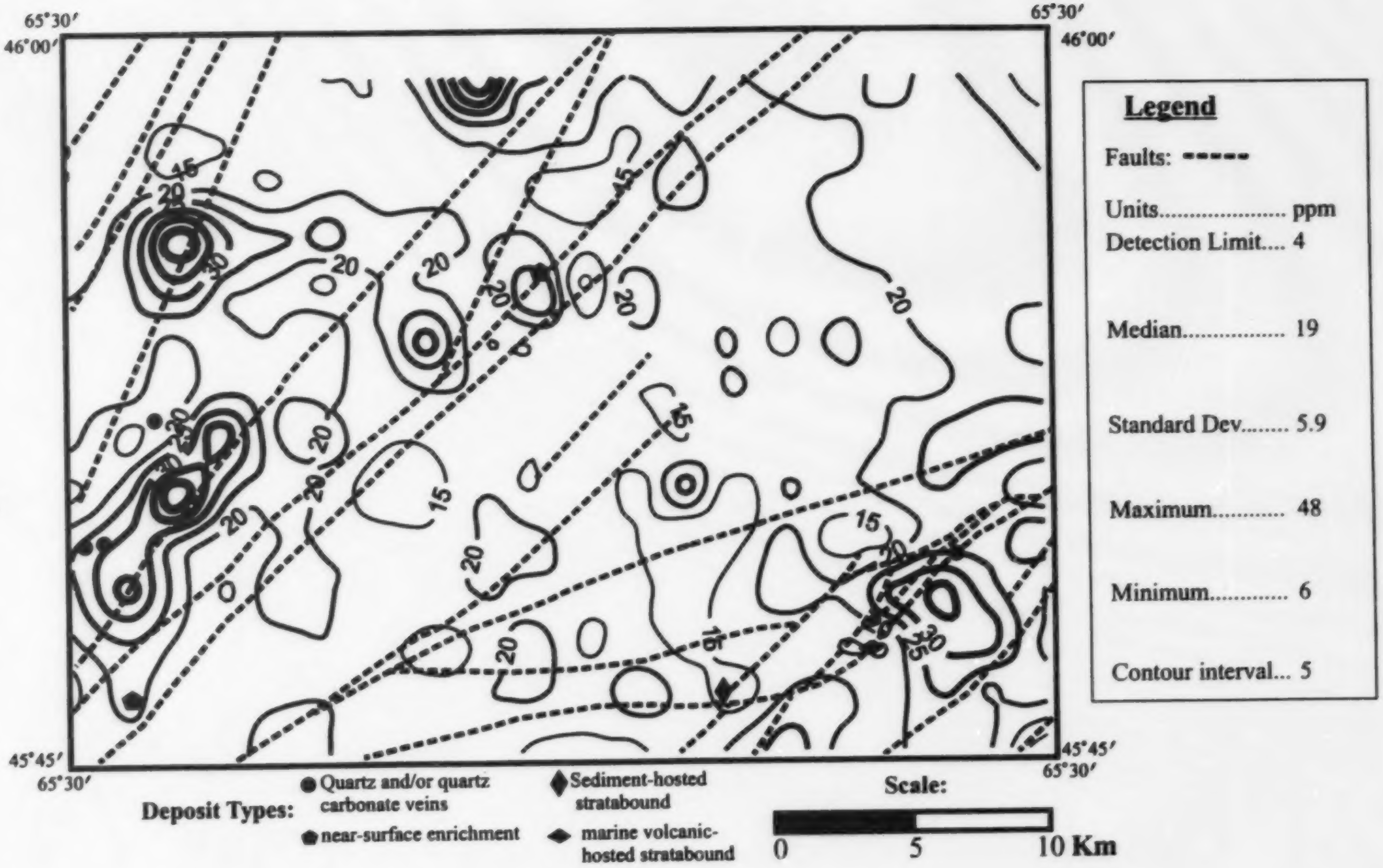

Figure 5.19: Contouring of lead concentrations in the till matrix.

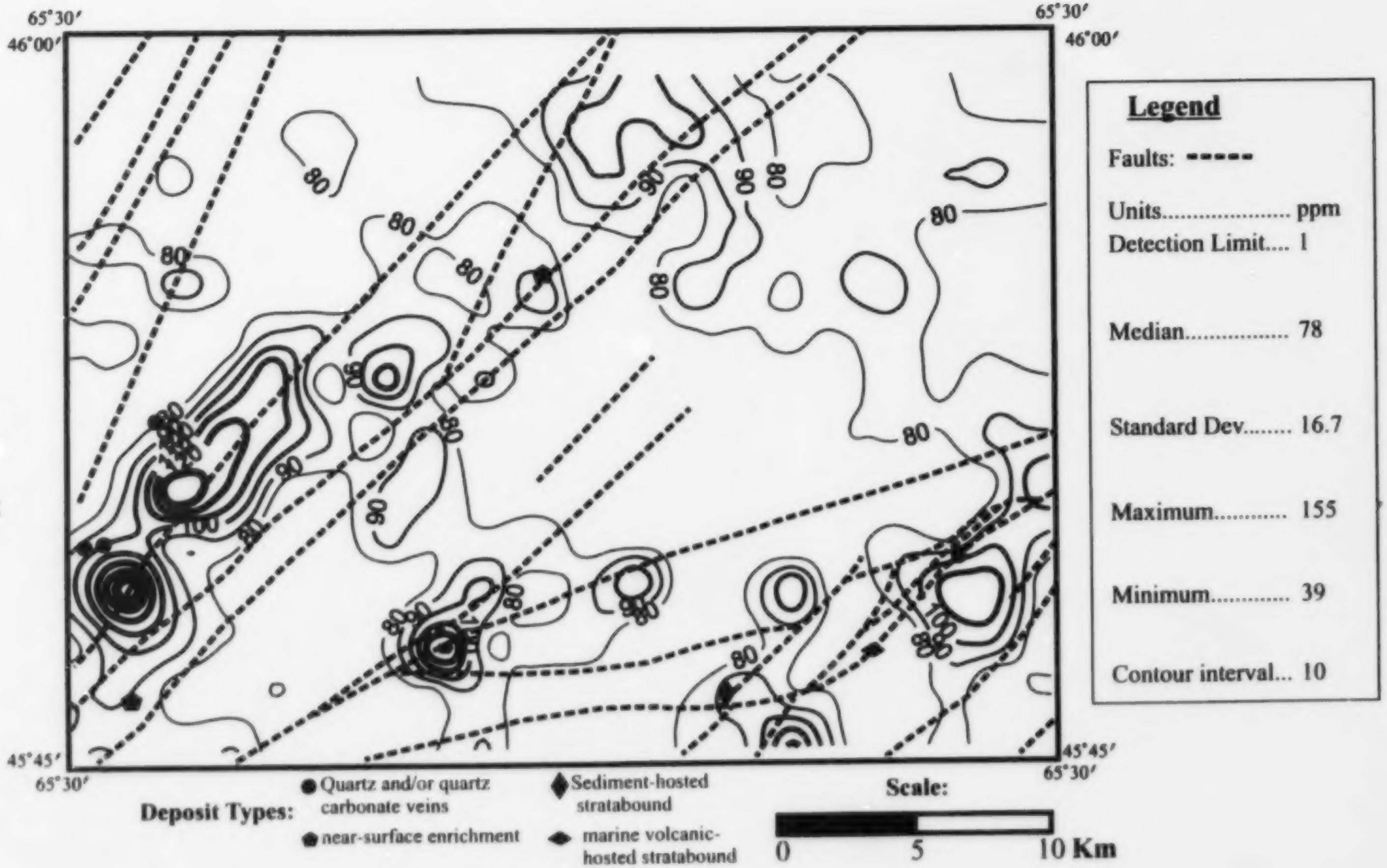

Figure 5.20: Contouring of zinc concentrations in the till matrix.

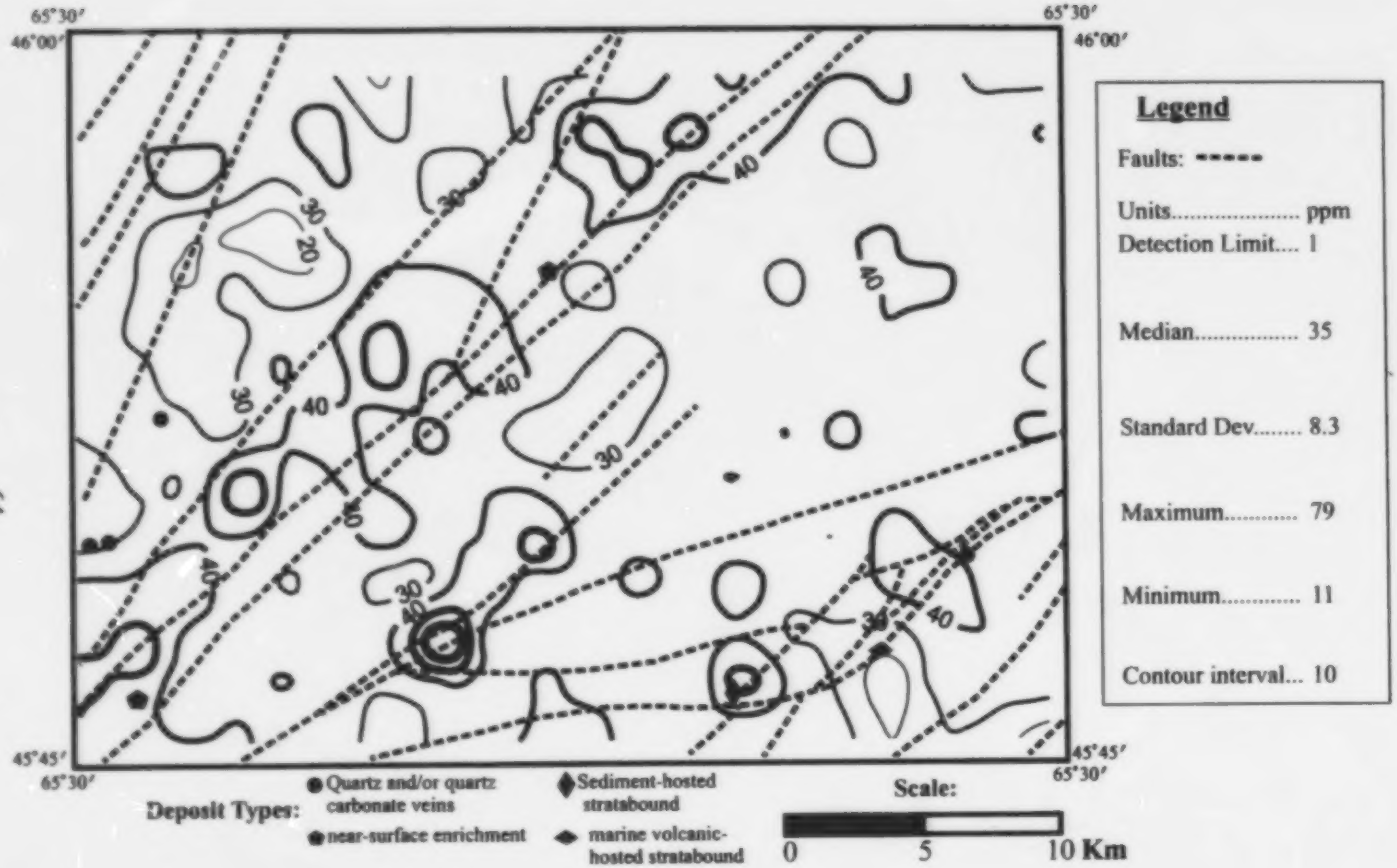

Figure 5.21: Contouring of nickel concentrations in the till matrix.

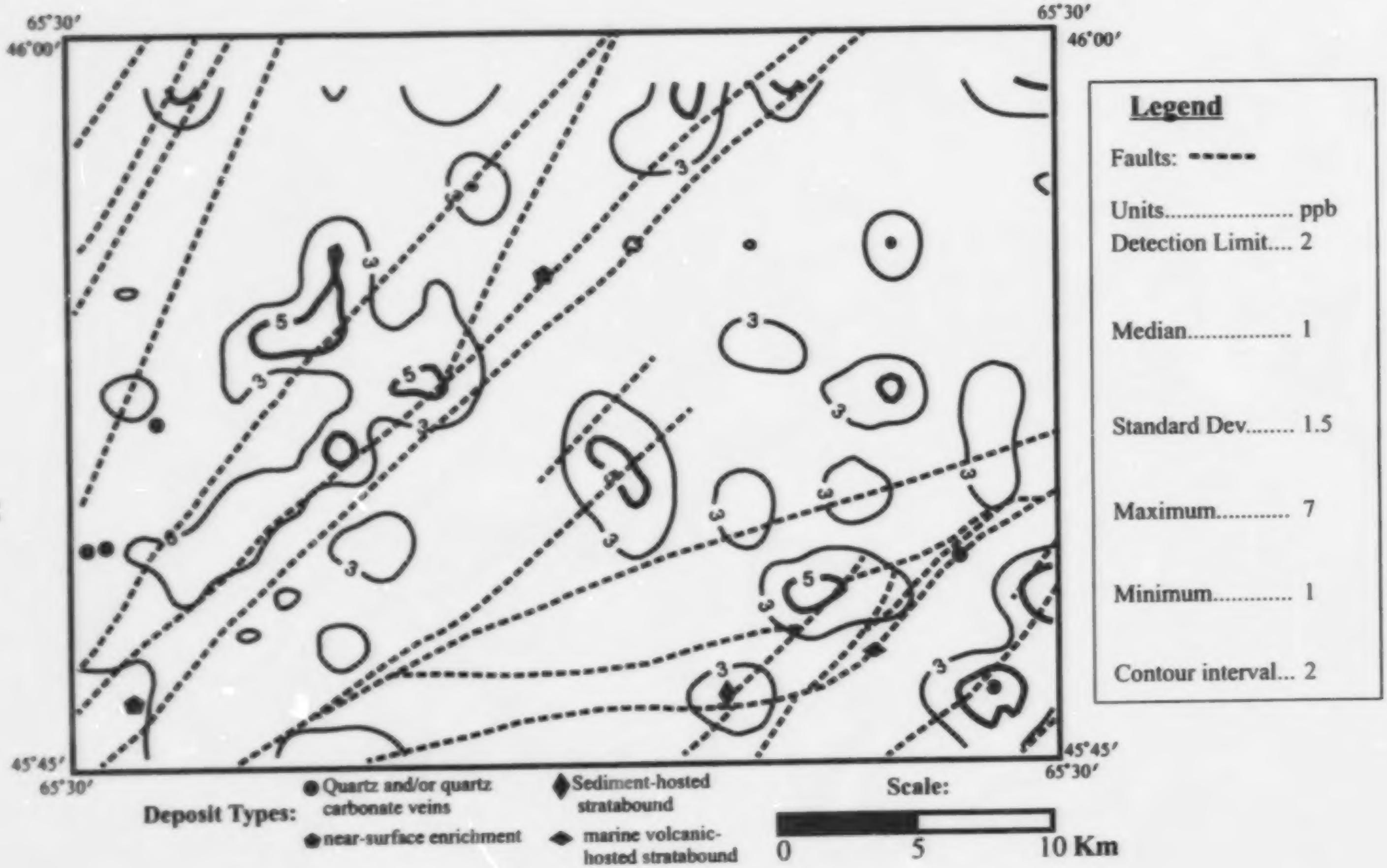

Figure 5.22: Contouring of gold concentrations in the till matrix.

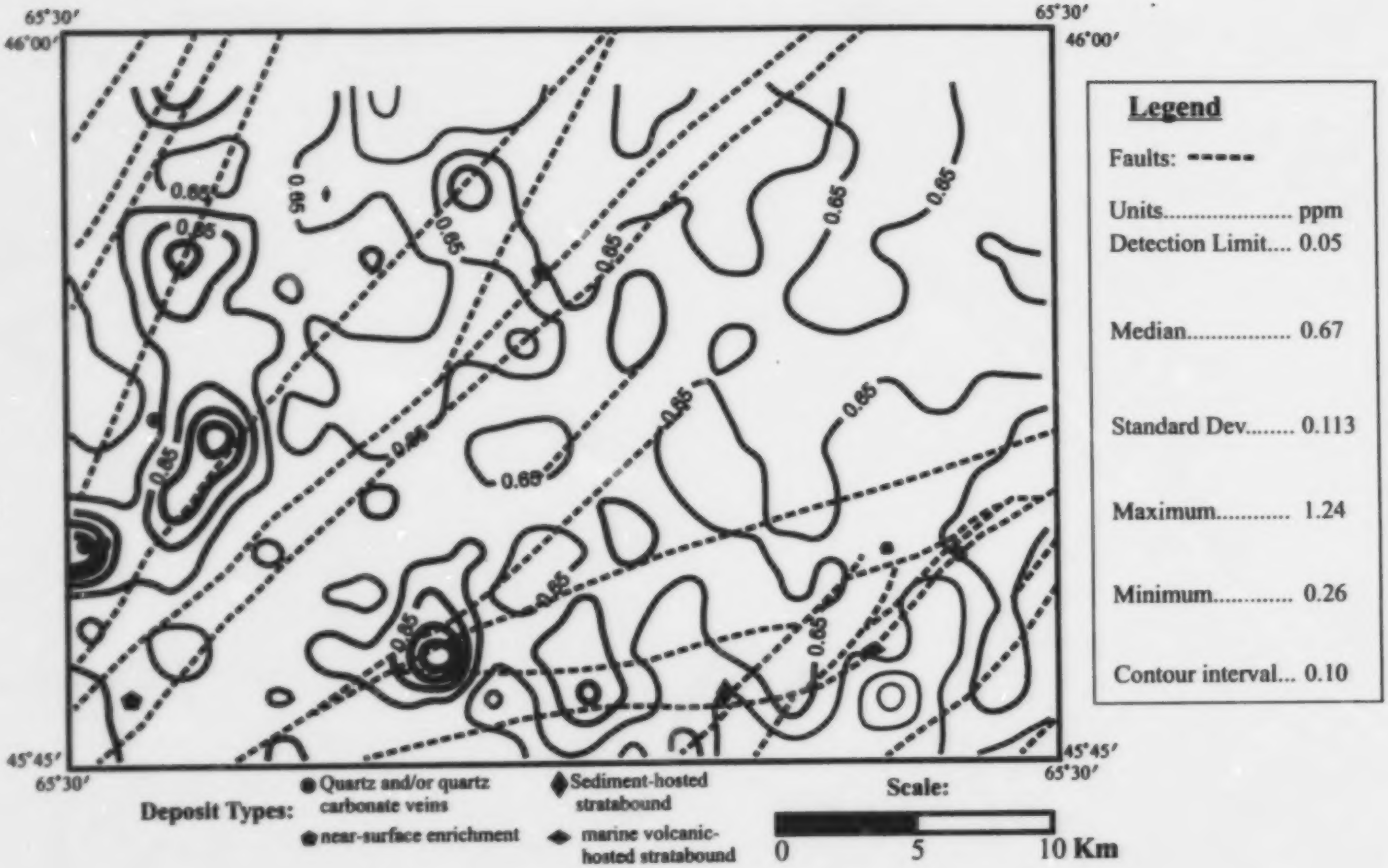

Figure 5.23: Contouring of lutetium concentrations in the till matrix.

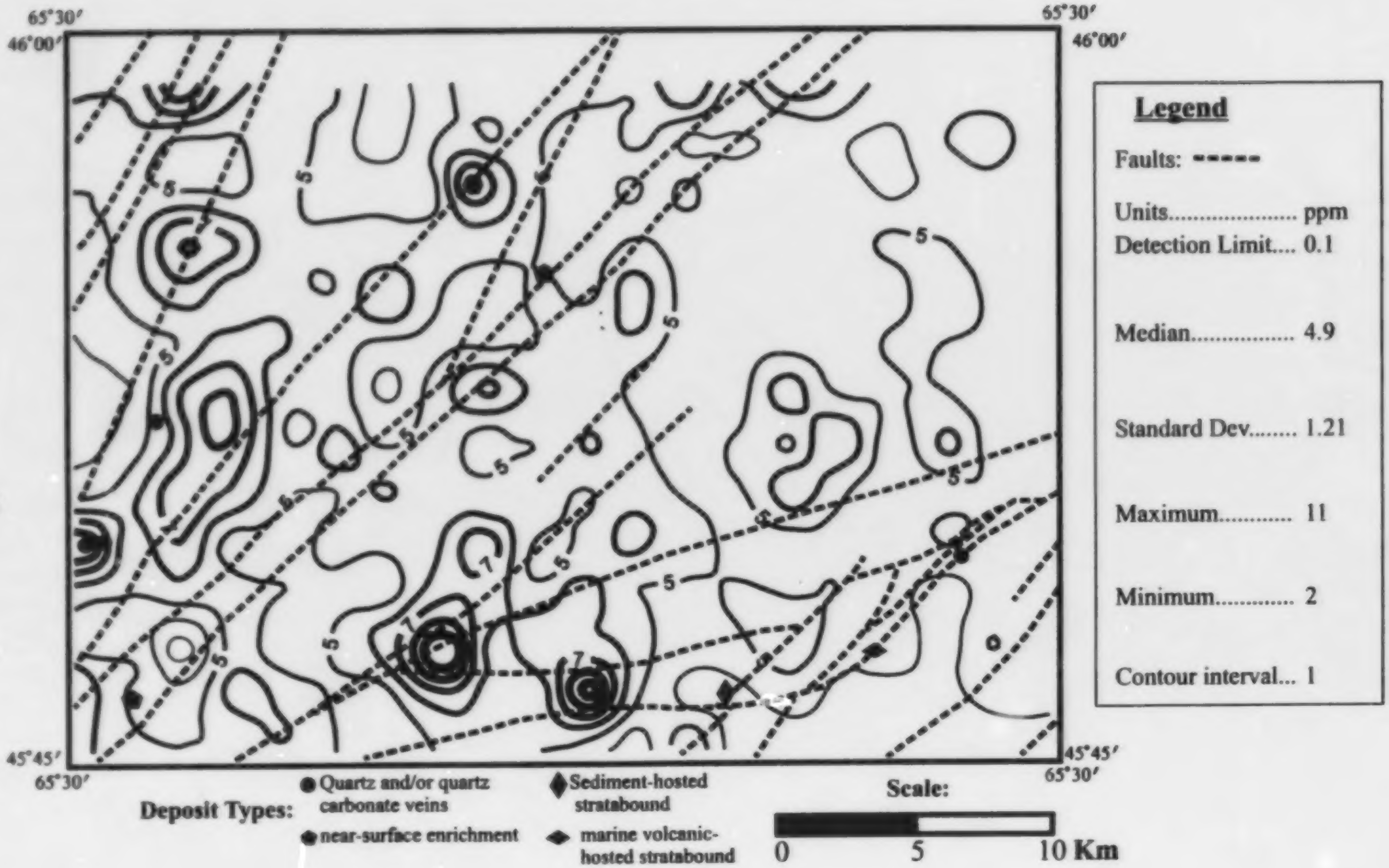

Figure 5.24: Contouring of samarium concentrations in the till matrix.

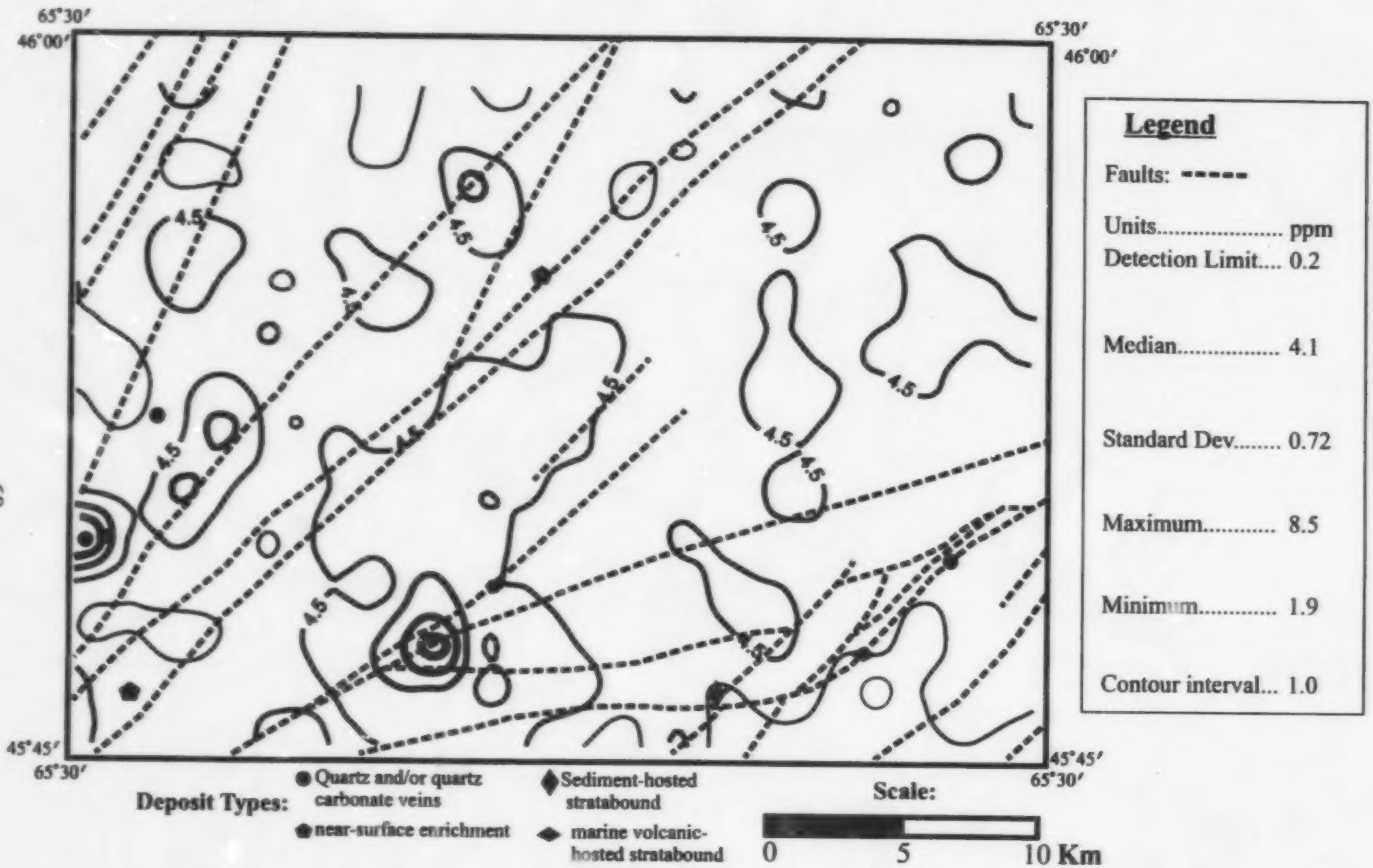

Figure 5.25: Contouring of ytterbium concentrations in the till matrix.

5.4. Indicators of Ice-flow Direction

Poor bedrock exposure hampered the determination of ice-flow patterns from micro-scale features (<1 m) of glacial erosion (e.g., striations, nail heads, and rat-tails) in the Petitcodiac area. Often, the available bedrock outcrops have been deeply weathered or are modified by human activity, destroying many glacial micro-scale features. Fluvial erosion during recent spring and fall run-off has effectively removed overburden without disturbing the erosion indicators. For this reason, it is suggested that further studies in southern New Brunswick, in areas where striae sites are sparsely distributed, be conducted immediately following periods of heavy rain.

Well-preserved striae sites were mainly limited to the eastern section of the study area (Figures 5.26, 5.27). In the northeast, two striated bedrock outcrops (Figure 5.26, Sites 1, 2) located on the eastern face of a moderate slope display numerous rat-tails, crag-and tails, and nail heads that record multiple ice movements trending at 045°, 050°, 060°, 070°, 090°, 105°, 120°, 150°, 160°, 170°. From cross-cutting relationships, the relative ages from oldest to youngest are; 1) 150°–170°, 2) 095°–105° 3) 070°–088°, and 4) 060°–040°. The 120° striae did not appear to be well preserved on the outcrops and its trend and relative age could not be evaluated. Toward the southeast near the base of the Caledonia Zone (sensu stricto, Rampton et al., 1984), striated outcrops demonstrate ice-flow directions from southeast to south-southwest.

In the north-central region of the study area the orientation and shape of drumlinoid features indicate an easterly ice-flow event (Figure 5.26). However, in the southwestern area, below Jordan Mountain, drumlinoid features and striae imply southwesterly ice movement.

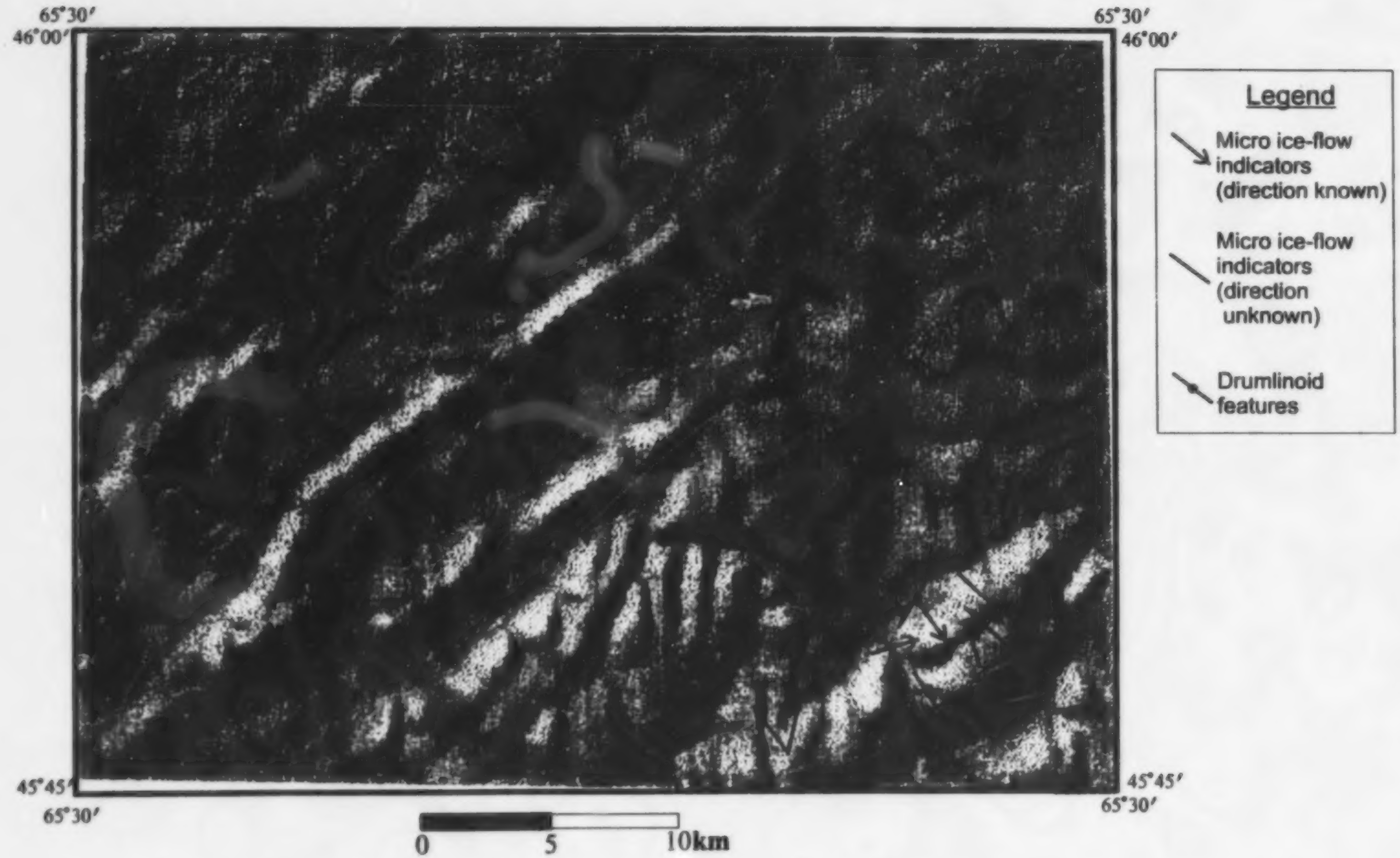

Figure 5.26: Glacial ice-flow indicators superimposed on a shaded elevation image generated using a Digital Terrain Model (DTM).

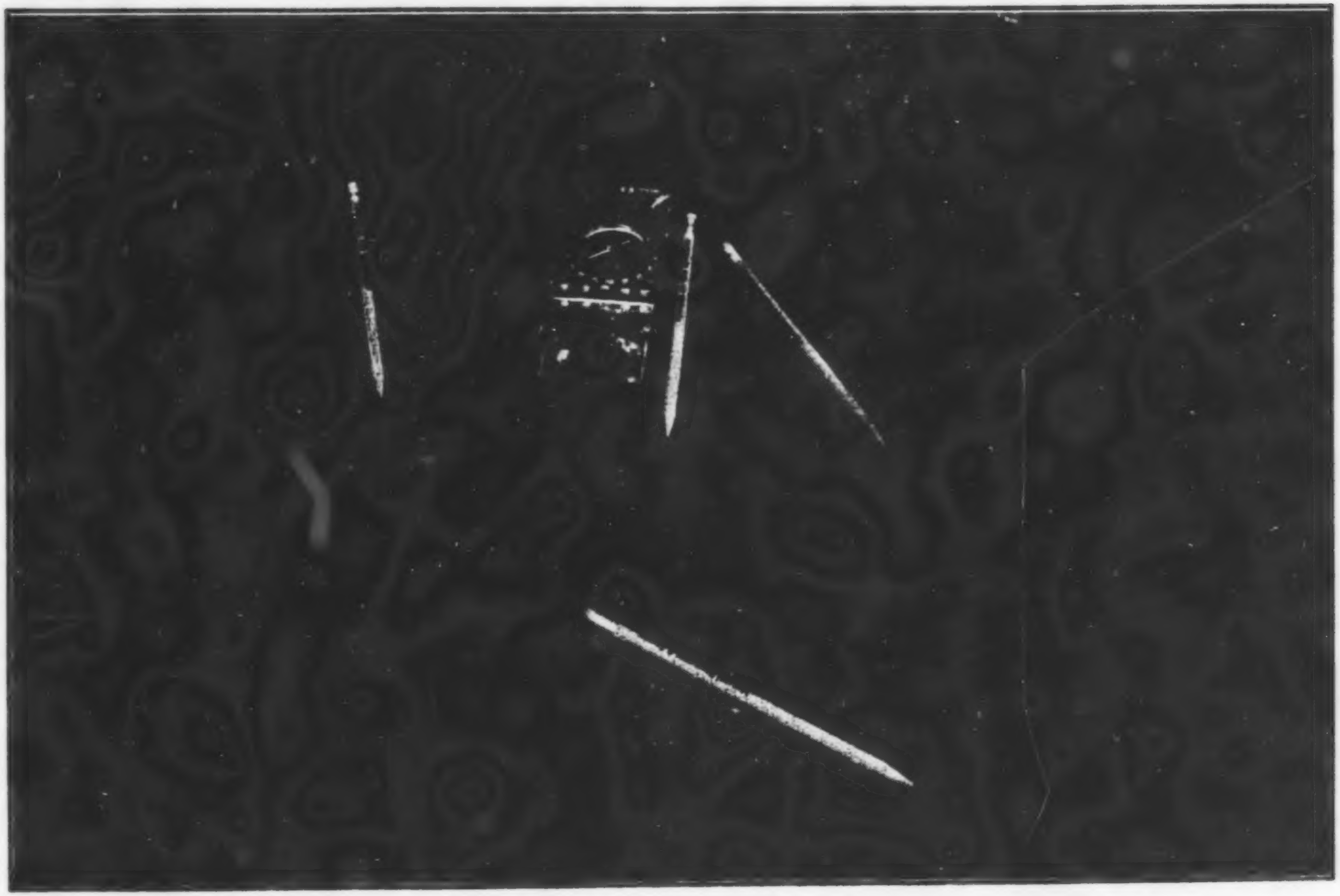

Figure 5.27: Striae site #2 located in the northeast corner of the Petitcodiac map sheet area recording multiple ice flow directions (long axis of the compass is approximately 20cm)

5.5. Topographic Influences

Many of the dispersal patterns appear to curve around areas of significant positive relief or terminate on the western or northwestern slopes of major topographical features. The most significant obstacles to local glacial dispersal are the Anagance Ridge, Jordan Mountain, and the Caledonia Zone (Figure 5.28). North of the Anagance Ridge, aluminium forms a long (approximately 10 km) ribbon-shaped dispersal train trending toward the southeast (Figure 5.29). Chromium (Figure 5.30), scandium (Figure 5.31), and vanadium (Figure 5.32) form dispersal trains close to the northern extremity of the Anagance Ridge. These trains appear to be diverted eastward around the Anagance Ridge, and are short (approximately 6 km). Felsic intrusive clasts (Figure 5.33) form a wide (approximately 7 km) dispersal train that appears to be bisected by the Anagance Ridge into two narrower dispersal trains elongated southwest and southeastward. Furthermore, the branch of this train that is diverted toward the southwest is considerably longer than its counterpart trending toward the southeast. Further south, the sodium (Figure 5.34) dispersal train is interrupted by the west side of the Anagance Ridge.

In the Caledonia Zone (Figure 5.28), short geochemical dispersal trains (<6 km) are common. For example, copper (Figure 5.35) and lead (Figure 5.36) appear to terminate against the northeast face of Collier Mountain (Figure 5.28) only 5 km from heads of their dispersal trains.

5.6. Statistical Correlations: Spearman's Rank Correlation Coefficient

The Spearman's rank correlation analysis is a nonparametric technique useful for quantifying the strength of association between two variables (Pangano and Gauvreau, 1993, p.369–371). Version 8 of the Statistical Package for the Social Sciences (SPSS

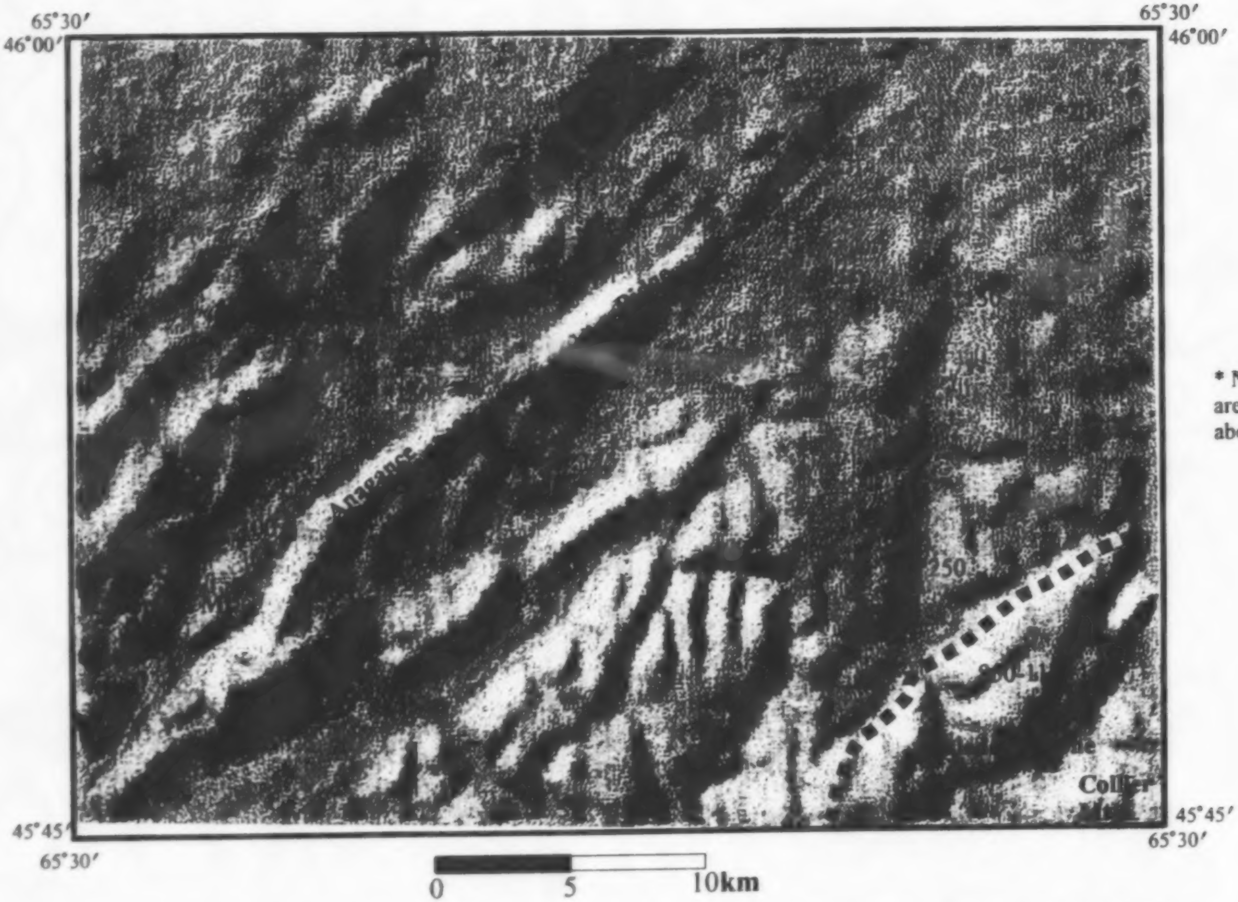

* **Note**: Point Elevations are measured in feet above sea level.

Figure 5.28: Point elevations for significant physiographic obstacles to ice-flow superimposed on a shaded elevation image generated using a Digital Terrain Model (DTM).

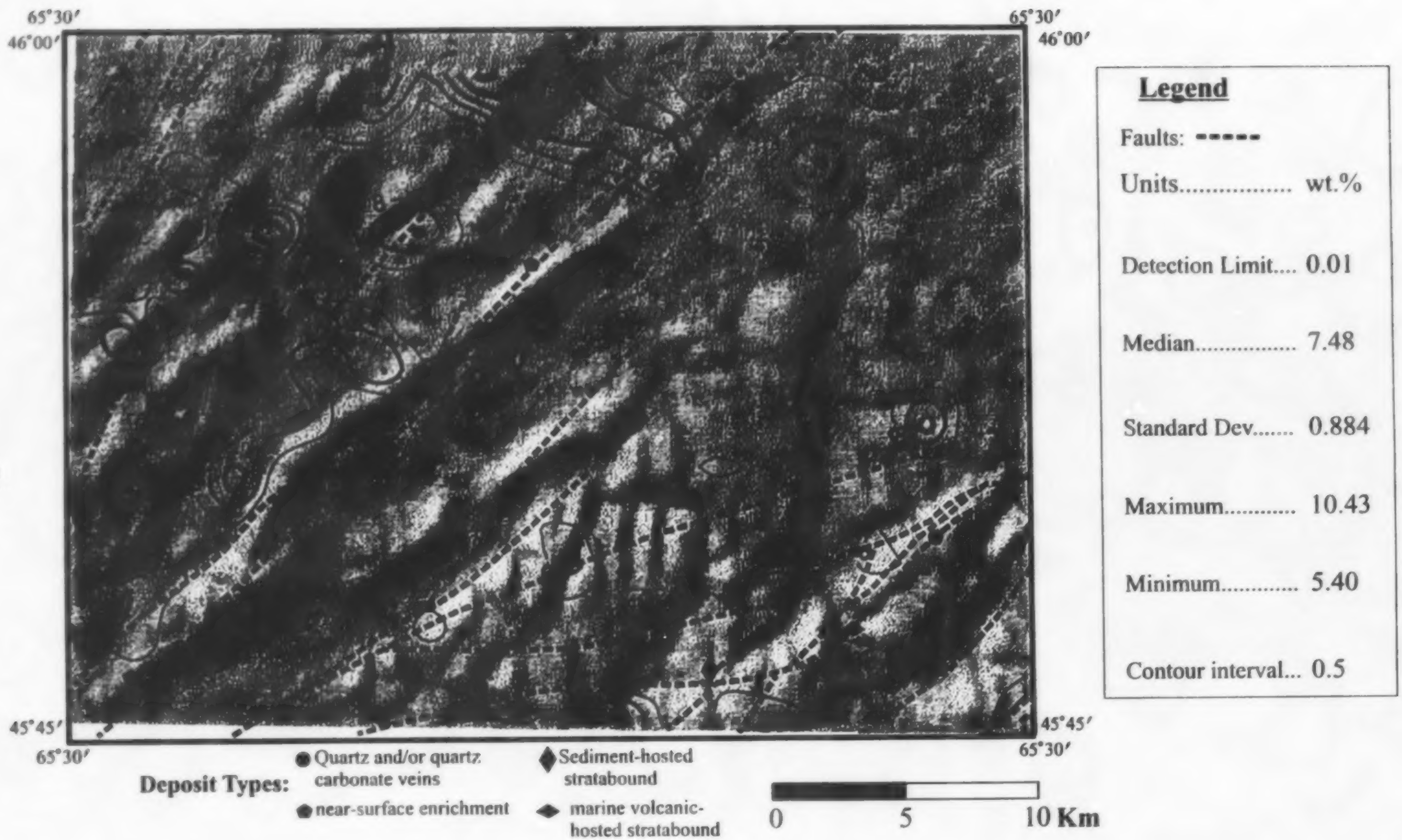

Figure 5.29: Topographic influence on aluminium dispersal in the till matrix. Geochemical contours are superimposed on a shaded elevation image generated using a Digital Terrain Model (DTM).

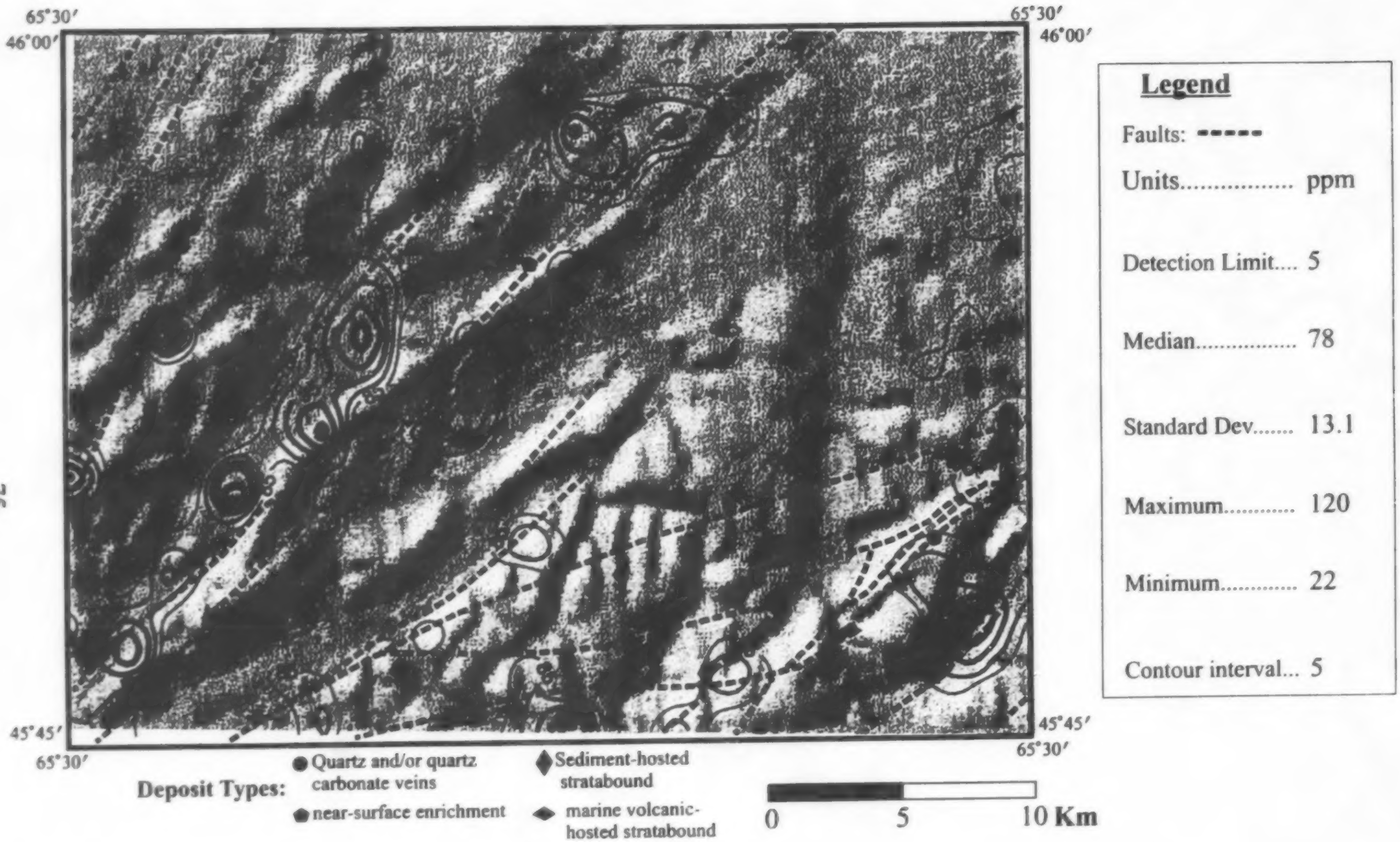

Figure 5.30: Topographic influence on chromium dispersal in the till matrix. Geochemical contours are superimposed on a shaded elevation image generated using a Digital Terrain Model (DTM).

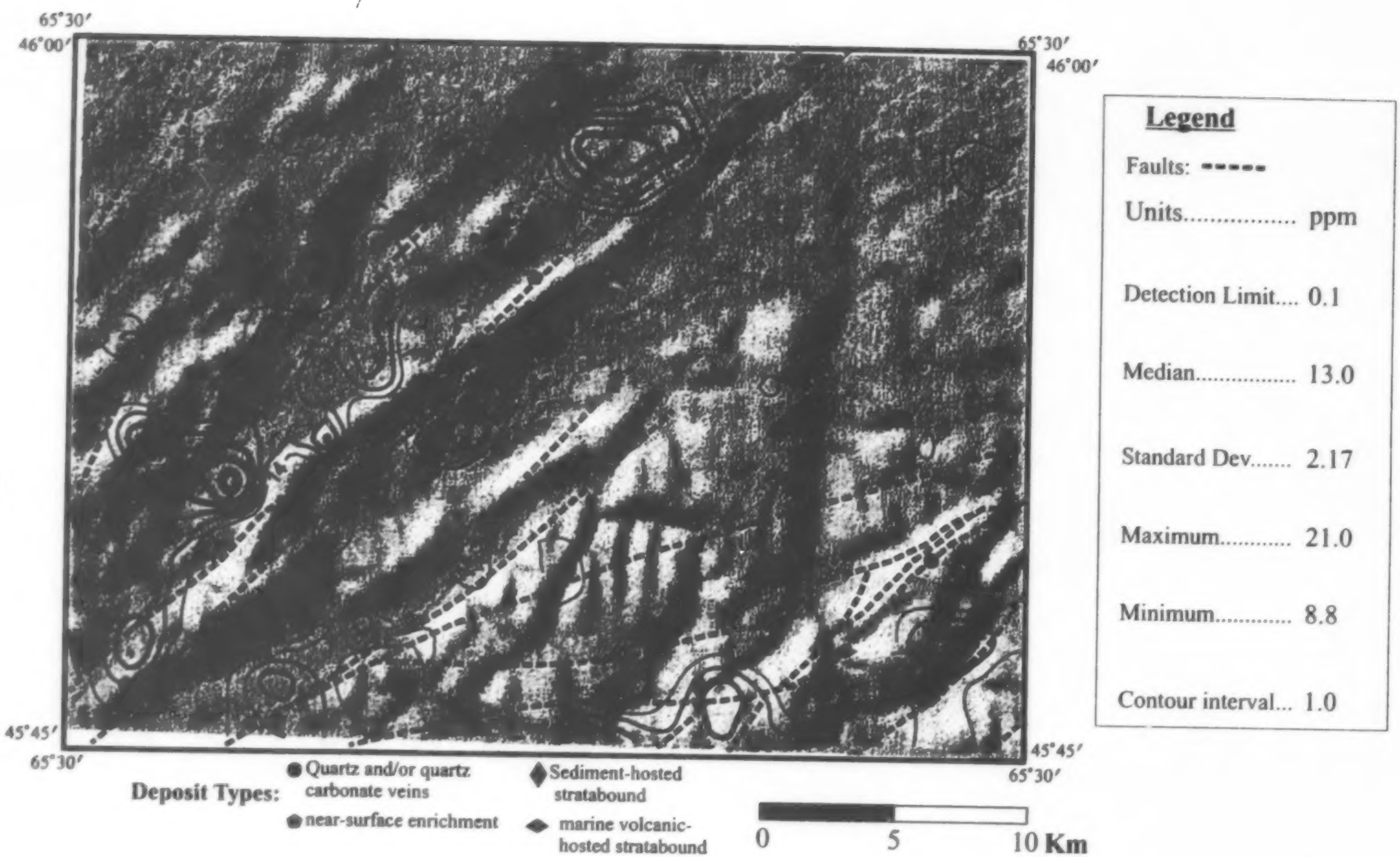

Figure 5.31: Topographic influence on scandium dispersal in the till matrix. Geochemical contours are superimposed on a shaded elevation image generated using a Digital Terrain Model (DTM).

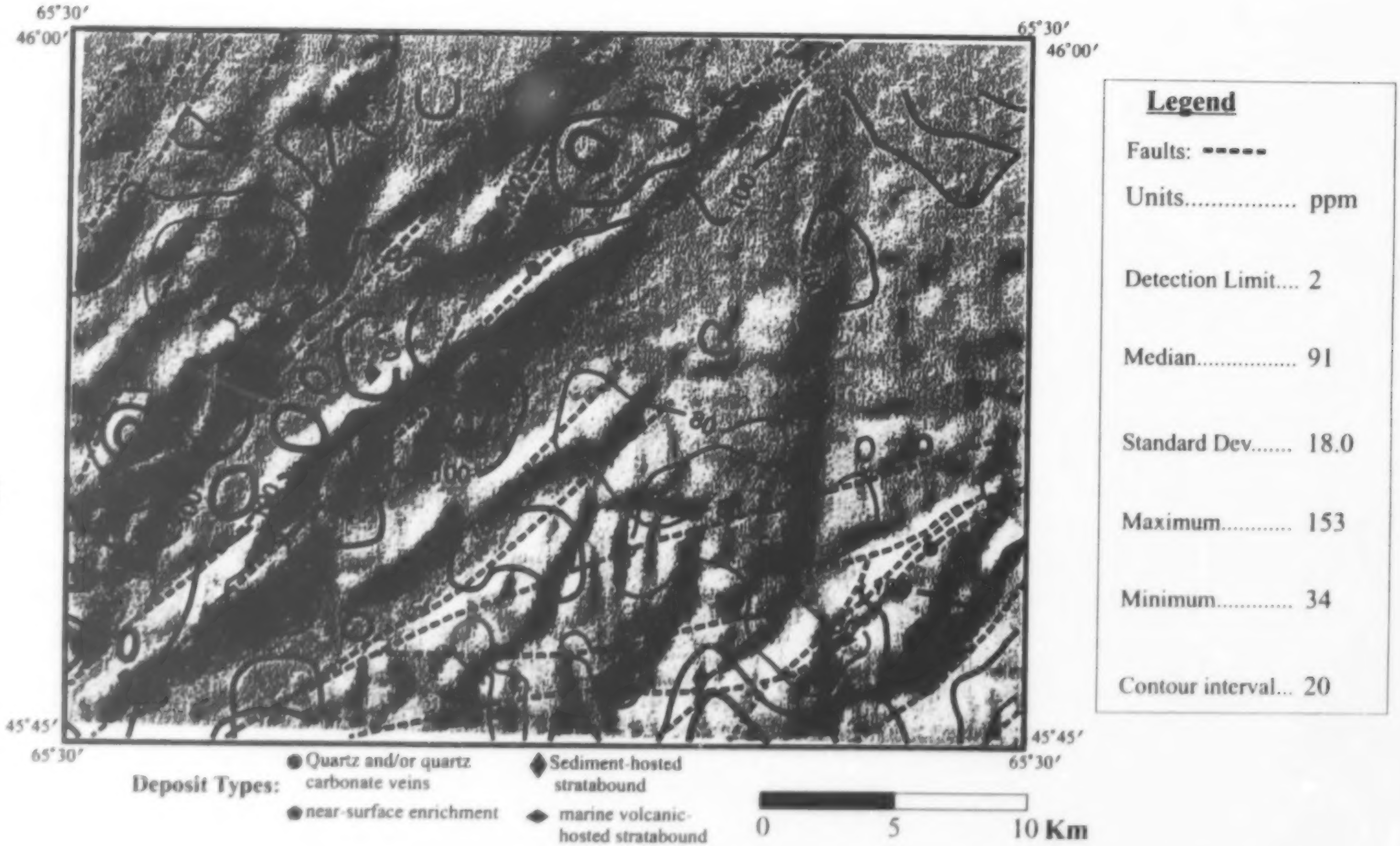

Figure 5.32: Topographic influence on vanadium dispersal in the till matrix. Geochemical contours are superimposed on a shaded elevation image generated using a Digital Terrain Model (DTM).

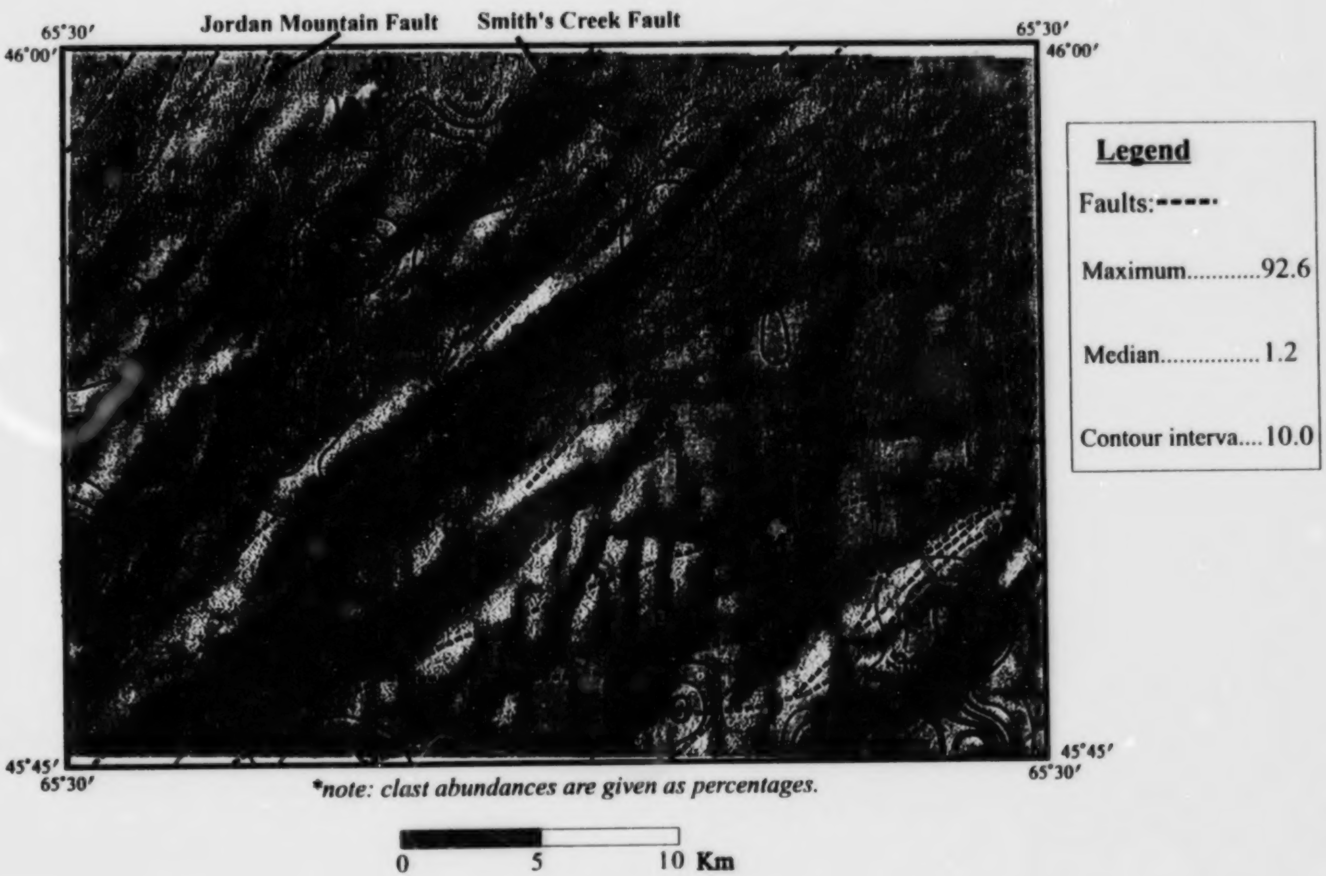

Figure 5.33: Topographic influence on granite and granodiorite clast dispersal in till. Contours of clast abundance are superimposed on a shaded elevation image generated using a Digital Terrain Model (DTM).

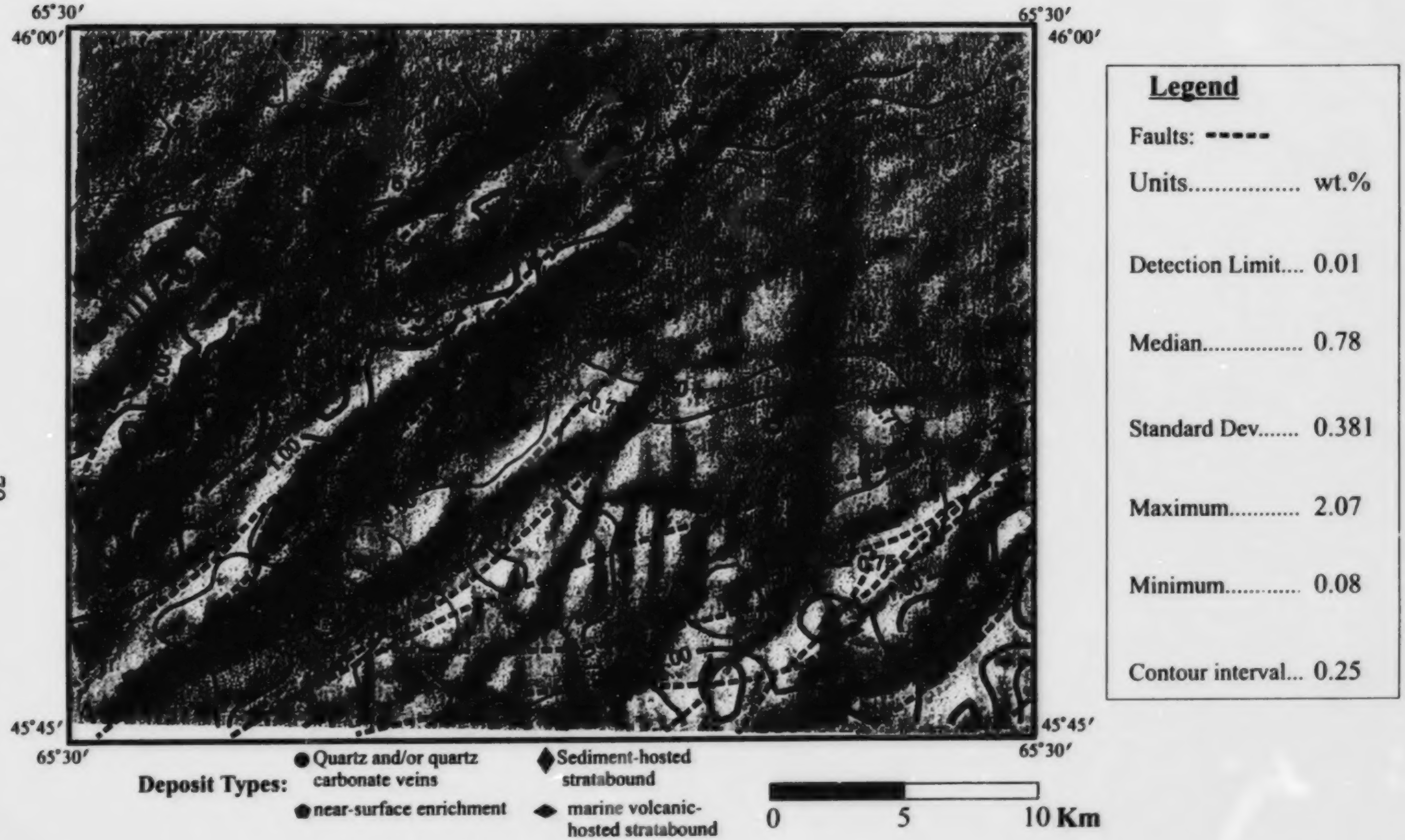

Figure 5.34: Topographic influence on sodium dispersal in the till matrix. Geochemical contours are superimposed on a shaded elevation image generated using a Digital Terrain Model (DTM).

Figure 5.35: Topographic influence on copper dispersal in the till matrix. Geochemical contours are superimposed on a shaded elevation image generated using a Digital Terrain Model (DTM).

Figure 5.36: Topographic influence on lead dispersal in the till matrix. Geochemical contours are superimposed on a shaded elevation image generated using a Digital Terrain Model (DTM).

8.0 for Windows®) was used to compare selected granulometric, lithological, and geochemical data (Appendix VI: Table VI–b).

Correlations between the physical attributes of the sample site (i.e. drainage, texture, and consistency) and the granulometric and geochemistry were also calculated. Correlation coefficients (r) with absolute values greater than 0.599, that is greater than a 35.9% correlation between the datum sets (Silk, 1979), are considered indicative of a significant association between the variables, and will be the only values discussed herein (Table 5.1).

One type of "false correlation" possibly encountered in the application of this statistical method, termed "closure", can occur when examining correlations among grouped variables that sum to a fixed total (Broster, 1986; Stumpf, 1995). Closure implies that the analysis of such data sets will display some degree of correlation, independent of the relationship between variables. In the case of the granulometric data containing three variable data sets (i.e. sand, silt, and clay) that sum to a fixed total of 100%, two of the correlations will always be negative, and one positive. Therefore, the strong negative correlation between sand and clay (-0.845) in the granulometric data suggests some degree of association between these two variables, but the influence of closure may be exaggerating the magnitude of the negative correlation (Table 5.1). However, it is possible that this correlation may be partially reflecting the process of glacial comminution contributing to the clay fraction at the expense of the sand fraction. A similar argument can be used to explain the negative correlation (-0.815) between the sand- and silt- sized fractions of the till (Table 5.1).

Table 5.1: Significant Spearman's Rank Correlation Coefficients (r) for Till Matrix Geochemistry, Till Clast Lithologies, and Selected Sample Site Charcteristics.

Additional Spearman's rank correlation coefficients are presented in Table VI-a.

	NI	CU	FE	HG	CA	MG	K	NA	AL	TH	CE	ND	EU	YB	LU	SM	V	CO	CS	Texture	Sand	Silt
NI	1																					
CU	.501(**)	1																				
FE	.483(**)	.432(**)	1																			
AS	.287(**)	-0.002	.344(**)																			
HG	-.124(*)	-.176(**)	-0.021	1																		
CA	-.147(*)	.223(**)	0.002	0.051	1																	
MG	.325(**)	.491(**)	.464(**)	-.210(**)	.157(**)	1																
K	.330(**)	0.102	.329(**)	-.323(**)	-.235(**)	.431(**)	1															
NA	-0.039	0.004	0.001	.203(**)	.487(**)	.442(**)	.140(*)	1														
AL	.367(**)	.134(*)	.688(**)	0.058	-0.036	.500(**)	.530(**)	0.086	1													
TH	0.015	-0.106	.161(**)	-0.099	-.246(**)	0.047	.464(**)	0.103	.241(**)	1												
CE	-0.021	-.138(*)	0.06	-0.065	-.229(**)	-0.013	.412(**)	.139(*)	0.108	.708(**)	1											
ND	.139(*)	0.005	.138(*)	-.131(*)	-.190(**)	-0.062	.301(**)	0.059	0.05	.481(**)	.616(**)	1										
EU	0.081	0.092	.157(**)	-0.062	-0.014	-.216(**)	0.007	-0.032	-.120(*)	.270(**)	.510(**)	.642(**)	1									
TB	0.022	-0.048	-0.086	-0.104	-.120(*)	-.210(**)	0.117	-0.117	-.160(**)	.185(**)	.261(**)	.348(**)	.316(**)									
YB	-0.03	-0.082	-0.095	-.248(**)	-.155(*)	-.322(**)	0.061	-.158(**)	-.272(**)	.127(**)	.485(**)	.526(**)	.598(**)	1								
LU	-0.081	-0.015	-0.082	-.162(**)	-0.085	-.182(**)	.136(*)	-0.02	-.274(**)	.345(**)	.447(**)	.552(**)	.495(**)	.683(**)	1							
SM	0.068	-0.053	0.024	-.123(*)	-.199(**)	-.123(*)	.352(**)	0.094	-0.042	.594(**)	.789(**)	.719(**)	.601(**)	.602(**)	.672(**)	1						
SR	0.106	.271(**)	0.102	0.01	.657(**)	.481(**)	0.097	.744(**)	0.112	-.125(*)	-0.046	0.012	0.03	-0.091	-0.014	-0.031						
V	.622(**)	.667(**)	.687(**)	-.274(**)	0.075	.522(**)	.180(**)	0.061	.505(**)	-0.047	-0.096	0.051	0.059	-0.07	-.155(*)	-0.053	1					
BR	-.223(**)	-.265(**)	0.005	.743(**)	.222(**)	0.038	-.323(**)	.298(**)	0.102	-0.119	-.164(**)	-.275(**)	-.218(**)	-.297(**)	-.149(*)	-.207(**)	-.217(**)					
CO	.694(**)	.658(**)	.678(**)	-.204(**)	0.009	.441(**)	.227(**)	-0.076	.361(**)	0.001	0.017	0.095	.163(**)	0.007	-0.05	-0.013	.649(**)	1				
CS	.310(**)	.279(**)	.401(**)	-.365(**)	-.134(*)	.558(**)	.609(**)	0.07	.449(**)	.307(**)	.203(**)	.218(**)	-0.099	-0.028	.127(*)	.187(**)	.412(**)	.328(**)	1			
RB	.268(**)	.150(*)	.402(**)	-.345(**)	-.238(**)	.342(**)	.758(**)	0.012	.502(**)	.382(**)	.342(**)	.250(**)	0.029	.190(**)	0.076	.246(**)	.436(**)	.295(**)	.635(**)			
SC	.435(**)	.497(**)	.727(**)	-.249(**)	0.063	.599(**)	.547(**)	.192(**)	.612(**)	.229(**)	.191(**)	.233(**)	.156(*)	0.012	0.055	.174(**)	.743(**)	.594(**)	.562(**)			
LA	0.048	-0.093	0.1	-.207(**)	-.345(**)	0.01	.554(**)	0.041	.179(**)	.720(**)	.890(**)	.782(**)	.606(**)	.479(**)	.548(**)	.840(**)	0.034	-0.007	.313(**)			
Texture	.283(**)	.435(**)	.299(**)	-.530(**)	-0.093	.203(**)	.172(**)	-.309(**)	.124(*)	-0.11	-.152(*)	0.019	-0.004	0.049	-0.041	-.124(*)	.479(**)	.341(**)	.407(**)	1		
Drainage	0.092	.214(**)	.149(*)	-.369(**)	-0.012	0.057	0.054	-.171(**)	0.023	-0.027	-0.048	0.09	0.058	0.064	0.012	-0.007	.250(**)	.133(*)	.212(**)	.458(**)		
Consistency	.196(**)	.272(**)	.121(*)	-.621(**)	-.130(*)	.188(**)	.347(**)	-.173(**)	0.108	0.101	0.108	.137(*)	0.043	.126(*)	0.024	0.101	.289(**)	.209(**)	.349(**)	.512(**)		
Sand	-.282(**)	-.469(**)	-.226(**)	.649(**)	0.105	-.212(**)	-.144(*)	.297(**)	-0.044	.186(**)	.179(**)	0.001	0.03	-0.092	0.003	0.112	-.485(**)	-.388(**)	-.412(**)	-.761(**)	1	
Silt	0.111	.360(**)	0.025	-.480(**)	0.067	.196(**)	-0.037	-0.042	-.164(**)	-.220(**)	-.191(**)	-0.03	-0.054	0.07	0.061	-0.085	.252(**)	.231(**)	.241(**)	.502(**)	-.815(**)	1
Clay	.345(**)	.453(**)	.325(**)	-.684(**)	-.196(**)	.194(**)	.276(**)	-.421(**)	.209(**)	-0.102	-0.111	0.027	0.005	0.092	-0.065	-0.1	.557(**)	.419(**)	.456(**)	.757(**)	-.845(**)	.417 (**)

Note: ** Correlation is significant at the 0.01 level (2-tailed)

* Correlation is significant to the 0.05 level (2-tailed)

The magnitude of the closure effect decreases as the number of variables that sum to make the final total increases (Stumpf, 1995). In both the granulometric and till clast data, their variable data sets add up to 100%, but the magnitude of the closure effect would be less significant in the till clast data due to the larger number of variables (i.e. 18) involved in their fixed total.

Only positive correlations are observed in the geochemical data (Table 5.1). Significant correlations exist between a number of the transition metals. For example, vanadium exhibits moderately strong correlations with nickel (0.622), copper (0.667), iron (0.687), scandium (0.743), and cobalt (0.649). Other correlations are found between several of the rare earth elements (Sm, Nd, Ce, Eu, Y, and Tb). Of the alkali metals, potassium displays moderate correlations with cerium and rubidium. Mercury and bromine display a moderately strong correlation (0.743), which may be attributed to the anomalous concentrations of both elements in the till overlying a large composite intrusion in the Caledonia Zone (Figure 5.17 and Appendix V: Part B: Figure 10).

No correlations are apparent between the till matrix geochemistry and clast lithologies or between the different lithologies types. Statistical comparisons between the geochemistry and the granulometric composition of the till matrix reveal that the concentration of mercury is positively correlated with the sand content of the till (0.649) and negatively correlated with the clay content (-0.604). These correlations suggest that the elevated mercury is associated with a bedrock unit(s) whose terminal grade lies predominantly in the sand-sized particle grade.

Good correlation was found between the granulometric composition and texture of the till matrix (Table 5.1). Therefore the standard loam test (Appendix III) used to

determine texture (after Zelazny et al., 1989) during field sampling provides a reliable approximation of the sand, silt, and clay content of the till matrix.

CHAPTER 6

DISCUSSION

The study of the geochemical and lithological components of till provided insight into the glacial ice-flow dynamics in the study area. Only one stratigraphic till unit and few glacial erosional features were observed; thus the direction of ice movement was inferred mainly from the areal distribution of till constituents (cf. Dreimanis and Vagners, 1969; Shilts, 1976; Gilberg, 1977; Broster, 1986; Clark, 1987; Broster and Seaman, 1991).

Dreimanis and Vagner (1969) suggested that the matrix-sized fraction of till is produced at the expense of the clast-sized fraction through the process of glacial comminution (see Chapter 2.2.3.). This relationship was not supported by the Spearman's multivariate analysis, which indicates that there is no significant correlation between the clast and matrix composition in the till. Previous studies have shown that till is often composed of sediments that have undergone multiple modes of transport and redeposition (Gilberg, 1977; Broster, 1982), which may explain the poor correlation. This interpretation is further substantiated by the relatively short transport distances for till clasts, which were probably deposited before they were significantly reduced to the matrix-sized fraction of the till. Therefore it is likely that the basal sediment load did not establish an erosive equilibrium with the underlying bedrock, but was composed mainly of pre-glacial sediment and disintegrated (highly weathered) local bedrock.

6.1. Clast Dispersal Patterns

Several of the clast dispersal trains are truncated at the boundaries of the study area. However, when the data are examined in conjunction with clast dispersal information from Munn (1995) from the Waterford map area (NTS 21 H/11) located directly to the south of the present study area, several conclusions can be drawn with respect to the regional ice-flow directions.

Similar to the results of Munn (1995), dispersal patterns of all lithologies in the study area indicate that the clast material is locally derived. Lithologic concentrations are highest near their respective bedrock sources and decrease rapidly in a down-ice direction. Clasts of felsic tuff display the longest dispersal train, trending south for approximately 15 km (Figure 5.2). Often, irregularly shaped dispersal trains were observed (e.g. mafic volcanic clasts, Figure 5.3), possibly reflecting the structural characteristics and shape of the bedrock source.

Multiple ice-flow directions are recorded by clast dispersal. In the western region of the map area, felsic volcanic clasts appear to have been transported southeastward, eastward, and northeastward from their only known bedrock source located at Jordan Mountain (Figure 5.1). However, the northeastward dispersal of felsic volcanic clasts seem to have multiple "heads" and does not conform to the idealised model of a glacial dispersal train (Shilts, 1976). The irregular shape of this dispersal train suggests that there may be unmapped felsic volcanic bedrock located somewhere northeast of Jordan Mountain. Similar felsic volcanic bedrock units found elsewhere in the region contain mineralisation; therefore, the new bedrock units implied by the erratic dispersal pattern represent potential prospecting targets.

Based on clast dispersal patterns and the local geologic setting, there are two likely source areas of unmapped felsic volcanic units northeast of Jordan Mountain. One possibility is that the two thrust faults (the Jordan Mountain Fault and Smiths Creek Fault, Figure 5.1) orientated northeast-southwest at the base of Jordan Mountain may have uplifted part of the Cambrian basement rock, exposing a felsic volcanic unit. An unmapped volcanic unit associated with the fault could explain the high abundance of felsic volcanic erratics found at considerable distances north of Jordan Mountain. A second possible source for the clasts lies in the north face of Jordan Mountain. There, immature felsic volcanic pebbles were discovered in Horton Group conglomerate indicating that pre-glacial fluvial transport and deposition during the Carboniferous period may now be obscuring the glacial dispersal pattern. Furthermore, based on the tectonostratigraphic history of the Petitcodiac area, sedimentary material in the Carboniferous was likely transported in a northeastward direction by the predominant river systems of the period (see Chapter 3.2.2.).

The high abundance of angular quartz clasts in till overlying some of the faults indicates that these faults may have acted as conduits for hydrothermal activity (Figure 5.5). A similar conclusion was reached by Clint St. Peter (1992), who suggested that faults may have acted as conduits for copper-bearing meteoric water, producing the copper deposit near Goshen (Figure 3.2, Site 6). Therefore, it is likely that there may be some local zones of mineralisation associated with the faults, which is supported by geochemical anomalies found in the till overlying faults during this study.

In the eastern half of the study area, the absence of clasts from the Caledonia Zone in the Moncton Subbasin suggests that area was not eroded by northward-moving

ice. This conclusion is supported by glacial studies by Munn (1995), who found no conclusive evidence of northward ice flow in the Waterford map area (NTS 21/H11) located immediately south of the study area. The absence of evidence supporting a late northward ice-flow event indicated that the late stage remnant ice cap on the Caledonian Highlands proposed by Chalmers (1890) and Foisy and Prichonnet (1990) did not affect the study area or was not very erosive.

The preservation of the weathered surface of a conglomerate bedrock unit near sample site E9 (Figure 1.3), and the low abundance of sedimentary clasts in till overlying the western half of the study area (Figures 5.6, 5.7), may indicate that the glacial ice was not a powerful agent of bedrock erosion locally. This suggestion is further substantiated by the poor correlation between the granulometric data (Table 5.1) and the underlying sedimentary bedrock units in this region, implying that the till in the area is not entirely composed of material derived from glacial erosion of underlying bedrock. Conversely, in the eastern half of the study area, grey sandstones (Figure 5.8) are abundant in the overlying till. Furthermore, in the east the till has a high sand content, possibly indicating that glacial comminution of the sedimentary clasts was the dominant process contributing to the till matrix.

The apparent regional variation on the erosive power of the glacial ice may be explained by the presence of a "contaminating layer" at the basal ice/bedrock interface (Drewry, 1986, p. 53). During pre-glacial times a thick blanket of sediments likely covered the wide "U-shaped" valleys in the western half of the study area. When the ice sheet advanced into this region, the basal ice probably entrained large volumes of the thick sediment blanket. For ice travelling over most bedrock types, glacial erosion by

basal ice is greatest when the debris concentration is about 10 to 30% by volume (Drewry, 1986, p.54). When the debris concentration is above this range, the particle content begins to significantly stiffen the basal layer, reducing creep and erosion rates. Therefore, the thick blanket of pre-glacial sediments may have impeded glacial dispersal of the sedimentary bedrock units lining the bases of these valleys.

6.2. Geochemical Dispersal Patterns

6.2.1. Ice-flow Directions

Generally, geochemical dispersal trains are short (<10 km), and irregularly shaped. The heads or maximum concentrations of dispersal trains often correspond with known mineral occurrences, geochemically unique bedrock units, or structural trends. The dominant dispersal direction varies up to 45° degrees, probably reflecting the influence of topography on ice flow.

In the western half of the map area, dispersal trains appear to follow the Smiths Creek valley (Figure 1.4), forming ribbon-shaped anomalies that are elongated toward the southwest and northeast (e.g. Figures 5.12, 5.14). The dispersal of sodium suggests that ice was deforming around the northwest edge of the Anagance Ridge (Figure 5.34).

In the north-central section of the study area, geochemical dispersal trains that occur in close proximity to the Anagance Ridge (Figure 5.28) appear to be diverted from a southeasterly trend toward a more easterly direction (Figures 5.30, 5.31, 5.32). An aluminium dispersal train located approximately 2 km northeast of the ridge does not deviate significantly from its southeasterly trend, producing the longest geochemical anomaly (Figure 5.29). The aluminium dispersal train does not encounter any significant

topographic features; therefore, it is free of topographic influences and probably records the regional ice-movement direction.

In the eastern half of the study area, geochemical dispersal trains from known mineral occurrences in the Caledonia Zone are elongated toward the southeast. All three deposits in the Caledonia Zone (Figure 3.2, Sites 6, 7, 8) show geochemical anomalies of mercury, copper, lead, or zinc in the overlying till (Figures 5.17, 5.18, 5. 19, 5.20).

6.2.2. Mineral Potential and Coincident Anomalies

Genetic models for mineral deposit types can serve as valuable guides to mineral exploration. They provide information about the typical geologic setting, host rocks, associated rocks, and mineral phases present for most deposit types. Therefore, the bedrock and structural geology of the project area can be used as a first approximation of the mineral potential for the study area, and may aid in the determination of which till geochemical anomalies represent important indicators of local mineral potential.

The tectonostratigraphic history of the Moncton Subbasin (see Chapter 3.2.2), suggests there is potential for mineralisation in the study area. Diagenesis during sedimentation under semi-arid or arid conditions in basinal environments may produce syngenic enrichment in sedimentary rocks. Examples of syngenic mineral deposit types associated with a similar basinal setting to that of the Moncton Subbasin include Mississippi Valley Type Pb-Zn (Sangster, 1984a), Sandstone Lead (Sangster, 1984b), Sedimentary Copper (Kirkham, 1984), and Sediment Hosted Barite (Lydon and Dawson, 1984).

The fault-controlled or thermal-related subsidence that occurred in the Moncton Subbasin (St. Peter, 1992) could also have produced mineralisation in the study area.

Basinal subsidence can produce epigenic enrichment of sedimentary strata, forming deposit types such as the Cu, Pb sedimentary exhalative (Sedex) deposits (Lydon, 1995). St. Peter (1992) has suggested that copper and barite occurrences in the Moncton Subbasin are related to fluid migration within fault zones. This may indicate that epigenetic mobilisation of metals occurred during subsidence.

Anomalous concentrations of several elements are found in the till matrix overlying faults. The most notable examples include barium, lead, and zinc concentrations in the Jordan Mountain area (Figures 5.10, 5.19, 5.20). Given the tectonostratigraphic history of the Petitcodiac area, these three elements may be valuable indicators for Mississippi Valley Type Pb-Zn (Sangster, 1995) and Sedimentary Exhalative (Sedex) deposits (Lydon, 1995).

6.3. Striae and Streamlined bedrock features

In the eastern half of the study area, striae indicate that the dominant ice-flow direction varied between south-southwest and southeast (Figure 5.26). These ice-flow directions are well documented in southeastern New Brunswick (Rampton et al., 1984; Foisy and Prichonnet, 1991; Seaman, 1991; Munn, 1995; Munn et al., 1996). Based on the model proposed by Rampton et al. (1984), the ice movement could have been associated with the expansion of the Escuminac Ice Centre near the north end of Prince Edward Island during the Chignecto phase approximately 15 to 18 ka.

Two striae sites in the Moncton Subbasin show multiple flow directions. Cross-cutting relationships among striae at these sites record a counter-clockwise shift in ice-flow from the south toward the northeast (Figure 5.27, Sites 1, 2). Using the Rampton et al. (1984) model, these striae sets may record the gradual expansion of the Gaspereau Ice

Centre located to the west of the study area in the interior of New Brunswick. Thus, as the Gaspereau Ice Centre expanded during the Bantalor phase (sensu stricto Rampton et al., 1984) approximately 14 ka, the flow direction probably underwent a gradual shift from southeast toward the east or northeast in the study area.

Striae sites at higher elevations (i.e. in the Caledonia Zone, Figure 5.29) record only the south-southwest to southeasterly ice movement, which is likely associated with ice from the Escuminac Ice Centre during the Chignecto phase approximately 15 to 18 ka. (Rampton et al., 1984). No evidence of the late stage eastward or northeastward ice-flow event was found in the Caledonia Zone, suggesting that ice during this time was too thin to override and scour the Caledonia Zone.

Streamlined bedrock features found in the western part of the study area indicate that ice flowed around the Anagance Ridge (Figure 5.27). The diversion of ice flow around the ridge suggests that the ice was probably thin and flowing under topographic control and erosive at some time during last glacial period.

6.4. Ice-flow Dynamics

Both the dispersal data and glacial erosional features indicate that topography significantly influenced ice flow. Generally, shifts in ice-flow direction appear to be related to fluctuations in the ice thickness. To simplify the discussion of the evolution of ice-flow dynamics during the Late Wisconsinan, the glacial history of the Petitcodiac map sheet area is divided into three stages. When possible, the ice-flow stages will be discussed in the context of the New Brunswick ice sheet model proposed by Rampton et al. (1984).

6.4.1. Stage 1: Glacial Advance

During stage 1, glacial ice advanced into the study area. The shape of the glacier is unknown, but it is likely that the ice sheet was thin and flowed under topographic control. This stage is not preserved in the glacial erosional record. During this stage, ice probably moved over disintegrated bedrock and thick pre-glacial sediments and would have had limited contact with competent bedrock capable of preserving striae. According to Rampton et al. (1984), glacial advance may have occurred at the onset of the Chignecto phase, approximately 18 ka.

6.4.2. Stage 2: Glacial Maximum

During stage 2, ice became sufficiently thick to override the Caledonia Zone and establish a regional ice-flow pattern that varied between south-southwestward to southeastward over the entire area. This may have occurred during the Chignecto phase of Rampton et al. (1984), approximately 15 to 18 ka. Most of the glacial dispersal in the Caledonia Zone occurred during this stage.

At the onset of stage 2, ice from the Escuminac Ice Centre likely expanded across the study area, eventually establishing a regional southwesterly ice-flow direction (Figure 6.1). Gradually the regional ice-flow direction shifted as the Gaspereau Ice Centre expanded, diverting ice flowing from the Escuminac Ice Centre toward the southeast.

In the western half of the area, there is little evidence of a regional ice-flow direction. The thick pre-glacial sediments in the valleys may have compromised the erosive power of the ice sheet, or basal ice may have continued to flow around the Anagance Ridge under topographic control.

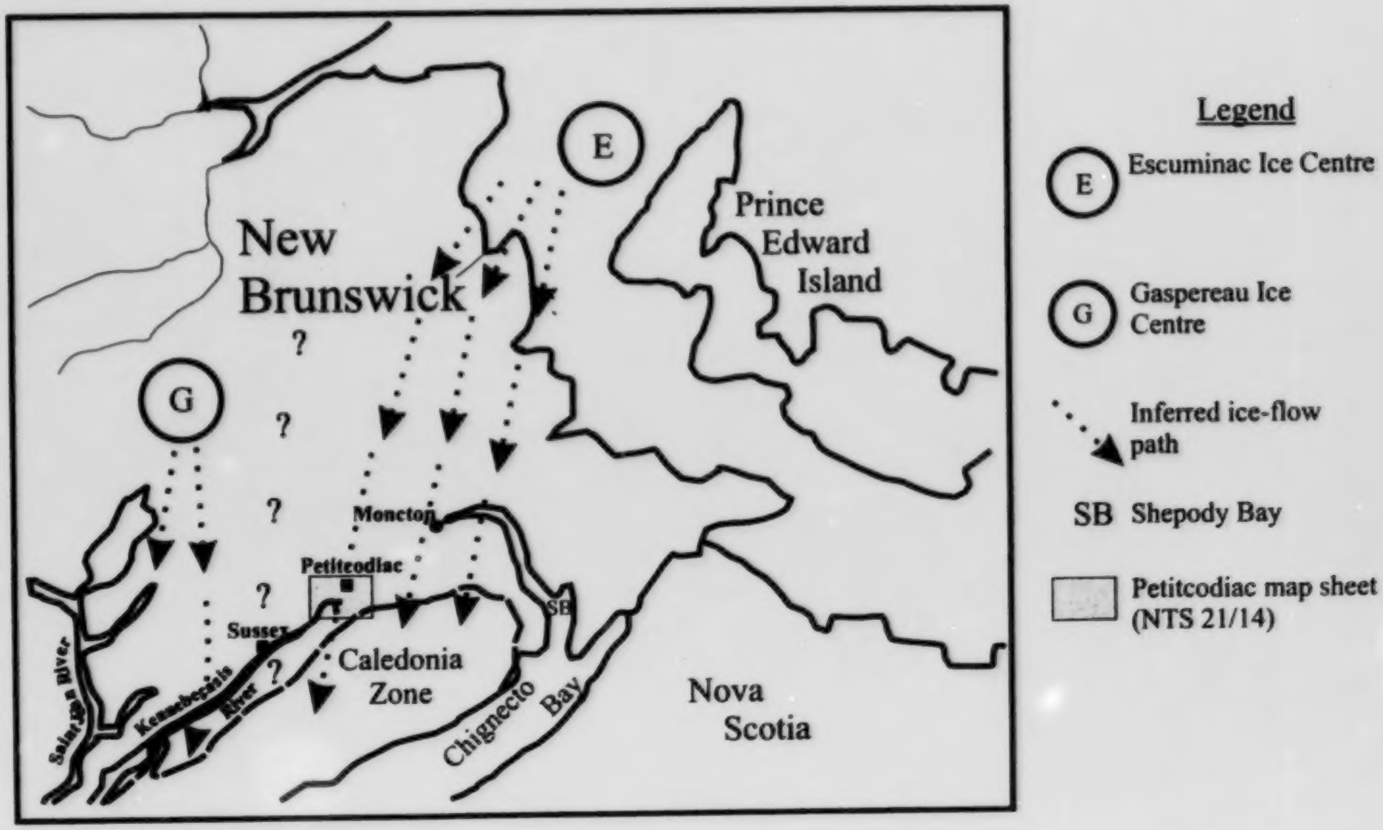

Figure 6.1: Ice sheet flow dynamics during glacial maximum (position of ice centres based on Rampton et al., 1984).

6.4.3. Stage 3: Retreat of the Escuminac Ice Centre

Near the conclusion of the Chignecto phase, approximately 14 ka., sea level began to rise, marking the retreat of the Escuminac Ice Centre (Rampton et al., 1984). Gaspereau ice likely advanced into the study area as the Escuminac ice retreated northeastward toward its centre near Prince Edward Island (Figure 6.2). Once the Gaspereau Ice Centre reached its maximum extent, it probably overrode most of the Petitcodiac map area, shifting the local ice movement from southeast toward a more easterly direction. However, based on present striae data, it is unlikely that the eastward moving ice from the Gaspereau Ice Centre was thick enough to completely override the Caledonia Zone; consequently ice was flowing under topographic control (Chapter 6.3). According to Rampton et al. (1984) the Gaspereau Ice Centre reached its maximum extent during the Bantalor phase 13.3 to 13.5 ka.

6.4.4. Stage 4: Late Stage Deglaciation

The rise in sea level may have eventually triggered the formation of a calving margin in the Bay of Fundy, causing thinning of the ice sheet in southeastern New Brunswick. Eventually the calving margin probably migrated northward up the Bay of Fundy and into Chignecto Bay (Figure 1.1). Drawdown on the ice sheet caused by rapid ice calving into Chignecto Bay may have began pulling ice northeastward around the Caledonia Zone and into the Bay of Fundy (Figure 6.3). When the ice sheet became too thin (<500 m) to override the Caledonia Zone, an ice-flow divide developed as ice streamed around its northwestern slope (Figure 1.2). The ice-flow divide would have separated ice moving south-southwest down the Kennebecasis River valley from ice moving northeast around the northern end of the Caledonia Zone toward Chignecto Bay.

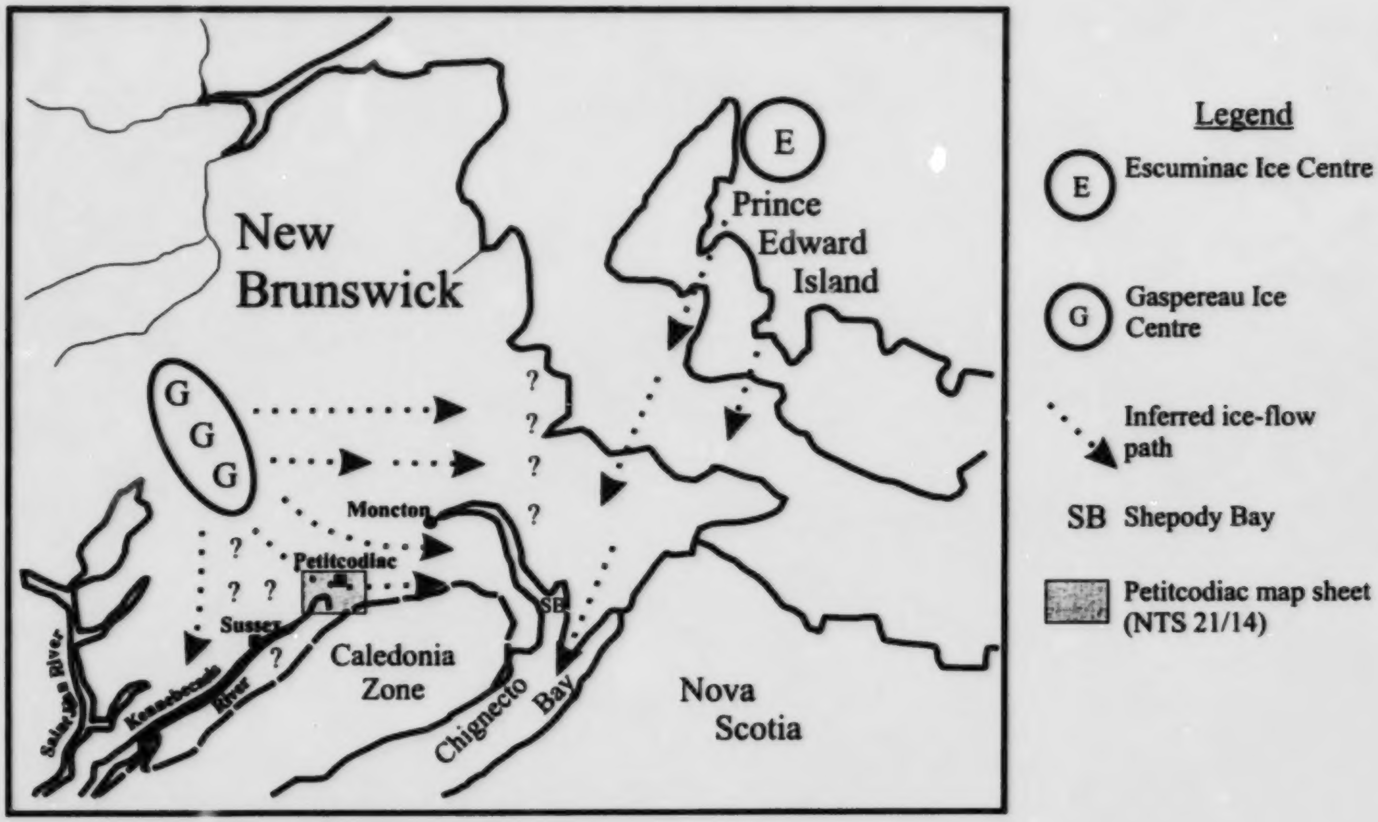

Figure 6.2: Ice sheet flow dynamics during the retreat of the Escuminac Ice Centre (position of ice centres based on Rampton et al., 1984).

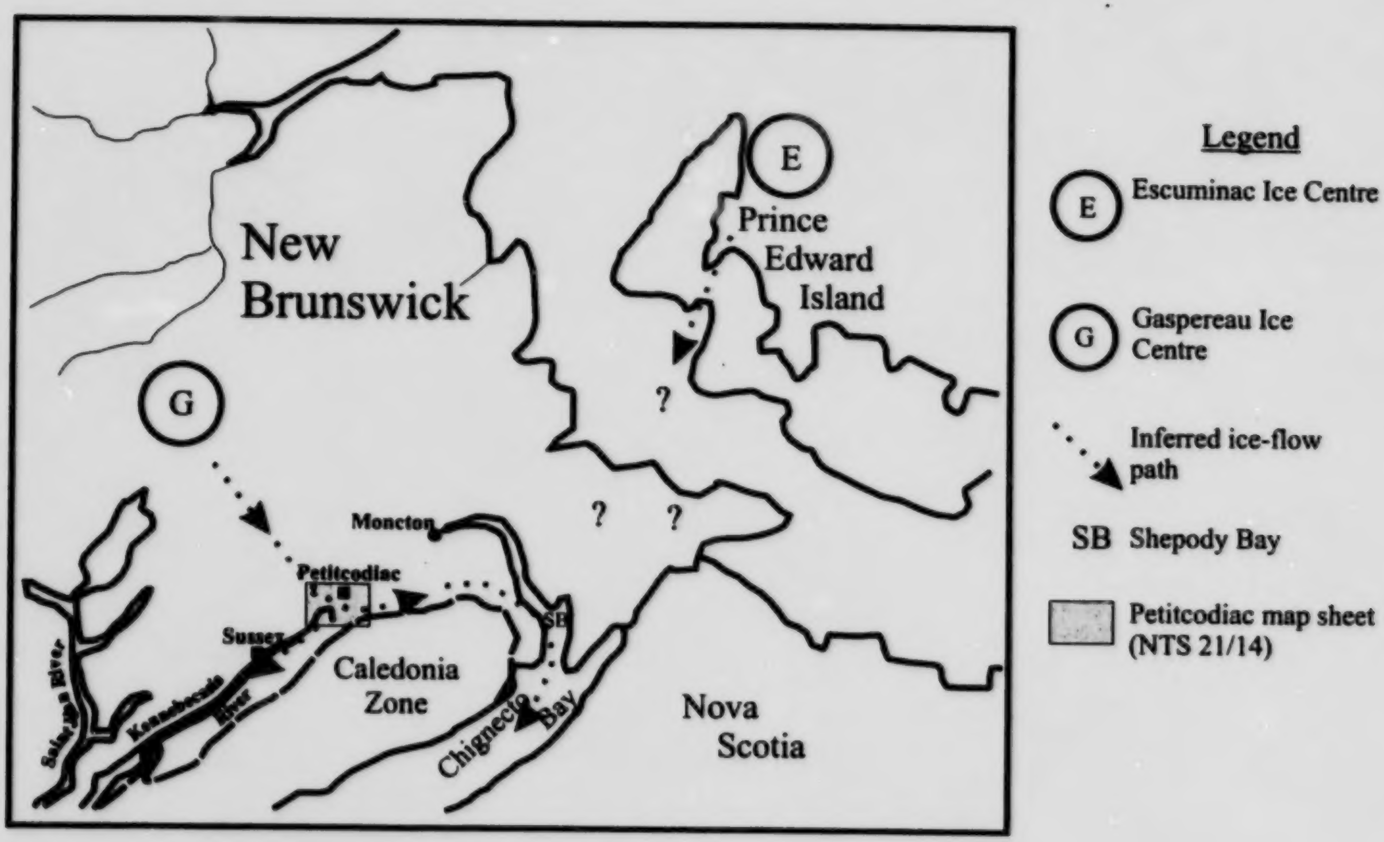

Figure 6.3: Ice sheet flow dynamics during late stage deglaciation (position of ice centres based on Rampton et al., 1984).

Figure 6.4: Glacial flow pattern in the Petitcodiac map area (21 H/14) during deglaciation. The dashed line denotes the approximate position of an "ice-flow divide".

Within the western half of the map area, ice movement once again flowed around Jordan Mountain and the Anagance Ridge under topographic control (Figure 6.4).

Based on the topographic influence evident in the dispersal pattern outside of the Caledonia Zone, it is likely that significant glacial erosion and till deposition occurred during this phase. Glaciofluvial ice-contact stratified drift and ablation moraine are limited mainly to valleys, indicating that the ice may have remained active during deglaciation with melting of the ice sheet being facilitated by the flooding of low-lying valleys with sea water. Deglaciation likely proceeded slowly under active ice conditions to provide sufficient time to produce the well-defined east-southeast to eastward-trending glacial dispersal trains thought to be associated with stage 3. Eastward dispersal and valley melting support an ice-flow model proposed by Prest (1970), Stea (1984), Stea and Mott (1989), and Stea et al. (1998), suggesting a slow glacial retreat during deglaciation in the Bay of Fundy region, with approximately 40 m of isostatic rebound in the Petitcodiac area and 20m to 30m in the Chignecto Bay area. Due to delayed crustal isostatic re-equilibration, because of continued removal of the ice mass that occurred during glacial retreat, significant encroachment of the sea accompanied deglaciation (Stea et al., 1998). The gradual encroachment of the sea probably accelerated the calving rates in Chignecto Bay, possibly increasing ice-flow velocities.

CHAPTER 7

CONCLUSIONS

The glacial erosional features examined are believed to record the events of the Late Wisconsinan Glaciation. The absence of glacial erosional features predating the regional ice-flow event in the study area suggests that the earlier glacial advance was either: 1) cold-based and none erosive; 2) vary rapid; or 3) completely overprinted by later glacial movements. However, the presence of preserved weathered bedrock surfaces under till in several areas indicates it is unlikely that subsequent glacial movements during the Late Wisconsinan were erosive enough to completely overprint all evidence of a highly erosive glacial advance.

Mapping of geomorphological ice–flow indicators suggests that there were several fluctuations in the ice-flow dynamics during the last period of glaciation. Glacial erosional features and dispersal data record multiple ice-flow directions implying that ice-flow movement in the Petitcodiac area was complex. However, the stratigraphic continuity of the till unit demonstrates that only one stratigraphic till sheet is present at surface. This is interpreted to be the result of fluctuations in ice-flow direction that occurred gradually under continuous ice cover.

Characterisation of the areal distribution of lithological and chemical components of the till in the Petitcodiac map area was instrumental for modelling local deviations in flow patterns as well as till matrix and clast dispersal. Generally, till clast and geochemical dispersal distances are short (<10 km) within the study area, with the head of the dispersal train occurring near an identifiable bedrock source. Most dispersal trains

are irregularly shaped, possibly reflecting the shape and structure of the source. Felsic volcanic clast dispersal patterns suggest that there may be unmapped bedrock sources located northeast of Jordan Mountain.

Several till geochemistry anomalies appear to be associated with faults, suggesting they may be local sources of mineralisation. Coincident geochemical anomalies of lead, zinc, and barium in the till matrix may be glacially dispersed from unidentified zones of local mineralisation related to Mississippi Valley Type (MVT) Pb-Zn or Sedimentary Exhalative (SEDEX) deposits.

In the Caledonia Zone, striae and dispersal data record a regional ice-flow direction ranging from south-southwest to southeast. This suggests that the portion of the Caledonia Zone within the study area was overridden by glacial ice during the glacial maximum.

In the Moncton Subbasin, two striae sites record a counter-clockwise rotation in the ice-flow direction from south-southeast toward the northeast. Clast and till matrix dispersal patterns in the Moncton Subbasin vary between east-southeast and eastward. Cross-cutting relationships in the striae record indicate the east-southeast and eastward flow events occurred following the southeastward regional ice-flow. No evidence of late eastward deviation from the regional ice–flow direction is found at higher elevations, suggesting that the till at lower elevations continued to be transported and deposited sometime after the glacial maximum.

The gradual northeasterly shift in ice-flow direction in the Moncton Subbasin can be attributed to the increasing influence of local topography on a thinning ice sheet during deglaciation. Encroachment of the sea possibly initiated ice calving in Chignecto

Bay, causing local drawdown on the ice sheet toward the northeast. Thin ice (<500 m thick) was probably diverted by topography, creating an ice-flow divide separating ice streaming around the Caledonia Zone (Figure 6.3) toward Chignecto Bay from ice moving south-southwest down the Kennebecasis River valley.

A significant statistical correlation was found between sample sites with a sand-rich till matrix and high mercury concentrations in the minus 63 μm fraction of the till, possibly reflecting the terminal grade of the source lithology. Evaluation of the precision and accuracy of the sampling procedures and instrumental analyses show that the minus 63 μm fraction of the till is an acceptable sampling medium for characterising the geochemistry of the till matrix.

As a result of this study, indications of northward flow in the northeastern part of the study area are attributed to deviation of southeastward flowing regional ice around the Caledonia Highlands and not attributed to a separate flow event as suggested by previous workers.

REFERENCES

Aalund, H. and Wicklund, R. E. 1950. Soil survey report of southeastern New Brunswick. Third Report of the New Brunswick Soil Survey, Dominion Department of Agriculture, 108 p.

Agriculture Canada Expert Committee on Soil Survey 1987. The Canadian System of Soil Classification, 2nd ed. Agriculture Canadian Publication, Ottawa, 1646, 164 p.

Balzer, S. A., and Broster, B. E. 1994. Comparison of clast and matrix dispersal in till: Canterbury area, New Brunswick. Atlantic Geology, **30**: 9–17.

Berrow, M. L. and Mitchell, R. L. 1991. Trace elements in soil profiles: total contents of particle-size separates. Transactions of the Royal Society of Edinburgh, **82**: 195–209.

Bolviken, B. and Gleeson, C. F. 1979. Focus on the use of soils for geochemical exploration in glaciated terrane; *In* Geophysics and Geochemistry in the Search for Metallic Ores. *Edited by* Peter J. Hood; Geological Survey of Canada, Economic Report 31, pp. 295–326.

Bostock, 1970. Physiographic subdivisions of Canada. *In* Geology and economic minerals of Canada. *Edited by* R.J.W. Douglas. Geological Survey of Canada, Economic Geology Report 1, pp. 10–42.

Bouyoucos, G. J. 1962. Hydrometer method improved for making particle size analysis of soils. Agronomy Journal, **54**(5): 464–465.

Bradley, D. C. 1982. Subsidence in Late Paleozoic basins in the northern Appalachians. Tectonics, **1**: 107-123.

Broster, B. E. 1982. Compositional variations in the St. Joseph till units of the Goderich area, Ontario. Ph.D thesis, University of Western Ontario, London, Ontario, 103 p.

-------------- 1986. Till variability and compositional stratification: examples from Port Huron lobe. Canadian Journal of Earth Sciences, **23**: 1823–1841.

Broster, B. E. and Dreimanis, A. 1981. Deposition of multiple lodgement tills by competing glacial flows in a common ice sheet, Cranbrook, British Columbia. Arctic and Alpine Research, **13**(2): 197–204.

Broster, B. E. and Huntley, D. H. 1995. Effective low-cost reconnaissance drift prospecting in area of variable terrain: An example from the south-east Taseko Lakes area, central British Columbia. *In* Drift Exploration in the Canadian Cordillera. *Edited by* P. T. Bobrowsky, S. J. Sibbick, J. M. Newell, and P. F Matysek. Canadian Cataloguing in Publication Data. Mineral Resources Division, Geological Survey Branch, Paper 1995-2, pp. 121–126.

Broster B. E. and Seaman, A. A. 1991. Glacigenic rafting of weathered granite: Charlie Lake, New Brunswick. Canadian Journal of Earth Sciences, **28**: 649–654.

Chalmers, R. 1884. Report on the surface geology of western New Brunswick with special reference to the area included in York and Carleton Counties. Geological Survey of Canada, Report of Progress, 1882–1884, Part XI.

---------------- 1885. Preliminary report on the surface geology of New Brunswick. Geological and Natural History of Canada, Annual Report: **1,** Part GG, 58 p.

---------------- 1890. Surface geology of southern New Brunswick. Geology Canada, Summary Report 1889, **4,** Part N, 92p.

---------------- 1895. Report on the surface geology of eastern New Brunswick, northwestern Nova Scotia and a portion of Prince Edward Island. Geological Survey of Canada, Annual Report 1894, **7,** Part M, 135 p.

---------------- 1902. Report on the surface geology shown on the Fredericton and Andover quarter-sheet maps, New Brunswick. Geological Survey of Canada, Annual Report 1899, **12,** Part M, 41 p.

Clark, P. U. 1987. Subglacial sediment dispersal and till composition. Journal of Geology, **95**: 527–541.

Coker, W. B. and DiLabio, R. N. W. 1989. Geochemical exploration in glaciated terrain: geochemical responses. *In* Proceedings of Exploration '87. *Edited by* G. D. Garland. Third Decennial International Conference on Geochemical Exploration for Minerals and Groundwater. Ontario Geological Survey, Special Volume 3, pp. 336–383.

David, P. P. and Lebuis, J. 1985. Glacial maximum and deglaciation of western Gaspé, Québec, Canada. Geological Society of America, Special Paper 197, pp. 85–109.

DiLabio, R. N. W. 1988. Residence sites of gold, PDE and rare lithophile elements in till. *In* Prospecting in areas of glaciated terrain-1988. *Edited by* D. R. MacDonald and K. A. Mills. Canadian Institute of Mining and Metallurgy. Department of Mines and Energy, Halifax, Nova Scotia, pp. 121–140.

Dreimanis, A. 1976. Tills: their origin and properties. *In* Glacial Till: an Interdisciplinary Study. *Edited by* R. F. Legget. Royal Society of Canada Special Publications, Ottawa, **12**, pp. 11–49.

Dreimanis, A. and Fenton, M, M. 1976. Method of stratigraphic correlation of till in central and western Canada. *In* Glacial Till, an Interdisciplinary Study. *Edited by* R. F. Legget. Royal Society of Canada Special Publications, Ottawa, **12**, pp. 67–82.

Dreimanis, A. and Vagners, U. J. 1969. The effect of the lithology upon the texture of till. *In* Quaternary Geology and Climate. *Edited by* H. E. Wright Jr. National Academy of Science, Publication 1701, Washington, D.C., pp. 93-98.

-- 1971. Bimodal distribution of rock and mineral fragments in basal till. *In* Till, a Symposium. *Edited by* R. P. Goldthwait. Ohio State University Press, Columbus, OH, pp. 237–250.

Drewry, D. J. 1986. Glacial Geologic Processes. Edward Arnold, London, 276 p.

Flint, R. F. 1951. Highland centers of former glacial outflow in northeastern North America. Geological Society of America Bulletin, **62**: 21–38.

Foisy, M. and Prichonnet, G. 1991. A reconstruction of glacial events in southeastern New Brunswick. Canadian Journal of Earth Sciences, **28**: 1594–1612.

Gilberg, G. 1977. Redeposition: a process in till formation. Geologiska Föreningens i Stockholm Förhandlingar, **99**: 246–253.

Goldschmidt, V. M. 1937. The principles of distribution of chemical elements in minerals and rocks. Journal of the Chemical Society, **1937**: 655–673.

-------------------------- 1954. Geochemistry, Oxford University Press, 730 p.

Grant, D. R. 1977. Glacial style and ice limits, the Quaternary stratigraphic record in the Atlantic Province, Canada. Géographie physique et Quaternaire, **XXXI**: 247–260.

Hamilton, J. B. and Caroll, D. J. J. 1975. Sand and gravel in New Brunswick. New Brunswick Department of Natural Resources Branch, Report of Investigation No. 16, 107 p.

Hornibrook, E. R. C., Broster, B. E., Gardner, W. W., and Pronk, A. G. 1991. Glacial dispersal of heavy minerals in the late Wisconsinan till, central New Brunswick. Atlantic Geology, **27**: 199–208.

Hughes, T., Borns, Jr. H. W., Fastook, J. L., Hyland, M. R., Kite, J. S. and Lowell, T. V. 1985. Models of glacial reconstruction and deglaciation applied to Maritime Canada and New England. *In* Late Pleistocene History of the Northeastern New England and Adjacent Québec. *Edited By* H.W. Borns, Jr., P. LaSalle, and W.B. Thompson, Geological Society of America, Special Paper 197, pp. 139–150.

Kauranne, K., Salminen, R and Erikson, K. 1992. Regolith exploration geochemistry in arctic and temperate terrains. *In* Handbook of Exploration Geochemistry. *Edited by* G. J. S. Govett. Elsevier, Amsterdam, 5, 443p.

Kirkham, R. V. 1984. Sedimentary Copper. *In* Canadian Mineral Deposit Types: A Geologic Synopsis. *Edited by* O. R. Eckstrand. Geologic Survey of Canada, Economic Geology Report 36, pp. 27.

Levinson, A. A. 1974. Introduction to Exploration Geochemistry. Applied Publishing Ltd., Matwood, Illinois, 614 p.

Lydon, J. W. 1995. Sedimentary exhalative sulphides (Sedex). *In* Geology of Canadian Mineral Deposit Types. *Edited by* O. R. Eckstrand, W. D. Sinclair, and R. I. Thorpe. Geological Survey of Canada, Geology of Canada, 8, pp. 130–152.

Lydon, J. W. and Dawson, K. R. 1984. Sediment-hosted barite. *In* Canadian Mineral Deposit Types: A Geologic Synopsis. *Edited by* O. R. Eckstrand. Geologic Survey of Canada, Economic Geology Report 36, pp. 36.

Matthew, G. F. 1872. On the surface geology of New Brunswick. Canadian Naturalist, New Series: VI, pp. 89–107.

------------------ 1879. Report on the superficial geology of southern New Brunswick. Geological Survey of Canada, Report of Progress 1877-1878, Part X, 36p.

McLeod, M. J., Johnson, S. C. and Ruitenberg, A. A. 1994. Geological map of southeastern New Brunswick. New Brunswick Department of Natural Resources and Energy, Mineral Resources, Map NR-6. Scale 1:250 000.

Merlini, S. (Comp) 1998. New Brunswick computerised mineral occurrence database (revised 1998). New Brunswick department of Natural Resources and Energy, Minerals and Energy Division, Open File 98-21, digital mineral occurrence files.

Munn, M. D. 1995. Till lithology and geochemistry in the Waterford area, New Brunswick. New Brunswick Department of Natural Resources and Energy, Mineral Resources, Open File Report 95-6, 170 p.

Munn, M. D., Broster, B. E. and Pronk A. G. 1996. Geochemical dispersion in till: Waterford area, New Brunswick. Atlantic Geology, **32**: 269–279.

Nichol, I. and Bjorklund, A. 1973. Glacial geology as a key to geochemical exploration in areas of glacial overburden with particular reference to Canada. Journal of geochemical Exploration, **2**: 133–170.

Pangano, M. and Gauvreau. 1993. Principles of Biostatistics. Wadsworth Publishing Company, California, 524 p.

Prest, V. 1970. Quaternary geology of Canada. *In* Geology and economic minerals of Canada. *Edited by* R. J. W. Douglas. Geologic Survey of Canada Economic Geology Report 1, pp. 676–764.

Pronk, A. G., Bobrowsky, P. T. and Parkhill, M. A. 1989. An interpretation of Late Quaternary glacial flow indicators in the Baie Des Chaleurs Region, Northern New Brunswick. Géographie physique et Quaternaire, **43** (2): 179–190.

Rampton, V. N., Gauthier, R. C. Thibault, J. and Seaman, A. A. 1984. Quaternary Geology of New Brunswick. Geological Survey of Canada, Memoir 416, 77p.

Rampton, V. N. and Paradis, S. 1981. Quaternary geology of Amherst map area (21 H), New Brunswick. New Brunswick Department of Natural Resources, Mineral Development Branch, Map Report 81-3, 36 p.

Rappol, M. 1989. Glacial history and stratigraphy of northwestern New Brunswick. Géographie physique et Quaternaire, **43**(2): 191–206.

Rose, D. G. and Johnson, S. C. 1990. New Brunswick computerised mineral occurrence database. New Brunswick department of Natural Resources and Energy, Mineral and Energy Division, Report 3, 69p.

Sangster, D. F. 1984a. Mississippi Valley Lead Zinc. *In* Canadian Mineral Deposit Types: A Geologic Synopsis. *Edited by* O. R. Eckstrand. Geologic Survey of Canada, Economic Geology Report 36, pp. 25.

---------------- 1984b. Sandstone lead. *In* Canadian Mineral Deposit Types: A Geologic Synopsis. *Edited by* O. R. Eckstrand. Geologic Survey of Canada, Economic Geology Report 36, pp. 26.

---------------- 1995. Mississippi Valley-Type lead-zinc. *In* Geology of Canadian Mineral Deposit Types. *Edited by* O. R. Eckstrand, W. D. Sinclair, and R. I. Thorpe; Geological Survey of Canada, Geology of Canada, **8**, pp. 253-261.

Seaman, A. A. 1987. Granular aggregate resources Petitcodiac (NTS 21 H/14) map area, New Brunswick. New Brunswick Department of Natural Resources and Energy, Mineral Resources, Open File Report 87-1, 98 p.

---------------- 1989. Glacial striae trends in New Brunswick: a compilation. New Brunswick Department of Natural Resources and Energy, Mineral Resources, Open File Report 89-34, 136 p.

---------------- 1991. Complex glacial ice-flow events in New Brunswick with particular reference to the Oromocto Lake area, and implications for drift prospecting. New Brunswick Department of Natural Resources and Energy, Mineral Resources, Open File Report 82-6, 48 p.

---------------- 1992. Till Geochemistry of the Forest City (NTS 21 G/12) map area, York County, New Brunswick. New Brunswick Department of Natural Resources and Energy, Mineral Resources, Open File Report 92-6, 192 p.

Shilts, W. W. 1976. Glacial till and mineral exploration. *In* Glacial Till, an Inter-disciplinary Study. *Edited by* R. F. Legget. Royal Society of Canada Special publications, Ottawa, **12**, pp. 205–224.

----------------- 1984. Till geochemistry in Finland and Canada. Journal of Geochemical Exploration, **21**: 95–117.

----------------- 1993. Geological Survey of Canada's contributions to the understanding of composition of glacial sediments. Canadian Journal of Earth Sciences, **30**: 333–353.

---------------- 1995. Geochemical partitioning in till. *In* Drift Exploration in the Canadian Cordillera. *Edited by* P. T. Bobrowsky, S. J. Sibbick, J. M. Newell, and P. F. Matysek. Canadian Cataloguing in Publication Data, Mineral Resources Division, Geological Survey Branch, Paper 1995-2, pp. 149-164.

Silk, J. 1979. Statistical Concepts in Geography. George Allen and Unwin, London, 256 p.

Stea, R. R. 1984. The sequence of glacial movements in northern mainland Nova Scotia determined through mapping and till provenance studies. *In* Correlation of Quaternary Chronologies. *Edited by* W. C. Mahaney. Geo Books, Norwich, England, pp. 279–297.

Stea, R. R. and Mott, R. J. 1989. Deglaciation Environments and Evidence for Glaciers of Younger Dryas age in Nova Scotia, Canada. Boreas, **18**: 169-187.

Stea, R. R., Piper, D. J. W., Fader, G. J. and Boyd. R. 1998. Wisconsinan glacial and sea level history of Maritime Canada and the adjacent continental shelf: a correlation of land and sea events. Geological Society of America Bulletin, **110**: 821–845.

St. Peter, C. 1992. Lithofacies, seismic facies, and strike-slip setting of the Lower Carboniferous alluvial/fluvial/lacustrine Albert Formation of New Brunswick. New Brunswick Department of Natural Resources and Energy, Mineral Resources, Open File Report 92-2, 145 p.

Stumpf, A. J. 1995. Quaternary geology and dispersal patterns of the McAdam (NTS 21 G/11) map area, York County, New Brunswick. New Brunswick Department of Natural Resources and Energy, Mineral Resources, Open File Report 95-5, 218 p.

Szabo, J. P. and Angle, M. P. 1983. The influence of the local bedrock: an important consideration in the interpretation of the textural and mineralogic analysis of till. Journal of Sedimentary Petrology, **53**(3): 981–989.

Vincent, J. S. and Prest, V. K. 1987. The early Wisconsinan history of the Luarentide Ice Sheet. Géographie physique et Quaternaire, **41**: 199-213.

Williams, E. P. 1974. Geology and petroleum possibilities in and around the Gulf of St. Lawrence. American Association of Petroleum Geologists Bulletin, **58**: 1137-1155.

Zelazny, V. F., Ng, T. T. M., Hayter, M. G., Bowling, C. L. and Bewick, D. A. 1989. Field guide to forest site classification in New Brunswick, Harvey-Harcourt-Fundy site regions. New Brunswick Department of Natural Resources and Energy, 43p.

APPENDICES

APPENDIX I

SAMPLE SITE LOCATIONS

Collection of 274 till and soil samples (including field duplicates) at 2-km spacing (one sample per $4km^2$) during fieldwork in the Petitcodiac map area (21 H/14) was based on the local U.T.M. grid, NAD 27 (North American Datum 1927). The geographic locations of the sample sites were measured within an accuracy of 50 metres. Samples were labelled using a letter-number code with letter designations increasing (from A to X) eastward across the map area and number designations increasing (from 1 to 14) toward the south.

APPENDIX I: U.T.M. Sample Site Locations

Sample Site Number	Easting (metres)	Northing (metres)
A8	306050	5080975
A9	306000	5078975
A10	306100	5077000
A11	306000	5075000
A12	306000	5073000
A13	305750	5071600
B1	308000	5095000
B2	307900	5093000
B3	308000	5090950
B4	307600	5088700
B5	307800	5087100
B6	307925	5084925
B7	308100	5083100
B8	308100	5081100
B9	308200	5079200
B10	308000	5077000
B11	307900	5075200
B12	308350	5072250
B13	307800	5070800
C1	310000	5095000
C2	310000	5093000
C3	310000	5091250
C4	310100	5089150
C5	310100	5087150
C6	309800	5085000
C7	310000	5083000
C8	309750	5081300
C9	309900	5078900
C10	310000	5077000
C11	309900	5075100
C12	310000	5072950
C13	310000	5071200
D1	312500	5094900
D2	311950	5093100
D3	312000	5091000
D4	312000	5089000
D5	312000	5086850
D6	311900	5084950
D7	311950	5083000
D8	311600	5081500
D9	312500	5078700
D10	311650	5077150
D11	311900	5075100
D12	312400	5073650
D13	312200	5071400
D14	312100	5068950

APPENDIX I: U.T.M. Sample Site Locations

Sample Site Number	Easting (metres)	Northing (metres)
E1	313850	5094850
E2	313900	5093000
E3	313900	5091000
E4	314000	5089100
E5	314000	5087000
E6	313400	5085400
E7	313750	5083700
E8	314800	5081600
E9	314250	5078850
E10	314000	5077000
E11	314000	5075000
E12	313950	5073100
E13	313900	5071250
E14	314000	5069250
F1	316100	5094850
F2	315800	5093500
F3	315700	5090800
F4	316100	5089100
F5	315750	5087400
F6	315400	5085400
F7	315750	5083350
F8	316100	5081000
F9	316000	5079000
F10	316000	5077000
F11	316000	5075000
F12	316000	5073000
F13	316000	5070600
F14	316250	5069150
G1	318000	5095000
G2	317950	5092950
G3	318000	5091200
G4	318000	5089000
G5	318150	5086700
G6	317800	5084750
G7	318000	5083400
G8	317700	5081450
G9	318000	5079000
G10	318000	5077000
G11	318000	5075000
G12	317550	5073500
G13	317850	5071000
G14	318000	5069000
H1	320000	5094900
H2	319950	5093100
H3	319900	5090900
H4	319900	5089200

APPENDIX I: U.T.M. Sample Site Locations

Sample Site Number	Easting (metres)	Northing (metres)
H5	320000	5087250
H6	319900	5085000
H7	320150	5083050
H8	319950	5080700
H9	320000	5079000
H10	320100	5077000
H11	319550	5075450
H12	320350	5072600
H13	319900	5070950
H14	320000	5069000
K1	322050	5095050
K2	322100	5093150
K3	321450	5091450
K4	322350	5089350
K5	321900	5086800
K6	322100	5084900
K7	322000	5083200
K8	321950	5081300
K9	322450	5078450
K10	321850	5077000
K11	322000	5075200
K12	321950	5072950
K13	322150	5071000
K14	322000	5069000
L1	323650	5094650
L2	324000	5093000
L3	324350	5091050
L4	323750	5088750
L5	324400	5086700
L6	323750	5085050
L7	323950	5082900
L8	324250	5081000
L9	323600	5079150
L10	324200	5076250
L11	324000	5075000
L12	324000	5073000
L13	324200	5071100
L14	324000	5069000
M1	326000	5095000
M2	326050	5093250
M3	325950	5090850
M4	326250	5088900
M5	326000	5087100
M6	325750	5085250
M7	326300	5082750
M8	326000	5080900

APPENDIX I: U.T.M. Sample Site Locations

Sample Site Number	Easting (metres)	Northing (metres)
M9	326000	5078850
M10	325950	5077000
M11	325650	5075000
M12	326000	5073000
M13	326000	5071000
M14	326050	5069000
N1	328150	5094900
N2	328000	5093000
N3	328000	5091000
N4	328000	5089100
N5	327900	5087200
N6	328150	5085550
N7	328050	5083200
N8	327850	5081100
N9	328300	5079000
N10	327650	5077250
N11	328000	5075400
N12	327950	5072900
N13	328000	5071000
N14	327850	5069100
P1	330000	5095000
P2	330050	5093000
P3	329950	5090900
P4	330050	5089200
P5	330200	5086950
P6	330000	5085000
P7	329900	5083150
P8	330000	5081000
P9	330000	5079000
P10	330000	5077250
P11	330150	5075000
P12	330100	5073100
P13	330100	5070800
P14	330000	5069000
Q1	332000	5094950
Q2	332000	5093000
Q3	331750	5091000
Q4	332200	5088800
Q5	332050	5086950
Q6	332000	5085000
Q7	332000	5083000
Q8	332000	5080400
Q9	332000	5079000
Q10	332000	5077800
Q11	331950	5074750
Q12	332000	5072900

APPENDIX I: U.T.M. Sample Site Locations

Sample Site Number	Easting (metres)	Northing (metres)
Q13	332000	5071000
Q14	332000	5069000
R1	333850	5095300
R2	334000	5093250
R3	334100	5090850
R4	333975	5088950
R5	334000	5086900
R6	334000	5085000
R7	333800	5083000
R8	334000	5081000
R9	334050	5079000
R10	333950	5076750
R11	334100	5074950
R12	333850	5073200
R13	334050	5070750
R14	334000	5068900
S1	335400	5094700
S2	336600	5092650
S3	335950	5090950
S4	336200	5089000
S5	335950	5086800
S6	336000	5085000
S7	336000	5083000
S8	336000	5081100
S9	336000	5079000
S10	336000	5077000
S11	335650	5075500
S12	336150	5072900
S13	335950	5070800
S14	335950	5068950
T1	338500	5094800
T2	337850	5093000
T3	338050	5090900
T4	338000	5089000
T5	338000	5086850
T6	338100	5085000
T7	338050	5083050
T8	338000	5081000
T9	337700	5078800
T10	338000	5077000
T11	337950	5074800
T12	338050	5073000
T13	338000	5071000
T14	338000	5069000
V1	340000	5094850
V2	340000	5093000

APPENDIX I: U.T.M. Sample Site Locations

Sample Site Number	Easting (metres)	Northing (metres)
V3	339950	5091050
V4	340000	5088900
V5	340200	5087000
V6	340050	5085050
V7	340000	5083000
V8	340250	5081000
V9	339100	5078950
V10	340250	5077250
V11	340050	5074950
V12	340000	5073000
V13	339800	5071150
V14	339800	5068850
W1	342000	5095000
W2	341950	5092950
W3	341900	5091050
W4	341850	5088950
W5	341950	5087050
W6	342000	5085000
W7	342000	5083000
W8	342000	5081000
W9	342000	5079000
W10	342050	5076950
W11	342200	5074950
W12	342000	5073100
W13	342000	5071150
W14	341850	5069000
X1	344000	5095000
X2	344100	5093150
X3	343900	5091150
X4	344050	5088800
X5	344000	5087000
X6	344000	5085000
X7	344000	5083000
X8	344000	5081500
X9	344000	5079000
X10	343850	5077100
X11	344000	5075100
X12	344250	5072600
X13	344000	5071000
X14	344050	5068750

APPENDIX II

QUALITY CONTROL

Four lake sediment standards provided by the Geochemistry Division at the Geological Survey of Canada were analyzed at random intervals with the field samples to evaluate the instrumental accuracy for the geochemical analysis. The DNRE accepted values for these standards were compared with their experimental values measured during this project (Table V-a).

Four field duplicates were collected from approximately the same depth in the glacial till at random sites to evaluate the local geochemical variability of the till matrix in the study area. The primary and duplicate samples were compared graphically using an X–Y plot of the two datum sets. A trend line through the origin was fitted to the data by performing a simple linear regression "least squares fit" using the Microsoft® Excel 97 computer spreadsheet software.

Ten sample splits were prepared from random till matrix samples and to investigate the geochemical variability within the sample. The sample splits were compared graphically in the same manner as the field duplicates.

APPENDIX II: Quality Control

Table II-a: Comparision of Experimental and Accepted Values for Geochemical Standards

ICP-ES Experimental Values:													
Element			Hg	Cu	Pb	Zn	Ag	Ni	Mn	Sr	Cd	Bi	V
Units			ppb	ppm	ppm	ppm	ppm	ppm	ppm	ppm	ppm	ppm	ppm
Detection Limit			5	1	4	1	0.4	1	1	1	0.5	5	2
Standards	LKSD-1	Run 1	107	42	93	295	0.8	16	639	244	1.4	2.5	48
		Run 2	106	37	84	261	0.2	14	574	230	1.4	2.5	43
		Run 3	99	38	81	278	0.5	16	581	236	1.4	5	44
	LKSD-2		179	39	46	190	1.2	27	1886	222	1.2	2.5	72
	LKSD-3	Run 1	246	34	286	132	2.8	53	1374	247	0.6	2.5	77
		Run 2	265	37	27	130	3.1	50	1314	237	0.6	2.5	75
		Run 3	265	32	32	131	2.6	51	1345	239	1.0	2.5	75
		Run 4	254	30	30	118	2.0	46	1250	224	0.7	6	69
	LKSD-4	Run 1	152	32	95	178	0.6	34	479	121	2.1	2.5	47
		Run 2	164	31	88	165	0.5	33	443	116	1.9	2.5	44
ICP-ES Accepted Values:													
Element			Hg	Cu	Pb	Zn	Ag	Ni	Mn	Sr	Cd	Bi	V
Units			ppb	ppm	ppm	ppm	ppm	ppm	ppm	ppm	ppm	ppm	ppm
Standards	LKSD-1	avg.	n/a	41	80	300	0.8	14	539	248	1.1	2	45
		std.dev	n/a	3.6	8.7	34.8	0.17	3.2	128.0	6.3	0.17	0.5	4.5
		max.	n/a	45	98	342	1.2	19	714	256	1.5	3	48
		min.	n/a	32	64	214	0.5	8	310	237	0.9	1	37
	LKSD-2	avg.	n/a	37	40	194	0.8	25	1798	231	0.8	2	71
		std.dev.	n/a	2.7	5.0	18.5	0.20	3.2	104.4	5.5	0.16	0.5	2.1
		max.	n/a	42	50	227	1.2	30	1981	236	1.1	3	74
		min.	n/a	32	32	157	0.5	20	1594	218	0.5	1	67
	LKSD-3	avg.	n/a	34	28	135	2.6	48	1287	246	0.5	3	74
		std.dev.	n/a	2.4	6.4	14.2	0.24	5.8	116.2	8.1	0.165	0.3	6.3
		max.	n/a	39	42	158	3	58	1525	258	0.80	3	83
		min.	n/a	31	18	113	2	40	1140	236	0.25	3	61
	LKSD-4	avg.	n/a	30	86	170	0.3	30	425	120	1.8	2	42
		std.dev.	n/a	3.0	9.5	21.9	0.16	4.2	63.4	5.2	0.25	0.8	4.1
		max.	n/a	35	104	212	0.7	40	559	127	2.2	3	49
		min.	n/a	23	70	132	0.1	23	318	112	1.4	1	36

APPENDIX II: Quality Control

Table II-a: Comparision of Experimental and Accepted Values for Geochemical Standards

ICP-ES Experimental Values:										
Element			Ca	P	Mg	Ti	Al	K	Y	Be
Units			wt.%	wt.%	wt.%	wt.%	wt.%	wt.%	ppm	ppm
Detection Limit			0.01	0.001	0.01	0.01	0.01	0.01	2	2
Standards	LKSD-1	Run 1	8.74	0.066	0.91	0.25	3.77	0.9	23	1
		Run 2	8.00	0.065	0.87	0.22	3.72	0.84	22	1
		Run 3	8.28	0.065	0.88	0.23	3.89	0.86	23	1
	LKSD-2		1.80	0.122	0.94	0.27	6.19	2.09	49	1
	LKSD-3	Run 1	2.00	0.104	1.15	0.27	6.25	1.84	34	1
		Run 2	1.93	0.099	1.12	0.26	6.07	1.74	34	1
		Run 3	1.90	0.106	1.1	0.26	6.35	1.8	34	1
		Run 4	1.85	0.099	1.07	0.24	6.19	1.66	30	1
	LKSD-4	Run 1	1.57	0.143	0.52	0.17	2.96	0.64	28	1
		Run 2	1.49	0.14	0.52	0.15	3.01	0.58	25	1
ICP-ES Accepted Values:										
Element			Ca	P	Mg	Ti	Al	K	Y	Be
Units			wt.%	wt.%	wt.%	wt.%	wt.%	wt.%	ppm	ppm
Standards	LKSD-1	avg.	7.70	0.068	0.95	0.25	3.83	0.92	21	1
		std.dev.	0.717	0.0030	0.050	0.014	0.198	0.033	2.8	0.0
		max.	9.07	0.072	1.00	0.26	4.20	0.96	26	1
		min.	7.01	0.062	0.84	0.22	3.44	0.86	18	1
	LKSD-2	avg.	1.77	0.126	0.99	0.27	6.27	2.06	48	1
		std.dev.	0.219	0.0059	0.041	0.009	0.236	0.069	4.9	0.3
		max.	1.97	0.138	1.03	0.29	6.57	2.19	54	2
		min.	1.45	0.119	0.91	0.26	5.79	1.98	42	1
	LKSD-3	avg.	1.78	0.108	1.18	0.27	6.38	1.79	31	1
		std.dev.	0.210	0.0045	0.054	0.007	0.308	0.064	3.4	0.5
		max.	2.15	0.114	1.25	0.28	6.77	1.94	35	2
		min.	1.59	0.1	1.09	0.26	6	1.72	26	1
	LKSD-4	avg.	1.43	0.144	0.54	0.16	2.90	0.63	24	1
		std.dev.	0.127	0.0066	0.031	0.008	0.137	0.048	1.4	0.3
		max.	1.60	0.153	0.58	0.17	3.05	0.71	26	2
		min.	1.18	0.136	0.49	0.15	2.72	0.55	22	1

APPENDIX II: Quality Control

APPENDIX II: Quality Control

Table II-a: Comparision of Experimental and Accepted Values for Geochemical Standards

INAA Experimental Values:

Element			Au	As	Ba	Br	Co	Cr	Cs	Fe	Hf	Ir	Mo
Units			ppb	ppm	ppm	ppm	ppm	ppm	ppm	wt.%	ppm	ppb	ppm
Detection Limit			2	0.5	50	0.5	1	5	1	0.01	1	5	1
Standards	LKSD-1	Run 1	3	37.0	390	10	9	26	0.5	2.95	5	2.5	15
		Run 2	2	35.0	430	11	9	24	1	2.94	5	2.5	11
		Run 3	9	32.0	350	10	9	26	0.5	2.68	5	2.5	14
	LKSD-2		6	11.0	680	17	16	50	2	4.14	9	2.5	4
	LKSD-3	Run 1	1	23.0	540	15	27	72	2	3.71	5	2.5	4
		Run 2	3	23.0	540	16	27	71	2	3.78	4	2.5	5
		Run 3	10	25.0	670	13	25	74	2	3.93	5	2.5	0.5
		Run 4	4	23.0	510	14	29	92	3	4.15	6	2.5	10
	LKSD-4	Run 1	5	18.0	420	50	11	45	2	3.23	4	2.5	0.5
		Run 2	2	17.0	380	49	11	32	0.5	2.95	3	2.5	24

INAA Accepted Values:

Element			Au	As	Ba	Br	Co	Cr	Cs	Fe	Hf	Ir	Mo
Units			ppb	ppm	ppm	ppm	ppm	ppm	ppm	wt.%	ppm	ppb	ppm
Standards	LKSD-1	avg.	7	35.8	445	10.4	10	30	1	2.84	4	n/a	8
		std.dev.	8.4	1.96	55.7	0.82	0.6	2.6	0.2	0.180	0.5	n/a	5.4
		max.	34	40.0	590	12.0	12	37	1	3.27	5	n/a	18
		min.	1	33.0	340	8.6	9	25	1	2.55	3	n/a	1
	LKSD-2	avg.	2	10.4	763	17.2	16	52	2	4.12	7	n/a	2
		std.dev.	1.8	1.77	98.9	1.39	1.5	5.4	0.5	0.246	0.7	n/a	2.8
		max.	6	18.0	930	21.0	20	68	3	4.62	9	n/a	9
		min.	1	8.4	530	15.0	13	41	2	3.63	6	n/a	1
	LKSD-3	avg.	3	28.0	693	15.1	28	81	2	3.99	5	n/a	2
		std.dev.	2.8	10.38	87.0	1.35	2.4	8.4	0.4	0.354	0.6	n/a	2.5
		max.	12	76.0	820	17.0	34	97	3	4.64	7	n/a	10
		min.	1	21.0	510	13.0	24	63	1	3.44	4	n/a	1
	LKSD-4	avg.	3	15.6	376	50.1	10	35	1	2.92	3	n/a	8
		std.dev.	3.3	2.36	74.0	6.93	1.8	6.3	0.7	0.395	0.6	n/a	9.9
		max.	15	19.0	550	62.0	13	50	3	3.62	4	n/a	40
		min.	1	5.5	160	18.0	3	11	1	1.16	1	n/a	1

APPENDIX II: Quality Control

Table II-a: Comparision of Experimental and Accepted Values for Geochemical Standards

INAA Experimental Values:													
Element			Na	Rb	Sb	Sc	Se	Sn	Ta	Th	U	W	La
Units			wt.%	ppm	ppm	ppm	ppm	wt.%	ppm	ppm	ppm	ppm	ppm
Detection Limit			0.01	15	0.1	0.1	3	0.01	0.5	0.2	0.5	1	0.5
Standards	LKSD-1	Run 1	1.50	7.5	1.2	7.5	1.5	0.005	0.25	1.8	8.4	0.5	17.0
		Run 2	1.51	33	1.1	7.4	1.5	0.005	0.25	2.0	8.4	0.5	17.0
		Run 3	1.48	38	1.0	7.3	1.5	0.005	0.25	2.0	10.0	0.5	15.0
	LKSD-2		1.41	72	1.0	12.0	1.5	0.005	1.4	11.0	6.2	0.5	75.0
	LKSD-3	Run 1	1.77	78	1.6	11.0	1.5	0.005	0.25	10.0	3.6	0.5	53.0
		Run 2	1.75	81	1.1	11.0	1.5	0.005	1.6	11.0	2.8	0.5	53.0
		Run 3	1.69	82	1.1	11.0	3	0.005	0.9	11.0	4.7	0.5	52.0
		Run 4	1.80	66	1.5	12.0	1.5	0.005	0.25	10.0	3.4	0.5	54.0
	LKSD-4	Run 1	0.65	7.5	1.7	7.3	1.5	0.005	1.9	5.5	34.0	0.5	30.0
		Run 2	0.61	7.5	2.0	7.1	1.5	0.005	1.8	4.8	25.0	0.5	29.0
INAA Accepted Values:													
Element			Na	Rb	Sb	Sc	Se	Sn	Ta	Th	U	W	La
Units			wt.%	ppm	ppm	ppm	ppm	wt.%	ppm	ppm	ppm	ppm	ppm
Standards	LKSD-1	avg.	1.48	25	1.2	7.7	n/a	n/a	0.5	2.3	9.9	n/a	15.8
		std.dev.	0.124	13.7	0.12	0.56	n/a	n/a	0.63	0.19	1.11	n/a	1.03
		max.	1.70	60	1.5	9.0	n/a	n/a	3.2	2.7	13.0	n/a	18.0
		min.	1.26	7.5	1.0	7.0	n/a	n/a	0.3	1.9	8.0	n/a	14.0
	LKSD-2	avg.	1.39	74	1.0	11.9	n/a	n/a	0.5	13.0	7.5	n/a	68.7
		std.dev.	0.095	15.3	0.12	0.81	n/a	n/a	0.47	1.26	1.04	n/a	4.57
		max.	1.56	92	1.3	14.0	n/a	n/a	2.0	16.0	9.4	n/a	78.0
		min.	1.21	7.5	0.8	11.0	n/a	n/a	0.3	11.0	5.5	n/a	59.0
	LKSD-3	avg.	1.68	65	1.2	11.7	n/a	n/a	0.5	11.8	4.6	n/a	52.3
		std.dev.	0.153	18.2	0.22	1.03	n/a	n/a	0.39	1.19	0.67	n/a	4.36
		max.	1.91	96	1.7	14.0	n/a	n/a	1.5	14.0	6.4	n/a	62.0
		min.	1.39	7.5	0.9	10.0	n/a	n/a	0.3	9.9	3.5	n/a	43.0
	LKSD-4	avg.	0.56	30	1.7	6.9	n/a	n/a	0.4	5.6	33.0	n/a	27.9
		std.dev.	0.087	13.7	0.31	0.96	n/a	n/a	0.24	0.90	5.71	n/a	3.98
		max.	0.73	60	2.3	8.8	n/a	n/a	1.2	7.8	46.0	n/a	35.0
		min.	0.20	7.5	0.5	2.7	n/a	n/a	0.3	2.1	12.0	n/a	9.9

APPENDIX II: Quality Control

Table II-a: Comparision of Experimental and Accepted Values for Geochemical Standards

INAA Experimental Values:									
Element			Ce	Nd	Sm	Eu	Tb	Yb	Lu
Units			ppm	ppm	ppm	ppm	ppm	ppm	ppm
Detection Limit			3	5	0.1	0.2	0.5	0.2	0.05
Standards	LKSD-1	Run 1	26	15	3.4	1.0	2.5	2.3	0.43
		Run 2	23	18	3.3	1.0	0.7	2.3	0.42
		Run 3	28	18	3.1	1.1	2.5	2.5	0.41
	LKSD-2		110	55	10	2.1	2.5	4.6	0.83
	LKSD-3	Run 1	86	35	7.1	1.4	0.7	3.4	0.50
		Run 2	87	36	7.2	1.5	1.0	3.2	0.41
		Run 3	77	45	6.2	1.5	2.5	3.2	0.53
		Run 4	93	47	7.1	1.9	0.8	3.6	0.54
	LKSD-4	Run 1	49	31	4.7	1.4	2.5	2.8	0.50
		Run 2	48	35	4.8	1.5	0.7	2.6	0.47
INAA Accepted Values:									
Element			Ce	Nd	Sm	Eu	Tb	Yb	Lu
Units			ppm	ppm	ppm	ppm	ppm	ppm	ppm
Standards	LKSD-1	avg.	29	15	3.4	1.1	0.5	2.4	0.36
		std.dev.	2.6	3.1	0.33	0.13	0.21	0.20	0.066
		max.	34	23	4.2	1.5	0.8	3.0	0.46
		min.	23	10	2.8	0.9	0.3	2.1	0.17
	LKSD-2	avg.	111	55	9.6	2.0	1.3	4.7	0.73
		std.dev.	9.1	6.6	0.76	0.16	0.22	0.37	0.076
		max.	130	74	11	2.3	1.5	5.7	0.90
		min.	98	44	8.2	1.8	0.3	4.1	0.61
	LKSD-3	avg.	90	39	7.1	1.6	0.8	3.2	0.48
		std.dev.	10.5	5.7	0.71	0.21	0.34	0.39	0.062
		max.	120	50	9.1	2.2	1.2	4.1	0.63
		min.	75	31	5.7	1.3	0.3	2.4	0.38
	LKSD-4	avg.	52	25	4.3	1.3	0.6	2.4	0.41
		std.dev.	8.1	5.1	0.66	0.22	0.41	0.37	0.074
		max.	64	36	5.6	1.7	2.2	3.3	0.57
		min.	21	12	1.8	0.5	0.3	0.9	0.16

APPENDIX II: Quality Contol

Table II-b: Geochemistry of Sample Splits for Selected Elements

Inductively Coupled Plasma Emission Spectrometry (ICP-ES):

Element	Hg	Cu	Pb	Zn	Ni	Sr	V	Al	Y
unit	ppb	ppm	ppm	ppm	ppm	ppm	ppm	wt.%	ppm
Detection Limit	5	1	4	1	1	1	2	0.01	2
A 9	22	19	13	59	23	94	61	5.46	22
A9D	21	19	12	59	23	95	64	5.61	23
C 10	15	26	21	75	38	126	98	6.96	30
C10D	15	27	22	76	39	127	101	7.47	31
E 2	20	31	20	80	38	55	101	7.86	26
E2D	21	29	16	77	38	55	99	7.84	26
G 8	46	21	17	65	33	67	79	6.54	19
G8D	45	22	17	66	34	68	81	6.55	18
K 4	27	22	19	89	40	86	104	7.66	25
K4D	27	21	15	89	40	84	103	7.68	26
M 8	9	18	15	56	28	70	73	5.97	28
M8D	12	17	17	55	26	68	71	5.83	29
P 11	38	16	13	64	36	70	81	6.86	22
P11D	37	16	13	64	35	69	81	6.80	20
R 3	16	24	19	73	31	63	83	6.54	24
R3D	17	24	16	71	31	62	84	6.44	24
T 10	49	17	13	88	45	47	79	8.01	25
T10D	49	17	15	88	43	47	78	7.89	24
W 8	98	24	28	93	38	73	83	7.52	23
W8D	93	23	20	90	34	71	81	7.39	23

Instrumental Neutron Activation Analysis (INAA):

Element	Au	As	Ba	Cr	Na	Sc	Th	Sm	Lu
unit	ppb	ppm	ppm	ppm	ppm	ppm	ppm	wt.%	ppm
Detection Limit	2	0.5	50	5	0.01	0.1	0.20	0.1	0.05
A 9	1	6.5	340	110	1.27	9.4	9.1	4.3	0.75
A9D	1	6.1	300	97	1.15	8.7	8.2	4.0	0.68
C 10	1	20.0	390	86	0.96	16	12.0	7.3	0.85
C10D	1	20.0	510	80	0.89	15	12.0	6.7	0.73
E 2	1	12.0	360	72	0.46	15	12.0	6.0	0.66
E2D	1	11.0	280	72	0.43	14	12.0	5.9	0.70
G 8	1	12.0	360	73	1.05	10	10.0	4.3	0.55
G8D	1	12.0	330	76	1.12	11	10.0	4.6	0.60
K 4	1	18.0	430	87	1.22	13	11.0	5.6	0.69
K4D	1	15.0	290	78	1.11	12	10.0	5.2	0.66
M 8	5	4.5	380	70	0.95	11	11.0	6.2	0.68
M8D	4	5.0	300	62	0.88	10	9.5	6.0	0.73
P 11	1	11.0	370	73	0.97	11	11.0	4.8	0.60
P11D	1	12.0	390	86	1.08	12	12.0	5.5	0.76

*Note: Sample site labels ending in "D" denote the sample split.

APPENDIX II: Quality Contol

Table II-b: Geochemistry of Sample Splits for Selected Elements

Instrumental Neutron Activation Analysis (INAA):									
Element	Au	As	Ba	Cr	Na	Sc	Th	Sm	Lu
unit	ppb	ppm	ppm	ppm	ppm	ppm	ppm	wt.%	ppm
Detection Limit	2	0.5	50	5	0.01	0.1	0.20	0.1	0.05
R3D	2	8.2	350	71	0.49	12	11.0	4.8	0.72
T 10	1	13.0	420	72	0.42	11	11.0	5.0	0.66
T10D	3	12.0	390	76	0.43	12	9.8	5.1	0.64
W 8	3	11.0	280	85	0.65	11	10.0	4.5	0.61
W8D	1	11.0	230	82	0.64	11	10.0	4.4	0.62

*Note: Sample site labels ending in "D" denote the sample split.

APPENDIX II: Quality Control

Table II-c: Geochemistry of Field Duplicates for Selected Elements

Inductively Coupled Plasma Emission Scepectrometry (ICP-ES):

	Element	Hg	Cu	Pb	Zn	Ni	Sr	V	Al	Y
	unit	ppb	ppm	ppm	ppm	ppm	ppm	ppm	wt.%	ppm
	Detection Limit	5	1	4	1	1	1	2	0.01	2
Sample Sites	B 2	21	27	17	76	40	53	105	7.89	26
	B2FD	20	26	16	66	35	54	93	7.00	23
	E 10	52	19	20	61	31	62	75	6.72	23
	E10FD	39	17	19	54	29	63	67	6.41	20
	H 2	25	24	16	64	32	54	88	7.53	20
	H2FD	25	22	17	60	35	56	82	7.18	20
	X 4	21	20	21	70	34	58	89	7.79	24
	X4FD	18	20	21	66	32	59	91	7.61	25

Instrumental Neutron Activation Analysis (INAA):

	Element	Au	As	Ba	Cr	Na	Sc	Th	Sm	Lu
	unit	ppb	ppm	ppm	ppm	ppm	ppm	ppm	wt.%	ppm
	Detection Limit	2	0.5	50	5	0.01	0.1	0.20	0.1	0.05
Sample Sites	B 2	1	18.0	340	84	0.41	15.0	12.00	5.8	0.68
	B2FD	1	13.0	390	84	0.51	14.0	12.00	5.8	0.76
	E 10	1	13.0	280	66	0.64	9.1	10.00	4.6	0.64
	E10FD	5	11.0	290	65	0.86	8.6	9.70	4.5	0.61
	H 2	1	11.0	410	74	0.58	12.0	13.00	4.9	0.52
	H2FD	1	10.0	240	74	0.62	11.0	13.00	5.1	0.67
	X 4	1	9.2	230	85	0.16	12.0	11.00	4.2	0.66
	X4FD	1	9.3	220	94	0.20	13.0	11.00	4.6	0.69

*Note: Sample site labels ending in "FD" denote the duplicate sample.

APPENDIX II: QUALITY CONTROL

Figures 1 to 8: Graphical Analysis of Field Duplicates

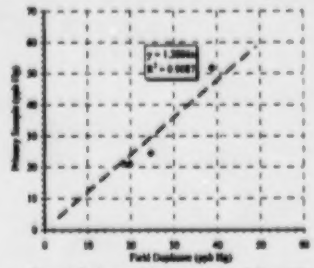

Figure 1: Evaluation of the precision of the field sampling procedure for Hg.

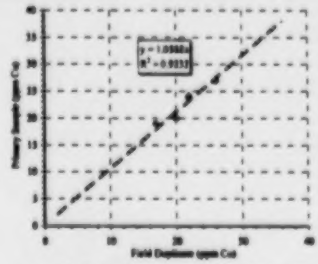

Figure 2: Evaluation of the precision of the field sampling procedure for Cu.

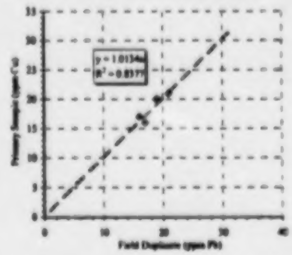

Figure3: Evaluation of the precision of the field sampling procedure for Pb.

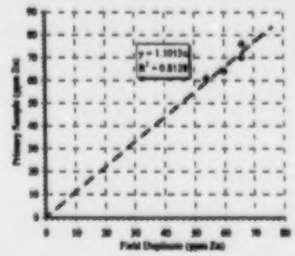

Figure 4: Evaluation of the precision of the field sampling procedure for Zn.

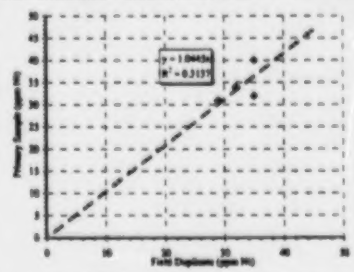

Figure 5: Evaluation of the precision of the field sampling procedure for Ni.

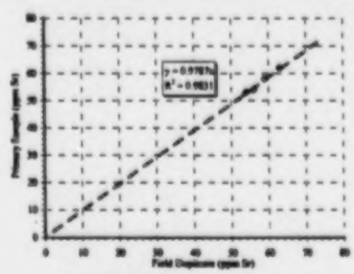

Figure 6: Evaluation of the precision of the field sampling procedure for Sr.

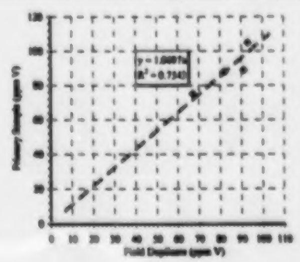

Figure 7: Evaluation of the precision of the field sampling procedure for V.

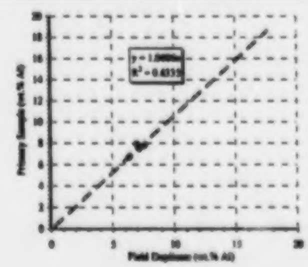

Figure 8: Evaluation of the precision of the field sampling procedure for Al.

APPENDIX II: QUALITY CONTROL

Figures 9 to 16: Graphical Analysis of Field Duplicates

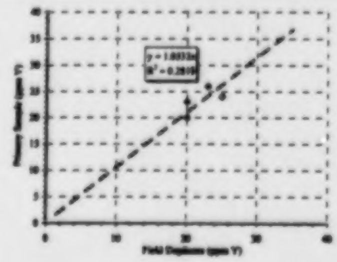

Figure 9: Evaluation of the precision of the field sampling procedure for Y.

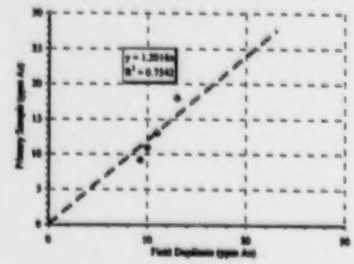

Figure 10: Evaluation of the precision of the field sampling procedure for As.

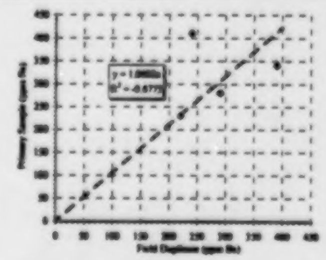

Figure 11: Evaluation of the precision of the field sampling procedure for Ba.

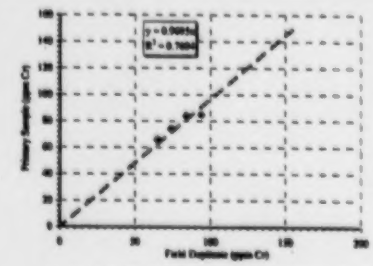

Figure 12: Evaluation of the precision of the field sampling procedure for Cr.

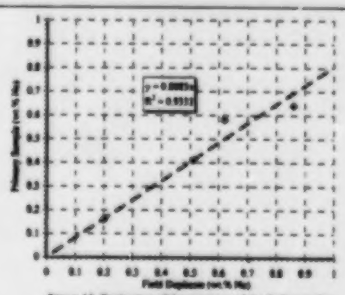

Figure 13: Evaluation of the precision of the field sampling procedure for Na.

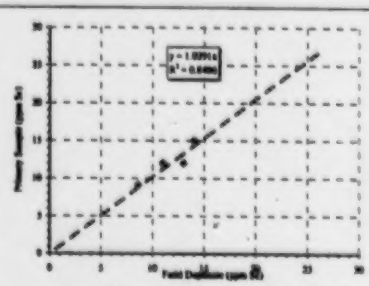

Figure 14: Evaluation of the precision of the field sampling procedure for Sc.

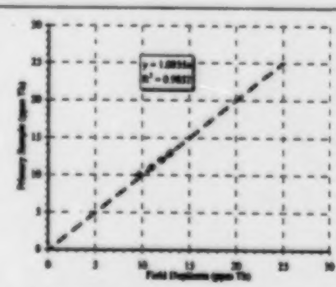

Figure 15: Evaluation of the precision of the field sampling procedure for Th.

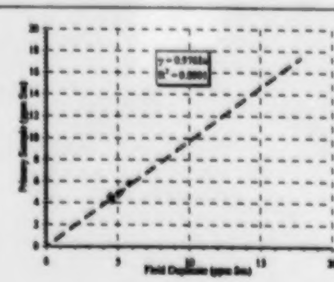

Figure 16: Evaluation of the precision of the field sampling procedure for Sm.

APPENDIX II: QUALITY CONTROL

Figure 17: Graphical Analysis of Field Duplicates

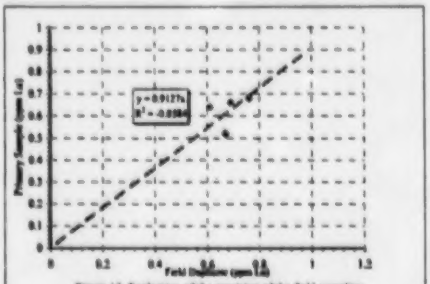

Figure 17: Evaluation of the precision of the field sampling procedure for La.

APPENDIX II: Quality Control

Figures 18 to 25: Graphical Analysis of Sample Splits

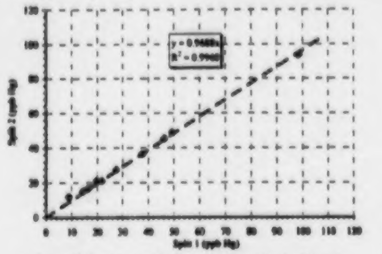

Figure 18: Evaluation of the Hg variability within the till matrix samples.

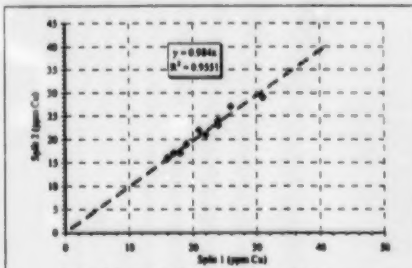

Figure 19: Evaluation of the Cu variability within the till matrix samples.

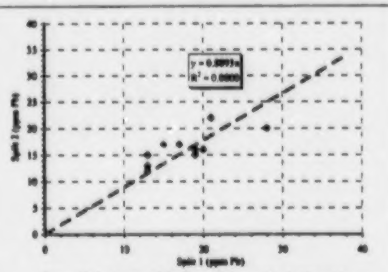

Figure 20: Evaluation of the Pb variability within the till matrix samples.

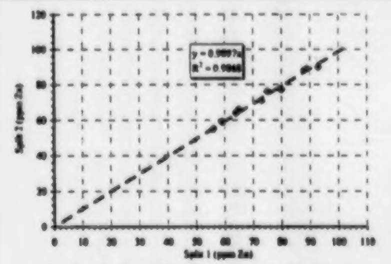

Figure 21: Evaluation of the Zn variability within the till matrix samples.

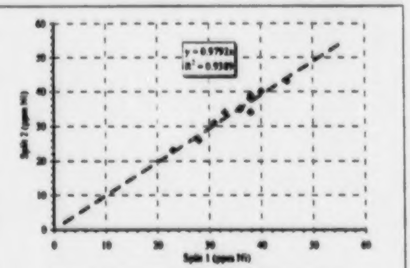

Figure 22: Evaluation of the Ni variability within the till matrix samples.

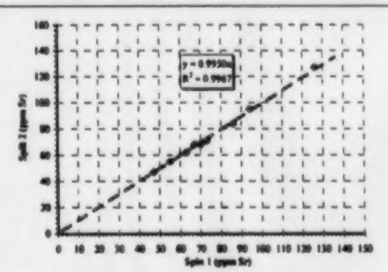

Figure 23: Evaluation of the Sr variability within the till matrix samples.

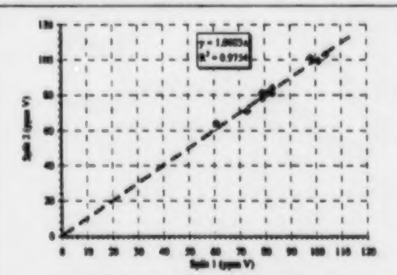

Figure 24: Evaluation of the V variability within the till matrix samples.

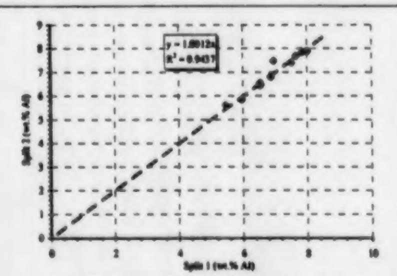

Figure 25: Evaluation of the Al variability within the till matrix samples.

APPENDIX II: Quality Control

Figures 26 to 33: Graphical Analysis of Sample Splits

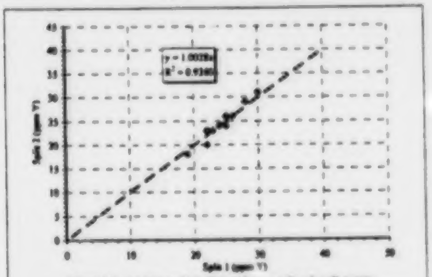

Figure 26: Evaluation of the Y variability within the till matrix samples.

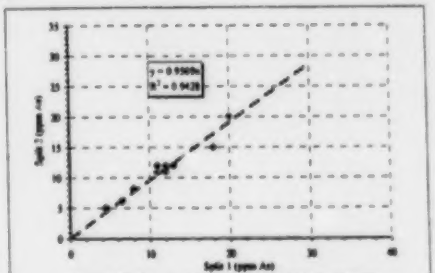

Figure 27: Evaluation of the As variability within the till matrix samples.

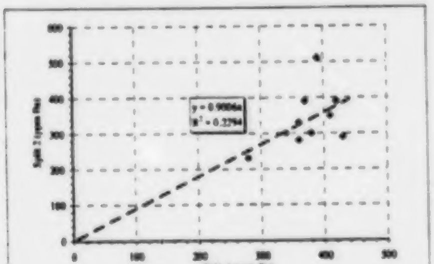

Figure 28: Evaluation of the Ba variability within the till matrix samples.

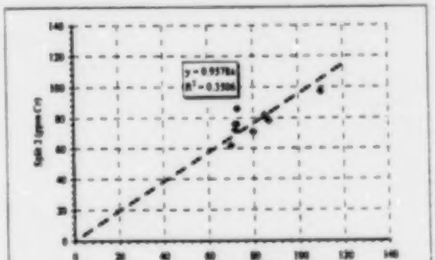

Figure 29: Evaluation of the Cr variability within the till matrix samples.

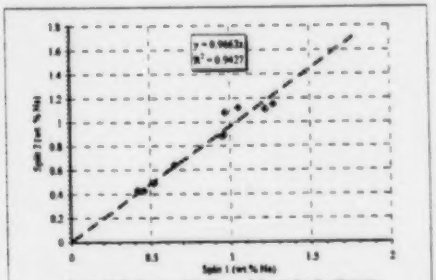

Figure 30: Evaluation of the Na variability within the till matrix samples.

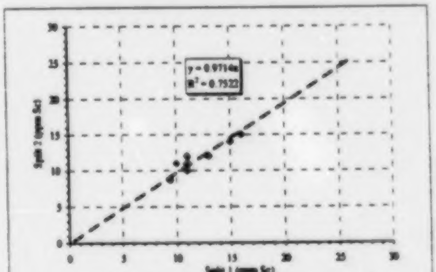

Figure 31: Evaluation of the Sc variability within the till matrix samples.

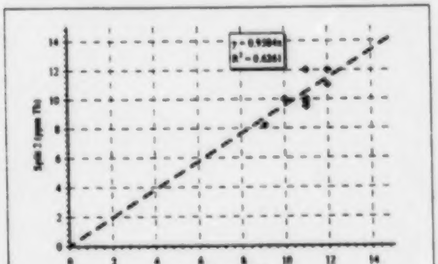

Figure 32: Evaluation of the Th variability within the till matrix samples.

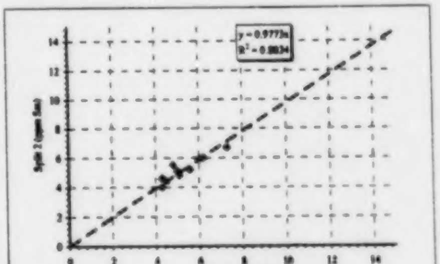

Figure 33: Evaluation of the Sm variability within the till matrix samples.

APPENDIX II: Quality Control

Figure 34: Graphical Analysis of Sample Splits

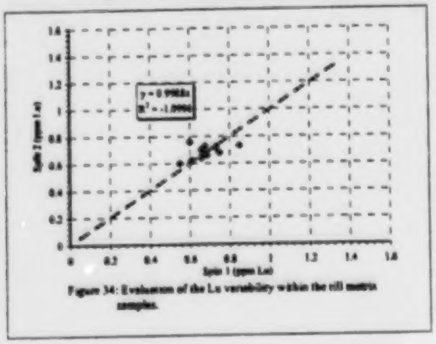

APPENDIX III

SITE CHARACTERISTICS AND GRANULOMETRIC ANALYSIS

The sample texture and consistency, as well as the local drainage were determined using the criteria outlined by Zelazny (1989) for each sample site. The field observations were assigned numeric values, permitting a Spearman rank correlation analysis of the data. The following numbering system was used to quantify the field observations:

Texture: Numbers increase approximately in the direction of increasing fine particle content.

Sand	1	Silty Clay Loam	6
Sandy Loam	2	Clay Loam	7
Silt Loam	3	Sandy Clay	8
Loam	4	Silty Clay	9
Sandy Clay Loam	5	Clay	10

Consistency: Numbers increase in the direction of increasing till compactness.

Loose	1	Friable	3
Very Friable	2	Firm	4

Drainage: Numbers increase in the direction of increasingly poor drainage.

Rapidly	1	Imperfectly	4
Well	2	Poorly	5
Moderately Well	3	Very Poorly	6

A granulometric analysis was performed on each of the 270 samples. Exactly 100 grams of the <2mm fraction of each till sample were dispersed in a 5% Calgon® solution. Two hydrometer readings were taken to determine the sand (2.00-0.05mm), silt (0.5-0.004 mm), and clay (<0.004 mm) fractions of the till (After Bouyoucos, 1962).

APPENIX III: Site Characteristics and Granulometric Anaylsis

Sample Site	Field Data			Granulometric Anaysis		
	Sample		Local	Sand	Silt	Clay
	Texture	consistency	Drainage	wt.%	wt.%	wt.%
A8	3	3	2	64	21	15
A9	4	3	4	59	30	11
A10	5	1	2	65	24	11
A11	4	2	2	57	29	14
A12	2	2	2	68	22	10
A13	2	2	2	69	20	11
B1	4	4	2	42	32	26
B2	5	4	3	48	21	31
B3	5	3	3	51	33	16
B4	2	3	2	64	24	12
B5	2	2	2	54	32	14
B6	1	2	1	72	19	9
B7	2	2	2	71	16	13
B8	4	4	2	42	51	7
B9	2	4	2	68	17	15
B10	2	2	2	56	32	12
B11	5	3	3	49	33	18
B12	5	2	2	33	45	22
B13	5	4	2	42	32	26
C1	4	4	3	48	40	12
C2	4	3	2	57	29	14
C3	4	3	2	50	36	14
C4	1	2	1	67	25	8
C5	2	4	2	70	18	12
C6	2	3	2	55	35	10
C7	3	3	3	54	38	8
C8	4	3	2	52	33	15
C9	4	2	3	48	39	13
C10	5	4	3	40	39	21
C11	5	2	2	50	33	17
C12	5	4	3	33	41	26
C13	2	3	2	65	25	10
D1	2	3	3	62	28	10
D2	4	4	2	52	36	12
D3	3	2	2	56	26	18
D4	2	4	2	73	19	8
D5	5	3	2	43	35	22
D6	2	3	2	57	32	11
D7	2	2	2	67	20	13
D8	2	3	2	61	30	9
D9	5	4	3	16	42	42
D10	4	4	1	52	24	24
D11	2	1	2	71	17	12
D12	2	2	2	67	23	10
D13	5	4	2	34	38	28

APPENIX III: Site Characteristics and Granulometric Anaylsis

Sample Site	Field Data			Granulometric Anaysis		
	Sample		Local	Sand	Silt	Clay
	Texture	consistency	Drainage	wt.%	wt.%	wt.%
D14	5	4	3	47	27	26
E1	4	3	3	51	29	20
E2	5	3	3	37	35	28
E3	1	3	2	69	21	10
E4	2	4	1	73	18	9
E5	2	3	2	70	19	11
E6	5	4	2	45	37	18
E7	4	3	3	51	29	20
E8	5	3	4	38	27	35
E9	4	4	2	55	30	15
E10	2	2	2	61	24	15
E11	5	2	2	65	23	12
E12	2	3	2	58	25	17
E13	7	5	2	19	28	53
E14	4	4	3	48	30	22
F1	4	3	4	55	26	19
F2	4	3	3	54	28	18
F3	4	3	2	55	22	23
F4	4	3	2	67	17	16
F5	3	3	2	60	28	12
F6	5	4	3	59	21	20
F7	2	5	2	67	15	18
F8	5	4	3	43	24	33
F9	4	4	3	65	14	21
F10	10	5	3	32	27	41
F11	2	1	2	67	17	16
F12	3	1	2	54	29	17
F13	5	4	3	19	48	33
F14	3	4	2	37	35	28
G1	4	3	2	67	20	13
G2	4	3	2	55	24	21
G3	4	3	2	58	25	17
G4	4	3	2	71	15	14
G5	5	4	3	37	35	28
G6	5	4	2	39	29	32
G7	5	5	3	14	40	46
G8	3	2	2	59	30	11
G9	4	4	2	47	30	23
G10	1	1	1	73	14	13
G11	2	1	2	72	15	13
G12	2	3	2	55	25	20
G13	5	3	2	46	27	27
G14	3	2	1	62	25	13
H1	5	4	3	37	31	32
H2	5	3	2	51	29	20

APPENIX III: Site Characteristics and Granulometric Anaylsis

Sample Site	Field Data			Granulometric Anaysis		
	Sample		Local	Sand	Silt	Clay
	Texture	consistency	Drainage	wt.%	wt.%	wt.%
H3	4	3	2	52	29	19
H4	1	4	2	73	15	12
H5	5	3	2	49	34	17
H6	3	3	2	53	36	11
H7	2	4	1	64	20	16
H8	5	4	3	27	37	36
H9	3	3	2	28	48	24
H10	2	2	1	54	30	16
H11	2	1	2	71	16	13
H12	2	2	2	62	23	15
H13	2	4	2	73	17	10
H14	2	1	1	71	17	12
K1	4	3	2	60	23	17
K2	4	3	2	49	30	21
K3	2	3	2	56	30	14
K4	5	3	2	41	36	23
K5	3	3	2	40	43	17
K6	5	4	2	53	22	25
K7	10	4	2	35	24	41
K8	6	4	2	23	37	40
K9	5	4	3	35	42	23
K10	2	4	n/a	73	13	14
K11	5	5	n/a	37	37	26
K12	1	2	1	75	19	6
K13	3	2	3	64	24	12
K14	1	2	2	63	25	12
L1	2	3	2	74	16	10
L2	4	4	2	64	24	12
L3	4	4	2	42	32	26
L4	1	3	2	64	24	12
L5	2	4	2	70	18	12
L6	1	2	1	72	21	7
L7	7	4	3	32	37	31
L8	5	4	4	36	32	32
L9	5	3	3	56	30	14
L10	3	3	2	40	33	27
L11	2	3	2	56	31	13
L12	3	3	2	60	23	17
L13	1	1	2	82	11	7
L14	2	2	2	70	20	10
M1	4	3	2	58	24	18
M2	5	5	3	45	23	32
M3	5	5	3	20	46	34
M4	4	5	2	50	32	18
M5	4	3	2	38	33	29

APPENIX III: Site Characteristics and Granulometric Anaylsis

Sample Site	Field Data			Granulometric Anaysis		
	Sample		Local	Sand	Silt	Clay
	Texture	consistency	Drainage	wt.%	wt.%	wt.%
M6	4	4	2	49	29	22
M7	4	4	3	46	37	17
M8	3	4	2	50	40	10
M9	4	3	2	56	31	13
M10	3	3	2	36	31	33
M11	4	4	2	49	21	30
M12	1	1	2	85	8	7
M13	2	1	2	64	19	17
M14	10	4	3	42	23	35
N1	4	3	2	57	24	19
N2	5	5	2	42	28	30
N3	5	5	2	26	32	42
N4	5	4	2	44	33	23
N5	5	4	4	44	29	27
N6	4	4	2	51	28	21
N7	2	2	n/a	58	21	21
N8	4	3	3	66	24	10
N9	2	2	n/a	68	23	9
N10	4	3	2	63	24	13
N11	2	2	2	70	19	11
N12	2	4	2	66	19	15
N13	4	1	2	71	22	7
N14	2	1	2	64	23	13
P1	5	5	3	53	26	21
P2	5	4	3	26	34	40
P3	1	2	2	46	48	6
P4	5	4	2	41	30	29
P5	4	3	2	57	17	26
P6	5	3	4	44	26	30
P7	5	4	2	45	27	28
P8	2	3	2	65	24	11
P9	2	4	2	71	20	9
P10	1	2	2	73	17	10
P11	3	3	2	58	18	24
P12	5	4	3	55	27	18
P13	5	1	2	73	14	13
P14	5	1	2	58	28	14
Q1	5	3	n/a	60	19	21
Q2	5	4	3	32	37	31
Q3	5	2	4	35	39	26
Q4	5	2	2	45	29	26
Q5	5	4	3	44	45	11
Q6	5	3	3	37	37	26
Q7	5	4	3	34	38	28
Q8	3	4	2	63	26	11

APPENIX III: Site Characteristics and Granulometric Anaylsis

Sample Site	Field Data			Granulometric Anaysis		
	Sample		Local	Sand	Silt	Clay
	Texture	consistency	Drainage	wt.%	wt.%	wt.%
Q9	2	2	2	68	20	12
Q10	1	2	1	69	26	5
Q11	4	4	2	60	31	9
Q12	5	4	2	55	27	18
Q13	2	1	2	74	21	5
Q14	2	1	2	68	27	5
R1	5	4	3	42	30	28
R2	5	4	3	38	30	32
R3	5	3	3	43	35	22
R4	5	4	2	40	36	24
R5	4	3	n/a	63	21	16
R6	5	3	3	35	37	28
R7	5	4	4	34	38	28
R8	2	3	2	58	33	9
R9	2	3	2	63	23	14
R10	2	3	2	62	27	11
R11	3	3	2	72	21	7
R12	2	1	2	71	19	10
R13	4	2	2	47	31	22
R14	4	3	2	50	31	19
S1	4	4	2	63	23	14
S2	4	3	3	47	30	23
S3	5	4	3	47	29	24
S4	5	4	4	43	26	31
S5	5	4	3	38	31	31
S6	4	4	3	55	23	22
S7	4	3	4	53	27	20
S8	4	3	2	71	14	15
S9	2	3	2	67	20	13
S10	2	2	2	68	21	11
S11	3	2	n/a	64	20	16
S12	3	1	2	62	28	10
S13	3	1	2	66	24	10
S14	2	1	2	73	22	5
T1	5	3	2	55	25	20
T2	5	4	4	42	33	25
T3	5	4	3	47	28	25
T4	7	4	4	37	31	32
T5	5	4	2	34	32	34
T6	5	3	n/a	33	36	31
T7	4	3	2	61	22	17
T8	4	3	2	61	27	12
T9	2	2	2	64	24	12
T10	3	2	2	63	24	13
T11	7	5	2	45	26	29

APPENIX III: Site Characteristics and Granulometric Anaylsis

Sample Site	Field Data			Granulometric Anaysis		
	Sample		Local	Sand	Silt	Clay
	Texture	consistency	Drainage	wt.%	wt.%	wt.%
T12	10	4	3	44	33	23
T13	3	1	3	80	15	5
T14	3	4	2	69	27	4
V1	4	3	2	57	28	15
V2	4	4	4	42	31	27
V3	5	3	4	40	33	27
V4	4	4	2	40	35	25
V5	5	3	n/a	33	35	32
V6	7	4	3	29	27	44
V7	5	4	4	40	28	32
V8	2	3	2	68	12	20
V9	4	4	2	53	28	19
V10	4	4	2	58	21	21
V11	3	2	n/a	59	25	16
V12	2	1	3	56	31	13
V13	2	1	2	59	27	14
V14	5	2	3	47	35	18
W1	4	3	3	52	31	17
W2	5	3	3	49	32	19
W3	7	4	4	31	32	37
W4	7	4	4	33	31	36
W5	5	4	n/a	30	37	33
W6	5	3	3	35	28	37
W7	4	3	n/a	51	27	22
W8	4	3	2	50	31	19
W9	4	3	2	60	25	15
W10	4	2	3	47	31	22
W11	4	3	2	62	23	15
W12	3	2	2	47	31	22
W13	10	3	n/a	41	39	20
W14	3	2	2	43	40	17
X1	3	4	3	48	36	16
X2	5	4	n/a	45	29	26
X3	5	4	2	40	29	31
X4	7	4	3	32	32	36
X5	7	4	n/a	32	31	37
X6	7	4	4	35	35	30
X7	4	3	n/a	48	28	24
X8	2	4	2	57	27	16
X9	4	3	2	61	28	11
X10	2	2	2	58	28	14
X11	3	3	2	63	25	12
X12	4	3	2	46	40	14
X13	5	3	2	69	19	12
X14	1	1	1	70	21	9

APPENDIX IV

LITHOLOGICAL ANALYSIS

Approximately 50 to 100 till clasts between 2cm to 10cm in diameter were collected from the C-horizon at the 270 sample sites. These clasts were categorized into 18 broad lithological groups:

Intrusive Rocks	Sedimentary Rocks	Miscellaneous
1) Felsic	7) Red Conglomerate	14) Rounded Quartz
2) Mafic	8) Grey Conglomerate	15) Angular Quartz
3) Diabase	9) Red Sandstone	16) Chert/Jasper
Extrusive Rocks	10) Grey Sandstone	17) Metamorphosed Sedimentary
4) Felsic Flow	11) Red Silt/mudstone	
5) Mafic Flow	12) Grey Silt/mudstone	18) Quartzite
6) Felsic Tuff	13) Greywacke	

The concentrations/abundances for these 18 lithologies are expressed as percentages of the total number of clasts collected at each site.

The lithological data was contoured using Surfer® 6.01 computer software. A linear isotropic variogram model was used to interpolate grid nodes between sample sites for contouring. Kriging, a geostatistical gridding method, was employed to generate lithological contour maps for the study area from the grid nodes.

APPENDIX IV: Till Clast Lithological Analysis

Sample Site	Rounded Quartz	Felsic			Diabase	Mafic		Quartzite
		Intrusive	Volcanic	Tuffs		Intrusive	Volcanic	
A8	4	0	12	0	0	0	0	19
A9	0	21	21	0	0	4	5	6
A10	0	93	0	0	0	0	2	0
A11	2	2	27	32	0	3	6	2
A12	0	0	0	0	0	0	0	0
A13	2	1	1	10	0	0	3	0
B1	5	0	0	0	0	3	0	2
B2	12	2	3	0	0	0	0	0
B3	6	0	1	0	0	1	0	0
B4	3	2	2	0	0	2	2	0
B5	4	15	45	0	0	4	0	0
B6	26	9	33	0	0	0	23	0
B7	0	0	5	0	0	0	0	0
B8	0	0	0	0	0	100	0	0
B9	0	0	0	0	0	0	0	0
B10	2	0	26	0	0	1	3	0
B11	0	0	18	0	0	3	0	0
B12	0	0	0	0	0	0	0	0
B13	5	1	0	0	0	4	1	0
C1	4	0	1	8	0	0	34	0
C2	3	1	1	59	0	5	3	0
C3	15	0	0	48	0	0	35	0
C4	0	2	63	33	0	0	2	0
C5	0	1	29	69	0	0	1	0
C6	4	1	9	1	0	1	6	0
C7	0	0	64	33	0	0	0	0
C8	3	1	52	17	0	1	17	0
C9	0	0	0	0	0	0	0	0
C10	3	4	16	8	0	0	63	0
C11	0	1	36	0	0	0	8	0
C12	3	3	55	0	0	0	7	0
C13	4	0	2	5	0	2	0	0
D1	0	0	0	100	0	0	0	0
D2	21	0	4	19	0	0	31	0
D3	5	5	14	28	0	6	6	0
D4	0	0	47	53	0	0	0	0
D5	0	4	28	13	0	7	4	0
D6	0	3	64	0	0	3	7	0
D7	4	6	77	0	0	0	4	0
D8	0	0	3	10	0	0	0	0
D9	0	0	0	0	0	0	0	0
D10	3	10	28	0	0	1	0	0
D11	0	0	0	1	0	0	0	0
D12	0	0	1	0	0	1	0	0
D13	7	0	9	3	0	0	2	0
D14	1	9	62	18	0	1	3	0
E1	4	1	0	4	0	0	62	0
E2	5	5	5	24	0	2	0	0

APPENDIX IV: Till Clast Lithological Analysis

Sample Site	Rounded Quartz	Felsic Intrusive	Felsic Volcanic	Felsic Tuffs	Diabase	Mafic Intrusive	Mafic Volcanic	Quartzite
E3	0	0	23	15	0	2	18	0
E4	10	5	31	21	0	5	12	0
E5	0	0	1	0	0	0	0	2
E6	2	0	18	34	0	2	5	0
E7	5	2	52	1	0	2	4	0
E8	0	35	24	0	0	11	0	1
E9	9	6	21	10	0	0	3	0
E10	0	0	5	0	0	0	0	0
E11	1	0	0	0	0	0	0	0
E12	0	0	1	0	0	0	0	2
E13	29	6	17	0	0	0	3	3
E14	0	0	33	7	0	0	0	0
F1	4	0	0	0	0	0	4	0
F2	0	11	56	0	0	0	33	0
F3	0	14	14	0	0	0	7	0
F4	3	33	19	0	0	0	0	0
F5	2	8	0	0	0	0	0	1
F6	0	30	26	2	0	8	0	0
F7	3	16	55	0	0	11	0	0
F8	0	2	20	0	0	4	0	0
F9	0	5	15	0	0	3	0	2
F10	0	2	8	0	0	0	0	0
F11	0	3	0	0	0	3	0	0
F12	0	0	0	0	0	0	0	1
F13	10	3	54	0	0	7	0	0
F14	3	22	55	0	0	3	0	0
G1	0	43	37	0	0	0	0	14
G2	0	13	29	15	0	0	0	5
G3	0	5	20	7	0	1	1	0
G4	0	42	36	0	0	0	0	0
G5	0	2	12	0	0	0	0	0
G6	0	2	7	0	0	0	0	0
G7	0	4	6	0	0	0	0	6
G8	0	0	4	0	0	0	0	0
G9	0	1	1	0	0	0	0	0
G10	0	1	26	0	0	0	0	0
G11	0	0	0	0	0	0	0	0
G12	6	0	13	0	0	0	0	6
G13	0	0	2	0	0	0	0	0
G14	0	12	86	0	0	0	0	0
H1	0	18	14	0	0	0	0	6
H2	0	6	10	0	0	2	0	6
H3	0	14	19	0	0	1	1	0
H4	0	4	74	0	0	0	4	0
H5	0	0	0	0	0	0	0	0
H6	0	3	5	0	0	0	0	0
H7	0	1	3	0	0	0	0	0
H8	0	3	0	0	0	0	0	0

APPENDIX IV: Till Clast Lithological Analysis

Sample Site	Rounded Quartz	Felsic			Diabase	Mafic		Quartzite
		Intrusive	Volcanic	Tuffs		Intrusive	Volcanic	
H9	2	0	2	0	0	0	0	0
H10	1	0	9	0	0	0	0	0
H11	2	0	0	0	0	0	0	0
H12	0	0	0	0	0	0	0	0
H13	0	0	0	0	0	0	0	0
H14	0	2	3	0	0	0	0	0
K1	0	50	8	0	0	0	0	4
K2	0	6	39	0	0	0	0	7
K3	4	11	44	0	0	1	0	5
K4	0	1	5	0	1	0	0	0
K5	0	0	2	0	0	0	1	0
K6	0	0	23	0	0	0	0	1
K7	0	2	1	0	0	0	0	2
K8	0	0	0	0	0	0	0	10
K9	0	0	0	0	0	0	0	0
K10	0	2	53	0	0	0	0	8
K11	0	0	0	0	0	0	0	0
K12	0	0	0	0	0	0	0	0
K13	0	0	0	0	0	0	0	0
K14	0	0	0	0	0	0	0	0
L1	0	23	62	0	0	1	2	0
L2	0	28	41	0	0	4	0	17
L3	0	3	12	0	0	0	0	0
L4	0	0	10	0	0	0	2	0
L5	12	7	10	0	0	0	0	8
L6	0	0	0	0	0	0	0	0
L7	0	1	5	0	0	1	0	0
L8	0	3	3	0	0	0	0	0
L9	0	3	4	0	0	0	0	3
L10	5	0	5	0	0	0	0	0
L11	0	0	1	0	0	0	0	1
L12	0	0	0	0	0	0	0	0
L13	0	0	0	0	0	0	0	0
L14	0	0	0	0	0	0	0	0
M1	7	17	52	0	0	0	2	0
M2	0	6	10	0	0	0	4	2
M3	0	1	6	0	0	0	2	1
M4	6	1	0	0	0	0	0	0
M5	4	0	0	0	0	0	0	1
M6	1	0	3	0	0	0	0	2
M7	5	5	5	0	0	0	0	5
M8	0	0	2	0	0	0	0	0
M9	5	0	17	0	0	0	0	3
M10	0	0	0	0	0	0	0	0
M11	0	0	0	0	0	0	0	0
M12	0	0	0	0	0	0	0	0
M13	0	0	0	0	0	0	0	0
M14	1	0	1	0	0	0	0	0

APPENDIX IV: Till Clast Lithological Analysis

Sample Site	Rounded Quartz	Felsic			Diabase	Mafic		Quartzite
		Intrusive	Volcanic	Tuffs		Intrusive	Volcanic	
N1	0	23	38	0	0	0	0	8
N2	0	11	20	0	0	0	0	7
N3	0	0	0	0	0	0	0	0
N4	0	5	25	0	0	0	0	2
N5	3	0	16	0	0	0	0	5
N6	2	2	16	0	0	0	0	0
N7	2	0	1	0	0	0	0	5
N8	0	0	0	0	0	0	0	0
N9	0	0	0	0	0	0	0	0
N10	3	0	0	0	0	0	0	0
N11	0	0	0	0	0	0	0	0
N12	0	0	0	0	0	0	0	0
N13	0	0	0	0	0	0	0	0
N14	0	21	64	3	2	0	0	0
P1	0	8	30	0	0	0	0	0
P2	0	0	0	0	0	0	0	12
P3	4	32	20	0	0	2	0	14
P4	3	21	0	0	0	0	0	0
P5	5	1	9	0	0	0	1	5
P6	2	0	5	0	0	0	0	0
P7	2	0	0	0	0	0	0	0
P8	0	0	4	0	0	0	0	1
P9	2	0	0	0	0	0	0	0
P10	0	0	0	0	0	0	0	0
P11	0	1	0	0	0	0	0	0
P12	0	0	2	0	0	0	0	0
P13	0	33	44	1	0	1	0	0
P14	2	11	55	0	0	9	0	0
Q1	2	4	33	0	0	0	0	10
Q2	2	2	3	0	0	0	0	14
Q3	0	0	0	0	0	0	0	3
Q4	0	3	10	0	0	0	0	0
Q5	4	2	8	0	0	0	0	12
Q6	0	0	0	0	0	0	0	0
Q7	0	0	5	0	0	0	0	0
Q8	0	0	0	0	0	0	0	0
Q9	0	0	0	0	0	0	0	0
Q10	0	0	0	0	0	0	0	0
Q11	0	0	0	0	0	0	0	0
Q12	0	1	3	0	0	0	0	0
Q13	0	0	69	0	0	0	0	0
Q14	0	0	92	0	0	0	0	0
R1	0	3	32	0	0	0	0	10
R2	0	12	10	0	0	0	0	14
R3	8	0	18	0	0	0	0	0
R4	6	0	2	0	0	2	0	4
R5	6	6	21	0	0	0	0	32
R6	0	7	0	0	0	0	0	2

APPENDIX IV: Till Clast Lithological Analysis

Sample Site	Rounded Quartz	Felsic Intrusive	Felsic Volcanic	Felsic Tuffs	Diabase	Mafic Intrusive	Mafic Volcanic	Quartzite
R7	0	0	3	0	0	3	0	0
R8	0	0	2	0	0	3	0	0
R9	0	0	0	0	0	2	0	0
R10	0	0	0	0	0	0	0	0
R11	0	0	0	0	0	0	0	0
R12	0	0	0	0	0	0	0	0
R13	0	0	16	0	0	7	0	7
R14	0	1	31	23	0	0	0	0
S1	0	5	41	0	0	0	0	3
S2	4	2	22	0	0	0	0	9
S3	0	0	2	0	0	0	0	7
S4	9	0	7	0	0	0	0	2
S5	0	0	0	0	0	0	0	0
S6	0	0	0	0	0	0	0	0
S7	0	2	4	0	0	8	0	2
S8	0	0	0	0	0	0	0	0
S9	0	0	0	0	0	0	0	0
S10	0	0	0	0	0	0	0	0
S11	0	0	0	0	0	0	0	0
S12	0	0	0	0	0	0	0	0
S13	0	1	22	1	0	0	0	3
S14	0	79	0	21	0	0	0	0
T1	3	12	17	0	0	2	0	0
T2	0	6	6	0	0	0	0	9
T3	2	4	13	0	0	0	0	22
T4	3	6	3	0	0	0	0	11
T5	0	0	0	0	0	0	0	0
T6	0	0	5	0	0	0	0	5
T7	2	2	11	0	0	0	0	2
T8	0	3	4	0	0	0	0	2
T9	0	5	5	0	0	0	0	0
T10	0	0	0	0	0	0	0	0
T11	0	6	10	0	0	0	0	3
T12	0	2	21	0	0	0	10	0
T13	0	19	80	0	0	0	0	0
T14	0	40	14	0	0	0	0	0
V1	2	0	3	0	0	0	0	72
V2	9	3	6	0	0	0	0	0
V3	2	0	15	0	0	0	0	5
V4	0	0	0	0	0	0	0	0
V5	0	6	0	0	0	0	0	3
V6	0	0	0	0	0	0	0	0
V7	0	6	3	0	0	3	0	0
V8	0	0	0	0	0	0	0	0
V9	0	0	0	0	0	0	0	0
V10	0	0	9	0	0	5	0	0
V11	0	26	29	0	0	0	0	0
V12	0	24	44	0	0	0	0	2

APPENDIX IV: Till Clast Lithological Analysis

Sample Site	Rounded Quartz	Felsic			Diabase	Mafic		Quartzite
		Intrusive	Volcanic	Tuffs		Intrusive	Volcanic	
V13	0	55	11	0	0	0	0	1
V14	0	30	31	0	0	1	0	0
W1	5	3	36	0	0	0	0	8
W2	2	2	19	0	0	0	0	7
W3	7	0	0	0	0	0	0	4
W4	0	0	0	0	0	0	0	0
W5	0	0	23	0	0	0	0	0
W6	0	0	0	0	0	0	0	0
W7	0	0	6	0	0	0	0	2
W8	0	7	13	0	0	1	0	1
W9	0	2	20	0	0	0	0	0
W10	0	0	11	0	0	0	0	0
W11	0	21	57	0	0	0	0	0
W12	0	28	55	0	0	0	0	0
W13	0	8	38	0	0	0	0	0
W14	0	77	13	0	0	0	0	1
X1	5	0	18	0	0	2	0	0
X2	0	8	6	0	0	0	0	2
X3	2	2	12	0	0	2	0	14
X4	0	8	0	0	0	0	0	0
X5	0	0	0	0	0	0	0	0
X6	0	0	3	0	0	0	0	0
X7	0	8	27	0	0	0	0	0
X8	1	17	7	0	0	0	0	0
X9	0	3	33	0	0	0	0	6
X10	0	13	57	0	0	0	7	0
X11	0	11	83	0	0	0	0	0
X12	0	6	43	0	0	0	0	0
X13	1	2	11	0	0	0	0	1
X14	0	0	100	0	0	0	0	0

APPENDIX IV: Till Clast Lithological Analysis

Sample Site	Angular Quartz	Chert/ Jasper	Metamorphosed Sedimentary	Conglomerate		Sandstone
				Grey	Red	Grey
A8	0	0	0	0	0	0
A9	0	5	4	0	5	14
A10	0	0	0	0	0	0
A11	0	0	6	0	4	16
A12	0	0	0	10	69	21
A13	0	0	0	0	80	1
B1	0	0	0	3	0	88
B2	0	0	0	9	0	74
B3	0	0	0	10	0	9
B4	0	0	0	0	64	25
B5	0	0	0	0	0	30
B6	0	0	0	0	0	7
B7	0	0	0	0	0	0
B8	0	0	0	0	0	0
B9	0	0	0	0	100	0
B10	0	0	0	0	46	5
B11	0	0	2	0	14	0
B12	0	0	2	0	0	6
B13	0	0	0	7	0	48
C1	0	0	0	7	0	45
C2	0	4	0	8	0	16
C3	0	0	0	0	1	0
C4	0	0	0	0	0	0
C5	0	0	0	0	0	0
C6	0	0	0	0	12	1
C7	1	0	1	0	0	0
C8	0	0	0	0	7	0
C9	0	0	0	0	61	0
C10	0	0	0	0	3	4
C11	0	0	0	1	0	0
C12	0	0	0	0	0	31
C13	0	0	0	0	57	0
D1	0	0	0	0	0	0
D2	0	0	0	0	0	25
D3	0	0	0	0	0	37
D4	0	0	0	0	0	0
D5	0	0	0	0	28	7
D6	0	0	3	6	0	14
D7	0	0	0	0	4	2
D8	0	0	0	0	87	0
D9	0	0	0	0	0	0
D10	0	0	0	3	3	51
D11	0	0	0	91	0	8
D12	0	0	0	0	43	42
D13	0	0	0	5	13	56
D14	0	0	0	0	0	0
E1	0	0	0	8	0	19
E2	0	0	6	5	0	42

APPENDIX IV: Till Clast Lithological Analysis

Sample Site	Angular Quartz	Chert/ Jasper	Metamorphosed Sedimentary	Conglomerate		Sandstone
				Grey	Red	Grey
E3	0	0	0	0	0	38
E4	0	0	1	0	0	12
E5	0	0	0	20	0	0
E6	0	0	2	0	0	0
E7	0	0	2	0	9	0
E8	0	0	5	0	0	1
E9	0	0	1	6	0	34
E10	0	0	0	42	0	53
E11	0	0	0	14	0	83
E12	0	0	0	20	0	0
E13	0	0	3	0	0	34
E14	0	0	0	7	7	4
F1	0	0	0	3	0	87
F2	0	0	0	0	0	0
F3	0	0	1	0	0	64
F4	0	0	0	0	0	41
F5	0	0	4	0	0	83
F6	0	0	0	0	0	18
F7	0	0	0	2	0	8
F8	0	0	0	0	0	47
F9	0	0	0	0	0	69
F10	0	0	2	3	0	42
F11	0	0	0	0	0	95
F12	0	0	0	0	16	9
F13	0	0	0	2	0	22
F14	0	0	1	0	0	12
G1	0	0	4	0	0	2
G2	15	0	16	0	0	7
G3	5	0	13	2	0	42
G4	19	0	0	0	0	1
G5	0	0	0	0	0	40
G6	2	0	3	0	0	73
G7	4	0	0	0	0	0
G8	0	1	0	3	0	91
G9	0	0	0	1	0	84
G10	5	0	0	2	0	66
G11	0	0	0	0	0	100
G12	0	0	0	4	0	45
G13	0	0	0	0	0	98
G14	1	0	2	0	0	0
H1	4	0	4	0	0	53
H2	0	0	2	2	0	70
H3	2	0	0	2	0	59
H4	7	0	0	0	11	2
H5	7	0	0	0	93	0
H6	2	0	1	90	0	0
H7	1	0	0	52	0	43
H8	0	0	0	0	0	77

APPENDIX IV: Till Clast Lithological Analysis

Sample Site	Angular Quartz	Chert/ Jasper	Metamorphosed Sedimentary	Conglomerate		Sandstone
				Grey	Red	Grey
H9	0	0	0	0	0	13
H10	0	0	0	42	0	48
H11	0	0	0	9	0	89
H12	0	0	0	0	0	100
H13	0	0	0	9	0	91
H14	0	0	0	0	0	95
K1	0	0	0	0	0	38
K2	1	0	0	0	0	41
K3	1	0	0	0	0	0
K4	2	0	0	0	0	2
K5	0	0	0	0	0	15
K6	9	0	3	3	0	61
K7	0	0	0	10	0	32
K8	0	0	0	10	0	65
K9	0	0	0	0	0	100
K10	0	0	0	4	0	34
K11	0	0	0	0	0	100
K12	0	0	0	0	0	100
K13	0	0	0	0	0	100
K14	0	0	0	0	0	100
L1	2	0	9	0	0	1
L2	9	0	0	0	0	0
L3	3	0	0	0	1	3
L4	2	0	0	1	0	38
L5	0	0	0	11	0	0
L6	0	0	0	0	0	100
L7	1	0	0	9	0	51
L8	0	0	0	0	0	12
L9	0	0	0	0	0	91
L10	0	0	0	0	0	12
L11	0	0	0	8	0	82
L12	0	0	0	0	0	95
L13	0	0	0	0	0	100
L14	0	0	0	0	0	100
M1	0	0	0	0	0	2
M2	0	0	0	0	0	6
M3	2	0	0	0	1	1
M4	0	0	3	5	0	4
M5	0	0	0	1	0	92
M6	1	0	0	17	0	49
M7	0	3	5	0	8	61
M8	0	0	0	0	0	98
M9	0	2	0	0	6	0
M10	0	0	0	0	0	100
M11	0	0	0	0	0	100
M12	0	0	0	0	0	100
M13	0	0	0	0	0	100
M14	0	0	0	0	0	91

APPENDIX IV: Till Clast Lithological Analysis

Sample Site	Angular Quartz	Chert/ Jasper	Metamorphosed Sedimentary	Conglomerate		Sandstone
				Grey	Red	Grey
N1	0	0	0	0	0	29
N2	0	0	0	0	0	7
N3	0	0	0	0	0	100
N4	2	0	5	7	0	34
N5	0	0	0	24	0	53
N6	0	0	2	13	0	49
N7	0	0	0	2	0	89
N8	0	0	2	39	0	59
N9	0	0	0	0	0	100
N10	0	0	0	19	0	39
N11	0	0	0	0	0	100
N12	0	0	0	0	0	100
N13	0	0	0	15	0	85
N14	0	0	4	0	0	5
P1	0	0	20	0	0	32
P2	0	0	0	0	0	2
P3	0	0	0	0	5	0
P4	0	0	0	0	0	76
P5	0	0	0	0	0	18
P6	0	5	5	0	0	49
P7	0	0	4	4	0	90
P8	0	0	0	0	0	87
P9	0	0	6	40	0	0
P10	0	0	0	3	0	97
P11	0	0	0	6	0	93
P12	0	0	0	0	0	98
P13	0	0	4	0	0	16
P14	0	0	5	0	0	0
Q1	0	0	0	0	0	10
Q2	0	0	0	0	0	15
Q3	0	0	0	0	0	67
Q4	0	0	10	0	11	3
Q5	0	0	0	0	0	46
Q6	0	0	2	0	0	31
Q7	0	0	0	5	0	80
Q8	0	0	0	0	0	98
Q9	0	0	0	0	0	98
Q10	0	0	0	0	0	100
Q11	0	0	0	0	0	100
Q12	0	0	0	0	0	96
Q13	0	0	0	31	0	0
Q14	2	0	6	0	0	0
R1	0	0	3	0	0	6
R2	0	0	0	0	0	48
R3	0	0	0	1	0	72
R4	0	0	0	0	0	20
R5	0	0	0	0	0	35
R6	0	0	0	0	15	31

APPENDIX IV: Till Clast Lithological Analysis

Sample Site	Angular Quartz	Chert/ Jasper	Metamorphosed Sedimentary	Conglomerate		Sandstone
				Grey	Red	Grey
R7	0	0	0	3	0	85
R8	0	0	0	0	0	95
R9		0	0	0	0	98
R10	0	0	0	0	0	100
R11	0	0	0	0	0	100
R12	0	0	0	0	0	100
R13	0	0	0	0	0	65
R14	0	0	29	1	0	14
S1	2	0	0	0	0	0
S2	0	0	0	0	0	9
S3	0	0	0	0	0	11
S4	0	0	0	2	0	69
S5	2	0	0	24	0	32
S6	0	0	0	23	0	48
S7	0	0	2	0	0	78
S8	0	0	0	0	0	100
S9	0	0	0	0	0	100
S10	0	0	0	0	0	100
S11	0	0	0	0	0	100
S12	0	0	0	0	0	100
S13	1	0	0	1	0	70
S14	0	0	0	0	0	0
T1	0	0	0	0	0	2
T2	0	0	0	9	6	35
T3	0	0	0	2	0	30
T4	0	0	0	6	0	63
T5	0	0	0	0	0	27
T6	0	0	0	3	0	44
T7	0	0	0	3	0	82
T8	0	0	0	1	0	87
T9	0	0	0	0	0	90
T10	0	0	0	0	0	100
T11	0	0	1	0	0	54
T12	0	0	0	2	0	66
T13	0	0	0	0	0	1
T14	0	0	32	10	0	4
V1	0	0	0	0	16	3
V2	0	0	0	0	0	32
V3	0	0	0	7	0	7
V4	0	0	0	9	0	18
V5	0	0	0	0	0	52
V6	0	0	0	12	0	16
V7	0	0	0	0	0	66
V8	0	0	0	0	0	100
V9	0	0	0	0	0	100
V10	0	0	0	0	0	86
V11	0	0	7	0	0	38
V12	0	0	19	0	0	11

APPENDIX IV: Till Clast Lithological Analysis

Sample Site	Angular Quartz	Chert/ Jasper	Metamorphosed Sedimentary	Conglomerate		Sandstone
				Grey	Red	Grey
V13	0	0	17	0	0	16
V14	0	0	14	0	0	24
W1	0	0	0	0	0	32
W2	0	0	0	0	0	31
W3	0	0	0	0	0	70
W4	0	0	0	7	0	43
W5	0	0	0	6	0	23
W6	0	0	0	56	0	44
W7	0	0	0	0	2	82
W8	0	0	0	0	4	73
W9	0	0	2	2	0	73
W10	0	0	0	29	0	60
W11	0	0	0	0	0	21
W12	0	0	0	0	0	17
W13	1	0	1	0	0	26
W14	0	0	8	0	0	0
X1	0	0	0	0	0	33
X2	2	2	0	4	0	10
X3	0	0	0	2	0	14
X4	0	0	0	38	54	0
X5	0	0	0	0	0	38
X6	0	0	0	0	0	6
X7	0	0	0	0	0	63
X8	0	0	0	0	0	72
X9	0	0	2	5	0	50
X10	0	0	0	0	0	10
X11	0	0	0	0	0	0
X12	0	0	1	1	0	4
X13	0	0	0	1	1	75
X14	0	0	0	0	0	0

APPENDIX IV: Till Clast Lithological Analysis

Sample Site		Mudstone/siltstone		Grey-wacke
	Red	Grey	Red	
A8	25	0	39	0
A9	14	0	0	2
A10	6	0	0	0
A11	0	0	0	0
A12	0	0	0	0
A13	0	0	0	0
B1	0	0	0	0
B2	0	0	0	0
B3	0	72	0	0
B4	0	0	0	0
B5	0	0	2	0
B6	0	0	2	0
B7	33	0	62	0
B8	0	0	0	0
B9	0	0	0	0
B10	16	0	0	0
B11	60	2	0	0
B12	81	0	0	11
B13	0	26	8	0
C1	0	0	0	0
C2	0	0	0	0
C3	0	0	0	0
C4	0	0	0	0
C5	0	0	0	0
C6	61	0	1	0
C7	0	0	0	0
C8	0	0	0	0
C9	39	0	0	0
C10	0	0	0	0
C11	52	2	0	0
C12	0	0	0	0
C13	2	2	25	2
D1	0	0	0	0
D2	0	0	0	0
D3	0	0	0	0
D4	0	0	0	0
D5	7	0	2	0
D6	0	0	0	0
D7	4	0	0	0
D8	0	0	0	0
D9	0	0	100	0
D10	0	0	3	0
D11	0	0	0	0
D12	4	1	7	0
D13	0	3	1	0
D14	6	0	0	0
E1	1	0	0	1
E2	2	5	0	0

APPENDIX IV: Till Clast Lithological Analysis

Sample Site		Mudstone/siltstone		Grey-wacke
	Red	Grey	Red	
E3	0	2	0	2
E4	0	0	2	0
E5	76	0	0	0
E6	34	2	0	0
E7	10	12	0	0
E8	1	7	14	0
E9	1	1	6	0
E10	0	0	0	0
E11	1	0	0	0
E12	76	0	0	0
E13	6	0	0	0
E14	38	4	0	0
F1	1	0	0	0
F2	0	0	0	0
F3	0	0	0	0
F4	1	1	1	0
F5	1	0	0	0
F6	16	0	0	0
F7	3	2	0	0
F8	20	6	2	0
F9	5	2	0	0
F10	0	44	0	0
F11	0	0	0	0
F12	74	0	0	0
F13	0	2	0	0
F14	5	0	0	0
G1	0	0	0	0
G2	0	0	0	0
G3	3	1	1	0
G4	0	0	1	0
G5	47	0	0	0
G6	13	0	0	0
G7	79	0	0	0
G8	0	0	0	0
G9	12	0	0	0
G10	0	0	0	0
G11	0	0	0	0
G12	26	0	0	0
G13	0	0	0	0
G14	0	0	0	0
H1	0	0	0	0
H2	2	0	0	0
H3	0	1	0	0
H4	0	0	0	0
H5	0	0	0	0
H6	0	0	0	0
H7	0	0	0	0
H8	21	0	0	0

APPENDIX IV: Till Clast Lithological Analysis

Sample Site		Mudstone/siltstone		Grey-wacke
	Red	Grey	Red	
H9	2	0	82	0
H10	0	0	0	0
H11	0	0	0	0
H12	0	0	0	0
H13	0	0	0	0
H14	0	0	0	0
K1	0	0	0	0
K2	6	0	0	0
K3	34	0	0	0
K4	87	1	0	0
K5	0	1	80	0
K6	0	0	0	0
K7	53	0	0	0
K8	0	16	0	0
K9	0	0	0	0
K10	0	0	0	0
K11	0	0	0	0
K12	0	0	0	0
K13	0	0	0	0
K14	0	0	0	0
L1	0	0	0	0
L2	0	0	0	0
L3	62	16	0	0
L4	30	16	0	0
L5	52	0	0	0
L6	0	0	0	0
L7	31	0	0	0
L8	82	0	0	0
L9	0	0	0	0
L10	0	0	77	0
L11	8	0	0	0
L12	5	0	0	0
L13	0	0	0	0
L14	0	0	0	0
M1	0	19	0	0
M2	0	71	0	0
M3	3	16	65	0
M4	60	9	12	0
M5	0	2	0	0
M6	25	0	0	0
M7	2	0	0	0
M8	0	0	0	0
M9	67	0	0	0
M10	0	0	0	0
M11	0	0	0	0
M12	0	0	0	0
M13	0	0	0	0
M14	6	0	0	0

APPENDIX IV: Till Clast Lithological Analysis

Sample Site	Red	Mudstone/siltstone Grey	Red	Grey-wacke
N1	1	1	0	0
N2	15	28	13	0
N3	0	0	0	0
N4	20	0	0	0
N5	0	0	0	0
N6	16	0	0	0
N7	0	0	0	0
N8	0	0	0	0
N9	0	0	0	0
N10	0	39	0	0
N11	0	0	0	0
N12	0	0	0	0
N13	0	0	0	0
N14	0	0	0	0
P1	2	5	3	0
P2	0	8	78	0
P3	21	0	2	0
P4	0	0	0	0
P5	54	3	5	0
P6	33	0	0	0
P7	0	0	0	0
P8	0	7	0	0
P9	0	53	0	0
P10	0	0	0	0
P11	0	0	0	0
P12	0	0	0	0
P13	0	0	0	0
P14	18	0	0	0
Q1	0	14	27	0
Q2	0	3	61	0
Q3	0	5	24	0
Q4	0	62	0	0
Q5	21	2	6	0
Q6	63	4	0	0
Q7	0	4	5	0
Q8	0	2	0	0
Q9	0	2	0	0
Q10	0	0	0	0
Q11	0	0	0	0
Q12	0	0	0	0
Q13	0	0	0	0
Q14	0	0	0	0
R1	0	13	32	0
R2	17	0	0	0
R3	0	0	0	0
R4	66	0	0	0
R5	0	0	0	0
R6	46	0	0	0

APPENDIX IV: Till Clast Lithological Analysis

Sample Site	Mudstone/siltstone			Grey-wacke
	Red	Grey	Red	
R7	3	3	0	0
R8	0	0	0	0
R9	0	0	0	0
R10	0	0	0	0
R11	0	0	0	0
R12	0	0	0	0
R13	5	0	0	0
R14	0	0	0	0
S1	18	21	10	0
S2	55	0	0	0
S3	67	2	11	0
S4	11	0	0	0
S5	0	2	41	0
S6	0	0	29	0
S7	4	0	0	0
S8	0	0	0	0
S9	0	0	0	0
S10	0	0	0	0
S11	0	0	0	0
S12	0	0	0	0
S13	0	0	0	0
S14	0	0	0	0
T1	22	41	0	0
T2	29	0	0	0
T3	26	0	2	0
T4	9	0	0	0
T5	73	0	0	0
T6	44	0	0	0
T7	0	0	0	0
T8	1	0	1	0
T9	0	0	0	0
T10	0	0	0	0
T11	0	26	0	0
T12	0	0	0	0
T13	0	0	0	0
T14	0	0	0	0
V1	0	3	0	0
V2	50	0	0	0
V3	66	0	0	0
V4	73	0	0	0
V5	39	0	0	0
V6	70	2	0	0
V7	16	6	0	0
V8	0	0	0	0
V9	0	0	0	0
V10	0	0	0	0
V11	0	0	0	0
V12	0	0	0	0

APPENDIX IV: Till Clast Lithological Analysis

Sample Site		Mudstone/siltstone		Grey-wacke
	Red	Grey	Red	
V13	0	0	0	0
V14	0	0	0	0
W1	12	5	0	0
W2	38	0	0	0
W3	19	0	0	0
W4	50	0	0	0
W5	48	0	0	0
W6	0	0	0	0
W7	6	2	0	0
W8	0	0	0	0
W9	0	0	0	0
W10	0	0	0	0
W11	0	0	0	0
W12	0	0	0	0
W13	26	0	0	0
W14	0	0	0	0
X1	42	0	0	0
X2	8	20	39	0
X3	53	0	0	0
X4	0	0	0	0
X5	62	0	0	0
X6	90	0	0	0
X7	0	0	2	0
X8	2	0	0	0
X9	0	0	2	0
X10	0	0	12	0
X11	7	0	0	0
X12	0	0	44	0
X13	10	0	0	0
X14	0	0	0	0

APPENDIX V

PART A–GEOCHEMICAL ANALYSIS

Geochemical analyses were performed on the <0.063 mm fraction of the till samples by Activation Laboratories Limited (Ancaster, Ontario) using inductively coupled plasma emission spectrometry (I.C.P.) and induced neutron activation analysis (I.N.A.A.). The samples were kiln dried at 95°C and dry-sieved in stainless sieves at the New Brunswick Department of Natural Resources and Energy sample preparation lab.

A "total digestion" of the sample was performed by ACTLABS for the I.C.P. analysis. Total digestion of the sample employed 4 acids; hydrochloric, nitric, perchloric, and hydrofluoric acids. However, according to ACTLABS, some mineral phase (e.g. barite, gahnite, chromite, and casserite) may remain insoluble in the 4 acid digestion reagent. Furthermore, other mineral phases (e.g. zircon, sphene, and magnetite) may only partially dissolve. To improve the detection limit for the I.C.P. mercury analysis, ACTLABS used a cold vapor Flow Injection Mercury System (FIMS).

A total of 48 elements (Ag, Al, As, Au, Ba, Be, Bi, Br, Ca, Cd, Ce, Co, Cr, Cs, Cu, Eu, Fe, Hf, Hg, Ir, K, La, Lu, Mg, Mn, Mo, Na, Nd, Ni, Pb, P, Rb, Sb, Sc, Se, Sm, Sn, Sr, Ta, Tb, Th, Ti, U, V, W, Y, Yb, Zn) were analyzed ACTLABS. The results are presented on the following pages in this appendix. For elemental concentrations below the detection limit, a value equal to one-half the detection limit inserted to permit statistical treatment of the data.

APPENDIX V: Part A- Geochemical Analysis (ICP Data)

Sample Site	Hg (ppb)	Cu (ppm)	Pb (ppm)	Zn (ppm)	Ag (ppm)	Ni (ppm)	Mn (ppm)	Sr (ppm)	Cd (ppm)	Bi (ppm)
A8	47	17	21	76	0.2	31	581	60	0.25	2.5
A9	22	19	13	59	0.2	23	387	94	0.25	2.5
A10	54	13	26	89	0.2	24	443	87	0.25	2.5
A11	51	27	24	100	0.6	43	709	95	0.25	2.5
A12	74	23	19	73	0.5	43	408	73	0.25	2.5
A13	30	25	13	89	0.2	54	373	84	0.25	2.5
B1	17	28	16	65	0.2	36	537	58	0.25	2.5
B2	21	27	17	76	0.5	40	1025	53	0.25	2.5
B3	25	24	16	66	0.4	34	615	46	0.25	2.5
B4	45	32	21	90	0.2	34	558	64	0.25	2.5
B5	41	22	22	65	0.6	32	548	80	0.25	2.5
B6	57	14	25	89	0.2	29	868	46	0.25	2.5
B7	50	14	23	73	0.2	35	649	50	0.5	2.5
B8	28	30	12	76	0.2	35	851	122	0.25	2.5
B9	28	20	24	95	0.2	32	757	75	0.25	2.5
B10	38	24	32	101	0.4	31	577	75	0.5	2.5
B11	25	23	38	155	0.6	41	708	131	0.25	2.5
B12	21	40	22	96	0.2	58	448	96	0.5	2.5
B13	34	31	22	91	0.2	44	623	68	0.25	2.5
C1	14	25	17	57	0.2	31	797	56	0.25	2.5
C2	48	20	14	76	0.2	35	618	45	0.25	2.5
C3	28	27	15	88	0.2	51	762	52	0.5	2.5
C4	36	11	47	64	0.2	21	392	59	0.25	2.5
C5	7	6	34	103	0.2	17	567	89	0.25	2.5
C6	72	13	18	53	0.2	28	368	77	0.25	2.5
C7	40	19	16	67	0.2	21	316	72	0.25	2.5
C8	27	23	18	89	0.2	38	427	50	0.25	2.5
C9	17	9	48	149	0.2	28	531	73	0.6	2.5
C10	15	26	21	75	0.2	38	553	126	0.5	2.5
C11	60	30	23	95	0.2	50	352	85	0.8	2.5
C12	15	35	18	94	0.2	37	542	63	0.25	2.5
C13	28	26	15	71	0.2	31	420	70	0.25	2.5
D1	40	31	20	71	0.7	40	504	68	0.25	2.5
D2	49	21	15	68	0.2	39	424	61	0.25	2.5
D3	80	21	18	61	0.2	37	438	68	0.25	2.5
D4	45	11	31	75	0.2	18	476	62	0.25	2.5
D5	21	22	19	80	0.2	37	533	87	0.25	2.5
D6	48	18	24	69	0.2	24	384	71	0.25	2.5
D7	44	12	24	101	0.2	29	400	64	0.25	2.5
D8	28	9	40	125	0.2	21	531	78	0.25	2.5
D9	15	31	20	108	0.2	64	438	100	0.25	2.5
D10	51	19	17	91	0.2	40	338	81	0.25	2.5
D11	45	17	14	74	0.2	34	459	60	0.25	2.5
D12	86	13	17	80	0.4	38	435	51	0.25	2.5
D13	11	27	17	70	0.2	35	693	69	0.25	2.5

APPENDIX V: Part A- Geochemical Analysis (ICP Data)

Sample Site	Hg (ppb)	Cu (ppm)	Pb (ppm)	Zn (ppm)	Ag (ppm)	Ni (ppm)	Mn (ppm)	Sr (ppm)	Cd (ppm)	Bi (ppm)
D14	32	25	18	92	0.2	43	568	71	0.25	2.5
E1	15	26	16	72	1.1	35	551	54	0.25	2.5
E2	20	31	20	80	0.4	38	651	55	0.5	2.5
E3	31	20	13	65	0.2	28	544	56	0.25	2.5
E4	33	10	27	66	0.2	11	463	51	0.5	2.5
E5	26	14	18	68	0.2	23	381	58	0.25	2.5
E6	21	17	19	87	0.2	33	429	56	0.25	2.5
E7	68	22	22	123	0.5	43	492	71	0.5	2.5
E8	30	18	14	107	0.2	42	348	92	0.25	2.5
E9	45	18	23	66	0.5	31	339	67	0.25	2.5
E10	52	19	20	61	0.4	31	422	62	0.25	2.5
E11	47	19	26	60	0.2	29	388	60	0.25	2.5
E12	16	29	17	69	0.7	31	398	74	0.6	2.5
E13	12	28	18	83	0.2	42	595	65	0.25	2.5
E14	12	31	25	68	0.2	31	1244	83	0.25	2.5
F1	24	21	15	62	0.2	32	492	50	0.25	2.5
F2	25	28	20	89	0.9	46	894	64	0.7	2.5
F3	24	27	19	82	0.5	40	743	56	0.25	2.5
F4	25	26	29	69	0.4	34	760	66	0.7	2.5
F5	44	13	12	51	0.4	20	278	70	0.25	2.5
F6	9	24	26	94	0.5	37	699	83	0.25	2.5
F7	16	21	23	64	1	31	533	103	0.5	2.5
F8	21	37	23	90	0.2	46	541	88	0.25	2.5
F9	44	21	18	73	0.2	40	431	72	0.25	2.5
F10	19	26	19	69	0.4	37	414	66	0.25	2.5
F11	51	19	20	67	0.2	34	749	60	0.25	2.5
F12	47	29	20	72	0.4	34	527	114	0.25	2.5
F13	9	27	20	71	0.5	35	495	84	0.25	2.5
F14	8	31	19	76	0.2	37	546	89	0.7	2.5
G1	28	8	14	62	0.2	15	263	37	0.25	2.5
G2	22	17	19	77	0.6	29	479	44	0.5	2.5
G3	53	26	17	67	0.2	38	496	54	0.25	2.5
G4	51	27	21	90	0.2	33	481	76	0.25	2.5
G5	20	40	20	83	0.2	47	804	103	0.25	2.5
G6	34	43	17	96	0.2	54	513	93	0.25	2.5
G7	28	22	16	123	0.2	58	358	90	0.5	2.5
G8	46	21	17	65	0.2	33	368	67	0.25	2.5
G9	23	27	10	92	0.2	39	644	67	0.25	2.5
G10	69	29	19	96	0.2	47	582	56	0.6	2.5
G11	89	9	20	65	0.2	24	214	46	0.25	2.5
G12	17	36	16	74	0.2	34	672	140	0.6	2.5
G13	19	21	17	67	0.2	31	183	41	0.25	2.5
G14	50	21	17	79	0.2	19	392	103	0.25	2.5
H1	12	35	22	87	0.2	43	661	48	0.8	2.5
H2	25	24	16	64	0.2	32	462	54	0.25	2.5

APPENDIX V: Part A- Geochemical Analysis (ICP Data)

Sample Site	Hg (ppb)	Cu (ppm)	Pb (ppm)	Zn (ppm)	Ag (ppm)	Ni (ppm)	Mn (ppm)	Sr (ppm)	Cd (ppm)	Bi (ppm)
H3	43	20	17	66	0.2	28	431	60	0.5	2.5
H4	45	14	24	80	0.2	31	309	74	0.25	2.5
H5	24	26	19	76	0.2	42	413	82	0.5	5
H6	30	22	34	98	1.3	40	321	76	0.25	2.5
H7	45	20	20	74	0.2	35	971	59	0.25	2.5
H8	21	31	15	101	0.2	43	722	66	0.5	2.5
H9	14	19	13	92	0.2	33	539	60	0.25	2.5
H10	40	28	16	81	0.2	40	516	62	0.25	2.5
H11	67	11	20	72	0.4	24	169	49	0.25	2.5
H12	44	19	11	144	0.2	79	259	47	0.25	2.5
H13	28	17	19	72	0.2	35	978	67	0.25	2.5
H14	69	19	17	79	0.8	34	295	61	0.5	2.5
K1	32	30	48	89	0.2	33	706	73	0.7	2.5
K2	42	20	21	70	0.2	33	470	57	0.25	2.5
K3	24	18	20	74	0.2	27	490	82	0.25	2.5
K4	27	22	19	89	0.2	40	350	86	0.25	2.5
K5	24	22	16	77	0.4	40	278	80	0.25	2.5
K6	16	26	15	80	0.5	46	711	57	0.25	2.5
K7	29	28	19	95	0.2	45	532	67	0.25	2.5
K8	14	24	18	57	0.9	32	278	64	0.25	2.5
K9	21	27	22	74	0.2	41	410	56	0.25	2.5
K10	26	33	20	81	0.2	39	854	68	0.25	2.5
K11	8	47	21	107	0.9	50	740	74	0.6	2.5
K12	57	13	16	76	0.2	33	475	49	0.25	2.5
K13	71	15	20	85	0.8	32	366	60	0.25	2.5
K14	78	21	18	95	0.2	39	1709	55	0.6	2.5
L1	75	10	23	86	0.2	28	483	77	0.25	2.5
L2	41	12	23	86	0.2	29	498	79	0.25	2.5
L3	17	20	13	69	0.2	39	380	88	0.25	2.5
L4	23	31	22	82	0.2	38	480	77	0.25	2.5
L5	13	28	34	103	0.5	34	731	79	0.25	2.5
L6	34	16	15	74	0.2	35	766	62	0.25	2.5
L7	32	30	17	74	0.2	39	571	57	0.25	2.5
L8	13	21	15	46	0.4	18	240	61	0.25	2.5
L9	39	25	14	70	0.2	38	573	62	0.25	2.5
L10	26	27	23	96	0.2	58	491	66	0.25	2.5
L11	27	19	16	52	0.2	29	372	65	0.25	2.5
L12	38	18	24	90	0.2	39	633	59	0.25	2.5
L13	116	24	21	69	0.2	42	334	59	0.25	2.5
L14	57	20	14	58	0.2	41	188	41	0.25	2.5
M1	34	20	22	88	0.2	30	597	78	0.6	2.5
M2	27	41	23	110	0.2	56	906	72	0.6	2.5
M3	14	21	12	97	0.2	38	293	147	0.25	2.5
M4	20	27	16	74	0.2	40	410	84	0.25	2.5
M5	42	16	7	59	0.2	23	208	25	0.7	2.5

APPENDIX V: Part A- Geochemical Analysis (ICP Data)

Sample Site	Hg (ppb)	Cu (ppm)	Pb (ppm)	Zn (ppm)	Ag (ppm)	Ni (ppm)	Mn (ppm)	Sr (ppm)	Cd (ppm)	Bi (ppm)
M6	28	25	16	77	0.2	35	554	58	0.25	2.5
M7	9	23	15	56	0.2	26	450	61	0.25	2.5
M8	9	18	15	56	0.9	28	340	70	0.25	2.5
M9	12	34	20	78	0.2	32	600	101	0.6	2.5
M10	36	15	16	71	0.2	33	547	72	0.25	2.5
M11	32	24	17	85	0.2	34	599	76	0.25	2.5
M12	65	15	13	90	0.2	37	370	60	0.25	2.5
M13	90	20	17	70	0.6	34	2370	59	0.25	2.5
M14	27	18	14	57	0.2	47	194	41	0.25	2.5
N1	62	21	19	107	0.2	35	478	74	0.5	2.5
N2	22	29	13	95	0.2	46	463	83	0.25	2.5
N3	21	34	15	98	0.2	54	406	72	0.25	2.5
N4	14	23	18	82	0.4	36	355	60	0.25	2.5
N5	16	22	22	69	0.2	35	649	76	0.25	2.5
N6	22	24	21	72	0.4	31	588	65	0.5	2.5
N7	28	15	15	76	0.2	25	353	71	0.25	2.5
N8	42	18	17	60	0.2	29	427	65	0.25	2.5
N9	46	19	12	65	0.2	34	406	65	0.25	2.5
N10	39	21	16	65	0.2	33	552	66	0.25	2.5
N11	32	16	17	117	0.2	44	354	69	0.25	2.5
N12	40	17	17	61	0.4	36	457	67	0.6	2.5
N13	55	18	25	73	0.2	36	355	78	0.7	2.5
N14	65	29	14	75	0.2	31	683	175	0.25	2.5
P1	20	30	23	92	0.2	44	437	169	0.25	7
P2	17	33	20	107	0.6	54	653	106	0.25	2.5
P3	62	19	26	70	0.2	36	492	88	0.25	5
P4	24	22	14	72	0.2	34	393	60	0.25	2.5
P5	36	23	18	102	0.2	35	554	60	0.25	2.5
P6	20	24	17	76	0.2	33	379	61	0.25	2.5
P7	19	25	15	74	9.9	33	456	64	0.25	2.5
P8	43	19	14	69	0.4	40	360	64	0.25	2.5
P9	42	21	29	72	0.2	39	682	63	0.25	116
P10	32	16	9	61	0.2	33	596	68	0.25	2.5
P11	38	16	13	64	0.2	36	362	70	0.25	2.5
P12	38	19	12	57	0.4	33	476	72	0.25	2.5
P13	57	31	19	82	0.2	31	542	144	0.25	2.5
P14	71	25	17	82	0.2	38	530	95	0.25	2.5
Q1	27	20	18	78	0.6	37	449	77	0.25	2.5
Q2	19	25	16	90	0.2	47	392	71	0.25	2.5
Q3	20	28	17	96	0.6	40	600	65	0.25	2.5
Q4	44	28	20	95	0.7	34	528	55	0.5	2.5
Q5	22	22	19	85	0.2	35	418	58	0.25	2.5
Q6	19	21	21	78	0.5	38	383	56	0.25	2.5
Q7	27	22	21	78	0.2	35	372	59	0.25	2.5
Q8	39	17	20	62	0.6	31	785	88	0.25	2.5

APPENDIX V: Part A- Geochemical Analysis (ICP Data)

Sample Site	Hg (ppb)	Cu (ppm)	Pb (ppm)	Zn (ppm)	Ag (ppm)	Ni (ppm)	Mn (ppm)	Sr (ppm)	Cd (ppm)	Bi (ppm)
Q9	69	16	11	79	0.9	42	1594	55	0.25	2.5
Q10	52	15	10	56	0.8	32	323	67	0.25	2.5
Q11	47	18	18	78	0.2	47	576	70	0.25	2.5
Q12	39	27	19	68	0.2	39	479	52	0.25	2.5
Q13	57	19	10	104	0.2	58	628	142	0.6	2.5
Q14	145	46	21	84	0.6	32	584	102	0.25	2.5
R1	20	28	24	81	0.2	49	820	105	0.25	2.5
R2	14	28	15	77	0.2	41	404	73	0.25	2.5
R3	16	24	19	73	0.2	31	446	63	0.25	2.5
R4	26	28	18	85	1	34	565	57	0.25	2.5
R5	34	16	18	76	0.2	25	421	59	0.25	2.5
R6	15	24	12	84	0.2	35	482	68	0.25	2.5
R7	22	24	18	72	0.2	36	648	66	0.25	2.5
R8	60	16	15	51	0.2	29	377	71	0.25	2.5
R9	35	21	21	70	0.2	37	1185	72	0.25	2.5
R10	56	17	23	68	0.2	32	664	63	0.25	2.5
R11	98	18	23	117	0.2	36	337	57	0.25	2.5
R12	49	14	17	86	0.5	27	423	53	0.25	2.5
R13	32	29	21	78	0.2	38	506	87	0.25	2.5
R14	86	27	29	125	0.2	31	430	68	0.5	2.5
S1	19	31	25	78	0.2	39	865	83	0.6	2.5
S2	26	19	17	69	0.2	22	415	59	0.25	2.5
S3	21	30	21	92	0.7	37	584	59	0.25	2.5
S4	14	23	21	88	0.2	39	430	60	0.25	2.5
S5	23	24	18	90	0.2	38	496	58	0.25	2.5
S6	29	22	22	78	0.2	37	635	65	0.5	2.5
S7	30	17	19	72	0.5	34	325	68	0.25	2.5
S8	54	19	16	81	0.2	44	802	60	0.6	2.5
S9	49	15	20	72	0.2	35	1145	60	0.6	2.5
S10	69	13	10	76	0.2	29	347	52	0.25	2.5
S11	36	17	20	67	0.2	33	501	52	0.25	2.5
S12	47	23	14	62	0.6	29	378	99	0.25	2.5
S13	53	20	24	79	0.2	29	371	81	0.25	2.5
S14	91	53	18	81	0.2	35	600	218	0.25	2.5
T1	21	28	17	89	0.2	43	537	72	0.5	2.5
T2	15	26	23	89	0.2	36	484	55	0.25	2.5
T3	21	22	22	82	0.2	31	488	57	0.25	2.5
T4	13	28	22	85	0.2	41	526	60	0.25	2.5
T5	12	24	19	97	0.2	40	419	55	0.25	2.5
T6	26	24	18	85	0.6	40	352	68	0.5	2.5
T7	37	19	20	87	0.2	37	474	66	0.25	2.5
T8	29	20	20	82	0.2	35	456	73	0.25	2.5
T9	39	18	21	60	0.2	36	418	84	0.25	2.5
T10	49	17	13	88	0.2	45	342	47	0.25	2.5
T11	38	28	32	86	0.7	43	868	79	0.6	2.5

APPENDIX V: Part A- Geochemical Analysis (ICP Data)

Sample Site	Hg (ppb)	Cu (ppm)	Pb (ppm)	Zn (ppm)	Ag (ppm)	Ni (ppm)	Mn (ppm)	Sr (ppm)	Cd (ppm)	Bi (ppm)
T12	36	92	15	54	0.4	25	329	83	0.25	2.5
T13	258	14	16	39	0.2	11	248	57	0.25	2.5
T14	107	18	18	48	0.2	18	396	122	0.5	2.5
V1	29	21	23	85	0.2	32	490	74	0.25	2.5
V2	14	23	24	81	0.2	36	626	71	0.25	2.5
V3	20	25	20	91	0.2	33	554	57	0.25	2.5
V4	12	23	20	72	0.2	31	396	51	0.25	2.5
V5	9	25	25	79	0.7	44	510	81	0.25	2.5
V6	13	23	21	75	0.2	35	283	62	0.25	2.5
V7	41	21	18	77	0.2	35	377	59	0.25	2.5
V8	39	22	27	80	0.4	39	2039	60	0.25	2.5
V9	40	25	26	74	0.2	35	841	75	0.25	2.5
V10	46	21	20	68	0.2	34	492	50	0.25	2.5
V11	100	32	38	117	0.2	47	509	64	0.5	2.5
V12	75	37	32	98	0.2	38	619	162	0.5	2.5
V13	55	52	26	88	0.2	36	760	144	0.25	2.5
V14	54	23	24	89	0.2	30	576	145	0.25	2.5
W1	31	17	18	68	0.2	28	417	77	0.25	2.5
W2	15	30	23	84	0.5	36	544	57	0.25	2.5
W3	19	25	24	93	0.2	35	395	54	0.25	2.5
W4	19	22	22	70	0.2	32	334	59	0.25	2.5
W5	13	23	20	63	0.4	31	257	62	0.25	2.5
W6	22	24	22	78	0.2	33	383	58	0.25	2.5
W7	39	22	23	87	0.2	39	466	69	0.25	2.5
W8	98	24	28	93	0.7	38	421	73	0.25	2.5
W9	45	24	21	74	0.2	38	427	78	0.5	2.5
W10	32	24	22	98	0.2	34	431	84	0.25	5
W11	84	24	25	117	0.2	35	544	91	0.5	2.5
W12	43	38	34	106	0.2	40	815	195	0.25	2.5
W13	27	24	19	66	0.2	34	646	77	0.25	2.5
W14	24	21	22	73	0.2	28	550	188	0.25	2.5
X1	15	23	13	63	0.2	27	462	60	0.25	2.5
X2	18	28	17	83	0.2	42	543	66	0.25	2.5
X3	22	26	21	88	0.2	33	479	56	0.25	2.5
X4	21	20	21	70	0.2	34	278	58	0.25	2.5
X5	36	21	22	78	0.2	34	318	61	0.25	2.5
X6	11	21	17	66	0.5	31	319	56	0.25	2.5
X7	105	17	22	83	0.6	26	322	66	0.25	2.5
X8	36	21	29	86	0.2	43	645	78	0.5	2.5
X9	56	16	13	113	0.2	34	373	82	0.5	2.5
X10	65	24	31	90	0.2	36	655	112	0.5	2.5
X11	41	27	20	69	0.2	30	570	191	0.25	2.5
X12	25	28	18	61	0.2	34	539	150	0.25	2.5
X13	58	21	25	88	0.2	38	505	77	0.25	2.5
X14	235	10	6	55	0.2	13	372	65	0.25	6

APPENDIX V: Part A- Geochemical Analysis (ICP Data)

Sample Site	V (ppm)	Ca (wt. %)	P (wt. %)	Mg (wt. %)	Ti (wt. %)	Al (wt. %)	K (wt. %)	Y (ppm)	Be (ppm)
A8	69	0.32	0.046	1.09	0.41	8.31	2.79	23	1
A9	61	0.6	0.034	0.74	0.48	5.46	1.52	22	1
A10	108	0.64	0.114	0.66	0.63	6.51	2.46	98	1
A11	127	0.61	0.066	1.57	0.6	7.7	2.35	26	1
A12	87	0.19	0.058	0.97	0.41	7.48	1.58	16	1
A13	100	0.28	0.041	1.36	0.4	7.55	2.06	36	1
B1	89	0.17	0.022	0.65	0.55	6.56	1.59	25	1
B2	105	0.13	0.054	0.7.	0.49	7.89	2.11	26	1
B3	75	0.16	0.028	0.75	0.42	6.05	1.64	20	1
B4	90	0.32	0.056	1.14	0.45	6.96	1.61	24	1
B5	75	0.35	0.032	0.8	0.47	6.91	1.73	23	1
B6	66	0.29	0.034	1.5	0.47	9.54	2.87	22	1
B7	73	0.29	0.054	1.58	0.41	8.45	2.63	18	1
B8	142	1.68	0.053	1.67	0.74	6.73	1.26	28	1
B9	79	0.17	0.03	1.14	0.39	8.8	3.07	26	1
B10	86	0.22	0.042	1.21	0.53	7.49	2.49	24	1
B11	113	0.44	0.063	1.55	0.54	8.38	2.6	26	2
B12	127	0.06	0.022	1.48	0.4	8.69	2.87	18	2
B13	108	0.16	0.03	1.32	0.48	7.52	2.08	20	1
C1	80	0.2	0.039	0.66	0.52	5.74	1.39	37	1
C2	77	0.18	0.158	1.03	0.38	7.3	1.68	19	1
C3	94	0.13	0.029	1.36	0.42	8.9	1.76	16	1
C4	46	0.25	0.072	0.53	0.35	6.04	2.02	34	1
C5	34	0.67	0.04	1.04	0.22	9.76	3.67	31	2
C6	72	0.41	0.06	0.65	0.5	5.98	1.34	20	1
C7	68	0.31	0.044	0.65	0.5	5.95	1.76	24	1
C8	92	0.06	0.028	1.38	0.46	7.82	2.63	18	2
C9	74	0.14	0.046	1.09	0.51	7.78	2.78	30	2
C10	98	0.42	0.041	1.19	0.42	6.96	1.95	30	1
C11	117	0.19	0.081	1.44	0.41	8.17	2.06	28	2
C12	101	0.34	0.02	1.69	0.43	7.38	2.18	14	1
C13	82	0.25	0.034	1.01	0.47	6.99	1.86	25	1
D1	95	0.16	0.03	0.91	0.46	6.94	1.61	28	1
D2	78	0.19	0.025	0.81	0.44	6.95	1.4	19	1
D3	85	0.23	0.048	0.69	0.46	8.1	1.35	20	1
D4	47	0.26	0.05	0.98	0.44	8.92	2.49	30	1
D5	91	0.58	0.042	1.32	0.49	7.31	2.12	25	1
D6	73	0.24	0.079	0.92	0.48	6.95	1.8	23	1
D7	81	0.13	0.067	1.24	0.41	8.28	2.06	22	1
D8	62	0.24	0.095	0.9	0.47	7.42	2.49	34	1
D9	150	0.31	0.05	1.96	0.41	9.6	2.95	25	2
D10	112	0.19	0.032	1.35	0.47	8.2	2.11	19	1
D11	82	0.16	0.051	0.72	0.41	7.53	1.78	23	1
D12	79	0.11	0.132	0.5	0.38	8.12	1.96	24	1
D13	97	0.28	0.031	1	0.45	7.47	2.11	36	1

APPENDIX V: Part A- Geochemical Analysis (ICP Data)

Sample Site	V (ppm)	Ca (wt. %)	P (wt. %)	Mg (wt. %)	Ti (wt. %)	Al (wt. %)	K (wt. %)	Y (ppm)	Be (ppm)
D14	102	0.29	0.034	1.09	0.45	7.85	2.11	22	1
E1	92	0.19	0.029	0.77	0.49	7.17	1.72	23	1
E2	101	0.17	0.033	0.87	0.52	7.86	1.91	26	1
E3	82	0.28	0.05	0.85	0.48	6.59	1.56	23	1
E4	38	0.18	0.046	1.45	0.27	10.43	2.79	18	1
E5	67	0.17	0.043	1.54	0.45	7.86	1.87	13	1
E6	84	0.13	0.023	1.37	0.48	7.49	2.5	22	1
E7	111	0.25	0.07	1.69	0.56	8.8	2.06	26	1
E8	134	0.2	0.047	1.56	0.45	9.07	2.63	20	1
E9	88	0.23	0.046	0.86	0.4	7.15	1.6	20	1
E10	75	0.16	0.03	0.65	0.48	6.72	1.85	23	1
E11	74	0.16	0.03	0.62	0.43	6.72	1.74	22	1
E12	82	0.37	0.019	0.97	0.43	6.32	1.7	20	1
E13	114	0.25	0.03	1.16	0.45	8.61	2.46	24	1
E14	92	0.53	0.055	1.04	0.45	6.45	2.08	34	1
F1	88	0.2	0.027	0.77	0.46	6.92	1.61	22	1
F2	104	0.36	0.066	1.27	0.48	8.11	2	26	1
F3	101	0.24	0.045	1.15	0.48	7.7	1.82	22	1
F4	90	0.31	0.062	1.18	0.47	7.25	1.98	28	1
F5	80	0.29	0.039	0.64	0.49	6.7	1.6	19	1
F6	111	0.28	0.059	1.75	0.61	9.07	2.83	29	2
F7	88	0.3	0.04	0.99	0.48	7.59	2.36	25	1
F8	123	0.4	0.046	1.32	0.41	8.2	2.36	38	1
F9	102	0.12	0.028	0.88	0.47	6.92	1.71	24	1
F10	107	0.07	0.024	0.68	0.44	7.66	1.8	20	1
F11	81	0.16	0.039	0.64	0.42	6.66	1.89	20	1
F12	97	0.9	0.107	1.11	0.42	7.32	1.74	36	1
F13	101	0.4	0.03	0.99	0.46	7.36	2.06	25	1
F14	100	0.44	0.026	1.08	0.5	7.29	2.03	24	1
G1	49	0.32	0.159	1.71	0.25	10.02	0.97	13	1
G2	82	0.34	0.063	1.43	0.4	8.32	1.45	13	1
G3	94	0.22	0.034	1.06	0.47	7.31	1.55	20	1
G4	103	0.3	0.06	1.35	0.56	8.87	2.04	19	1
G5	117	0.46	0.06	1.39	0.38	7.68	2.25	35	1
G6	137	0.12	0.04	1.66	0.44	8.59	2.44	20	1
G7	150	0.17	0.034	1.81	0.49	9.44	3.05	23	1
G8	79	0.17	0.025	0.83	0.4	6.54	1.63	19	1
G9	101	0.28	0.023	0.81	0.5	6.97	1.69	28	1
G10	105	0.14	0.049	0.73	0.44	7.65	1.64	20	1
G11	75	0.08	0.055	0.3	0.39	7.04	1.57	19	1
G12	106	1.16	0.034	1.19	0.49	7.52	2.02	37	1
G13	77	0.06	0.015	0.58	0.41	6.51	1.74	24	1
G14	96	0.7	0.042	1.25	0.48	8.12	2.09	25	1
H1	114	0.34	0.059	1.52	0.48	8	2.27	22	1
H2	88	0.2	0.026	0.96	0.48	7.53	1.53	20	1

APPENDIX V: Part A- Geochemical Analysis (ICP Data)

Sample Site	V (ppm)	Ca (wt. %)	P (wt. %)	Mg (wt. %)	Ti (wt. %)	Al (wt. %)	K (wt. %)	Y (ppm)	Be (ppm)
H3	83	0.24	0.04	0.9	0.46	7	1.53	18	1
H4	82	0.13	0.041	1.43	0.42	9.34	2.71	18	2
H5	100	0.19	0.047	1.12	0.48	7.68	2.06	23	1
H6	85	0.22	0.102	0.89	0.42	7.15	1.68	23	1
H7	91	0.11	0.074	0.85	0.45	8.14	2.16	26	1
H8	123	0.17	0.024	1.03	0.53	8.5	2.55	26	1
H9	88	0.2	0.023	0.84	0.48	6.48	1.74	24	1
H10	88	0.22	0.027	0.75	0.5	6.8	1.52	26	1
H11	88	0.07	0.062	0.35	0.49	7.42	2	26	1
H12	99	0.04	0.04	0.45	0.43	8.64	2.18	58	1
H13	85	0.14	0.055	0.63	0.43	7.1	2.13	30	1
H14	79	0.22	0.05	0.51	0.42	7.07	1.45	23	1
K1	93	0.3	0.058	1.54	0.48	10.1	2.95	23	2
K2	90	0.2	0.028	1.02	0.48	7.64	1.69	19	1
K3	84	0.3	0.058	1.13	0.59	7.37	1.97	32	1
K4	104	0.26	0.09	1.07	0.43	7.66	1.98	25	1
K5	99	0.23	0.031	1.14	0.43	7.54	1.92	18	1
K6	102	0.13	0.029	1.78	0.42	7.21	2.23	23	1
K7	132	0.11	0.022	0.93	0.54	9.35	2.7	35	1
K8	125	0.08	0.014	0.56	0.47	8.73	2.29	20	1
K9	91	0.1	0.03	0.87	0.5	7.12	2.22	25	1
K10	103	0.22	0.045	1.14	0.43	7.36	2.2	40	1
K11	107	0.53	0.067	1.42	0.43	7.77	2.81	32	2
K12	67	0.11	0.041	0.51	0.34	6.01	1.68	23	1
K13	83	0.14	0.051	0.57	0.35	7.4	1.8	23	1
K14	88	0.11	0.048	0.49	0.48	7.08	1.63	26	1
L1	86	0.2	0.073	1.34	0.52	9.8	2.43	22	2
L2	83	0.23	0.054	1.51	0.51	9.09	2.54	20	2
L3	109	0.36	0.033	1.17	0.47	7.61	2.25	20	1
L4	99	0.25	0.056	1.1	0.47	7.22	1.87	25	1
L5	98	0.4	0.051	1.54	0.53	7.37	2.18	29	1
L6	70	0.16	0.041	0.61	0.46	6.59	1.85	23	1
L7	104	0.14	0.023	0.91	0.53	7.63	1.89	28	1
L8	91	0.16	0.017	0.44	0.56	6.38	1.37	22	1
L9	92	0.23	0.038	0.75	0.52	7.04	1.66	30	1
L10	116	0.07	0.025	1.6	0.48	8.03	2.62	22	1
L11	76	0.28	0.023	0.62	0.44	6.29	1.59	23	1
L12	97	0.05	0.061	0.65	0.42	8.35	2.26	31	1
L13	78	0.22	0.057	0.54	0.33	7.12	1.57	23	1
L14	72	0.11	0.031	0.45	0.38	6.04	1.25	22	1
M1	84	0.28	0.104	1.47	0.53	8.99	2.6	24	1
M2	153	0.12	0.055	1.75	0.47	9.46	3.22	22	2
M3	124	0.23	0.023	1.23	0.54	7.97	2.19	19	1
M4	94	0.23	0.041	1.37	0.43	6.92	1.86	20	1
M5	95	0.02	0.036	0.38	0.37	7.34	1.95	25	1

APPENDIX V: Part A- Geochemical Analysis (ICP Data)

Sample Site	V (ppm)	Ca (wt. %)	P (wt. %)	Mg (wt. %)	Ti (wt. %)	Al (wt. %)	K (wt. %)	Y (ppm)	Be (ppm)
M6	87	0.19	0.026	0.74	0.47	6.65	1.69	28	1
M7	75	0.24	0.02	0.61	0.48	5.4	1.47	29	1
M8	73	0.23	0.017	0.66	0.5	5.97	1.62	28	1
M9	93	0.8	0.034	1.21	0.47	6.55	1.97	34	1
M10	105	0.23	0.037	0.77	0.47	8.04	2.04	23	1
M11	113	0.07	0.057	0.7	0.52	8.95	2.85	30	1
M12	76	0.18	0.059	0.53	0.41	7.31	1.65	26	1
M13	90	0.13	0.055	0.56	0.43	7.59	1.78	47	1
M14	116	0.05	0.022	0.53	0.41	8.45	1.86	22	1
N1	110	0.24	0.111	1.32	0.51	8.24	2.17	23	1
N2	137	0.18	0.034	1.46	0.5	9.18	2.96	25	1
N3	127	0.2	0.019	2.05	0.49	8.42	2.49	19	1
N4	85	0.1	0.022	1.16	0.44	6.2	1.91	23	1
N5	95	0.37	0.016	0.77	0.46	7.02	1.99	34	1
N6	87	0.23	0.024	0.71	0.47	6.5	1.76	32	1
N7	81	0.46	0.017	0.58	0.45	7.47	1.7	26	1
N8	78	0.18	0.032	0.64	0.48	6.64	1.81	26	1
N9	76	0.19	0.033	0.6	0.46	6.36	1.63	26	1
N10	84	0.19	0.044	0.67	0.47	6.74	1.9	31	1
N11	77	0.19	0.038	0.67	0.44	7.07	1.77	20	1
N12	88	0.18	0.046	0.67	0.42	7.57	2.06	23	1
N13	67	0.41	0.047	0.57	0.37	6.54	1.33	20	1
N14	91	1.52	0.1	1.6	0.39	9.51	1.6	19	1
P1	108	0.77	0.085	1.48	0.46	7.99	2.61	34	2
P2	135	0.34	0.042	2.1	0.47	8.92	2.81	23	2
P3	83	0.28	0.065	1.08	0.46	9.64	1.61	20	1
P4	92	0.14	0.019	0.79	0.46	7.27	1.87	25	1
P5	94	0.37	0.027	0.75	0.5	7.17	1.53	25	1
P6	97	0.19	0.017	0.8	0.5	7.41	1.87	25	1
P7	89	0.22	0.02	0.74	0.47	6.76	1.6	24	1
P8	68	0.24	0.04	0.57	0.42	6.58	1.69	22	1
P9	89	0.12	0.043	0.71	0.46	7.94	2.06	23	1
P10	79	0.18	0.036	0.62	0.46	6.46	1.72	25	1
P11	81	0.28	0.036	0.67	0.43	6.86	1.63	22	1
P12	85	0.29	0.036	0.63	0.44	7.4	1.64	22	1
P13	96	1.42	0.055	1.09	0.41	8.06	1.39	25	1
P14	100	1.09	0.077	1.15	0.45	7.38	1.47	43	1
Q1	95	0.29	0.053	1.46	0.47	7.16	2.05	20	1
Q2	110	0.2	0.027	1.81	0.48	7.61	2.25	19	1
Q3	110	0.13	0.03	0.97	0.47	8.11	2.1	28	1
Q4	100	0.3	0.022	0.78	0.52	7.12	1.64	26	1
Q5	99	0.19	0.016	0.83	0.46	7.63	1.92	28	1
Q6	102	0.08	0.018	0.78	0.46	7.94	1.96	26	1
Q7	91	0.11	0.022	0.75	0.47	6.94	1.52	25	1
Q8	80	0.48	0.036	0.64	0.47	6.67	1.83	28	1

APPENDIX V: Part A- Geochemical Analysis (ICP Data)

Sample Site	V (ppm)	Ca (wt. %)	P (wt. %)	Mg (wt. %)	Ti (wt. %)	Al (wt. %)	K (wt. %)	Y (ppm)	Be (ppm)
Q9	99	0.11	0.048	0.76	0.43	8.89	2.14	25	1
Q10	66	0.24	0.034	0.6	0.42	6.27	1.41	22	1
Q11	96	0.25	0.054	0.76	0.54	7.72	2.03	29	1
Q12	99	0.24	0.031	0.56	0.43	7.98	1.67	26	1
Q13	121	1.72	0.152	1.41	0.65	7.88	1.12	34	1
Q14	139	0.91	0.177	1.33	0.57	8.2	1.53	23	1
R1	108	0.67	0.064	1.48	0.45	8.63	2.32	44	2
R2	104	0.25	0.024	1.43	0.44	7.58	2.11	19	1
R3	83	0.3	0.015	0.77	0.5	6.54	1.48	24	1
R4	91	0.25	0.018	0.77	0.48	7.09	1.64	26	1
R5	79	0.31	0.017	0.6	0.46	7.2	1.35	24	1
R6	96	0.23	0.016	0.86	0.5	7.4	1.73	25	1
R7	95	0.14	0.033	0.78	0.45	7.74	2.09	36	1
R8	67	0.25	0.019	0.62	0.43	6.1	1.41	19	1
R9	89	0.34	0.055	0.72	0.43	7.63	1.83	36	1
R10	70	0.17	0.041	0.58	0.39	6.75	1.59	22	1
R11	75	0.16	0.061	0.63	0.39	7.77	1.6	20	1
R12	69	0.12	0.075	0.46	0.4	6.65	1.53	29	1
R13	93	0.47	0.038	1.11	0.47	7.48	1.87	25	1
R14	120	0.32	0.062	1.23	0.48	8.44	1.4	20	1
S1	96	0.41	0.069	1.24	0.47	7.75	2.21	32	1
S2	76	0.29	0.019	0.57	0.48	6.3	1.23	23	1
S3	101	0.24	0.018	0.83	0.52	7.5	1.8	29	1
S4	107	0.19	0.021	0.82	0.5	8.32	2.09	30	1
S5	103	0.14	0.018	0.81	0.47	8.15	1.84	26	1
S6	90	0.29	0.025	0.68	0.42	7.92	1.58	25	1
S7	85	0.19	0.019	0.65	0.49	7.02	1.61	25	1
S8	97	0.13	0.049	0.74	0.45	8.67	2.17	44	2
S9	82	0.13	0.062	0.58	0.42	7.42	2.08	28	1
S10	66	0.07	0.064	0.44	0.43	6.89	1.62	22	1
S11	86	0.05	0.048	0.62	0.45	7.81	2.15	25	1
S12	76	0.44	0.086	1.26	0.42	7.11	1.63	23	1
S13	74	0.46	0.057	0.85	0.42	6.81	1.32	20	1
S14	117	2.21	0.1	1.26	0.51	8.22	1.07	24	1
T1	107	0.18	0.029	1.64	0.5	8.71	2.49	23	1
T2	98	0.19	0.017	0.87	0.47	7.54	1.81	28	1
T3	92	0.25	0.017	0.73	0.49	7.34	1.61	26	1
T4	100	0.25	0.021	0.84	0.48	7.94	2.01	35	1
T5	101	0.08	0.024	0.7	0.46	7.95	1.81	25	1
T6	90	0.1	0.024	0.78	0.46	7.05	1.7	26	1
T7	91	0.22	0.039	0.8	0.5	7.89	2.23	24	1
T8	77	0.3	0.032	0.64	0.45	7.12	1.69	22	1
T9	76	0.44	0.036	0.65	0.45	7.12	1.55	23	1
T10	79	0.05	0.047	0.63	0.45	8.01	2.07	25	1
T11	105	0.36	0.049	1.23	0.46	8.2	1.94	26	1

APPENDIX V: Part A- Geochemical Analysis (ICP Data)

Sample Site	V (ppm)	Ca (wt. %)	P (wt. %)	Mg (wt. %)	Ti (wt. %)	Al (wt. %)	K (wt. %)	Y (ppm)	Be (ppm)
T12	73	0.47	0.026	0.77	0.43	6.37	1.49	25	1
T13	96	0.6	0.183	0.34	0.35	9.1	0.43	17	1
T14	81	1.01	0.197	0.59	0.42	6.86	0.9	22	1
V1	96	0.35	0.028	0.93	0.47	7.94	1.77	24	1
V2	102	0.44	0.019	1.06	0.5	7.46	1.97	26	1
V3	95	0.25	0.016	0.78	0.51	7.39	1.66	25	1
V4	86	0.11	0.015	0.72	0.42	6.77	1.53	28	1
V5	94	0.37	0.016	0.7	0.46	6.98	1.45	34	1
V6	91	0.07	0.016	0.65	0.43	7.5	1.69	28	1
V7	89	0.1	0.019	0.83	0.41	7.44	1.73	23	1
V8	104	0.11	0.083	0.71	0.46	9.53	2.67	41	2
V9	92	0.34	0.031	1	0.44	7.52	1.9	23	1
V10	85	0.08	0.048	0.63	0.43	7.34	2.01	26	1
V11	99	0.44	0.079	1.35	0.42	7.93	1.55	19	1
V12	130	1.69	0.092	1.65	0.63	8.14	1.4	24	1
V13	112	1.18	0.074	1.36	0.49	7.4	1.34	20	1
V14	101	1.18	0.066	1.2	0.46	7.07	1.46	20	1
W1	82	0.37	0.028	0.99	0.51	7.29	1.69	19	1
W2	106	0.2	0.02	0.89	0.48	7.69	1.88	31	1
W3	103	0.13	0.017	0.82	0.48	8	1.85	28	1
W4	93	0.17	0.017	0.75	0.44	7.42	1.66	22	1
W5	84	0.14	0.016	0.67	0.46	6.75	1.51	26	1
W6	85	0.11	0.023	0.68	0.4	7.05	1.65	24	1
W7	86	0.28	0.035	0.87	0.41	7.65	1.76	23	1
W8	83	0.3	0.041	0.83	0.41	7.52	1.52	23	1
W9	83	0.38	0.047	0.81	0.42	7.57	1.51	25	1
W10	81	0.49	0.033	1.06	0.45	6.89	1.49	28	1
W11	87	0.6	0.076	1.03	0.45	7.31	1.4	24	1
W12	122	2.14	0.06	1.6	0.48	7.94	1.46	36	1
W13	96	0.31	0.034	1.17	0.42	7.32	2.15	24	1
W14	105	1.9	0.047	1.14	0.43	7.06	1.47	24	1
X1	73	0.35	0.015	0.71	0.47	5.7	1.17	23	1
X2	101	0.2	0.023	1.31	0.5	7.98	2.15	25	1
X3	92	0.18	0.016	0.81	0.45	7.37	1.7	24	1
X4	89	0.08	0.014	0.73	0.4	7.79	1.6	24	1
X5	89	0.1	0.018	0.72	0.43	7.43	1.62	25	1
X6	80	0.12	0.015	0.67	0.42	6.73	1.63	28	1
X7	80	0.29	0.034	0.66	0.41	7.33	1.33	22	1
X8	91	0.37	0.052	0.93	0.43	7.93	1.77	24	1
X9	72	0.53	0.055	0.75	0.4	6.99	1.27	20	1
X10	101	0.74	0.075	1.21	0.58	8.03	1.38	37	1
X11	111	1.63	0.054	1.27	0.52	7.76	1.71	28	1
X12	94	1.24	0.034	1.2	0.43	7.52	1.55	24	1
X13	84	0.38	0.059	0.88	0.41	7.74	1.62	24	1
X14	58	0.62	0.182	0.4	0.27	9.23	0.64	24	1

APPENDIX V: Part A-Geochemical Analysis (INAA DATA)

Sample Site	Au PPB	As (ppm)	Ba (ppm)	Br (ppm)	Co (ppm)	Cr (ppm)	Cs (ppm)	Fe (wt. %)	Hf (ppm)	Ir (ppm)
A8	1	11	460	11	11	84	6	3.52	14	2.5
A9	1	6.5	340	8.5	7	110	4	2.57	21	2.5
A10	2	130	440	13	7	66	22	4.69	18	2.5
A11	1	17	380	7.4	14	90	7	4.17	13	2.5
A12	1	18	350	27	14	82	7	3.91	15	2.5
A13	4	20	420	6.9	16	93	6	4.49	14	2.5
B1	1	9.4	330	4.8	13	74	5	3.67	14	2.5
B2	1	18	340	1.5	16	84	7	4.75	12	2.5
B3	1	15	260	5.4	11	66	8	3.53	16	2.5
B4	1	31	300	15	12	75	6	4.1	15	2.5
B5	3	14	370	8.3	12	74	5	3.43	16	2.5
B6	1	16	410	8.7	12	54	6	4.33	9	2.5
B7	4	15	400	11	11	80	6	3.48	12	2.5
B8	1	22	260	15	18	75	3	4.65	12	2.5
B9	1	60	330	6.2	12	71	52	4.19	13	2.5
B10	3	14	330	8.6	11	84	14	3.8	20	2.5
B11	1	22	460	4.5	14	76	8	4.16	13	2.5
B12	3	40	510	4.5	22	110	9	5.1	11	2.5
B13	3	21	370	3.7	15	90	7	4.36	12	2.5
C1	6	11	310	-0.5	13	68	4	3.54	15	2.5
C2	1	13	350	12	13	71	9	4.29	14	2.5
C3	1	20	340	6	17	85	6	4.62	10	2.5
C4	1	18	360	8.3	6	54	5	2.53	18	2.5
C5	1	15	660	5.2	6	22	11	2.8	13	2.5
C6	1	8.2	270	16	9	120	3	3.15	22	2.5
C7	1	18	320	16	8	68	4	2.91	18	2.5
C8	1	15	340	7.5	14	84	18	4.23	13	2.5
C9	1	19	440	5.8	10	60	12	3.73	19	2.5
C10	3	20	390	1.7	14	86	8	4.22	13	2.5
C11	3	27	400	14	16	100	8	4.54	11	2.5
C12	1	10	330	3.1	18	75	6	4.55	8	2.5
C13	1	13	340	8	10	68	4	3.41	16	2.5
D1	1	25	560	8	12	82	6	3.8	17	2.5
D2	1	13	250	15	12	76	4	3.5	13	2.5
D3	2	13	270	15	13	71	5	3.7	14	2.5
D4	2	11	420	25	6	45	6	2.61	19	2.5
D5	1	15	350	5.7	12	96	8	3.71	15	2.5
D6	3	15	350	- 24	9	63	6	3.35	16	2.5
D7	3	25	510	15	11	68	15	5.04	13	2.5
D8	1	25	390	7.5	9	55	10	3.61	26	2.5
D9	4	19	600	1.2	18	120	11	4.49	6	2.5
D10	4	12	370	10	11	87	6	3.9	12	2.5
D11	1	14	280	14	10	75	4	3.69	14	2.5
D12	3	18	360	8.1	8	61	3	3.78	15	2.5
D13	2	12	400	0.9	13	72	5	3.98	11	2.5

APPENDIX V: Part A-Geochemical Analysis (INAA DATA)

Sample Site	Au PPB	As (ppm)	Ba (ppm)	Br (ppm)	Co (ppm)	Cr (ppm)	Cs (ppm)	Fe (wt. %)	Hf (ppm)	Ir (ppm)
D14	1	12	380	6.7	15	84	7	4.24	11	2.5
E1	1	11	280	2.6	13	72	6	3.81	11	2.5
E2	1	12	360	3.5	15	72	6	4.3	12	2.5
E3	1	15	410	7.5	10	67	5	3.38	14	2.5
E4	1	21	380	9.2	8	29	7	3.5	16	2.5
E5	1	13	340	3.9	11	56	6	3.69	18	2.5
E6	7	18	380	6.3	13	74	10	4.21	14	2.5
E7	1	17	170	17	14	78	11	4.89	11	2.5
E8	1	18	450	5.8	13	98	9	4.64	8	2.5
E9	3	14	350	21	11	70	5	3.55	15	2.5
E10	1	13	280	2.2	11	66	4	3.15	14	2.5
E11	3	12	300	4.1	9	71	4	3.3	15	2.5
E12	1	7.5	360	4.4	12	66	4	3.24	13	2.5
E13	1	13	420	-0.5	16	88	8	4.71	8	2.5
E14	3	11	350	-0.5	13	77	5	3.76	19	2.5
F1	3	12	340	5.5	11	85	6	4	16	2.5
F2	1	18	400	4.8	17	81	6	4.58	12	2.5
F3	1	15	250	5.6	14	82	6	4.17	14	2.5
F4	5	17	380	2.4	14	83	5	3.95	21	2.5
F5	5	6.9	290	17	7	77	4	2.5	16	2.5
F6	6	17	430	1.5	14	87	7	4.69	15	2.5
F7	1	14	520	2.4	9	91	6	3.59	16	2.5
F8	7	20	470	-0.5	17	110	9	4.47	12	2.5
F9	1	14	320	4.4	12	90	5	4.11	17	2.5
F10	3	11	290	1	14	95	6	4.46	15	2.5
F11	1	18	320	2.7	13	76	4	3.9	17	2.5
F12	4	8.1	410	17	14	80	3	4.32	15	2.5
F13	1	10	370	3.1	13	87	6	4.02	12	2.5
F14	4	12	390	4.3	16	95	6	4.27	12	2.5
G1	1	8.9	130	11	8	64	4	3.72	12	2.5
G2	1	14	220	6.7	14	92	7	4.82	13	2.5
G3	1	15	210	10	14	90	6	4.39	16	2.5
G4	1	10	320	12	15	87	7	4.9	19	2.5
G5	1	20	560	2	15	97	6	4.24	8	2.5
G6	3	22	480	7.8	16	110	8	4.54	7	2.5
G7	5	19	500	5	15	100	12	4.74	6	2.5
G8	1	12	360	4.6	11	73	3	3.03	11	2.5
G9	2	8.8	360	6	16	77	4	4.21	12	2.5
G10	4	14	380	3.1	17	74	4	4.42	13	2.5
G11	2	11	370	11	8	67	3	2.94	13	2.5
G12	2	7.6	430	1.3	13	76	3	3.93	11	2.5
G13	1	4.9	270	4.9	15	72	4	3.41	13	2.5
G14	3	6.3	340	8.5	10	55	3	3.79	11	2.5
H1	5	14	440	2.1	16	87	6	4.33	10	2.5
H2	1	11	410	9.8	14	74	6	3.9	13	2.5

APPENDIX V: Part A-Geochemical Analysis (INAA DATA)

Sample Site	Au PPB	As (ppm)	Ba (ppm)	Br (ppm)	Co (ppm)	Cr (ppm)	Cs (ppm)	Fe (wt. %)	Hf (ppm)	Ir (ppm)
H3	1	9.3	280	9.4	10	67	4	3.12	12	2.5
H4	1	19	350	14	10	63	6	3.72	13	2.5
H5	3	12	440	4.9	13	85	7	3.61	12	2.5
H6	4	13	250	12	10	71	4	3.03	12	2.5
H7	5	25	420	13	12	66	4	4.14	10	2.5
H8	1	11	470	6.1	18	96	6	4.78	8	2.5
H9	2	5	270	3.6	13	71	4	3.8	12	2.5
H10	1	9.1	380	8	15	74	4	3.8	11	2.5
H11	1	37	450	11	5	71	3	4.26	17	2.5
H12	1	6.4	340	7.9	29	92	7	3.42	10	2.5
H13	1	14	420	2	12	79	3	3.88	16	2.5
H14	1	10	310	10	9	82	3	3.44	15	2.5
K1	3	14	350	4.2	12	58	5	3.92	10	2.5
K2	1	11	280	13	11	72	5	3.48	12	2.5
K3	5	16	360	7.5	11	79	5	3.81	18	2.5
K4	2	18	430	8.1	13	87	8	4.04	10	2.5
K5	1	18	450	8	14	78	6	3.67	9	2.5
K6	2	26	300	2.4	16	91	7	3.96	9	2.5
K7	2	7.4	490	5.9	21	97	7	4.53	9	2.5
K8	1	8	400	3.1	10	96	6	3.79	8	2.5
K9	2	5.6	340	4.7	13	75	5	3.55	9	2.5
K10	1	14	390	1.7	14	74	5	4	11	2.5
K11	1	14	550	-0.5	14	85	6	4.12	8	2.5
K12	1	12	310	4	12	70	3	2.67	13	2.5
K13	2	18	370	10	11	71	3	3.72	13	2.5
K14	1	19	350	5.2	11	78	3	3.43	16	2.5
L1	1	13	410	30	11	62	5	4.08	13	2.5
L2	1	16	310	8.5	11	64	6	4.07	13	2.5
L3	1	14	480	-0.5	12	84	7	3.42	9	2.5
L4	1	16	420	4.2	12	80	6	3.62	12	2.5
L5	1	15	550	2.3	12	72	5	3.28	14	2.5
L6	1	12	330	4.3	11	57	2	2.8	11	2.5
L7	1	10	370	5.8	15	82	5	4.1	9	2.5
L8	1	5.2	320	1.3	-1	67	5	2.68	12	2.5
L9	1	10	190	9.4	12	75	4	3.33	14	2.5
L10	1	9.5	370	3.5	16	100	6	4.11	7	2.5
L11	1	6.4	320	5.6	9	78	4	2.84	15	2.5
L12	1	15	460	6.2	14	78	4	4.31	16	2.5
L13	1	17	370	13	9	94	3	3.75	16	2.5
L14	1	9.1	290	9.7	11	90	4	2.89	14	2.5
M1	1	13	350	6.6	11	64	6	3.75	12	2.5
M2	1	41	580	6.4	21	110	12	5.32	7	2.5
M3	1	13	450	1.4	13	91	7	3.6	8	2.5
M4	2	12	280	5.4	11	74	4	3.35	13	2.5
M5	2	13	280	6.7	7	100	10	3.04	13	2.5

APPENDIX V: Part A-Geochemical Analysis (INAA DATA)

Sample Site	Au PPB	As (ppm)	Ba (ppm)	Br (ppm)	Co (ppm)	Cr (ppm)	Cs (ppm)	Fe (wt. %)	Hf (ppm)	Ir (ppm)
M6	1	9	360	7	14	82	4	3.75	13	2.5
M7	3	8	330	1.5	10	70	3	2.97	14	2.5
M8	5	4.5	380	-0.5	9	70	3	2.65	13	2.5
M9	3	6.7	310	2	12	66	4	3.45	15	2.5
M10	1	15	340	10	11	81	5	3.95	13	2.5
M11	1	13	330	6.5	12	84	7	3.92	12	2.5
M12	1	14	340	11	10	81	3	3.22	26	2.5
M13	1	15	360	5.4	14	67	4	3.45	17	2.5
M14	1	9.1	350	3.8	9	110	8	4.23	11	2.5
N1	1	21	330	9.7	11	81	7	4.31	13	2.5
N2	5	17	490	2.9	14	93	9	4.63	8	2.5
N3	1	9.3	310	2	17	96	8	4.31	7	2.5
N4	3	11	330	2.2	10	80	4	3.04	16	2.5
N5	1	12	420	-0.5	13	74	5	3.98	13	2.5
N6	1	9.2	330	3.6	12	68	4	3.62	16	2.5
N7	1	9.3	290	6.9	8	54	3	2.97	16	2.5
N8	4	10	280	4	10	68	3	3.38	18	2.5
N9	5	9.3	300	-0.5	10	76	3	3.18	18	2.5
N10	4	12	270	5.2	10	74	4	3.89	20	2.5
N11	1	9	360	6.1	13	70	3	3.1	14	2.5
N12	1	15	260	9.8	12	75	5	3.62	13	2.5
N13	1	9.8	310	10	11	86	2	3.17	19	2.5
N14	1	5.6	370	31	14	70	3	4.62	9	2.5
P1	6	33	510	2.9	14	82	7	4.13	11	2.5
P2	4	15	490	1.9	20	100	9	4.99	6	2.5
P3	1	18	380	6	13	71	5	3.85	16	2.5
P4	1	9.4	360	4.6	12	69	4	3.53	10	2.5
P5	1	8.9	340	7.2	14	77	4	3.98	12	2.5
P6	1	11	320	2.2	12	81	5	3.68	11	2.5
P7	1	8	360	3.9	12	69	4	3.54	10	2.5
P8	1	11	360	3.4	11	69	3	3.11	10	2.5
P9	1	17	390	7.7	13	74	3	4.16	11	2.5
P10	1	8	390	2.5	10	83	3	3.48	17	2.5
P11	1	11	370	6	10	73	3	3.46	13	2.5
P12	1	10	340	5.1	11	72	4	3.49	13	2.5
P13	3	6.7	430	20	13	69	2	4.05	9	2.5
P14	1	12	370	6.3	12	95	5	4.23	10	2.5
Q1	1	12	420	4.2	12	80	5	3.42	10	2.5
Q2	1	10	370	2.2	14	92	6	3.92	8	2.5
Q3	1	15	340	3.2	14	79	5	4.21	9	2.5
Q4	3	7.9	290	6.4	13	73	5	3.79	11	2.5
Q5	1	10	280	2.4	12	79	5	4.05	12	2.5
Q6	4	9.8	380	1.5	12	87	6	4.35	10	2.5
Q7	1	8.5	330	5.1	12	75	5	3.73	11	2.5
Q8	1	13	380	2.6	11	65	3	3.41	11	2.5

APPENDIX V: Part A-Geochemical Analysis (INAA DATA)

Sample Site	Au PPB	As (ppm)	Ba (ppm)	Br (ppm)	Co (ppm)	Cr (ppm)	Cs (ppm)	Fe (wt. %)	Hf (ppm)	Ir (ppm)
Q9	5	11	530	4.6	17	68	4	4.23	9	2.5
Q10	4	9.8	470	3.9	12	74	3	3.01	15	2.5
Q11	1	13	420	2.7	15	81	3	4.03	13	2.5
Q12	1	9.5	260	7.5	13	82	5	4.05	11	2.5
Q13	5	13	420	22	15	98	2	4.41	10	2.5
Q14	2	230	320	45	14	81	4	4.97	6	2.5
R1	6	15	380	-0.5	12	85	6	4.07	9	2.5
R2	2	12	360	2.2	12	84	5	3.97	9	2.5
R3	1	8	410	1.8	12	80	5	3.77	14	2.5
R4	1	8.9	330	4	15	80	5	4.1	13	2.5
R5	1	8.7	360	8	9	63	3	3.09	14	2.5
R6	3	8.7	450	2.7	13	84	5	4.08	11	2.5
R7	2	11	560	-0.5	15	85	5	4.05	12	2.5
R8	1	8	310	2.3	13	86	3	3.11	15	2.5
R9	1	17	470	4.7	14	72	3	4.09	13	2.5
R10	1	15	440	6.7	13	77	3	3.44	12	2.5
R11	6	20	420	10	12	71	4	4.25	13	2.5
R12	2	12	380	16	9	74	3	3.78	14	2.5
R13	1	14	480	2.5	12	86	5	3.93	11	2.5
R14	1	17	330	39	14	74	5	4.92	6	2.5
S1	1	18	440	1.6	13	76	5	3.65	11	2.5
S2	1	5.2	210	2.2	8	55	4	2.48	13	2.5
S3	1	8.9	280	3.8	15	76	5	4.07	12	2.5
S4	1	10	470	1.1	13	87	5	4.21	11	2.5
S5	1	9	350	4.1	13	76	5	4.11	10	2.5
S6	1	10	370	2.8	13	69	4	3.7	12	2.5
S7	3	8.4	310	4.4	10	74	3	3.46	14	2.5
S8	2	15	240	1.7	13	64	4	4.54	9	2.5
S9	4	26	360	4.9	13	64	3	4.39	11	2.5
S10	2	16	370	5.3	8	58	3	3.38	13	2.5
S11	5	18	480	5.3	11	81	5	4.06	11	2.5
S12	1	19	310	15	10	66	4	3.31	11	2.5
S13	3	11	350	24	10	65	3	3.09	11	2.5
S14	1	6.8	370	47	14	76	2	4.16	9	2.5
T1	1	16	400	3.2	14	80	6	3.96	9	2.5
T2	1	8.9	280	2.5	13	67	5	3.88	10	2.5
T3	1	9.1	320	3.2	12	71	4	3.74	12	2.5
T4	5	8.5	510	-0.5	14	74	5	4.04	10	2.5
T5	2	7.5	350	-0.5	14	81	5	3.96	10	2.5
T6	1	9.5	270	4.7	14	79	5	3.92	12	2.5
T7	6	13	400	5.6	14	77	4	4.55	13	2.5
T8	1	9	280	6	11	70	2	3.21	12	2.5
T9	3	11	370	6.3	11	61	3	2.94	11	2.5
T10	1	13	420	6.7	12	72	4	3.47	9	2.5
T11	4	32	410	13	17	83	6	4.98	10	2.5

APPENDIX V: Part A-Geochemical Analysis (INAA DATA)

Sample Site	Au PPB	As (ppm)	Ba (ppm)	Br (ppm)	Co (ppm)	Cr (ppm)	Cs (ppm)	Fe (wt. %)	Hf (ppm)	Ir (ppm)
T12	1	8.8	350	3.3	7	62	4	2.25	12	2.5
T13	1	5.3	200	160	-1	43	-1	5.46	5	2.5
T14	1	6.3	310	79	9	72	2	3.67	13	2.5
V1	1	10	320	7.9	11	70	5	3.34	14	2.5
V2	1	12	380	2.1	13	83	5	3.85	13	2.5
V3	1	7.9	310	5.5	14	67	5	3.75	11	2.5
V4	1	6.6	260	2.1	11	72	4	3.21	15	2.5
V5	1	9.5	480	2.3	16	82	4	4.22	14	2.5
V6	1	9.8	330	1.9	12	80	5	3.86	12	2.5
V7	1	9.4	300	8.4	15	88	6	4.2	11	2.5
V8	2	12	390	3.1	15	74	4	4.77	10	2.5
V9	1	10	380	9.3	13	72	4	3.8	10	2.5
V10	1	14	330	12	11	80	3	4.06	14	2.5
V11	1	16	360	51	15	97	6	4.31	9	2.5
V12	1	8.1	320	39	16	81	3	4.09	6	2.5
V13	4	13	350	31	17	85	4	4.73	11	2.5
V14	1	8.5	230	25	13	79	4	4.42	11	2.5
W1	4	9.5	350	8.1	11	64	5	3.16	18	2.5
W2	1	14	240	3.1	15	84	5	4.31	14	2.5
W3	1	8.8	300	-0.5	12	89	4	4.1	14	2.5
W4	1	6.6	290	1.7	11	86	4	3.72	14	2.5
W5	1	7.2	220	2	11	82	4	3.41	19	2.5
W6	1	10	300	5.1	14	88	5	4.32	15	2.5
W7	5	13	300	7.1	13	82	4	3.69	14	2.5
W8	3	11	280	14	14	85	4	3.75	15	2.5
W9	4	17	340	8.8	14	93	4	4.19	17	2.5
W10	1	5.7	300	9.4	11	82	6	3.22	15	2.5
W11	3	11	260	38	13	88	4	3.76	16	2.5
W12	1	6.4	310	16	16	110	5	4.62	10	2.5
W13	7	16	370	3.7	14	94	6	3.82	19	2.5
W14	4	7.3	350	11	11	75	3	3.96	12	2.5
X1	5	7.8	240	3.3	12	69	4	3.04	18	2.5
X2	1	11	340	3.4	13	92	7	3.93	13	2.5
X3	3	10	290	3.8	15	81	5	4.19	13	2.5
X4	1	9.2	230	2.3	14	85	6	4.06	15	2.5
X5	1	8.6	240	3	12	83	5	3.96	14	2.5
X6	1	6.7	240	-0.5	12	79	5	3.52	17	2.5
X7	1	8.3	200	20	10	84	4	3.26	13	2.5
X8	1	14	410	9.9	15	86	4	4.5	14	2.5
X9	1	7.9	290	23	12	80	3	3.5	16	2.5
X10	1	11	240	17	12	87	4	3.64	11	2.5
X11	7	8.3	370	17	10	95	4	3.81	13	2.5
X12	3	8.4	210	7.8	14	83	4	3.89	12	2.5
X13	3	12	240	28	13	80	4	3.73	14	2.5
X14	1	5.4	250	150	8	43	1	4.33	6	2.5

APPENDIX V: Part A-Geochemical Analysis (INAA DATA)

Sample Site	Mo (ppm)	Na (wt. %)	Rb (ppm)	Sb (ppm)	Sc (ppm)	Se (ppm)	Sn (wt. %)	Ta (ppm)	Th (ppm)	U (ppm)
A8	3	0.52	120	1.5	12	3	0.005	1	11	2.8
A9	0.5	1.27	62	0.8	9.4	1.5	0.005	1.6	9.1	2.6
A10	8	1.25	130	2.9	11	1.5	0.005	2.2	13	2.7
A11	0.5	1.14	90	1.4	14	1.5	0.005	0.25	9.9	2.8
A12	0.5	0.97	100	1.6	12	1.5	0.005	1.8	10	2.5
A13	2	1.01	100	2	13	1.5	0.005	0.25	11	3.2
B1	4	0.46	84	1.3	12	1.5	0.005	2.2	10	2.4
B2	2	0.41	110	1.6	15	1.5	0.005	1.6	12	2.9
B3	3	0.37	73	1.5	11	1.5	0.005	1.3	11	2.4
B4	0.5	0.83	79	2.5	14	1.5	0.005	1.6	10	2.3
B5	0.5	1.11	73	1.9	11	1.5	0.005	0.9	13	2.8
B6	2	0.1	110	2.6	16	1.5	0.005	0.25	12	1.5
B7	0.5	0.23	95	1.9	12	1.5	0.005	1.1	11	2.3
B8	1	1.36	63	1	17	1.5	0.005	1	7.4	2.3
B9	0.5	1.18	150	2.5	15	1.5	0.005	1.3	17	2.9
B10	0.5	1.26	130	1.6	13	1.5	0.005	1.1	15	3.5
B11	0.5	1.28	130	1.6	15	1.5	0.005	3.1	13	4
B12	0.5	0.85	140	2.7	18	1.5	0.005	0.25	11	3.4
B13	0.5	0.77	100	1.9	15	1.5	0.005	2.2	11	3.4
C1	5	0.69	75	1.1	12	1.5	0.005	1.9	11	2.3
C2	0.5	0.5	91	1.3	12	1.5	0.005	1	10	1.6
C3	0.5	0.58	85	1.3	15	1.5	0.005	0.25	12	2.2
C4	0.5	1.09	100	1.7	13	1.5	0.005	2.1	15	3
C5	0.5	1.63	170	1.4	14	1.5	0.005	1.9	14	4
C6	1	1.15	75	0.8	11	1.5	0.005	1.5	12	2.1
C7	2	1.26	71	2.4	9.6	1.5	0.005	0.25	11	2.6
C8	1	0.93	150	1.5	16	1.5	0.005	1.6	12	2
C9	2	1.64	140	1.4	17	1.5	0.005	1.9	18	4.2
C10	3	0.96	110	2	16	1.5	0.005	2.1	12	3.1
C11	0.5	1.11	100	2.5	15	1.5	0.005	0.25	11	3.3
C12	0.5	0.56	110	0.7	14	1.5	0.005	1.3	8.1	2.1
C13	0.5	0.95	75	2	11	1.5	0.005	1.5	9.4	2.7
D1	3	0.61	70	3.2	12	1.5	0.005	0.25	11	3.1
D2	2	0.74	62	1.2	11	1.5	0.005	0.25	10	2.2
D3	3	0.83	78	1.1	11	1.5	0.005	1.7	13	2.4
D4	2	0.92	99	1.3	11	1.5	0.005	0.25	17	3
D5	4	1.22	100	1.3	13	1.5	0.005	1.4	11	1.8
D6	0.5	1.39	99	0.9	12	1.5	0.005	1.4	13	2.6
D7	0.5	1.1	140	1.6	16	1.5	0.005	1.8	14	2.8
D8	0.5	2.07	150	1.5	15	1.5	0.005	2	22	4.4
D9	4	1.04	130	2.4	21	1.5	0.005	0.25	12	3
D10	0.5	1.04	92	1.5	13	1.5	0.005	1.6	9.2	2.6
D11	4	0.68	96	0.9	11	1.5	0.005	2	10	2.6
D12	4	0.77	77	0.8	11	1.5	0.005	1.8	11	2.2
D13	0.5	0.68	97	1	14	1.5	0.005	1.1	11	2.6

APPENDIX V: Part A-Geochemical Analysis (INAA DATA)

Sample Site	Mo (ppm)	Na (wt. %)	Rb (ppm)	Sb (ppm)	Sc (ppm)	Se (ppm)	Sn (wt. %)	Ta (ppm)	Th (ppm)	U (ppm)
D14	0.5	0.72	100	1.1	14	1.5	0.005	0.25	9.8	2.7
E1	0.5	0.46	78	1.1	13	1.5	0.005	1.6	10	3
E2	0.5	0.46	100	1	15	1.5	0.005	1.5	12	2.5
E3	0.5	0.73	71	1.2	12	1.5	0.005	0.9	11	2.5
E4	2	0.92	140	1.2	12	1.5	0.005	0.25	17	3.3
E5	3	1.26	94	1.2	12	1.5	0.005	0.25	16	3.1
E6	2	0.93	150	1.3	16	1.5	0.005	1.6	13	2
E7	0.5	0.98	110	1.4	17	1.5	0.005	1.5	12	4.1
E8	4	0.98	140	1.5	15	1.5	0.005	0.25	8.8	3
E9	0.5	0.91	94	0.9	10	1.5	0.005	0.25	9.6	2.7
E10	2	0.64	73	0.8	9.1	1.5	0.005	1.8	10	2.6
E11	4	0.79	80	0.7	10	1.5	0.005	1.4	10	2.5
E12	0.5	0.72	84	0.7	11	1.5	0.005	1	10	2.5
E13	0.5	0.57	120	1.2	17	1.5	0.005	1	11	2.9
E14	4	0.94	71	1	15	6	0.005	2	12	4.3
F1	0.5	0.62	96	0.9	13	1.5	0.005	1.5	12	3.6
F2	0.5	0.63	110	1.9	14	1.5	0.005	1.4	12	2.9
F3	0.5	0.54	97	1.2	13	1.5	0.005	1	12	3.5
F4	0.5	0.82	110	1.6	13	1.5	0.005	1.4	14	4.9
F5	6	0.92	96	0.7	11	1.5	0.005	2.7	10	2.5
F6	0.5	1.19	160	1.3	15	1.5	-0.02	0.25	16	3.4
F7	0.5	1.71	120	1.7	13	1.5	-0.02	0.25	15	4.2
F8	0.5	1.3	120	2.1	18	1.5	-0.02	0.25	12	4.8
F9	0.5	0.44	100	1.1	12	1.5	0.005	0.25	11	3.8
F10	0.5	0.31	120	1.1	17	1.5	0.005	1.6	13	4.2
F11	0.5	0.79	110	0.8	12	1.5	0.005	1.4	11	3.1
F12	0.5	1.15	85	0.5	14	1.5	0.005	0.25	11	2.6
F13	0.5	0.93	120	1.2	15	1.5	0.005	1.5	11	3.3
F14	0.5	1.05	140	1.2	15	1.5	0.005	0.9	10	4.2
G1	9	0.44	61	0.8	10	1.5	0.005	0.25	8.3	2.1
G2	0.5	0.44	81	1.2	13	1.5	0.005	1.5	11	2.4
G3	0.5	0.64	83	1.1	14	1.5	0.005	1.7	14	3.1
G4	0.5	1.24	110	1.3	16	1.5	0.005	0.25	19	5
G5	0.5	1.25	130	3.1	17	1.5	-0.02	1.6	11	3.7
G6	7	1.05	150	2.9	17	1.5	-0.02	0.25	12	2.8
G7	3	0.86	170	2.8	17	1.5	-0.02	0.25	9.4	2.3
G8	0.5	1.05	82	1.6	10	1.5	0.005	1.5	10	2.6
G9	0.5	0.46	100	1.9	14	1.5	-0.02	0.25	12	2.7
G10	5	0.53	110	2.3	12	1.5	-0.02	0.25	12	2.6
G11	3	0.37	90	2	9.7	1.5	0.005	0.25	9.1	3
G12	5	1.1	110	1.8	16	1.5	-0.02	1.6	12	2.7
G13	0.5	0.58	89	1.8	11	1.5	0.005	1.6	11	2.3
G14	0.5	0.79	120	1	14	1.5	-0.02	1.3	11	2.3
H1	5	0.34	120	1.6	16	1.5	0.005	1.6	13	3.5
H2	5	0.58	89	1.6	12	1.5	-0.02	1.6	13	2.7

APPENDIX V: Part A-Geochemical Analysis (INAA DATA)

Sample Site	Mo (ppm)	Na (wt. %)	Rb (ppm)	Sb (ppm)	Sc (ppm)	Se (ppm)	Sn (wt. %)	Ta (ppm)	Th (ppm)	U (ppm)
H3	0.5	0.6	79	1.4	10	1.5	0.005	0.25	11	2.8
H4	4	1.38	140	2	13	1.5	-0.02	0.25	14	2.4
H5	0.5	1.22	120	2	14	1.5	-0.02	0.25	12	2.7
H6	4	1.36	76	1.6	9.6	1.5	0.005	1	10	2.9
H7	5	0.73	120	1.3	12	1.5	-0.02	0.9	11	2.8
H8	7	0.27	130	1.6	16	1.5	-0.02	1.7	11	2.9
H9	4	0.45	110	1.2	12	1.5	0.005	0.25	9.5	2.3
H10	2	0.58	83	1.2	12	1.5	0.005	0.25	11	2.4
H11	0.5	0.52	99	1.7	11	1.5	0.005	0.25	12	3.2
H12	0.5	0.19	130	1.6	15	1.5	-0.02	0.25	11	3.3
H13	2	0.83	85	1.1	13	1.5	0.005	1.7	12	3.2
H14	2	0.75	85	1.1	12	1.5	0.005	0.25	11	2.6
K1	6	0.92	160	1.8	13	1.5	-0.02	2.3	20	2.2
K2	0.5	0.61	98	1.4	12	1.5	0.005	0.25	13	2.3
K3	4	1.33	110	1.8	14	1.5	-0.02	0.25	21	3.7
K4	5	1.22	140	2.1	13	1.5	-0.02	1.3	11	3
K5	5	1.66	100	1.8	12	1.5	-0.02	1.6	9.4	2.6
K6	0.5	0.7	130	1.5	15	1.5	0.005	0.25	12	3.1
K7	1	0.26	160	1.6	17	1.5	-0.02	0.25	11	1.9
K8	0.5	0.29	130	1.7	16	1.5	-0.02	1.8	11	3.2
K9	8	0.49	110	1.1	13	1.5	0.005	0.25	11	2.5
K10	0.5	0.77	93	1.8	14	1.5	0.005	1.2	12	3
K11	3	0.79	110	1.9	15	1.5	0.005	0.25	11	2.6
K12	2	0.65	85	1.1	9.7	1.5	0.005	0.25	11	2.6
K13	2	0.73	100	1.3	11	1.5	0.005	1.5	12	2.6
K14	5	0.7	94	1.7	13	4	0.005	1.7	14	3
L1	3	1.1	110	1.9	13	1.5	-0.02	0.25	17	2.3
L2	0.5	1.16	130	1.7	13	1.5	-0.02	1.9	18	3.7
L3	6	1.38	130	1.4	14	1.5	-0.02	2	10	3.1
L4	7	1	110	1.3	12	1.5	-0.02	0.25	12	3.2
L5	5	1.19	100	1	12	1.5	-0.02	1.1	12	5.6
L6	4	0.97	94	0.5	8.9	1.5	0.005	0.25	10	2.7
L7	0.5	0.42	110	0.9	14	1.5	-0.02	0.25	11	2.6
L8	0.5	0.23	110	0.6	11	1.5	-0.02	2.3	9.3	2.4
L9	4	0.56	81	0.7	11	1.5	-0.02	1.3	11	2.8
L10	0.5	0.52	130	1	14	1.5	-0.02	1.1	11	2.5
L11	0.5	0.82	100	0.7	11	1.5	-0.02	1.9	11	3.2
L12	3	0.64	130	0.6	15	1.5	-0.02	1.4	13	3.9
L13	6	0.78	83	0.8	11	1.5	0.005	2.2	12	2.7
L14	0.5	0.44	84	0.7	10	1.5	0.005	1.3	11	3.5
M1	3	1.15	120	1.2	13	1.5	-0.02	1.8	16	3.1
M2	7	1.17	150	2.5	19	1.5	-0.02	0.25	13	4.3
M3	9	1.3	130	1.2	15	1.5	-0.02	1.8	9.2	2.5
M4	2	1.09	87	0.9	11	1.5	0.005	2	10	2.6
M5	2	0.08	110	0.7	14	1.5	0.005	1.3	10	2.3

APPENDIX V: Part A-Geochemical Analysis (INAA DATA)

Sample Site	Mo (ppm)	Na (wt. %)	Rb (ppm)	Sb (ppm)	Sc (ppm)	Se (ppm)	Sn (wt. %)	Ta (ppm)	Th (ppm)	U (ppm)
M6	0.5	0.45	92	0.7	12	1.5	0.005	1.6	12	2.9
M7	3	0.57	74	0.8	11	1.5	0.005	1.6	10	3
M8	0.5	0.95	82	0.7	11	1.5	0.005	0.25	11	2.7
M9	0.5	0.86	77	0.6	13	1.5	0.005	0.25	11	2.4
M10	0.5	0.71	92	0.7	14	1.5	0.005	1.9	12	2.5
M11	0.5	0.47	140	0.7	16	1.5	0.005	1.5	12	2.5
M12	0.5	0.74	75	0.8	11	1.5	0.005	1.6	13	3.3
M13	0.5	0.65	92	0.8	14	1.5	0.005	1.5	11	2.7
M14	0.5	0.24	100	1.3	16	1.5	0.005	1	11	2.9
N1	2	1.02	110	1.6	14	1.5	0.005	0.25	12	3.1
N2	0.5	1.54	190	1.7	19	1.5	-0.02	2.3	12	3.5
N3	2	1.01	120	1.2	17	1.5	0.005	1.8	9	2.8
N4	1	0.76	76	1.1	11	1.5	0.005	1	10	2.3
N5	0.5	0.39	100	0.9	13	1.5	0.005	1.3	10	3.2
N6	0.5	0.56	88	1	12	1.5	0.005	1.2	12	3.4
N7	2	0.38	83	1	10	1.5	0.005	2.3	9.1	2.4
N8	0.5	0.85	96	0.8	10	1.5	0.005	1.4	11	3
N9	2	0.89	82	0.8	11	1.5	0.005	1.6	11	2.9
N10	0.5	0.72	100	0.8	13	1.5	0.005	0.25	13	3.5
N11	0.5	0.83	72	0.7	10	1.5	0.005	1.3	9.2	2.5
N12	1	0.77	87	0.8	12	1.5	0.005	1.5	11	2.7
N13	3	1	57	0.6	9.9	1.5	0.005	1.3	10	2.2
N14	0.5	0.84	75	0.5	17	1.5	0.005	0.25	9.7	2
P1	0.5	1.32	120	1.9	16	1.5	0.005	0.25	15	3.8
P2	0.5	0.96	160	1.2	18	1.5	0.005	1.7	11	3.6
P3	7	1.1	90	1	13	1.5	0.005	0.25	17	3.6
P4	5	0.28	98	0.8	12	1.5	0.005	1.5	11	2.9
P5	0.5	0.25	78	0.7	12	1.5	0.005	0.25	9.9	2.4
P6	0.5	0.35	110	0.8	13	1.5	0.005	1.7	10	2.8
P7	4	0.33	110	0.8	11	1.5	0.005	1.4	10	2
P8	2	0.76	73	0.7	8.8	1.5	0.005	1.6	10	2.7
P9	0.5	0.86	110	1.2	13	1.5	0.005	0.25	12	2.8
P10	4	1.02	85	0.8	12	1.5	0.005	2.9	12	3.1
P11	0.5	0.97	95	0.7	11	1.5	0.005	0.25	11	2.8
P12	0.5	0.8	74	0.8	12	1.5	0.005	0.25	11	3.4
P13	3	1.08	71	0.5	14	1.5	0.005	1	11	2.1
P14	3	0.92	96	0.8	15	1.5	0.005	0.25	9.5	3.1
Q1	0.5	1.13	110	1.1	12	1.5	0.005	0.25	9.5	3.4
Q2	5	1.04	120	1	14	1.5	0.005	0.25	9.8	2.1
Q3	3	0.27	120	1	13	1.5	0.005	1.1	10	2.5
Q4	0.5	0.2	92	0.8	12	1.5	0.005	1.8	9.2	2.8
Q5	0.5	0.21	100	0.9	14	1.5	0.005	2.1	11	2.5
Q6	7	0.23	120	1.1	14	1.5	0.005	1.8	12	2.6
Q7	4	0.26	84	0.9	11	1.5	0.005	1.6	11	2.5
Q8	0.5	1.03	94	0.7	12	1.5	0.005	1.7	11	2.8

APPENDIX V: Part A-Geochemical Analysis (INAA DATA)

Sample Site	Mo (ppm)	Na (wt. %)	Rb (ppm)	Sb (ppm)	Sc (ppm)	Se (ppm)	Sn (wt. %)	Ta (ppm)	Th (ppm)	U (ppm)
Q9	0.5	0.78	91	0.8	14	1.5	0.005	0.25	12	3.3
Q10	0.5	0.91	66	0.7	9.2	1.5	0.005	1.8	11	2.8
Q11	5	0.67	110	0.7	13	1.5	0.005	0.25	12	2.6
Q12	2	0.39	90	1	13	1.5	0.005	0.25	12	2.8
Q13	0.5	1.47	59	1.1	17	1.5	0.005	0.25	6.6	2.9
Q14	7	1.3	75	3.3	16	1.5	-0.02	1.3	6.7	1.7
R1	3	0.82	130	1.4	15	1.5	0.005	0.25	12	2.9
R2	5	1.12	100	1.1	14	1.5	0.005	0.25	11	2.7
R3	0.5	0.52	92	0.9	13	1.5	0.005	2.1	12	2.7
R4	3	0.3	130	0.9	13	1.5	0.005	2.1	11	2.8
R5	0.5	0.33	93	0.8	10	7	0.005	1.5	9.9	3.3
R6	4	0.45	97	0.9	13	1.5	0.005	1.3	11	3.3
R7	6	0.5	120	0.9	15	1.5	0.005	0.25	12	2.5
R8	0.5	1.06	95	0.7	10	1.5	0.005	2.3	12	2.4
R9	2	0.76	120	0.8	14	1.5	0.005	1.3	11	2.7
R10	7	0.79	92	0.9	10	6	0.005	0.25	11	2.4
R11	4	0.9	92	0.6	11	1.5	0.005	0.25	11	1.9
R12	3	0.81	88	0.7	11	1.5	0.005	0.25	12	2.5
R13	9	0.94	110	0.9	15	1.5	0.005	0.25	11	2.7
R14	0.5	0.97	130	1	15	1.5	0.005	0.25	8.6	1.8
S1	0.5	1.3	120	1.5	13	1.5	0.005	1.4	14	3.4
S2	4	0.38	110	0.6	9.8	1.5	0.005	1.8	8.3	1.7
S3	6	0.22	110	0.9	13	1.5	0.005	1.4	10	2.4
S4	0.5	0.23	120	0.8	14	1.5	0.005	1.6	11	2.1
S5	3	0.21	98	0.9	13	1.5	0.005	1.3	11	1.8
S6	2	0.26	100	0.6	12	1.5	0.005	0.25	11	3.2
S7	0.5	0.6	81	0.7	11	5	0.005	1.3	11	2.9
S8	4	0.77	97	0.9	15	1.5	0.005	1.9	12	2.3
S9	0.5	0.84	120	1	13	1.5	0.005	1.4	12	3.2
S10	4	0.77	72	0.7	10	1.5	0.005	0.25	11	2.2
S11	4	0.65	120	0.9	13	1.5	0.005	2	12	2.7
S12	6	1.24	51	0.7	11	1.5	0.005	1.4	10	1.5
S13	3	0.76	55	0.7	9.4	1.5	0.005	1.3	9.4	2.2
S14	0.5	1.62	47	0.5	16	1.5	0.005	1.4	8.9	2.5
T1	5	1.03	110	1.2	14	1.5	0.005	1.5	12	2.7
T2	6	0.28	100	0.8	12	1.5	0.005	1.6	9.8	2.2
T3	3	0.29	100	0.9	12	1.5	0.005	1.2	9.8	2.2
T4	6	0.22	130	0.8	14	1.5	0.005	1.4	11	2.4
T5	4	0.11	97	0.9	13	1.5	0.005	1.6	11	2.5
T6	0.5	0.15	97	2.7	11	1.5	0.005	0.25	11	3.1
T7	0.5	0.68	120	2.7	13	1.5	-0.02	1.4	11	2.4
T8	2	0.83	86	1.8	9.9	1.5	0.005	0.25	10	2.5
T9	2	0.9	71	1.5	9.6	1.5	0.005	1.6	9.1	2.1
T10	1	0.42	92	1.6	11	1.5	0.005	1.3	11	2
T11	2	0.84	120	2.2	14	1.5	-0.02	1	11	3

APPENDIX V: Part A-Geochemical Analysis (INAA DATA)

Sample Site	Mo (ppm)	Na (wt. %)	Rb (ppm)	Sb (ppm)	Sc (ppm)	Se (ppm)	Sn (wt. %)	Ta (ppm)	Th (ppm)	U (ppm)
T12	3	0.98	94	1.4	11	1.5	0.005	1.8	10	3
T13	0.5	0.67	51	1.5	9.2	1.5	-0.02	0.6	12	2.5
T14	0.5	1.22	57	1.2	11	1.5	-0.02	1.2	9.4	2.6
V1	4	0.91	100	1.7	11	1.5	0.005	1.6	12	2.5
V2	0.5	0.69	110	2	13	1.5	0.005	1.5	10	2.8
V3	0.5	0.26	110	1.8	12	1.5	0.005	0.25	9.5	2.5
V4	2	0.12	82	1.6	11	1.5	0.005	1.4	11	2.1
V5	0.5	0.26	83	2	11	1.5	0.005	0.25	10	3.7
V6	4	0.15	100	2.1	12	1.5	0.005	1.8	11	2.7
V7	0.5	0.28	100	2.3	13	1.5	-0.02	1.4	11	2.5
V8	0.5	0.64	130	1.7	15	1.5	-0.02	0.9	11	2.7
V9	0.5	0.74	100	1.4	13	1.5	0.005	1.5	9.8	2.4
V10	0.5	0.5	99	1.3	12	1.5	0.005	2	12	3.2
V11	3	0.84	86	1.5	13	1.5	-0.02	1.5	9.7	2.4
V12	2	1.61	60	1.1	16	1.5	-0.02	0.25	8.3	2.1
V13	0.5	1.32	62	0.8	15	1.5	0.005	0.25	10	2.8
V14	3	1.22	77	0.5	14	1.5	0.005	0.25	8.7	3.2
W1	0.5	0.88	79	0.9	11	1.5	0.005	1.3	11	3.6
W2	0.5	0.5	100	1.1	15	1.5	0.005	1.4	11	4.2
W3	6	0.12	100	0.8	14	1.5	0.005	1.4	10	2.2
W4	0.5	0.21	100	0.8	12	1.5	0.005	1.3	10	2.9
W5	0.5	0.2	69	0.9	11	1.5	0.005	1.5	10	3
W6	0.5	0.28	99	0.9	12	1.5	0.005	1.5	11	3.6
W7	0.5	0.62	85	0.7	11	1.5	0.005	1.4	9.9	3.5
W8	4	0.65	95	0.8	11	1.5	0.005	1	10	3.3
W9	3	0.91	73	0.8	12	1.5	0.005	0.25	11	3.4
W10	0.5	1.19	99	0.5	11	1.5	0.005	0.25	9.3	3.3
W11	0.5	1.03	73	0.8	12	4	0.005	1.3	11	3.3
W12	0.5	1.39	90	0.6	17	1.5	0.005	1.2	8.5	3
W13	5	1.29	100	0.9	14	1.5	0.005	1.3	11	3.4
W14	4	1.66	67	0.6	15	1.5	0.005	1.5	7.8	2.2
X1	3	0.52	59	0.8	10	1.5	0.005	1.8	9.3	3.5
X2	5	0.74	100	1	14	1.5	0.005	0.25	11	2.6
X3	0.5	0.26	120	1	13	1.5	0.005	1.6	10	2.5
X4	3	0.16	110	0.8	12	1.5	0.005	1.1	11	2.9
X5	0.5	0.19	100	0.8	11	1.5	0.005	0.25	10	2.8
X6	2	0.14	77	0.9	12	1.5	0.005	1.5	10	2.8
X7	0.5	0.55	98	0.6	11	1.5	0.005	0.8	9.1	3.3
X8	0.5	0.78	89	1	12	1.5	0.005	1.7	12	3.1
X9	0.5	1.08	62	0.7	11	1.5	0.005	1.4	9.7	3.5
X10	0.5	1.29	63	0.9	13	1.5	0.005	0.25	8.9	2.6
X11	0.5	1.58	100	0.5	14	1.5	0.005	1.7	9.2	2.7
X12	0.5	1.55	90	0.9	14	1.5	0.005	0.25	9.5	2.4
X13	0.5	0.89	81	0.7	11	1.5	0.005	0.25	10	3.5
X14	0.5	0.92	-15	0.6	12	1.5	0.005	0.25	6.3	3

APPENDIX V: Part A-Geochemical Analysis (INAA DATA)

Sample Site	W (ppm)	La (ppm)	Ce (ppm)	Nd (ppm)	Sm (ppm)	Eu (ppm)	Tb (ppm)	Yb (ppm)	Lu (ppm)	Mass (g)
A8	0.5	36	67	19	3.8	1	0.25	3.8	0.66	26.63
A9	0.5	34	55	21	4.3	1.2	0.9	4.1	0.75	28.91
A10	3	44	130	36	9.7	2	2.4	8.4	1.24	24.58
A11	0.5	37	62	29	5.1	1.3	0.8	3.9	0.66	26.13
A12	0.5	37	64	20	4.3	1.1	0.25	3.3	0.65	26.95
A13	0.5	43	73	31	7.1	1.7	1.3	4.8	0.89	30.18
B1	0.5	44	79	27	6	1.3	1.2	3.9	0.69	24.76
B2	0.5	47	77	26	5.8	1.4	0.25	3.8	0.68	24.05
B3	0.5	38	69	25	5	1.2	1	3.8	0.73	29.92
B4	1	39	65	27	5.1	1.2	1.1	4	0.72	31.4
B5	0.5	43	89	26	5.3	1.1	1	3.9	0.69	29.4
B6	0.5	42	75	21	4.5	1	0.9	3.5	0.7	26.14
B7	0.5	36	70	17	4	1.1	1.1	3.2	0.58	25.74
B8	0.5	30	58	22	4.5	1.3	0.9	3.6	0.68	33.14
B9	0.5	58	100	26	5.8	1.3	0.9	3.8	0.71	23.39
B10	0.5	44	85	28	5	1	0.25	4.2	0.77	28.89
B11	0.5	45	72	28	5.1	1	1.1	3.7	0.71	24.75
B12	0.5	47	85	32	5.1	1.2	0.25	3.8	0.72	20.88
B13	0.5	41	67	23	4.8	1.1	0.25	4	0.7	23.83
C1	2	52	97	39	9.1	2.2	1.8	5.1	0.94	28.67
C2	0.5	38	65	26	4.5	1.1	0.25	3.4	0.66	26.55
C3	0.5	39	64	23	4.7	1.1	1.1	3.3	0.62	27.99
C4	2	57	110	40	8.5	1.4	1.8	5.4	0.99	29.37
C5	0.5	58	97	31	6.8	0.9	1.1	5.2	0.95	24.78
C6	0.5	37	73	21	4.8	1.2	1	4	0.77	29.01
C7	0.5	53	90	37	7.4	1.7	1	4.3	0.81	32.5
C8	0.5	49	77	32	6	1.2	0.25	4	0.79	26.08
C9	0.5	70	110	39	8.1	1.2	0.25	6	1.06	26.87
C10	0.5	48	81	36	7.3	1.7	1.1	4.7	0.85	25.03
C11	0.5	42	73	25	5.8	1.4	0.25	4.2	0.74	23.21
C12	2	28	35	8	2	0.7	0.25	2.9	0.56	25.76
C13	0.5	36	60	18	4.2	1.1	1.1	4	0.7	31.87
D1	0.5	46	73	31	6.1	1.4	1.1	4.1	0.76	33.29
D2	0.5	36	61	24	4.7	1	0.9	3.6	0.63	27.5
D3	2	37	76	25	4.7	1.1	0.8	3.5	0.63	29.29
D4	2	60	110	38	7.3	1.3	1.2	4.9	0.91	28.58
D5	2	37	63	27	4.8	1.1	0.9	3.8	0.72	25.33
D6	0.5	51	87	35	6.6	1.4	1.1	4.2	0.83	28.5
D7	2	60	100	41	8.2	1.7	1.2	4.7	0.86	25.73
D8	3	73	120	48	8.6	1.3	1.3	6.1	1.17	29.93
D9	0.5	46	79	32	6.3	1.5	1.2	4	0.7	21.42
D10	0.5	40	63	27	4.4	1	0.7	3.9	0.68	26.51
D11	0.5	45	73	29	5.3	1.3	0.9	3.8	0.68	28.18
D12	2	41	73	30	5.7	1.4	0.8	3.6	0.71	27.36
D13	0.5	50	82	37	6.9	1.7	1.2	4	0.73	28.47

APPENDIX V: Part A-Geochemical Analysis (INAA DATA)

Sample Site	W (ppm)	La (ppm)	Ce (ppm)	Nd (ppm)	Sm (ppm)	Eu (ppm)	Tb (ppm)	Yb (ppm)	Lu (ppm)	Mass (g)
D14	0.5	40	66	27	5	1.2	0.25	3.9	0.66	23.73
E1	0.5	39	66	27	5.3	1.3	1	3.9	0.69	25.38
E2	0.5	48	79	35	6	1.5	1	3.8	0.66	26.52
E3	0.5	41	70	29	5.4	1.2	0.9	4	0.78	27.82
E4	0.5	58	99	28	5.2	1.1	0.25	3.4	0.66	23.05
E5	0.5	55	92	33	5.5	1.2	0.9	3.3	0.63	26.95
E6	0.5	53	84	34	6.5	1.3	1.2	4.8	0.87	26.56
E7	2	44	74	31	5.3	1	0.8	3.9	0.66	22.13
E8	0.5	38	62	22	4.1	0.9	0.8	3.2	0.55	17.91
E9	2	39	67	26	4.9	1.1	1	4	0.71	26.18
E10	2	37	66	29	4.6	1.1	0.8	3.4	0.64	31.28
E11	0.5	41	83	28	5.1	1.2	1	3.7	0.7	26.14
E12	2	33	52	18	3.5	0.9	0.25	4.1	0.72	28.5
E13	0.5	42	69	29	5.6	1.4	0.8	3.6	0.62	19.05
E14	0.5	52	110	39	6.2	2	0.25	5.2	0.79	28.38
F1	0.5	38	77	29	5.3	1.5	1.3	4.4	0.72	24.94
F2	0.5	37	84	26	4.6	1.4	0.25	3.9	0.67	26.87
F3	0.5	35	73	22	4.4	1.3	0.25	3.6	0.51	27.9
F4	0.5	49	100	34	5.5	1.6	0.25	4.8	0.72	27.62
F5	0.5	36	65	21	4.7	1.5	0.25	4.2	0.68	27.89
F6	0.5	52	100	37	5.8	1.8	0.25	4.1	0.63	22.58
F7	0.5	48	100	47	6	1.9	0.25	4.4	0.69	23.71
F8	0.5	45	87	40	7.3	2.1	2.4	5	0.74	22.94
F9	0.5	38	74	36	4.8	1.5	0.25	4.5	0.69	27.77
F10	0.5	46	89	33	5.4	1.8	1	5.2	0.73	24.41
F11	5	39	83	29	4.8	1.6	1	4.5	0.64	30.68
F12	0.5	40	86	27	5.2	1.8	0.25	5.3	0.82	26.4
F13	0.5	40	74	28	4.9	1.5	1.2	4.4	0.65	25.93
F14	0.5	42	77	29	4.9	1.6	1	4.4	0.72	24.38
G1	0.5	38	80	16	3.3	1	0.25	2.5	0.38	16.78
G2	0.5	35	80	24	3.4	1.1	0.25	2.9	0.5	26.11
G3	0.5	39	85	34	4.8	1.5	0.25	4	0.66	29.17
G4	0.5	49	99	36	5.4	1.6	0.25	4.3	0.76	23.41
G5	0.5	42	76	25	7.2	1.8	1.1	5.1	0.75	23.8
G6	0.5	39	73	27	4.4	1	0.7	4.2	0.61	20.64
G7	0.5	37	68	23	3.5	0.8	0.25	3.8	0.55	19.12
G8	0.5	35	70	22	4.3	1	0.25	3.8	0.55	30.23
G9	0.5	46	86	32	6.3	1.5	0.25	5.4	0.79	23.54
G10	0.5	39	73	25	5.2	1.3	1	4.7	0.69	24.48
G11	0.5	35	62	25	4.2	1.1	0.7	3.8	0.61	25.65
G12	0.5	50	88	29	6.1	1.6	0.25	5	0.73	25.37
G13	0.5	37	67	24	4.3	1.1	0.8	5.2	0.73	25.35
G14	0.5	51	70	19	4	1.1	0.7	4.5	0.71	25
H1	0.5	41	84	21	4.6	1	0.25	3.9	0.57	24.9
H2	0.5	40	80	23	4.9	1.1	0.7	4.2	0.52	22.76

APPENDIX V: Part A-Geochemical Analysis (INAA DATA)

Sample Site	W (ppm)	La (ppm)	Ce (ppm)	Nd (ppm)	Sm (ppm)	Eu (ppm)	Tb (ppm)	Yb (ppm)	Lu (ppm)	Mass (g)
H3	0.5	34	64	18	4.2	0.9	0.6	3.6	0.59	29.3
H4	0.5	59	90	25	5.5	1.3	0.25	3.9	0.6	24.09
H5	0.5	44	81	27	5.2	1.1	0.8	4.5	0.7	25.94
H6	0.5	37	70	23	4.6	1.1	1.2	4.2	0.64	28.75
H7	0.5	44	92	28	5.7	1.4	1	4.3	0.62	23.54
H8	0.5	45	80	33	5.7	1.4	0.6	4.8	0.71	20.9
H9	0.5	38	69	25	5	1.1	0.8	4.6	0.67	29.43
H10	0.5	42	80	27	5.8	1.4	0.9	4.6	0.71	26.86
H11	0.5	47	81	26	5.8	1.4	0.9	5.7	0.86	25.2
H12	0.5	75	130	47	11	2.9	2	8.5	1.21	26.86
H13	0.5	51	110	33	6.5	1.5	0.8	5.3	0.72	28.78
H14	0.5	43	75	27	5.1	1.2	0.7	4.6	0.71	28.5
K1	0.5	59	110	27	5.8	1.2	0.25	3.4	0.43	25.28
K2	1	39	69	20	4.6	1.1	0.7	3.8	0.57	29.51
K3	0.5	76	140	40	8.6	1.7	1	6.1	0.87	27.77
K4	0.5	41	79	24	5.6	1.2	0.9	4.9	0.69	26.48
K5	0.5	37	65	27	4.1	0.9	0.6	3.9	0.58	26.55
K6	2	41	93	24	4.8	1.2	0.25	4	0.6	24.5
K7	0.5	52	97	33	7.6	1.8	1.3	5.6	0.75	19.67
K8	0.5	32	60	17	4.3	1.1	0.8	4.6	0.63	20.13
K9	0.5	43	84	27	5.3	1.4	1	4.4	0.65	25.35
K10	0.5	47	89	37	8.2	1.9	1.4	5.6	0.79	26.13
K11	0.5	42	72	31	6.6	1.6	0.9	4.5	0.66	27.59
K12	0.5	40	82	24	5.5	1.3	0.8	4.4	0.69	30.94
K13	3	40	78	22	5.2	1.3	0.8	4.1	0.51	26.14
K14	0.5	48	100	32	6.2	1.5	1	5.5	0.78	27.5
L1	0.5	55	99	32	5.6	1.1	0.9	3.5	0.53	24.79
L2	0.5	54	100	25	5.1	1.1	0.25	3.8	0.58	28.19
L3	0.5	43	82	30	4.9	1	0.25	4	0.55	25.22
L4	0.5	42	79	26	5.1	1.2	0.8	4.3	0.67	29.03
L5	0.5	45	81	27	5.5	1.3	0.8	4.5	0.7	31.58
L6	0.5	36	71	23	4.8	1.2	0.6	3.9	0.49	33.98
L7	0.5	47	85	33	5.9	1.5	1.1	4.7	0.72	25.26
L8	0.5	41	74	24	4.9	1.1	0.25	4.5	0.54	23.13
L9	0.5	40	84	27	6	1.4	1.1	4.8	0.7	27.83
L10	0.5	41	74	24	4.2	1.1	0.25	3.7	0.56	26.99
L11	0.5	42	93	24	5.3	1.2	0.25	4.6	0.6	29.41
L12	0.5	52	110	37	6.9	1.8	1.1	5.2	0.77	26.52
L13	0.5	41	75	26	5.3	1.3	0.9	4.8	0.66	27.61
L14	3	41	72	25	5.1	1.3	0.8	4.5	0.63	30.86
M1	4	51	90	24	5.4	1.1	0.8	3.8	0.6	25.16
M2	0.5	40	75	26	4.3	1	0.25	3.9	0.57	21.71
M3	0.5	43	79	28	4.5	1	0.8	4.2	0.61	22.18
M4	0.5	38	62	25	4.4	1	0.7	3.6	0.57	29.41
M5	0.5	36	59	22	4.4	1	0.9	3.7	0.6	27.63

APPENDIX V: Part A-Geochemical Analysis (INAA DATA)

Sample Site	W (ppm)	La (ppm)	Ce (ppm)	Nd (ppm)	Sm (ppm)	Eu (ppm)	Tb (ppm)	Yb (ppm)	Lu (ppm)	Mass (g)
M6	4	43	79	26	5.6	1.3	1.1	5.1	0.69	27.72
M7	3	41	79	26	5.8	1.4	0.9	4.7	0.71	33.08
M8	0.5	44	86	30	6.2	1.5	0.25	4.7	0.68	28.87
M9	0.5	38	67	22	4.7	1.2	0.8	4.1	0.75	30.58
M10	0.5	46	73	27	5.2	1.4	0.8	3.8	0.63	23.49
M11	0.5	62	94	31	6.7	1.6	1.2	4	0.77	25.56
M12	0.5	47	76	26	6	1.3	1.1	4.4	0.81	27.98
M13	0.5	60	120	50	10	2.5	2	5.2	0.89	27.52
M14	0.5	40	63	24	4.5	1.1	0.9	3.6	0.65	24.46
N1	0.5	47	75	30	4.9	1	0.25	3.6	0.67	22.3
N2	0.5	47	76	27	5.4	1.3	0.25	3.7	0.69	17.3
N3	1	35	54	18	3.6	0.9	0.5	3	0.57	23.77
N4	0.5	44	67	26	5.1	1.1	1.1	3.9	0.72	30.66
N5	0.5	46	80	33	6.7	1.5	1.2	4.5	0.79	27.13
N6	0.5	49	84	30	6.2	1.4	1.2	4.4	0.8	29.86
N7	0.5	34	54	21	4.5	1	0.8	4.2	0.74	26.23
N8	0.5	43	95	23	5.4	1.3	0.9	3.8	0.71	30.5
N9	2	44	82	28	5.6	1.3	1.1	3.9	0.72	31.6
N10	0.5	57	100	32	6.6	1.6	1.3	4.2	0.82	29.55
N11	0.5	38	61	27	4.9	1.1	0.25	3.5	0.69	29.17
N12	2	45	77	30	5.5	1.3	0.8	3.6	0.63	27.16
N13	0.5	39	61	28	5	1.2	1	4	0.72	31.76
N14	0.5	37	47	13	3.2	0.9	0.25	2.8	0.5	26.1
P1	0.5	53	94	43	7.5	2	1	4.8	0.69	23.16
P2	0.5	36	58	25	3.6	1	0.25	3.4	0.55	23.61
P3	0.5	58	94	39	5.6	1.4	0.25	4.2	0.66	26.19
P4	0.5	38	62	26	4.2	1.2	0.7	4	0.65	23.96
P5	0.5	36	58	27	4.3	1.3	0.8	4.4	0.69	30.85
P6	3	39	64	25	4.2	1.3	0.8	4.4	0.69	25.75
P7	0.5	37	62	25	4.2	1.2	0.9	4	0.65	28.34
P8	0.5	33	56	25	4.1	1.2	0.9	3.6	0.57	33.44
P9	0.5	42	79	28	4.7	1.3	0.25	4.1	0.63	24.92
P10	0.5	45	87	29	5.7	1.7	0.25	4.7	0.71	28.38
P11	0.5	40	69	30	4.8	1.3	0.25	4.2	0.6	33.1
P12	0.5	37	82	28	4.5	1.2	0.25	4	0.63	25.3
P13	0.5	33	52	21	3.5	1.1	0.25	3.7	0.57	27.33
P14	0.5	35	77	29	6.2	2	1.2	5	0.73	27.7
Q1	0.5	37	61	23	4.2	1.1	0.9	3.7	0.55	28.33
Q2	0.5	36	57	24	3.9	1	0.9	3.6	0.56	24.15
Q3	0.5	39	61	32	4.2	1.3	0.6	4	0.62	26.31
Q4	0.5	35	54	21	4.1	1.2	0.25	4	0.59	28.53
Q5	0.5	40	63	29	4.6	1.3	0.9	4.3	0.69	24.28
Q6	0.5	44	70	27	4.4	1.2	0.9	4.1	0.62	24.88
Q7	0.5	39	62	30	4.5	1.4	0.9	4.3	0.67	27.7
Q8	0.5	41	92	27	5.4	1.6	1.2	4.1	0.64	28.06

APPENDIX V: Part A-Geochemical Analysis (INAA DATA)

Sample Site	W (ppm)	La (ppm)	Ce (ppm)	Nd (ppm)	Sm (ppm)	Eu (ppm)	Tb (ppm)	Yb (ppm)	Lu (ppm)	Mass (g)
Q9	0.5	36	100	15	4.8	1.6	0.25	3.7	0.53	25.53
Q10	0.5	37	68	28	4.5	1.3	0.25	4.3	0.64	29.92
Q11	0.5	49	85	33	5.2	1.5	0.9	4.7	0.76	26.36
Q12	0.5	40	65	31	4.7	1.4	1	4.3	0.68	27.62
Q13	0.5	20	37	22	3.7	1.3	0.25	3.3	0.53	31.02
Q14	0.5	24	43	26	3.2	1.2	0.25	2.7	0.43	27.52
R1	0.5	48	76	39	7.1	2.1	1.6	4.7	0.69	29.22
R2	3	37	64	19	4	1.2	0.25	3.6	0.53	24.14
R3	4	42	70	34	5.1	1.5	0.9	5	0.73	27.5
R4	0.5	40	65	22	4.5	1.4	0.9	4.5	0.71	28.72
R5	0.5	36	63	20	4.3	1.3	0.25	4.7	0.65	27.91
R6	0.5	41	69	27	4.6	1.4	0.25	4.6	0.68	26.47
R7	0.5	52	84	43	6.9	2.1	1.2	5.2	0.76	28.78
R8	1	37	70	31	4.6	1.4	0.9	4.4	0.66	31.59
R9	0.5	46	84	40	7.1	2.2	1.2	4.9	0.74	29.75
R10	0.5	36	79	21	4.3	1.4	0.7	4	0.62	30.22
R11	0.5	40	70	35	4.8	1.5	0.25	4.6	0.64	28.05
R12	0.5	47	83	45	6.3	1.9	1.6	4.9	0.73	27.63
R13	0.5	40	69	28	4.6	1.4	1.6	4.2	0.72	27.4
R14	5	28	50	22	3.4	1	0.25	3.1	0.51	23.41
S1	0.5	48	100	36	6	1.7	0.25	4.6	0.68	27.96
S2	0.5	33	55	23	3.8	1.1	0.6	4.1	0.68	26.56
S3	0.5	39	64	30	4.7	1.4	1.1	4.3	0.65	25.16
S4	0.5	41	70	29	4.7	1.2	1	4.3	0.62	23.55
S5	0.5	38	65	30	4.4	1.3	0.25	4	0.58	24.73
S6	0.5	37	66	26	4.2	1.3	0.9	4.2	0.67	24.43
S7	0.5	40	66	31	4.6	1.4	0.25	4.6	0.68	29.2
S8	0.5	52	100	45	7.4	2.3	1.4	4.3	0.63	26.46
S9	0.5	44	88	32	5.1	1.5	0.8	4.5	0.65	28.22
S10	0.5	39	67	27	4.5	1.3	0.9	4.4	0.64	25.38
S11	0.5	44	80	30	5.1	1.5	0.25	4.1	0.67	23.31
S12	0.5	32	71	25	4.1	1.1	0.8	3.7	0.56	27.8
S13	0.5	31	56	21	3.6	1.2	0.6	3.4	0.55	27.71
S14	0.5	27	54	20	3.8	1.3	0.25	3.1	0.46	27.51
T1	0.5	44	75	34	4.3	1.2	0.25	3.3	0.55	26.38
T2	3	36	58	23	3.7	1.1	0.5	3.7	0.57	25.95
T3	0.5	35	56	21	3.7	1.1	1.2	4.1	0.57	26.13
T4	0.5	44	74	34	5.3	1.6	1.1	4.5	0.68	26.78
T5	0.5	40	64	27	4.3	1.3	0.9	4	0.58	24.76
T6	2	43	79	27	5.3	1.3	0.9	4.8	0.73	24.94
T7	0.5	42	71	24	4.9	1.3	1.1	4.2	0.62	21.68
T8	0.5	34	63	22	4.3	1	0.8	3.8	0.6	27.96
T9	0.5	33	61	22	4.2	1.2	0.8	3.5	0.56	29.99
T10	0.5	41	69	26	5	1.2	0.8	4.4	0.66	26.88
T11	2	34	72	19	4.2	1	0.7	3.8	0.56	21.22

APPENDIX V: Part A-Geochemical Analysis (INAA DATA)

Sample Site	W (ppm)	La (ppm)	Ce (ppm)	Nd (ppm)	Sm (ppm)	Eu (ppm)	Tb (ppm)	Yb (ppm)	Lu (ppm)	Mass (g)
T12	0.5	38	66	25	5	1.2	0.7	3.9	0.64	26.64
T13	0.5	28	50	17	3.7	0.9	0.25	1.9	0.26	17.16
T14	0.5	28	54	15	4	1.1	0.25	3.6	0.55	22.44
V1	0.5	40	69	26	4.6	1.1	0.7	4.3	0.63	26.6
V2	0.5	38	65	22	5	1.2	0.7	4.4	0.62	26.46
V3	4	36	62	20	4.2	1.1	0.25	4.4	0.64	26.15
V4	0.5	40	72	25	5.1	1.2	0.8	4.6	0.7	29.87
V5	0.5	40	73	29	6	1.5	1	5	0.75	27.18
V6	0.5	43	76	26	5	1.3	1	4.8	0.7	25.13
V7	2	42	76	20	5	1.2	0.25	4.6	0.7	22.87
V8	0.5	53	110	31	6.6	1.7	0.9	3.9	0.6	23.98
V9	0.5	35	79	24	4.4	1.1	0.7	3.5	0.55	27.6
V10	4	44	85	26	5.4	1.4	0.9	4.5	0.67	27.33
V11	0.5	27	60	16	3.4	0.9	0.25	3.5	0.47	23.91
V12	0.5	23	46	16	3.4	1	0.25	2.9	0.45	26.61
V13	0.5	28	67	23	3.8	1.4	0.25	3.6	0.55	26.1
V14	0.5	29	60	23	3.7	1.4	0.25	3.3	0.55	24.2
W1	0.5	39	72	24	4.5	1.4	0.9	3.9	0.69	28.87
W2	0.5	43	77	34	5.6	1.7	1.1	4.7	0.67	26.85
W3	0.5	40	76	32	4.7	1.4	0.25	4.4	0.71	23.69
W4	0.5	37	68	25	4.1	1.2	0.25	4	0.64	23.6
W5	0.5	39	73	30	4.7	1.5	0.25	4.9	0.68	27.37
W6	0.5	40	75	36	4.8	1.5	1.3	4.4	0.7	26.41
W7	0.5	33	63	24	4	1.3	0.25	3.7	0.61	26.15
W8	0.5	35	68	29	4.5	1.5	0.25	4	0.61	26.27
W9	0.5	38	78	28	4.9	1.5	1.1	4.4	0.73	29.75
W10	0.5	34	70	28	4.6	1.5	0.25	4.4	0.73	26.72
W11	0.5	33	68	27	4.2	1.4	0.25	3.9	0.66	28.34
W12	0.5	36	73	32	5.3	1.9	0.25	4.5	0.7	26.92
W13	0.5	36	72	24	4.3	1.4	0.9	4.4	0.72	27.83
W14	0.5	27	53	20	3.7	1.4	0.25	3.5	0.55	29.69
X1	0.5	36	68	21	4.6	1.5	1.3	4.9	0.72	28.02
X2	0.5	38	71	27	4.4	1.4	0.8	4.2	0.68	24.43
X3	0.5	38	69	28	4.2	1.3	1	4.3	0.7	24.53
X4	0.5	40	73	26	4.2	1.4	0.8	4.2	0.66	25.64
X5	0.5	37	67	25	4.3	1.4	0.25	4.2	0.61	26.54
X6	0.5	40	74	29	4.8	1.6	0.25	4.9	0.77	29.25
X7	0.5	34	62	25	4.3	1.4	0.25	3.9	0.6	24.39
X8	0.5	39	75	28	4.9	1.5	0.25	4.3	0.72	27.12
X9	0.5	34	68	25	4.4	1.4	0.25	4.3	0.67	27.51
X10	0.5	34	86	26	5.2	1.8	1.2	4.2	0.64	26.91
X11	0.5	27	56	22	3.9	1.4	0.25	3.5	0.6	24.89
X12	0.5	30	65	25	3.9	1.3	0.25	3.6	0.59	30.24
X13	0.5	36	82	29	4.4	1.5	0.25	3.9	0.61	28.6
X14	0.5	18	37	20	3.5	1.2	0.25	2.6	0.46	19.14

APPENDIX V

PART B–GEOCHEMICAL CONTOUR MAPS

The geochemical data was contoured using Surfer® 6.01 computer software in a similar manner as the lithological data. A linear isotropic variogram model was used to interpolate grid nodes for geochemical contouring. Kriging, a geostatistical gridding method, was employed to generate geochemical contour maps from the grid nodes for selected elements in the study area. The median value and standard deviation of the contour datum presented on each figure was calculated using Microsoft® Excel 97.

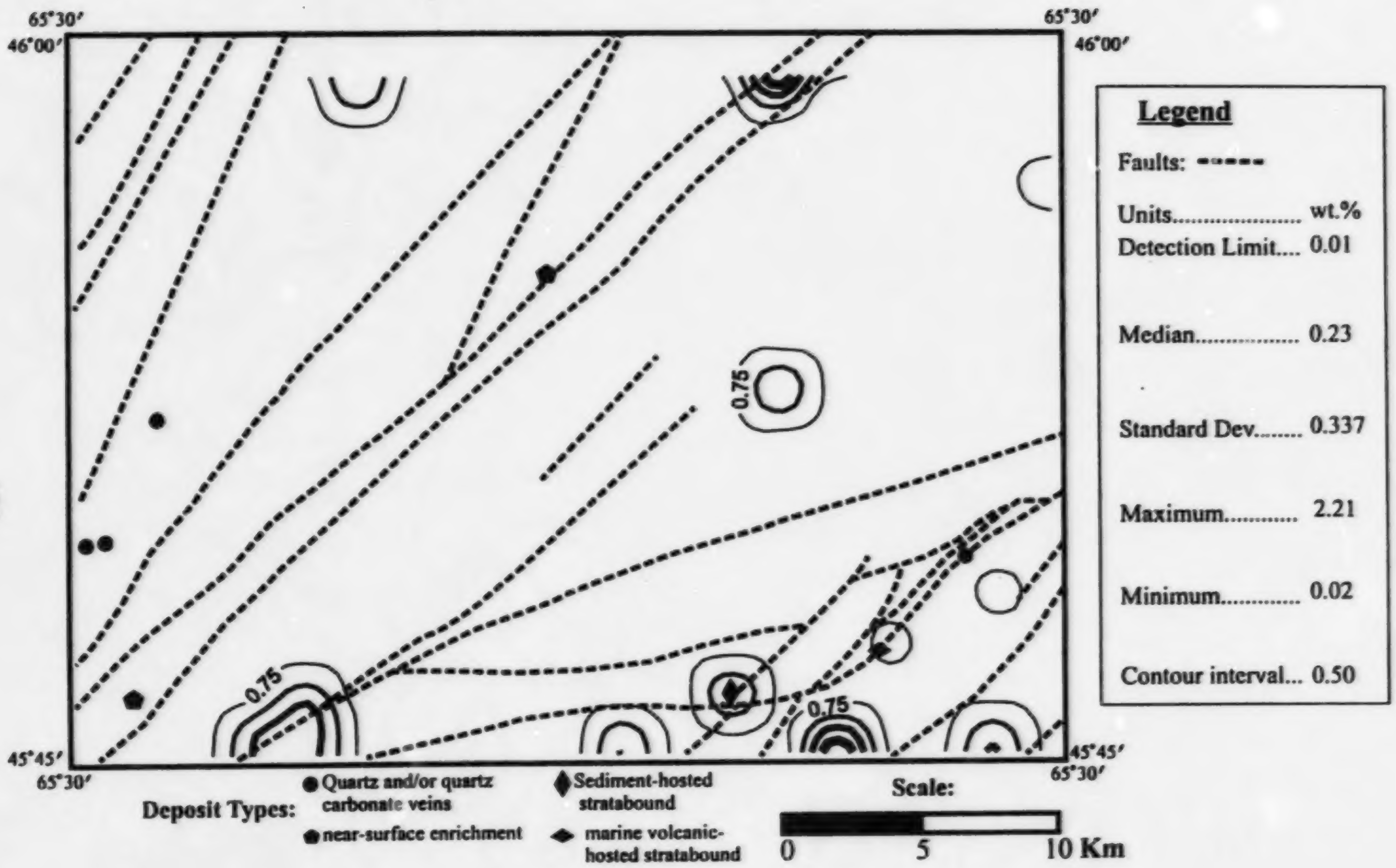

Appendix V: Figure 1: Contouring of calcium concentrations in the till matrix.

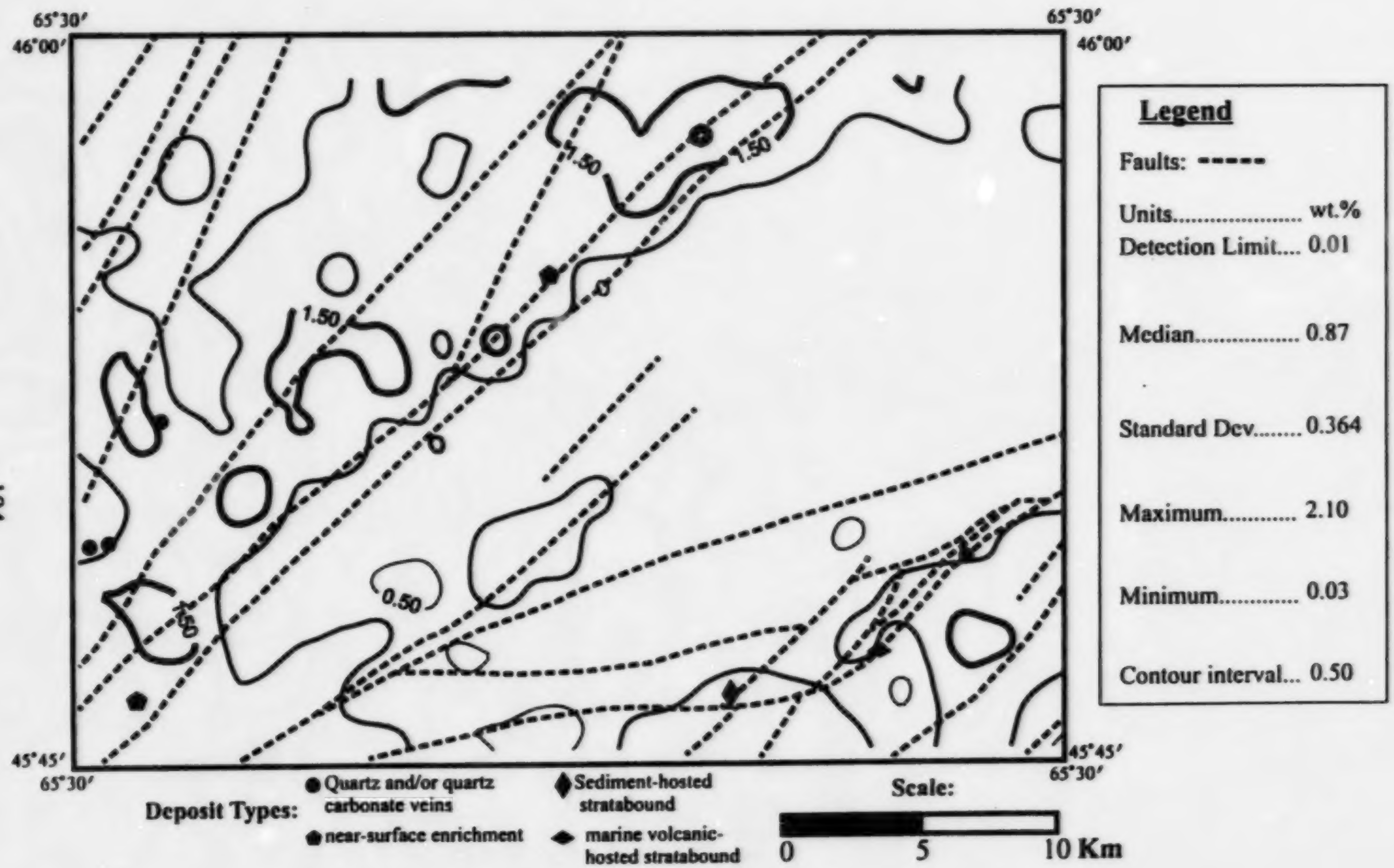

Appendix V: Figure 2: Contouring of magnesium concentrations in the till matrix.

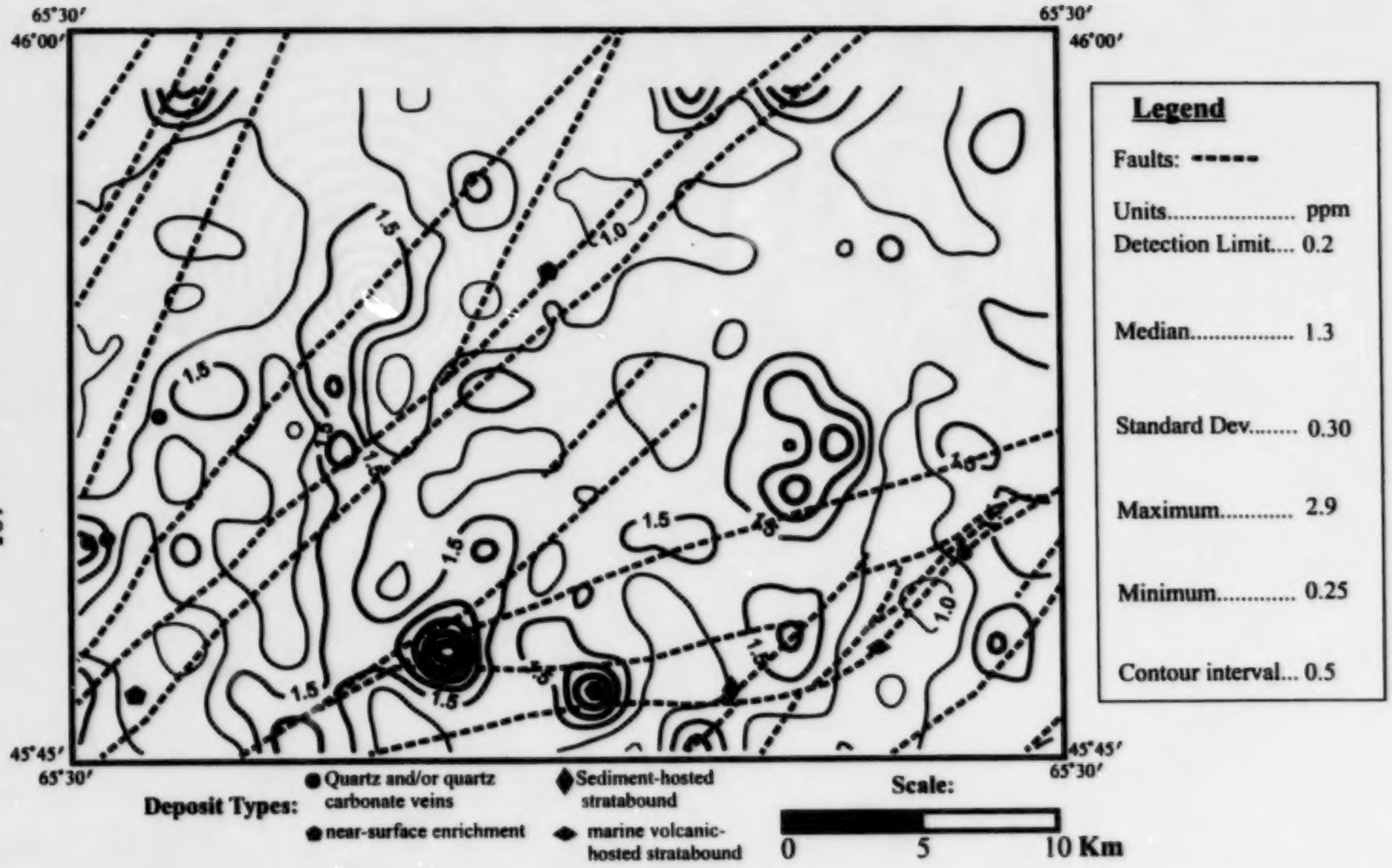

Appendix V: Figure 3: Contouring of europium concentrations in the till matrix.

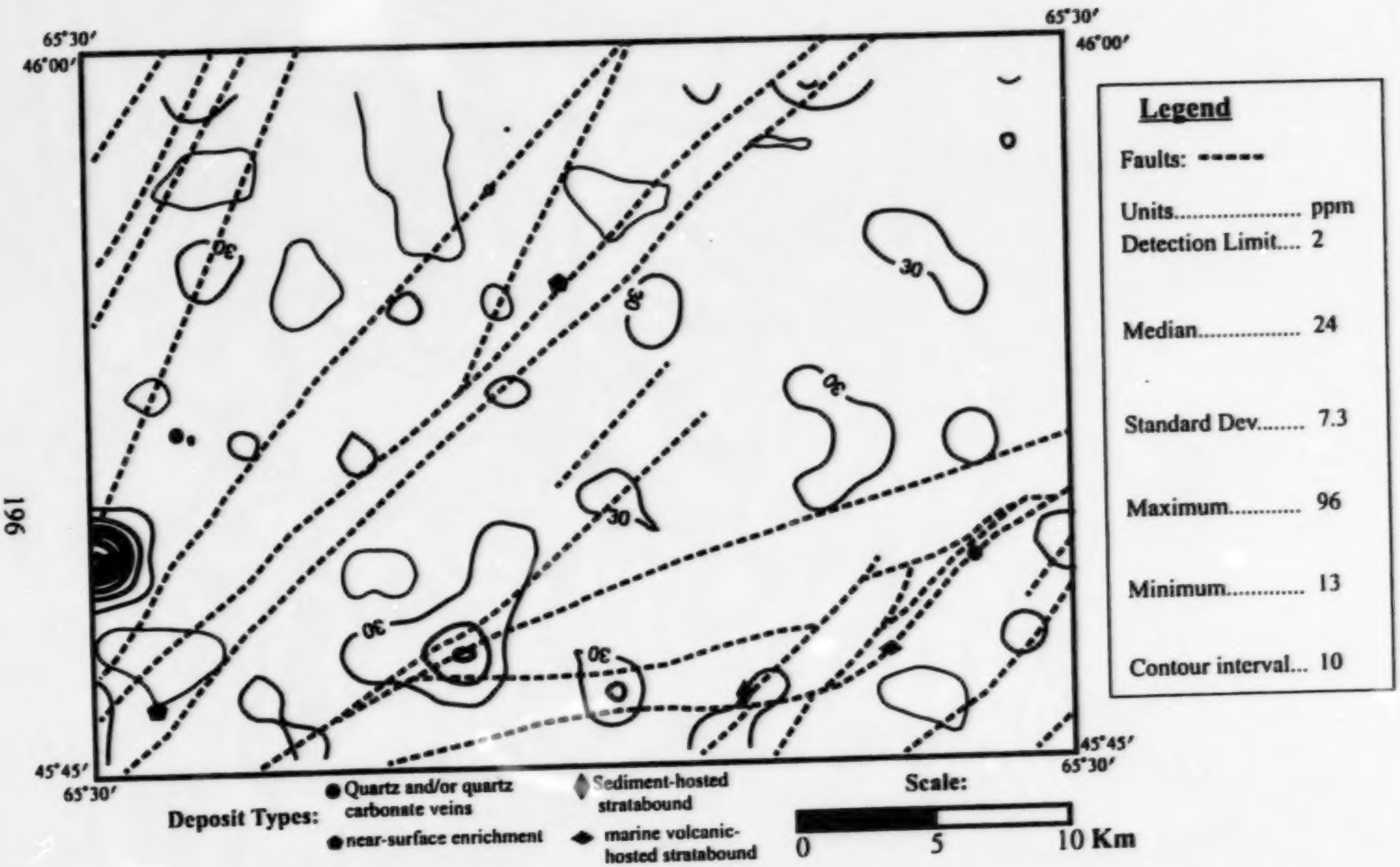

Appendix V: Figure 4: Contouring of yttrium concentrations in the till matrix.

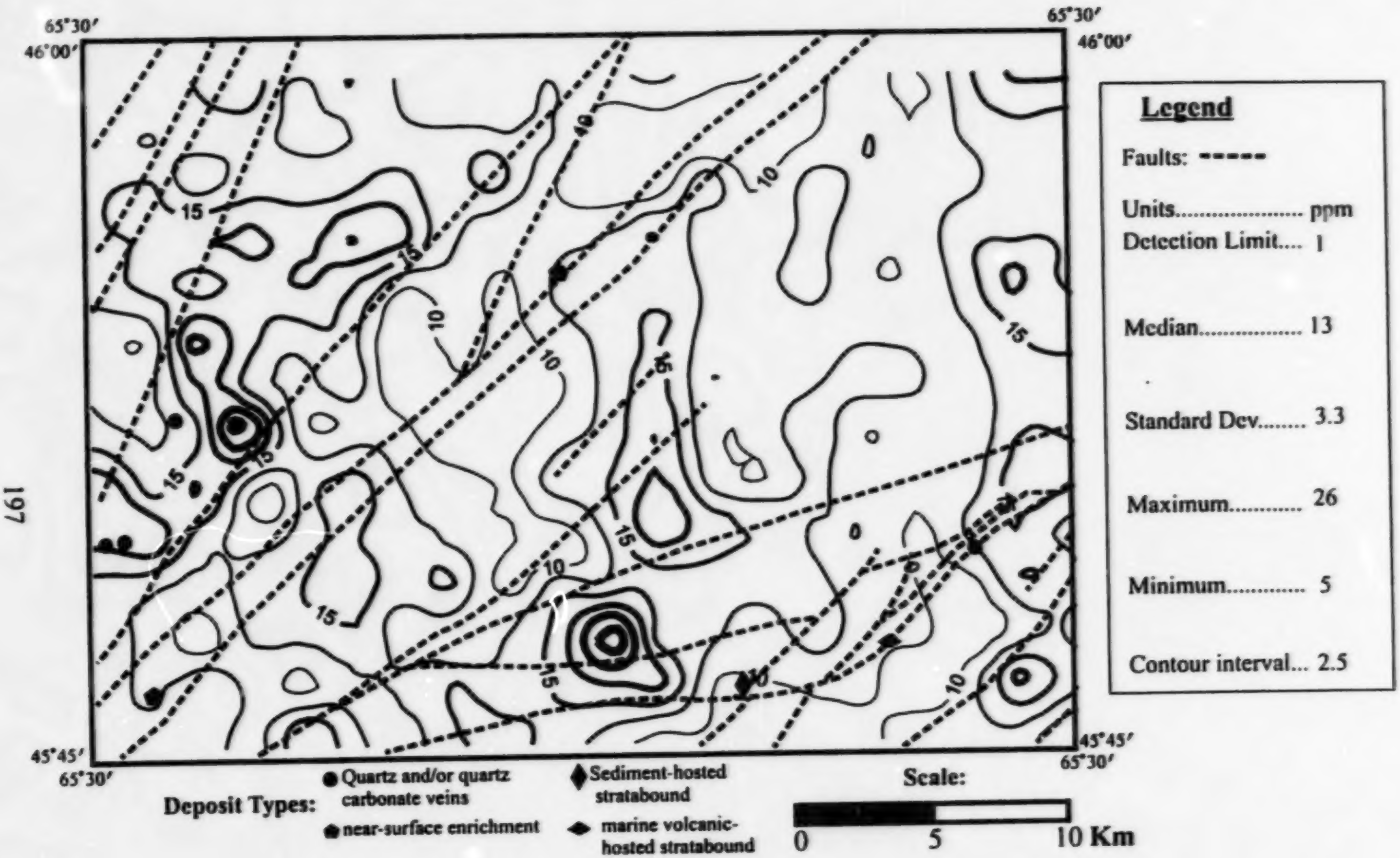

Appendix V: Figure 5: Contouring of hafnium concentrations in the till matrix.

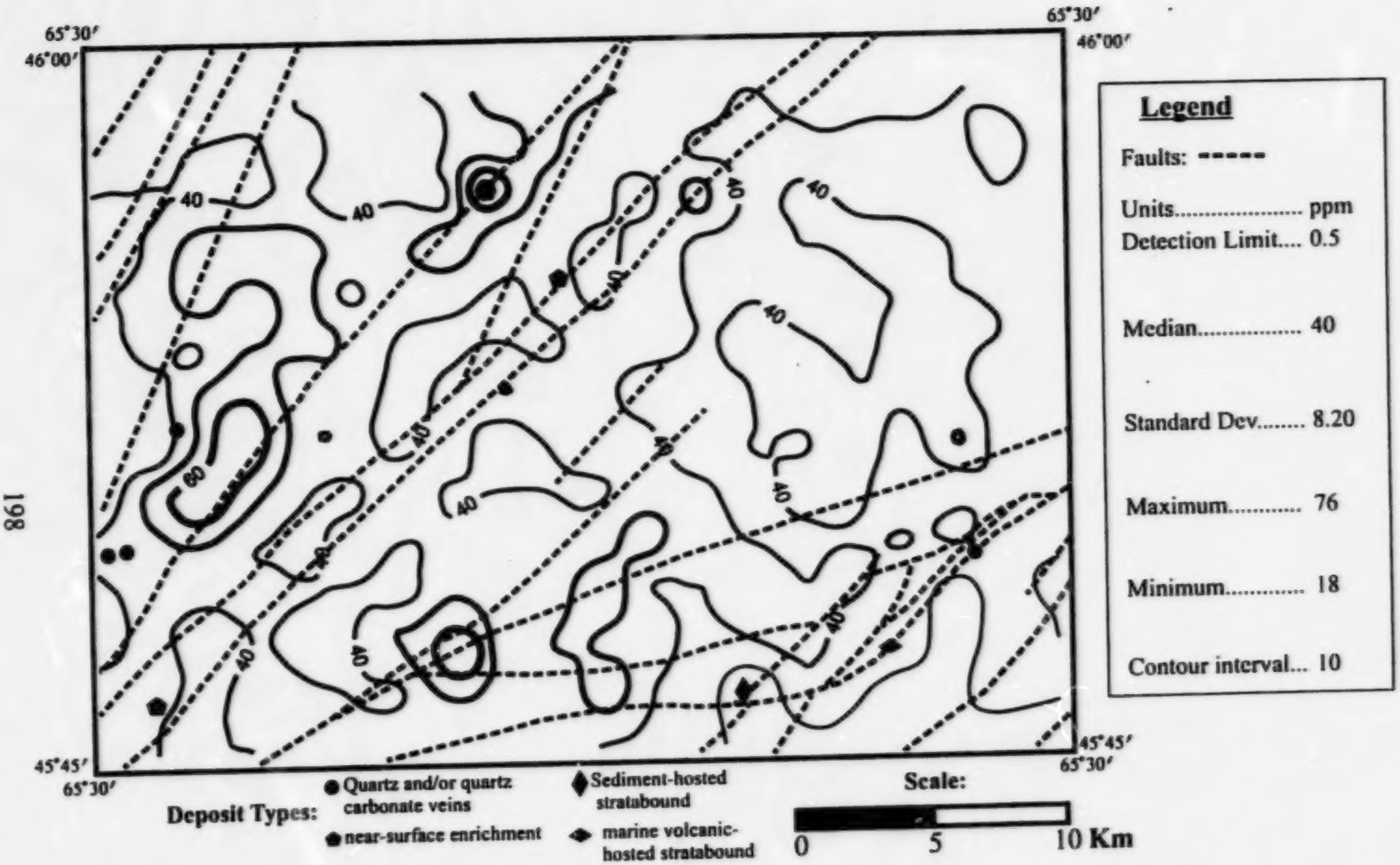

Appendix V: Figure 6: Contouring of lanthanum concentrations in the till matrix.

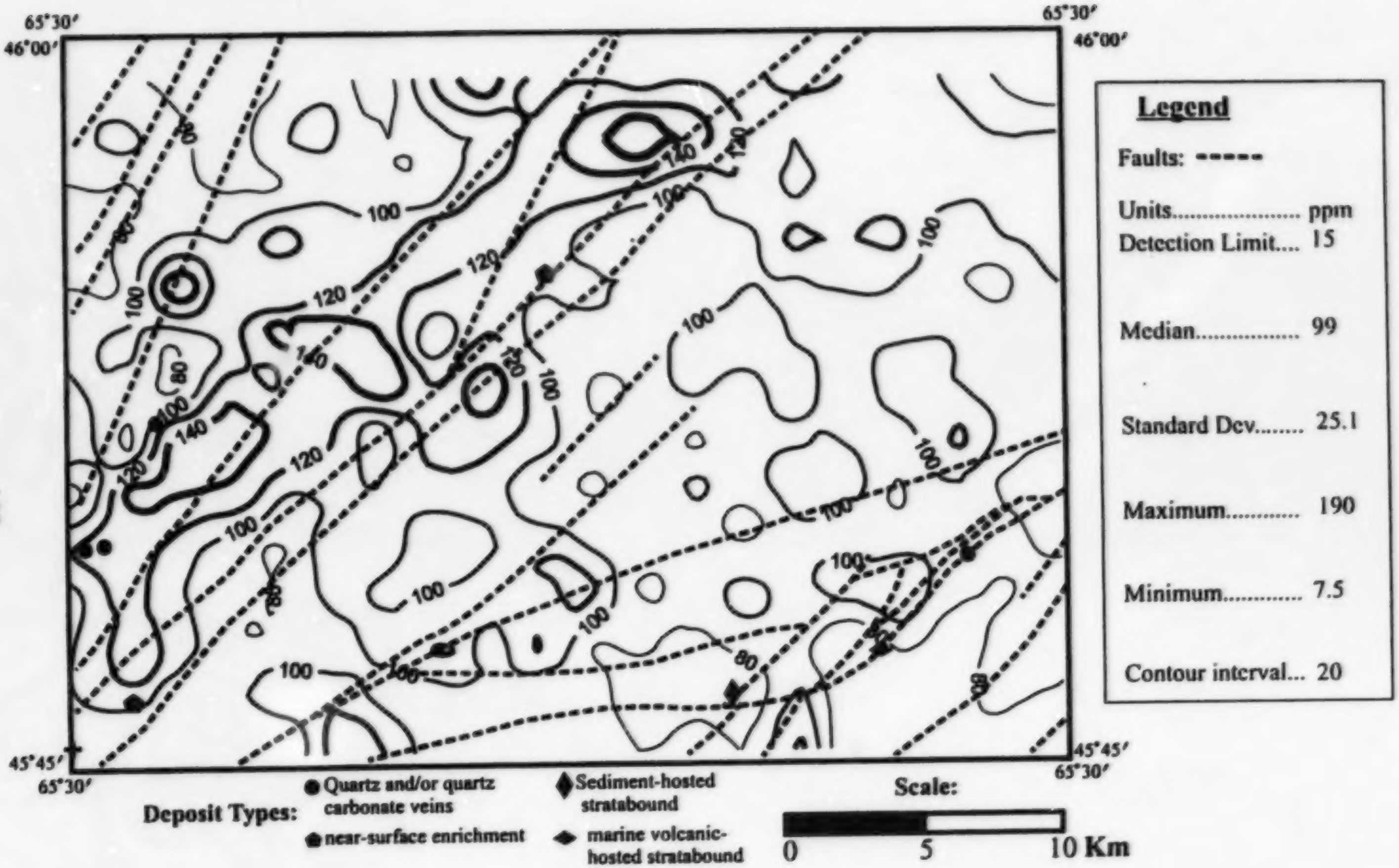

Appendix V: Figure 7: Contouring of rubidium concentrations in the till matrix.

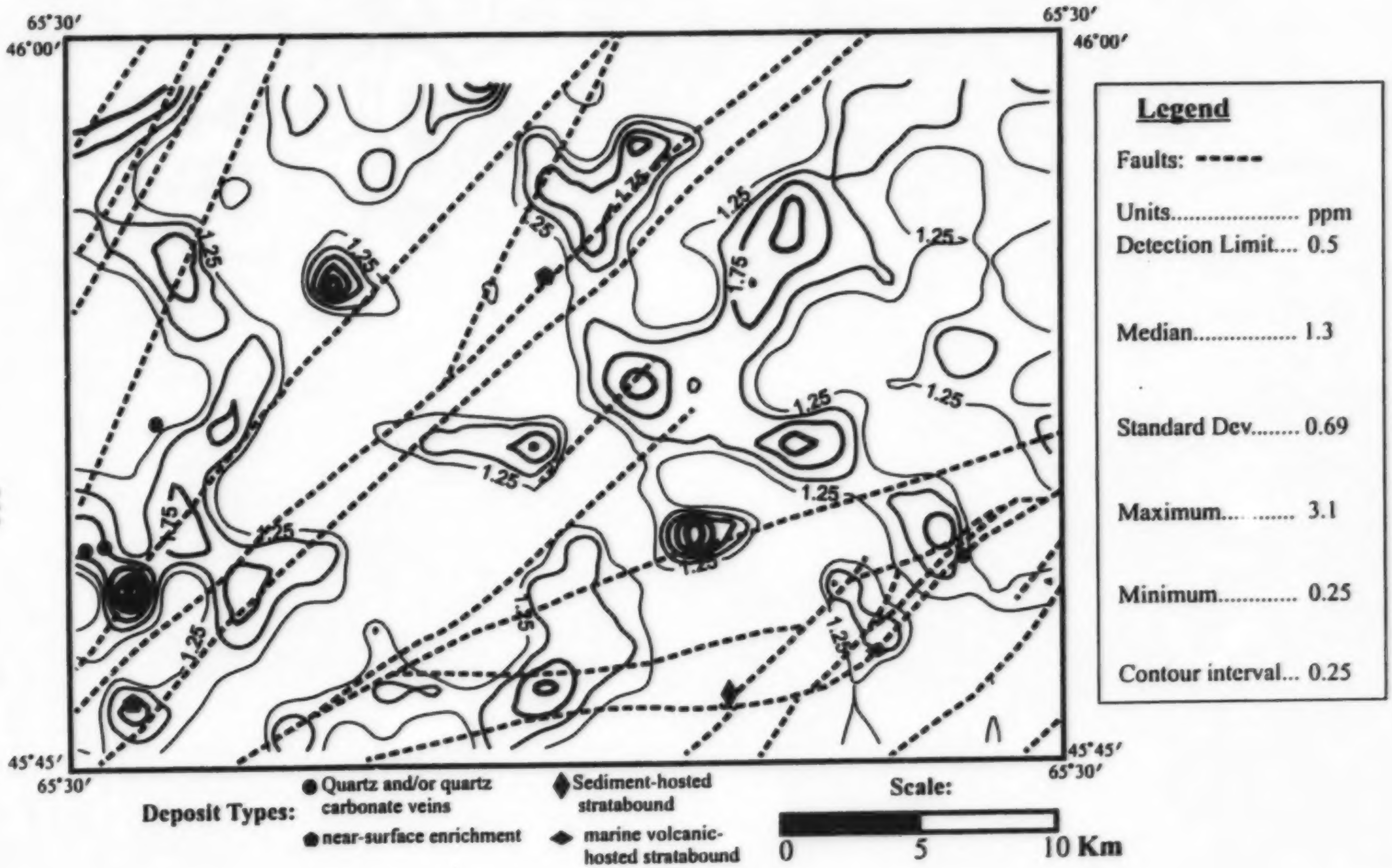

Appendix V: Figure 8: Contouring of tantalum concentrations in the till matrix.

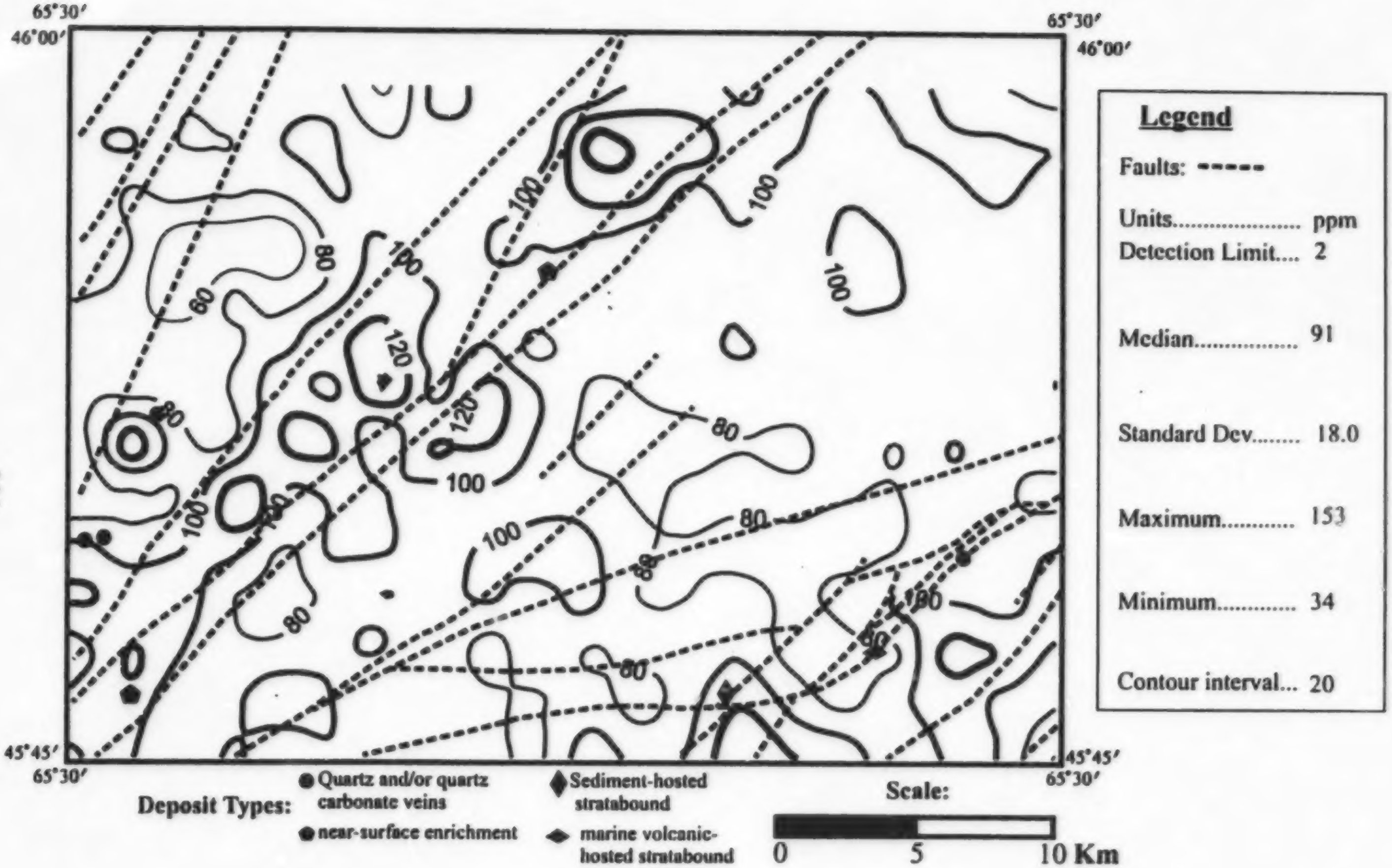

Appendix V: Figure 9: Contouring of vanadium concentrations in the till matrix.

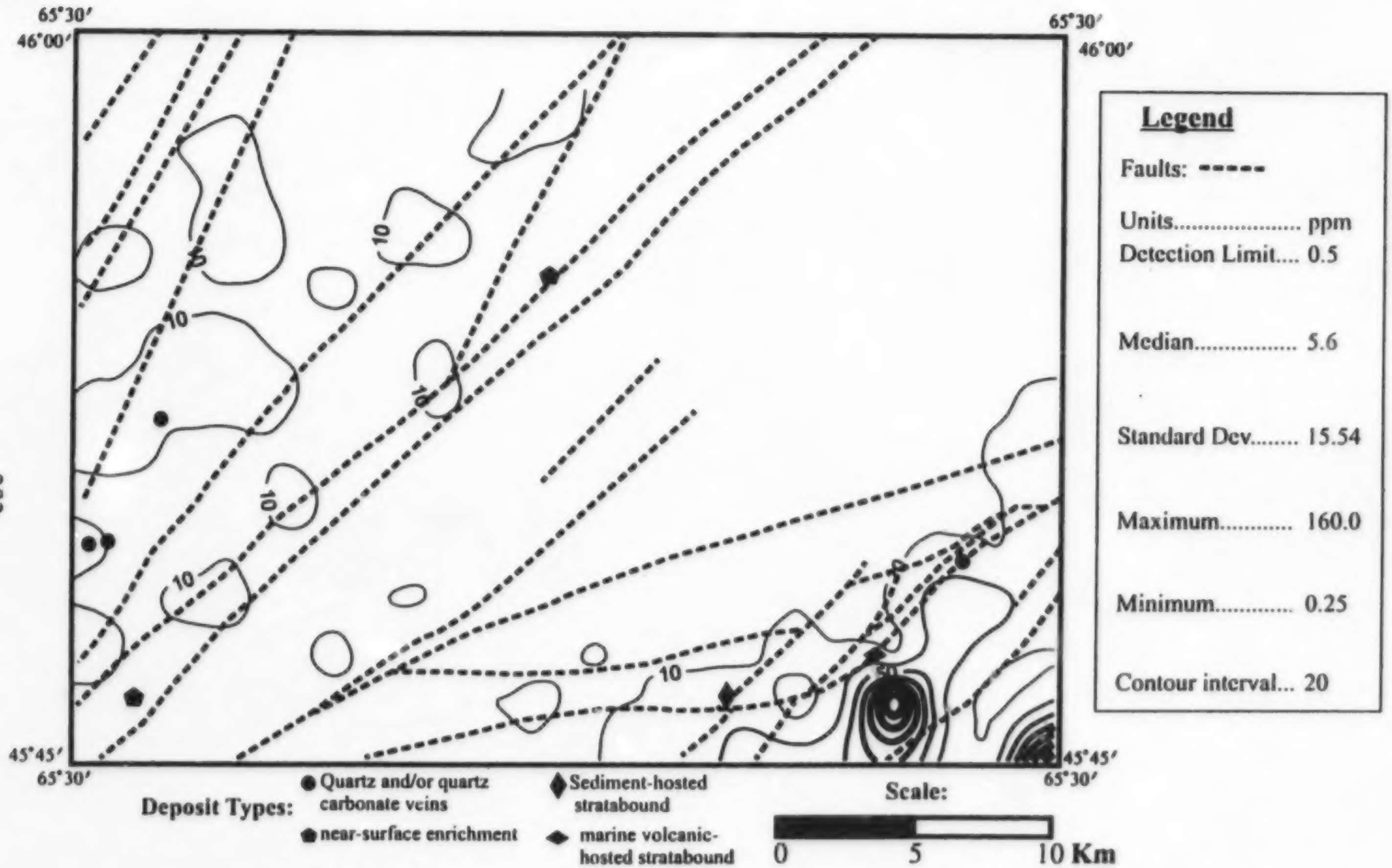

Appendix V: Figure 10: Contouring of bromine concentrations in the till matrix.

APPENDIX VI

STATISTICS

The median value and standard deviation each datum set in the geochemistry and lithological data were calculated using Microsoft® Excel 97. Median values for each element were used to define their regional background concentrations in the till matrix (Table VI-a). Geochemical anomalies were assigned threshold values outside two standard deviations from the population median concentrations.

Spearman's rank correlation analysis for selected site characteristics, granulometric, lithological, and geochemical data is presented in Table VI-b. For each comparison, the Spearman's rank correlation coefficient (r) is followed by its corresponding 2–tailed significance level (α). The significance levels 0.01 and 0.05 of the correlations is denoted in the table by (**) and (*), respectively.

APPENDIX VI: STATISTICS

Table VI-a: Elemental Background Concentrations in Till Matrix

Instrumental Neutron Activation Analysis (INAA)						
Element	Units	Detection Limit	Median	Standard Deviation	Max.	Min.
As	ppm	0.5	12.0	16.21	230.0	4.5
Au	ppb	2	1	1.5	7	1
Ba	ppm	50	350	80.4	660	130
Br	ppm	0.5	5.6	15.54	160.0	B.D.L.
Co	ppm	1	12	3.0	29	B.D.L.
Cr	ppm	5	78	13.1	120	22
Cs	ppm	1	5	3.8	52	B.D.L.
Fe	wt.%	0.01	3.88	0.559	5.46	2.25
Hf	ppm	1	13	3.3	26	5
Ir	ppb	5	3	0.0	3	3
Mo	ppm	1	1	2.1	9	0.5
Na	wt.%	0.01	0.78	0.381	2.07	0.08
Rb	ppm	15	99	25.1	190	B.D.L.
Sb	ppm	0.1	1.1	0.57	3.3	0.5
Sc	ppm	0.1	13.0	2.17	21.0	8.8
Se	ppm	3	2	0.6	7	2
Sn	wt.%	0.01	0.01	0.009	0.01	B.D.L.
Ta	ppm	0.5	1.3	0.69	3.1	0.25
Th	ppm	0.2	11.0	2.12	22.0	6.3
U	ppm	0.5	2.7	0.61	5.6	1.5
W	ppm	1	0.5	0.80	5	0.5
La	ppm	0.5	40	8.20	76	18
Ce	ppm	3	73	15.7	140	35
Nd	ppm	5	27	6.3	50	8
Sm	ppm	0.1	4.9	1.21	11	2
Eu	ppm	0.2	1.3	0.30	2.9	0.7
Tb	ppm	0.5	0.8	0.42	2.4	0.25
Yb	ppm	0.2	4.1	0.72	8.5	1.9
Lu	ppm	0.05	0.67	0.113	1.24	0.26

**Notes:* 1) The median concentration for each element was assumed to represent its background concentration.
2) "B.D.L." denotes values below detection limit.

APPENDIX VI: STATISTICS

Table VI-a: Elemental Background Concentrations in Till Matrix

Inducively Coupled Plasma Emission Spectrometry (ICP-ES)						
Element	Units	Detection Limit	Median	Standard Deviation	Max.	Min.
Cu	ppm	1	22	8.2	92	6
Pb	ppm	4	19	5.9	48	6
Zn	ppm	1	78	16.7	155	39
Ag	ppm	0.4	0.2	0.62	9.9	0.2
Ni	ppm	1	35	8.3	79	11
Mn	ppm	1	484	245.3	2370	169
Sr	ppm	1	67	26.9	218	25
Cd	ppm	0.5	B.D.L.	0.1	0.8	B.D.L.
Bi	ppm	5	3	6.9	116	2.5
V	ppm	2	91	18.0	153	34
Ca	wt.%	0.01	0.23	0.337	2.21	0.02
P	wt.%	0.001	0.039	0.0298	0.197	0.014
Mg	wt.%	0.01	0.87	0.364	2.10	0.30
Ti	wt.%	0.01	0.46	0.057	0.74	0.22
Al	wt.%	0.01	7.48	0.884	10.43	5.40
K	wt.%	0.01	1.81	0.450	3.67	0.43
Y	ppm	2	24	7.3	98	13
Be	ppm	2	1	0.3	2	B.D.L.
Hg (ICP-CV)	ppb	5	32	25.6	258	7

*Notes: 1) The median concentration for each element was assumed to represent its background concentration.
2) ICP-CV refers to ICP cold vapour FIMS.
3) "B.D.L." denotes values below detection limit.

APPENDIX VI: STATISTICS

Table VI-b: Spearman Correlation Coefficients for Selected Trace Element, Lithological, Site Characteristic, and Granulometic Data (N=20)

		Ni	Cu	Pb	Zn	Fe	Au	As	Hg	As
Ni	r	1	.501(**)	0.003	.493(**)	.483(**)	0.065	.287(**)	-.124(*)	0.009
	α		0	0.959	0	0	0.291	0	0.042	0.888
Cu	r		1	.134(*)	.313(**)	.432(**)	0.069	-0.002	-.376(**)	0.076
	α			0.028	0	0	0.261	0.975	0	0.21
Pb	r			1	.331(**)	.202(**)	0.077	.276(**)	0.035	0.029
	α				0	0.001	0.21	0	0.569	0.638
Zn	r				1	.494(**)	0.04	.266(**)	-0.032	-0.055
	α					0	0.513	0	0.601	0.37
Fe	r					1	.132(*)	.344(**)	-0.023	-0.038
	α						0.03	0	0.701	0.536
Au	r						1	.122(*)	-0.017	0.002
	α							0.046	0.779	0.968
As	r							1	.158(**)	0.042
	α								0.009	0.49
Hg	r								1	-0.076
	α									0.212
Ag	r									1
	α									
Ca	r									
	α									
Mg	r									
	α									
K	r									
	α									
Na	r									
	α									
Al	r									
	α									
Ti	r									
	α									
Mn	r									
	α									
Ba	r									
	α									
Cr	r									
	α									
Th	r									
	α									
U	r									
	α									
Ce	r									
	α									
Nd	r									
	α									
Eu	r									
	α									
Tb	r									
	α									
Yb	r									
	α									
Lu	r									
	α									

APPENDIX VI: STATISTICS

Table VI-b: Spearman Correlation Coefficients for Selected Trace Element, Lithological, Site Characteristic, and Granulometic Data (N=20)

		Ca	Mg	K	Na	Al	Ti	Mn	Ba	Cr
Ni	r	-.147(*)	.323(**)	.330(**)	-0.039	.367(**)	0.042	.248(**)	.301(**)	.575(**)
	α	0.016	0	0	0.52	0	0.49	0	0	0
Cu	r	.223(**)	.491(**)	0.102	0.004	.134(*)	.275(**)	.394(**)	0.11	.430(**)
	α	0	0	0.096	0.952	0.028	0	0	0.07	0
Pb	r	.187(**)	.269(**)	.215(**)	.172(**)	.264(**)	0.019	.271(**)	.153(*)	0.011
	α	0.002	0	0	0.005	0	0.754	0	0.012	0.854
Zn	r	0.038	.506(**)	.383(**)	.122(*)	.498(**)	.203(**)	.244(**)	.243(**)	.270(**)
	α	0.531	0	0	0.045	0	0.001	0	0	0
Fe	r	0.002	.464(**)	.329(**)	0.001	.608(**)	.127(*)	.401(**)	.261(**)	.424(**)
	α	0.971	0	0	0.986	0	0.037	0	0	0
Au	r	0.064	.125(*)	.119(*)	.184(**)	0.037	-0.001	0.039	.196(**)	0.07
	α	0.292	0.039	0.05	0.002	0.541	0.986	0.526	0.001	0.251
As	r	-0.103	.336(**)	.479(**)	.359(**)	.317(**)	-0.085	.286(**)	.389(**)	0.088
	α	0.09	0	0	0	0	0.162	0	0	0.148
Hg	r	0.051	-.210(**)	-.323(**)	.203(**)	0.058	-.239(**)	-0.09	-.152(*)	-.165(**)
	α	0.408	0.001	0	0.001	0.345	0	0.142	0.013	0.006
Ag	r	-0.017	-0.068	-0.03	-0.077	-0.101	0.036	0.001	-0.014	-0.02
	α	0.778	0.264	0.626	0.208	0.097	0.552	0.99	0.822	0.745
Ca	r	1	.357(**)	-.235(**)	.487(**)	-0.036	.141(*)	.245(**)	0.046	-0.012
	α		0	0	0	0.558	0.02	0	0.45	0.847
Mg	r		1	.431(**)	.442(**)	.500(**)	.242(**)	.337(**)	.269(**)	.304(**)
	α			0	0	0	0	0	0	0
K	r			1	.140(*)	.530(**)	.150(*)	.286(**)	.513(**)	.163(**)
	α				0.022	0	0.013	0	0	0.007
Na	r				1	0.086	0.069	0.099	.250(**)	0.033
	α					0.161	0.262	0.105	0	0.594
Al	r					1	0.041	.226(**)	.318(**)	.218(**)
	α						0.505	0	0	0
Ti	r						1	.268(**)	0.061	0.063
	α							0	0.318	0.303
Mn	r							1	.254(**)	0.032
	α								0	0.602
Ba	r								1	.149(*)
	α									0.014
Cr	r									1
	α									
Th	r									
	α									
U	r									
	α									
Ce	r									
	α									
Nd	r									
	α									
Eu	r									
	α									
Tb	r									
	α									
Yb	r									
	α									
Lu	r									
	α									

APPENDIX VI: STATISTICS

Table VI-b: Spearman Correlation Coefficients for Selected Trace Element, Lithological, Site Characteristic, and Granulometic Data (N=20)

		Th	U	Ce	Nd	Eu	Tb	Yb	Lu	Sm
Ni	r	0.015	0.119	-0.021	.139(*)	0.081	0.022	-0.03	-0.081	0.068
	α	0.811	0.051	0.731	0.023	0.187	0.717	0.62	0.185	0.263
Cu	r	-0.106	0.05	-.138(*)	0.005	0.092	-0.048	-0.002	-0.015	-0.053
	α	0.082	0.414	0.023	0.933	0.133	0.428	0.97	0.804	0.382
Pb	r	.233(**)	.190(**)	.210(**)	.183(**)	0.101	0.013	0.049	0.044	0.111
	α	0	0.002	0.001	0.003	0.097	0.835	0.423	0.47	0.07
Zn	r	0.024	0.05	-0.038	0.096	-0.062	-0.073	-0.011	-0.016	0.003
	α	0.697	0.409	0.536	0.115	0.309	0.23	0.861	0.789	0.962
Fe	r	.161(**)	0.093	0.06	.138(*)	.157(**)	-0.086	-0.095	-0.082	0.024
	α	0.008	0.128	0.328	0.023	0.01	0.158	0.12	0.178	0.691
Au	r	0.09	0.086	.128(*)	0.066	.208(**)	0.047	0.064	0.065	0.08
	α	0.139	0.16	0.035	0.277	0.001	0.44	0.297	0.284	0.19
As	r	.421(**)	.223(**)	.354(**)	.285(**)	0.04	.156(*)	-0.062	0.096	.322(**)
	α	0	0	0	0	0.511	0.01	0.313	0.115	0
Hg	r	-0.039	-.121(*)	-0.065	-.151(*)	-0.062	-0.104	-.248(**)	-.162(**)	-.123(*)
	α	0.519	0.046	0.289	0.013	0.308	0.089	0	0.008	0.043
Ag	r	-0.028	.131(*)	-0.03	0.011	0.029	-0.052	-0.024	-0.061	-0.009
	α	0.646	0.031	0.621	0.859	0.636	0.393	0.697	0.316	0.878
Ca	r	-.246(**)	0.058	-.229(**)	-.190(**)	-0.014	-.120(*)	-.155(*)	-0.085	-.199(**)
	α	0	0.34	0	0.002	0.825	0.049	0.011	0.163	0.001
Mg	r	0.047	0.068	-0.013	-0.062	-.216(**)	-.210(**)	-.322(**)	-.182(**)	-.123(*)
	α	0.443	0.268	0.834	0.311	0	0.001	0	0.003	0.044
K	r	.464(**)	.209(**)	.412(**)	.301(**)	0.007	0.117	0.061	.136(*)	.352(**)
	α	0	0.001	0	0	0.912	0.055	0.316	0.025	0
Na	r	0.103	.192(**)	.139(*)	0.059	-0.032	-0.117	-.158(**)	-0.02	0.094
	α	0.092	0.002	0.022	0.337	0.602	0.055	0.009	0.738	0.122
Al	r	.241(**)	0.041	0.108	0.05	-.120(*)	-.160(**)	-.272(**)	-.274(**)	-0.042
	α	0	0.503	0.077	0.409	0.049	0.008	0	0	0.492
Ti	r	0.043	-0.017	0.063	0.104	0.045	0	0.057	0.047	0.084
	α	0.477	0.784	0.301	0.088	0.457	1	0.352	0.437	0.168
Mn	r	.233(**)	.137(*)	.269(**)	.164(**)	.272(**)	0.066	-0.002	0.049	.221(**)
	α	0	0.025	0	0.007	0	0.278	0.971	0.424	0
Ba	r	.301(**)	.173(**)	.257(**)	.247(**)	.120(*)	0.08	.197(**)	.127(*)	.282(**)
	α	0	0.004	0	0	0.05	0.191	0.001	0.037	0
Cr	r	-0.041	.238(**)	-0.066	0.073	.149(*)	-0.079	0.064	0.031	-0.056
	α	0.502	0	0.279	0.23	0.014	0.196	0.293	0.606	0.363
Th	r	1	.337(**)	.708(**)	.481(**)	.270(**)	.185(**)	.327(**)	.345(**)	.594(**)
	α		0	0	0	0	0.002	0	0	0
U	r		1	.385(**)	.286(**)	.332(**)	-0.011	.307(**)	.247(**)	.309(**)
	α			0	0	0	0.854	0	0	0
Ce	r			1	.616(**)	.510(**)	.261(**)	.485(**)	.447(**)	.789(**)
	α				0	0	0	0	0	0
Nd	r				1	.642(**)	.348(**)	.526(**)	.552(**)	.719(**)
	α					0	0	0	0	0
Eu	r					1	.316(**)	.598(**)	.495(**)	.601(**)
	α						0	0	0	0
Tb	r						1	.380(**)	.491(**)	.496(**)
	α							0	0	0
Yb	r							1	.683(**)	.602(**)
	α								0	0
Lu	r								1	.672(**)
	α									0

APPENDIX VI: STATISTICS

Table VI-b: Spearman Correlation Coefficients for Selected Trace Element, Lithological, Site Characteristic, and Granulometic Data (N=20)

		Sr	Cd	V	Y	Br	Co	Cs	Hf
Ni	r	0.106	.147(*)	.622(**)	0.114	-.223(**)	.694(**)	.310(**)	-.449(**)
	α	0.082	0.016	0	0.062	0	0	0	0
Cu	r	.271(**)	.153(*)	.667(**)	.216(**)	-.265(**)	.650(**)	.279(**)	-.384(**)
	α	0	0.012	0	0	0	0	0	0
Pb	r	.206(**)	.177(**)	0.094	.163(**)	0.093	0.102	.211(**)	0.088
	α	0.001	0.004	0.122	0.007	0.128	0.093	0	0.148
Zn	r	.206(**)	.205(**)	.494(**)	.148(*)	0.06	.489(**)	.384(**)	-.346(**)
	α	0.001	0.001	0	0.015	0.322	0	0	0
Fe	r	0.102	.149(*)	.687(**)	0.109	0.005	.678(**)	.401(**)	-.414(**)
	α	0.094	0.014	0	0.074	0.934	0	0	0
Au	r	.163(**)	0.065	0.097	0.104	-0.045	0.082	0.007	0.02
	α	0.007	0.289	0.11	0.087	0.463	0.179	0.905	0.74
As	r	0.112	.182(**)	.150(*)	-0.004	0.107	.154(*)	.426(**)	0.017
	α	0.065	0.003	0.014	0.945	0.079	0.011	0	0.784
Hg	r	0.01	0.055	-.274(**)	-.255(**)	.743(**)	-.204(**)	-.365(**)	0.11
	α	0.87	0.37	0	0	0	0.001	0	0.071
Ag	r	-0.026	0.044	0.018	0.057	-0.098	0.023	0.018	0.047
	α	0.668	0.472	0.769	0.351	0.109	0.709	0.77	0.443
Ca	r	.657(**)	.120(*)	0.075	0.075	.222(**)	0.009	-.134(*)	-0.034
	α	0	0.048	0.222	0.22	0	0.889	0.028	0.574
Mg	r	.481(**)	.203(**)	.522(**)	-0.107	0.038	.441(**)	.558(**)	-.350(**)
	α	0	0.001	0	0.08	0.529	0	0	0
K	r	0.097	0.094	.380(**)	.183(**)	-.323(**)	.227(**)	.609(**)	-.231(**)
	α	0.11	0.124	0	0.003	0	0	0	0
Na	r	.744(**)	0.105	0.041	-0.09	.298(**)	-0.076	0.07	0.046
	α	0	0.084	0.503	0.142	0	0.212	0.251	0.451
Al	r	0.112	.174(**)	.505(**)	-0.021	0.102	.361(**)	.449(**)	-.483(**)
	α	0.067	0.004	0	0.737	0.094	0	0	0
Ti	r	.181(**)	0.038	.387(**)	.232(**)	-.148(*)	.151(*)	.150(*)	-0.085
	α	0.003	0.529	0	0	0.015	0.013	0.014	0.165
Mn	r	.149(*)	.210(**)	.324(**)	.369(**)	-.129(*)	.468(**)	0.111	-.157(**)
	α	0.014	0.001	0	0	0.034	0	0.069	0.01
Ba	r	.269(**)	0.053	.269(**)	.190(**)	-.187(**)	.224(**)	.262(**)	-.256(**)
	α	0	0.383	0	0.002	0.002	0	0	0
Cr	r	.212(**)	0.113	.568(**)	0.02	-.135(*)	.489(**)	.391(**)	-.154(*)
	α	0	0.065	0	0.742	0.026	0	0	0.011
Th	r	-.125(*)	.135(*)	-0.047	.174(**)	-0.119	0.001	.307(**)	.248(**)
	α	0.04	0.026	0.446	0.004	0.052	0.985	0	0
U	r	.203(**)	0.103	0.088	.207(**)	-.143(*)	0.077	.221(**)	.254(**)
	α	0.001	0.09	0.148	0.001	0.019	0.21	0	0
Ce	r	-0.046	0.079	-0.096	.364(**)	-.164(**)	0.017	.203(**)	.289(**)
	α	0.455	0.198	0.117	0	0.007	0.777	0.001	0
Nd	r	0.012	-0.012	0.051	.470(**)	-.275(**)	0.095	.218(**)	.264(**)
	α	0.848	0.842	0.4	0	0	0.118	0	0
Eu	r	0.03	-0.088	0.059	.601(**)	-.218(**)	.163(**)	-0.099	.257(**)
	α	0.629	0.15	0.333	0	0	0.007	0.104	0
Tb	r	-.134(*)	-.159(**)	-0.091	.393(**)	-.164(**)	-0.058	0.066	.158(**)
	α	0.027	0.009	0.138	0	0.007	0.341	0.281	0.009
Yb	r	-0.091	-0.085	-0.07	.577(**)	-.297(**)	0.007	-0.028	.320(**)
	α	0.138	0.163	0.251	0	0	0.912	0.641	0
Lu	r	-0.014	-0.042	-.155(*)	.493(**)	-.149(*)	-0.05	.127(*)	.533(**)
	α	0.815	0.493	0.011	0	0.014	0.409	0.037	0

APPENDIX VI: STATISTICS

Table VI-b: Spearman Correlation Coefficients for Selected Trace Element, Lithological, Site Characteristic, and Granulometic Data (N=20)

		Ir	Mo	Rb	Sb	Sc	Ta	W	La	Diorite
Ni	r	.	0.063	.268(**)	.255(**)	.435(**)	-.170(**)	-0.105	0.048	-0.06
	α	.	0.304	0	0	0	0.005	0.086	0.431	0.324
Cu	r	.	0.025	.150(*)	.180(**)	.497(**)	-0.077	-0.067	-0.093	0.048
	α	.	0.682	0.014	0.003	0	0.208	0.271	0.128	0.436
Pb	r	.	-0.039	.257(**)	.208(**)	.165(**)	-0.066	0.033	.145(*)	0.066
	α	.	0.529	0	0.001	0.007	0.283	0.594	0.017	0.282
Zn	r	.	0.043	.410(**)	.269(**)	.475(**)	-.153(*)	-0.033	0.07	-0.055
	α	.	0.487	0	0	0	0.012	0.591	0.248	0.366
Fe	r	.	-0.072	.402(**)	.297(**)	.727(**)	-.152(*)	-0.054	0.1	-0.073
	α	.	0.241	0	0	0	0.013	0.373	0.1	0.232
Au	r	.	0.07	0.075	0.036	0.117	-0.045	-0.045	0.078	0.066
	α	.	0.253	0.222	0.559	0.054	0.462	0.462	0.202	0.277
As	r	.	0.092	.333(**)	.485(**)	.307(**)	-0.037	0.061	.352(**)	-0.016
	α	.	0.13	0	0	0	0.545	0.321	0	0.792
Hg	r	.	-0.063	-.345(**)	-.143(*)	-.249(**)	-.172(**)	0.049	-.207(**)	0.04
	α	.	0.302	0	0.019	0	0.004	0.421	0.001	0.511
Ag	r	.	-0.117	-0.05	0.015	-0.089	0.029	0.008	-0.057	0.024
	α	.	0.054	0.409	0.802	0.144	0.636	0.894	0.35	0.692
Ca	r	.	-0.088	-.238(**)	-0.106	0.063	-0.063	-0.062	-.345(**)	.136(*)
	α	.	0.147	0	0.081	0.301	0.299	0.314	0	0.025
Mg	r	.	0.015	.342(**)	.349(**)	.599(**)	-.201(**)	-0.055	0.01	0.04
	α	.	0.812	0	0	0	0.001	0.366	0.871	0.51
K	r	.	0.045	.758(**)	.465(**)	.547(**)	0.02	0.001	.554(**)	-0.107
	α	.	0.46	0	0	0	0.742	0.987	0	0.078
Na	r	.	0.008	0.012	.128(*)	.192(**)	-0.067	-0.015	0.041	0.023
	α	.	0.901	0.846	0.035	0.002	0.273	0.812	0.503	0.705
Al	r	.	0.037	.502(**)	.302(**)	.612(**)	-.163(**)	-0.114	.179(**)	-0.026
	α	.	0.545	0	0	0	0.007	0.061	0.003	0.676
Ti	r	.	0.032	.187(**)	0.089	.267(**)	0.087	-0.009	.134(*)	-0.048
	α	.	0.598	0.002	0.145	0	0.153	0.884	0.028	0.432
Mn	r	.	-0.04	.179(**)	0.105	.471(**)	-0.054	-0.065	.151(*)	-0.042
	α	.	0.51	0.003	0.085	0	0.378	0.286	0.013	0.492
Ba	r	.	0.118	.438(**)	.327(**)	.379(**)	-0.085	-.137(*)	.343(**)	-.146(*)
	α	.	0.053	0	0	0	0.161	0.024	0	0.017
Cr	r	.	-0.065	.258(**)	.128(*)	.476(**)	-0.081	-.132(*)	-0.075	0.063
	α	.	0.288	0	0.036	0	0.183	0.03	0.22	0.302
Th	r	.	0.012	.382(**)	.333(**)	.229(**)	0.066	0.065	.720(**)	-0.032
	α	.	0.85	0	0	0	0.279	0.288	0	0.596
U	r	.	-.257(**)	.210(**)	.126(*)	.158(**)	-0.01	-0.044	.274(**)	0.014
	α	.	0	0.001	0.038	0.009	0.875	0.471	0	0.821
Ce	r	.	0.013	.342(**)	.243(**)	.191(**)	0.015	0.019	.800(**)	-0.009
	α	.	0.826	0	0	0.002	0.806	0.759	0	0.887
Nd	r	.	0.038	.250(**)	0.067	.233(**)	0.018	-0.046	.702(**)	-0.016
	α	.	0.531	0	0.272	0	0.773	0.454	0	0.791
Eu	r	.	-0.051	0.029	-.158(**)	.156(*)	-0.038	-0.102	.406(**)	0.079
	α	.	0.402	0.63	0.009	0.011	0.532	0.095	0	0.197
Tb	r	.	0.081	0.063	0.101	0.004	0.05	0.086	.359(**)	-0.067
	α	.	0.182	0.301	0.099	0.942	0.41	0.16	0	0.275
Yb	r	.	0.013	.190(**)	0.058	0.012	0.084	0.023	.479(**)	-0.025
	α	.	0.834	0.002	0.343	0.841	0.167	0.702	0	0.687
Lu	r	.	-0.098	0.076	0.113	0.055	0.076	0.027	.548(**)	-0.032
	α	.	0.109	0.213	0.063	0.366	0.213	0.658	0	0.6

APPENDIX VI: STATISTICS

Table VI-b: Spearman Correlation Coefficients for Selected Trace Element, Lithological, Site Characteristic, and Granulometic Data (N=20)

		Rnded Gabbro	Felsic Volc.	Mafic Intrus.	Felsic Volc.	Mafic Volc.	Quart-zite	Ang. Qtz.	Chert/ jasper	Tuffs
Ni	r	0.024	-0.014	-0.031	-.148(*)	-0.029	0.02	0.041	-0.084	-0.104
	α	0.691	0.825	0.613	0.015	0.632	0.744	0.5	0.168	0.089
Cu	r	-0.013	.160(**)	0.018	.127(*)	-0.001	.125(*)	0.051	0.033	-0.009
	α	0.831	0.009	0.769	0.037	0.985	0.04	0.401	0.595	0.878
Pb	r	0.021	.215(**)	0.017	.247(**)	0.049	0.031	-0.003	-.132(*)	0.023
	α	0.727	0	0.78	0	0.419	0.616	0.959	0.03	0.709
Zn	r	-0.009	.152(*)	-0.05	.129(*)	0.057	.124(*)	0.079	-0.098	-0.033
	α	0.88	0.012	0.414	0.034	0.349	0.041	0.198	0.107	0.593
Fe	r	0.032	.238(**)	0.098	0.118	0.078	-0.011	0.037	-0.114	0.025
	α	0.601	0	0.11	0.053	0.202	0.858	0.541	0.06	0.685
Au	r	-0.034	0.081	-0.041	0.06	-0.073	-0.006	0.077	-0.034	-0.044
	α	0.58	0.186	0.505	0.327	0.231	0.922	0.205	0.573	0.471
As	r	.142(*)	0.007	.150(*)	0.04	.257(**)	-.156(*)	.159(**)	-0.107	.178(**)
	α	0.019	0.908	0.014	0.511	0	0.01	0.009	0.078	0.003
Hg	r	0.095	0.052	0.059	0.05	0.026	-.250(**)	-0.01	-0.101	0.042
	α	0.121	0.395	0.33	0.414	0.673	0	0.869	0.099	0.497
Ag	r	0	-0.072	0.002	-0.075	-0.055	0.014	-0.069	-0.093	-0.027
	α	0.995	0.236	0.97	0.217	0.368	0.822	0.259	0.129	0.663
Ca	r	-0.098	.408(**)	0.068	.506(**)	0.066	.161(**)	-0.014	0.02	0.105
	α	0.108	0	0.267	0	0.28	0.008	0.825	0.746	0.085
Mg	r	0.039	.410(**)	.156(*)	.470(**)	.232(**)	.176(**)	.239(**)	-0.002	.151(*)
	α	0.526	0	0.01	0	0	0.004	0	0.974	0.013
K	r	0.092	-0.019	0.023	0.005	0.102	0.045	.128(*)	-0.049	-0.012
	α	0.13	0.755	0.704	0.931	0.095	0.465	0.036	0.423	0.847
Na	r	0.014	.260(**)	.153(*)	.348(**)	.162(**)	-0.118	.136(*)	-0.009	.131(*)
	α	0.818	0	0.012	0	0.007	0.053	0.026	0.884	0.032
Al	r	0.053	.236(**)	-0.016	.189(**)	0.036	0.08	.124(*)	-.138(*)	0.025
	α	0.387	0	0.791	0.002	0.556	0.19	0.042	0.024	0.678
Ti	r	-0.002	.184(**)	.157(**)	.161(**)	0.062	.207(**)	0.115	0.028	-0.034
	α	0.974	0.002	0.01	0.008	0.307	0.001	0.058	0.644	0.577
Mn	r	0.047	0.096	0.087	0.084	0.061	0.01	-0.036	-0.022	0.072
	α	0.439	0.117	0.155	0.169	0.314	0.869	0.553	0.723	0.237
Ba	r	-0.025	0.002	0	-0.029	0.027	-0.008	0.035	-0.057	0.009
	α	0.678	0.979	0.994	0.637	0.66	0.899	0.566	0.348	0.883
Cr	r	-0.064	0.118	0.084	0.027	-0.023	0.047	0.058	-0.006	-0.105
	α	0.294	0.054	0.171	0.659	0.703	0.44	0.342	0.923	0.086
Th	r	0.029	-0.012	0.106	0.006	.133(*)	-0.118	.134(*)	-0.112	0.075
	α	0.639	0.847	0.082	0.919	0.029	0.052	0.028	0.066	0.22
U	r	0.063	0.11	0.042	0.113	-0.058	-0.004	-0.017	-0.076	-0.109
	α	0.302	0.07	0.493	0.065	0.342	0.953	0.777	0.216	0.072
Ce	r	0.028	-0.059	0.036	-0.043	0.048	-.160(**)	.137(*)	-0.098	0.017
	α	0.642	0.335	0.561	0.482	0.436	0.008	0.024	0.107	0.783
Nd	r	0.028	-.135(*)	0.117	-0.074	0.051	-.160(**)	-0.039	-0.107	.124(*)
	α	0.651	0.026	0.054	0.227	0.4	0.009	0.52	0.079	0.042
Eu	r	-0.04	-0.064	0.01	-0.098	-.128(*)	-.130(*)	-.134(*)	-0.056	-0.069
	α	0.508	0.297	0.876	0.108	0.035	0.033	0.028	0.359	0.258
Tb	r	0.022	-.241(**)	0.083	-.158(**)	0.092	-0.094	-0.078	-0.031	0.1
	α	0.718	0	0.174	0.009	0.13	0.124	0.201	0.617	0.101
Yb	r	-0.044	-.197(**)	-0.046	-.151(*)	-0.116	-0.036	-0.02	-0.014	-0.104
	α	0.475	0.001	0.456	0.013	0.057	0.553	0.738	0.824	0.089
Lu	r	0.044	-.220(**)	.125(*)	-0.071	.136(*)	-.151(*)	-.121(*)	0.049	.139(*)
	α	0.473	0	0.04	0.248	0.025	0.013	0.047	0.42	0.022

APPENDIX VI: STATISTICS

Table VI-b: Spearman Correlation Coefficients for Selected Trace Element, Lithological, Site Characteristic, and Granulometic Data (N=20)

		Sedi-mentary	Congl-merate	Meta. seds	Texture	Drain-age	Consist.	Sand	Silt	Clay
Ni	r	.203(**)	-0.078	-0.034	.283(**)	0.092	.196(**)	-.282(**)	0.111	.345(**)
	α	0.001	0.202	0.573	0	0.132	0.001	0	0.069	0
Cu	r	-0.119	0.044	.131(*)	.435(**)	.214(**)	.272(**)	-.469(**)	.360(**)	.453(**)
	α	0.051	0.475	0.031	0	0	0	0	0	0
Pb	r	-.262(**)	0.046	0.079	0.013	0.004	0.027	0.041	-0.043	0.001
	α	0	0.453	0.198	0.831	0.944	0.657	0.5	0.48	0.987
Zn	r	-.124(*)	-0.057	0.038	.168(**)	0.04	0.019	-.152(*)	0.045	.216(**)
	α	0.042	0.347	0.538	0.006	0.512	0.759	0.012	0.46	0
Fe	r	-.194(**)	-0.107	.161(**)	.299(**)	.149(*)	.121(*)	-.226(**)	0.025	.325(**)
	α	0.001	0.08	0.008	0	0.014	0.047	0	0.683	0
Au	r	-0.005	-0.018	.153(*)	0.041	-0.041	-0.019	-0.004	0.043	-0.016
	α	0.934	0.768	0.012	0.501	0.507	0.754	0.942	0.477	0.792
As	r	-.154(*)	-0.052	0.03	-.157(**)	-0.1	-0.024	.210(**)	-.192(**)	-.171(**)
	α	0.011	0.392	0.628	0.01	0.102	0.696	0.001	0.002	0.005
Hg	r	-0.054	-.133(*)	0.048	-.530(**)	-.380(**)	-.621(**)	.649(**)	-.480(**)	-.604(**)
	α	0.377	0.029	0.428	0	0	0	0	0	0
Ag	r	0.096	0.005	0.09	0.047	0.004	-0.013	-0.044	0.045	0.055
	α	0.117	0.94	0.14	0.438	0.948	0.827	0.475	0.457	0.368
Ca	r	-.435(**)	-0.099	.210(**)	-0.093	-0.032	-.130(*)	0.105	0.067	-.196(**)
	α	0	0.104	0.001	0.128	0.598	0.033	0.085	0.274	0.001
Mg	r	-.480(**)	-0.047	.252(**)	.203(**)	0.057	.188(**)	-.212(**)	.196(**)	.194(**)
	α	0	0.439	0	0.001	0.348	0.002	0	0.001	0.001
K	r	0.014	-0.044	-0.096	.172(**)	0.054	.347(**)	-.144(*)	-0.037	.276(**)
	α	0.825	0.475	0.116	0.005	0.379	0	0.018	0.549	0
Na	r	-.397(**)	-0.018	.162(**)	-.309(**)	-.171(**)	-.173(**)	.297(**)	-0.042	-.421(**)
	α	0	0.768	0.008	0	0.005	0.004	0	0.489	0
Al	r	-.192(**)	-.186(**)	0.075	.124(*)	0.023	0.108	-0.044	-.164(**)	.209(**)
	α	0.001	0.002	0.222	0.042	0.706	0.077	0.475	0.007	0.001
Ti	r	-.167(**)	0.023	0.056	.170(**)	.219(**)	.157(**)	-.240(**)	.258(**)	.175(**)
	α	0.006	0.705	0.363	0.005	0	0.01	0	0	0.004
Mn	r	-.136(*)	-0.044	0.012	-0.054	0.005	0.093	0.056	-0.081	0.017
	α	0.025	0.471	0.846	0.379	0.941	0.126	0.358	0.185	0.777
Ba	r	0.043	-0.093	-0.074	-0.039	-0.014	0.093	0.017	-0.078	0.051
	α	0.479	0.127	0.224	0.52	0.821	0.127	0.782	0.2	0.404
Cr	r	0.075	-0.083	0.066	.375(**)	.148(*)	.204(**)	-.417(**)	.238(**)	.445(**)
	α	0.218	0.172	0.277	0	0.015	0.001	0	0	0
Th	r	-0.032	0.017	-0.101	-0.11	-0.027	0.101	.186(**)	-.220(**)	-0.102
	α	0.604	0.779	0.097	0.071	0.66	0.096	0.002	0	0.095
U	r	-0.054	0.016	-0.016	0.043	0.045	.129(*)	0.015	-0.104	0.079
	α	0.381	0.791	0.795	0.479	0.458	0.035	0.81	0.087	0.193
Ce	r	0.048	0.026	-0.114	-.152(*)	-0.048	0.108	.179(**)	-.191(**)	-0.111
	α	0.435	0.672	0.062	0.013	0.436	0.078	0.003	0.002	0.068
Nd	r	0.065	0.073	-.141(*)	0.019	0.09	.137(*)	0.001	-0.03	0.027
	α	0.29	0.231	0.02	0.757	0.141	0.025	0.984	0.627	0.654
Eu	r	.132(*)	-0.025	-.126(*)	-0.004	0.058	0.043	0.03	-0.054	0.005
	α	0.031	0.685	0.038	0.942	0.344	0.484	0.623	0.374	0.94
Tb	r	0.08	0.098	-0.096	0.009	0.054	0.059	-0.017	0.038	-0.021
	α	0.188	0.109	0.117	0.878	0.381	0.335	0.782	0.536	0.734
Yb	r	.232(**)	0.082	-.214(**)	0.049	0.064	.126(*)	-0.092	0.07	0.092
	α	0	0.18	0	0.422	0.292	0.039	0.131	0.25	0.131
Lu	r	-0.02	.241(**)	-.178(**)	-0.041	0.012	0.024	0.003	0.061	-0.065
	α	0.747	0	0.003	0.498	0.846	0.695	0.957	0.322	0.29

APPENDIX VI: STATISTICS

Table VI-b: Spearman Correlation Coefficients for Selected Trace Element, Lithological, Site Characteristic, and Granulometic Data (N=20)

		Sr	Cd	V	Y	Br	Co	Cs	Hf
Sm	r	-0.031	-0.007	-0.053	.539(**)	-.207(**)	-0.013	.187(**)	.316(**)
	α	0.612	0.913	0.383	0	0.001	0.829	0.002	0
Sr	r	1	0.11	.306(**)	0.101	.124(*)	0.11	0.05	-0.111
	α		0.071	0	0.099	0.041	0.07	0.41	0.069
Cd	r		1	.129(*)	0.017	0.061	.159(**)	0.101	-0.079
	α			0.034	0.778	0.322	0.009	0.096	0.198
V	r			1	.212(**)	-.217(**)	.649(**)	.432(**)	-.563(**)
	α				0	0	0	0	0
Y	r				1	-.306(**)	.139(*)	-0.036	0.047
	α					0	0.022	0.556	0.443
Br	r					1	-.200(**)	-.166(**)	0.107
	α						0.001	0.006	0.08
Co	r						1	.328(**)	-.427(**)
	α							0	0
Cs	r							1	-.157(**)
	α								0.01
Hf	r								1
	α								
Ir	r								
	α								
Mo	r								
	α								
Rb	r								
	α								
Sb	r								
	α								
Sc	r								
	α								
Ta	r								
	α								
W	r								
	α								
La	r								
	α								
Diorite	r								
	α								
Rnded Gabbro	r								
	α								
Felsic Intrus.	r								
	α								
Mafic Intrus.	r								
	α								
Felsic Volc.	r								
	α								
Mafic Volc.	r								
	α								
Quart-zite	r								
	α								
Ang. Qtz.	r								
	α								
Chert/ jasper	r								
	α								

APPENDIX VI: STATISTICS

Table VI-b: Spearman Correlation Coefficients for Selected Trace Element, Lithological, Site Characteristic, and Granulometic Data (N=20)

		Ir	Mo	Rb	Sb	Sc	Ta	W	La	Diorite
Sm	r	.	-0.016	.246(**)	.257(**)	.174(**)	0.058	0.039	.840(**)	-0.029
	α	.	0.799	0	0	0.004	0.341	0.521	0	0.637
Sr	r	.	-0.044	0.045	0.06	.278(**)	-0.099	-0.117	-0.085	0.061
	α	.	0.469	0.457	0.323	0	0.105	0.055	0.163	0.315
Cd	r	.	-0.035	0.086	.173(**)	.176(**)	-0.07	-0.005	0.026	0.066
	α	.	0.564	0.157	0.004	0.004	0.249	0.941	0.668	0.279
V	r	.	0.01	.436(**)	.264(**)	.743(**)	-0.1	-0.11	0.004	-0.056
	α	.	0.875	0	0	0	0.103	0.072	0.951	0.359
Y	r	.	-0.005	.151(*)	0.011	.244(**)	0.036	-0.025	.391(**)	-0.04
	α	.	0.94	0.013	0.86	0	0.555	0.682	0	0.51
Br	r	.	-0.105	-.328(**)	-0.027	-.176(**)	-.189(**)	0.041	-.278(**)	0.056
	α	.	0.084	0	0.664	0.004	0.002	0.503	0	0.358
Co	r	.	-0.06	.295(**)	.226(**)	.594(**)	-.168(**)	-0.06	-0.007	-0.028
	α	.	0.329	0	0	0	0.006	0.323	0.908	0.644
Cs	r	.	-0.017	.635(**)	.506(**)	.562(**)	0.031	0.058	.313(**)	-0.027
	α	.	0.784	0	0	0	0.616	0.343	0	0.658
Hf	r	.	-.122(*)	-.292(**)	-.159(**)	-.436(**)	.157(**)	0.068	.219(**)	0.106
	α	.	0.046	0	0.009	0	0.01	0.267	0	0.082
Ir	r		.	.	.	.	.	.	.	.
	α		.	.	.	.	.	.	.	.
Mo	r		1	0.058	0.021	-0.065	0.039	-0.074	0.044	-0.065
	α			0.345	0.734	0.288	0.528	0.225	0.473	0.29
Rb	r			1	.395(**)	.563(**)	0.044	0.039	.460(**)	-0.075
	α				0	0	0.476	0.528	0	0.22
Sb	r				1	.301(**)	-0.062	0.011	.312(**)	-0.034
	α					0	0.307	0.854	0	0.581
Sc	r					1	-0.046	-0.083	.284(**)	-0.062
	α						0.45	0.173	0	0.312
Ta	r						1	.172(**)	0.09	0.09
	α							0.005	0.139	0.141
W	r							1	0.016	-0.029
	α								0.797	0.633
La	r								1	-0.093
	α									0.126
Diorite	r									1
	α									
Rnded Gabbro	r									
	α									
Felsic Intrus.	r									
	α									
Mafic Intrus.	r									
	α									
Felsic Volc.	r									
	α									
Mafic Volc.	r									
	α									
Quart-zite	r									
	α									
Ang. Qtz.	r									
	α									
Chert/ jasper	r									
	α									

APPENDIX VI: STATISTICS

Table VI-b: Spearman Correlation Coefficients for Selected Trace Element, Lithological, Site Characteristic, and Granulometic Data (N=20)

		Rnded Gabbro	Felsic Volc.	Mafic Intrus.	Felsic Volc.	Mafic Volc.	Quart-zite	Ang. Qtz.	Chert/ jasper	Tuffs
Sm	r	0.037	-.159(**)	0.079	-0.109	.138(*)	-.199(**)	-0.027	-0.085	.133(*)
	α	0.545	0.009	0.196	0.073	0.023	0.001	0.654	0.163	0.029
Sr	r	-0.093	.319(**)	0.083	.327(**)	-0.008	0.05	0.059	-0.003	-0.011
	α	0.126	0	0.173	0	0.89	0.416	0.332	0.967	0.858
Cd	r	0.025	.151(*)	-0.081	.139(*)	0.053	-0.014	0.03	-0.018	-0.021
	α	0.683	0.013	0.185	0.022	0.386	0.818	0.626	0.769	0.728
V	r	-0.021	.234(**)	-0.013	0.1	-0.033	.131(*)	.121(*)	-0.085	-0.098
	α	0.726	0	0.835	0.102	0.593	0.031	0.047	0.164	0.108
Y	r	-0.049	-.163(**)	-0.095	-0.094	-.144(*)	-0.004	-.172(**)	-0.014	-0.04
	α	0.418	0.007	0.118	0.125	0.018	0.947	0.005	0.817	0.508
Br	r	0.042	.215(**)	0.093	.229(**)	.152(*)	-.152(*)	0.063	-0.071	.188(**)
	α	0.489	0	0.127	0	0.012	0.012	0.305	0.247	0.002
Co	r	-0.015	0.103	0.048	0.012	0.001	0.046	0.041	-0.083	-0.015
	α	0.801	0.092	0.433	0.839	0.982	0.453	0.498	0.176	0.81
Cs	r	0.038	.166(**)	.175(**)	.192(**)	.334(**)	0.038	.144(*)	-0.023	.175(**)
	α	0.532	0.006	0.004	0.002	0	0.539	0.018	0.703	0.004
Hf	r	0.057	-0.106	.176(**)	-0.046	0.055	-0.093	-0.098	0.063	.143(*)
	α	0.349	0.083	0.004	0.45	0.372	0.128	0.11	0.303	0.019
Ir	r	.	.	.	.	.	.	.	.	.
	α	.	.	.	.	.	.	.	.	.
Mo	r	-0.076	-0.018	-0.071	-.168(**)	-0.074	.119(*)	.141(*)	-0.059	-0.091
	α	0.214	0.771	0.246	0.006	0.224	0.05	0.02	0.338	0.135
Rb	r	0.033	0.051	0.039	0.014	0.049	0.091	.134(*)	-0.105	-0.103
	α	0.591	0.408	0.523	0.816	0.42	0.136	0.027	0.084	0.093
Sb	r	0.03	0.102	0.084	.158(**)	.211(**)	-0.028	.222(**)	-0.072	0.086
	α	0.618	0.093	0.169	0.009	0	0.651	0	0.238	0.157
Sc	r	0.008	.174(**)	0.084	.180(**)	0.101	0.013	0.081	-0.085	0.073
	α	0.893	0.004	0.169	0.003	0.099	0.832	0.185	0.162	0.233
Ta	r	0.045	-0.098	0.025	-.160(**)	0.025	-0.028	-.126(*)	0.016	0.011
	α	0.461	0.11	0.687	0.009	0.683	0.643	0.038	0.796	0.863
W	r	.140(*)	-0.029	0.037	0.05	0.114	-0.02	-0.05	0.079	.122(*)
	α	0.021	0.63	0.541	0.414	0.062	0.747	0.414	0.193	0.045
La	r	0.058	-.121(*)	0.065	-0.079	0.069	-.128(*)	0.079	-0.099	0.094
	α	0.346	0.047	0.286	0.195	0.259	0.036	0.196	0.106	0.122
Diorite	r	-0.071	.129(*)	-0.022	.149(*)	0.049	-0.044	0.019	-0.071	0.075
	α	0.247	0.034	0.715	0.014	0.425	0.475	0.758	0.247	0.219
Rnded Gabbro	r	1	0.002	.309(**)	-0.025	0.106	-0.105	0.007	-0.027	.125(*)
	α		0.972	0	0.685	0.081	0.086	0.913	0.663	0.039
Felsic Intrus.	r		1	.210(**)	.589(**)	.158(**)	.220(**)	.160(**)	0.02	0.044
	α			0.001	0	0.009	0	0.009	0.749	0.472
Mafic Intrus.	r			1	.248(**)	.203(**)	-0.05	-0.038	0.045	.211(**)
	α				0	0.001	0.41	0.538	0.459	0
Felsic Volc.	r				1	.263(**)	.171(**)	.240(**)	0.018	.190(**)
	α					0	0.005	0	0.765	0.002
Mafic Volc.	r					1	-.184(**)	0.001	0.047	.458(**)
	α						0.002	0.99	0.439	0
Quart-zite	r						1	0.077	0.088	-.190(**)
	α							0.21	0.149	0.002
Ang. Qtz.	r							1	0.01	-0.015
	α								0.865	0.803
Chert/ jasper	r								1	0.011
	α									0.853

APPENDIX VI: STATISTICS

Table VI-b: Spearman Correlation Coefficients for Selected Trace Element, Lithological, Site Characteristic, and Granulometic Data (N=20)

		Sedi-mentary	Congl-merate	Meta. seds	Texture	Drain-age	Consist.	Sand	Silt	Clay
Sm	r	0.049	.125(*)	-.182(**)	-.124(*)	-0.007	0.101	0.112	-0.085	-0.1
	α	0.422	0.04	0.003	0.042	0.912	0.097	0.065	0.165	0.101
Sr	r	-.314(**)	-0.02	.160(**)	-0.017	-0.025	-0.004	-0.033	.153(*)	-0.069
	α	0	0.747	0.008	0.786	0.688	0.945	0.592	0.012	0.26
Cd	r	-0.115	-0.001	0.1	-0.035	-0.089	-0.04	0.048	-0.035	0.001
	α	0.06	0.991	0.1	0.565	0.144	0.517	0.435	0.569	0.989
V	r	-0.069	-0.114	.138(*)	.479(**)	.250(**)	.289(**)	-.485(**)	.252(**)	.557(**)
	α	0.258	0.062	0.023	0	0	0	0	0	0
Y	r	0.078	0.078	-.167(**)	0.106	0.116	.125(*)	-0.09	0.043	0.111
	α	0.2	0.201	0.006	0.083	0.056	0.04	0.139	0.477	0.068
Br	r	-.335(**)	-0.054	.185(**)	-.422(**)	-.313(**)	-.495(**)	.467(**)	-.273(**)	-.498(**)
	α	0	0.379	0.002	0	0	0	0	0	0
Co	r	0.023	-0.089	0.074	.341(**)	.133(*)	.209(**)	-.388(**)	.231(**)	.419(**)
	α	0.701	0.143	0.222	0	0.029	0.001	0	0	0
Cs	r	-.256(**)	0.047	0.028	.407(**)	.212(**)	.349(**)	-.412(**)	.241(**)	.456(**)
	α	0	0.439	0.642	0	0	0	0	0	0
Hf	r	-0.073	.258(**)	-0.097	-.280(**)	-0.104	-.160(**)	.310(**)	-.150(*)	-.358(**)
	α	0.229	0	0.111	0	0.089	0.008	0	0.014	0
Ir	r	.	.	.	.	.	.	.	.	.
	α	.	.	.	.	.	.	.	.	.
Mo	r	.142(*)	-0.067	-0.017	0.052	0.058	0.014	-0.075	.123(*)	0.003
	α	0.02	0.272	0.784	0.393	0.345	0.823	0.217	0.044	0.96
Rb	r	0.019	-0.063	-0.063	.315(**)	.148(*)	.387(**)	-.318(**)	0.076	.449(**)
	α	0.754	0.3	0.306	0	0.015	0	0	0.21	0
Sb	r	-.216(**)	0.031	-0.024	0.069	-0.005	.166(**)	-0.084	0.03	0.118
	α	0	0.617	0.699	0.262	0.932	0.006	0.171	0.623	0.053
Sc	r	-.202(**)	-0.108	.143(*)	.293(**)	.183(**)	.245(**)	-.339(**)	.178(**)	.382(**)
	α	0.001	0.077	0.019	0	0.003	0	0	0.003	0
Ta	r	0.088	0.091	-0.087	0.042	0.104	0.078	-0.094	0.096	0.065
	α	0.15	0.135	0.154	0.487	0.087	0.203	0.122	0.115	0.287
W	r	-0.058	0.051	-0.016	-0.018	0.035	-0.003	0.006	-0.001	-0.007
	α	0.341	0.401	0.794	0.763	0.568	0.958	0.92	0.984	0.906
La	r	0.022	0.096	-.133(*)	-0.055	0.033	.207(**)	0.055	-0.111	0.005
	α	0.718	0.114	0.029	0.368	0.593	0.001	0.371	0.068	0.931
Diorite	r	-0.033	-0.063	0.053	0.078	-0.047	0.034	-0.023	0.014	0.034
	α	0.591	0.303	0.388	0.202	0.443	0.579	0.707	0.817	0.574
Rnded Gabbro	r	-0.035	.120(*)	0.015	-0.045	-0.014	-0.005	0.048	-0.039	-0.041
	α	0.565	0.048	0.802	0.46	0.818	0.934	0.435	0.527	0.503
Felsic Intrus.	r	-.525(**)	-.194(**)	.346(**)	.144(*)	0.013	0.045	-0.022	-0.023	0.081
	α	0	0.001	0	0.018	0.837	0.465	0.72	0.702	0.186
Mafic Intrus.	r	-.232(**)	0.025	0.119	0.026	0.076	0.034	-0.042	0.099	-0.008
	α	0	0.686	0.051	0.674	0.213	0.575	0.49	0.103	0.895
Felsic Volc.	r	-.669(**)	-0.101	.315(**)	0.008	-0.027	0.003	0.046	0.012	-0.039
	α	0	0.097	0	0.892	0.659	0.967	0.452	0.84	0.518
Mafic Volc.	r	-.360(**)	0.083	0.022	-0.05	0.007	0.014	0.03	0.065	-0.099
	α	0	0.176	0.715	0.409	0.911	0.825	0.622	0.285	0.104
Quart-zite	r	-0.075	-0.009	0.029	.216(**)	0.101	.152(*)	-.191(**)	0.102	.217(**)
	α	0.222	0.877	0.64	0	0.098	0.012	0.002	0.093	0
Ang. Qtz.	r	-.188(**)	0.04	.150(*)	0.029	-0.098	0.091	-0.011	0.031	0.021
	α	0.002	0.511	0.014	0.64	0.108	0.136	0.855	0.612	0.729
Chert/ jasper	r	-0.02	0.108	0.1	0.042	0.049	-0.001	-0.018	0.072	-0.031
	α	0.748	0.076	0.101	0.491	0.426	0.985	0.763	0.241	0.617

APPENDIX VI: STATISTICS

Table VI-b: Spearman Correlation Coefficients for Selected Trace Element, Lithological, Site Characteristic, and Granulometic Data (N=270)

		Sedi-mentary	Congl-merate	Meta. seds	Texture	Drain-age	Consist.	Sand	Silt	Clay
Conglom-erate	r		1	-0.024	0.025	0.054	0.056	-0.043	0.095	-0.001
	α			0.697	0.677	0.374	0.357	0.486	0.12	0.984
Meta. Seds.	r			1	0.117	0.043	-0.023	-0.044	0.086	-0.005
	α				0.055	0.48	0.703	0.469	0.161	0.939
Texture	r				1	.458(**)	.532(**)	-.761(**)	.502(**)	.757(**)
	α					0	0	0	0	0
Drainage	r					1	.307(**)	-.430(**)	.339(**)	.370(**)
	α						0	0	0	0
Consist.	r						1	-.533(**)	.308(**)	.556(**)
	α							0	0	0
Sand	r							1	-.815(**)	-.845(**)
	α								0	0
Silt	r								1	.417(**)
	α									0
Clay	r									1
	α									

VITA

Candidate's full name: Geoffrey Morgan Allaby

Place and date of birth: Vancouver, British Columbia

Permanent address: 249 Ragged Point Road,
Saint John New Brunswick

Universities attended:

University of New Brunswick
Saint John, New Brunswick
1992–1993 B.Sc. in Chemistry
(not completed).

University of New Brunswick
Fredericton, New Brunswick
1993–1994 B.Sc. in Chemistry
(not completed).

University of New Brunswick
Saint John, New Brunswick
1994–1997 B.Sc. (Major) in
Environmental Geochemistry.

University of New Brunswick
Fredericton, New Brunswick
1997–1999 M.Sc. Geology.

Publications:

Allaby, G. M., Broster, B. E., and Pronk, A. G. 1999. Late Wisconsinan glacial movement in the Petitcodiac map area, southeastern New Brunswick. *In* Program and Abstracts. Atlantic Geoscience Society Annual Meeting and Colloquium, p. 11.

Allaby, G. M., Pronk, A. G., and Broster, B. E. 1999. Till provenance study in the Petitcodiac area, southeastern New Brunswick. *In* Program and Abstracts. Joint meeting Canadian Quaternary Association-Canadian Geomorphology Research Group 1999, p. 2.

Allaby, G. M., Pronk, A. G., and Broster, B. E. 1999. Late Wisconsinan glacial movement in the Petitcodiac map area (21 H/14), southeastern New Brunswick. *In* Abstracts, 1999: 24th Annual Review of Activities. *Edited by* B. W. Carroll. Department of Natural Resources and Energy New Brunswick, Mineral and Energy Division, Information Circular 99-3, p. 1.